





DISSERTATIONES BIOLOGICAE UNIVERSITATIS TARTUENSIS  
143

**VLADIMIR VIMBERG**

Peptide mediated macrolide resistance



Faculty of Science and Technology, University of Tartu, Tartu, Estonia

Dissertation is accepted for the commencement of the degree of Doctor of Philosophy (PhD) in molecular biology on June 20, 2008, by the Council of the Institute of Molecular and Cell Biology, Faculty of Science and Technology, University of Tartu.

Supervisor: Ph.D. Professor Tanel Tenson,  
University of Tartu,  
Tartu, Estonia

Opponent: Lic. scient. (Ph.D.) Research Associate Professor  
Birte Vester,  
Department of Biochemistry and Molecular Biology,  
University of Southern Denmark.

Commencement will take place at the Institute of Molecular and Cell Biology, Riia 23, Tartu, on August 21, 2008, at 10.15.

ISSN 1024-6479  
ISBN 978-9949-11-916-5 (trükis)  
ISBN 978-9949-11-917-2 (PDF)

Autoriõigus Vladimir Vimberg, 2008

Tartu Ülikooli Kirjastus  
[www.tyk.ee](http://www.tyk.ee)  
Tellimus nr 297

# CONTENTS

LIST OF ORIGINAL PUBLICATIONS .....	7
LIST OF ABBREVIATIONS .....	8
INTRODUCTION.....	9
1. REVIEW OF LITERATURE.....	10
1.1. Protein biosynthesis in Bacteria .....	10
1.2. Antibiotics and the Ribosome.....	13
1.3. Macrolide Antibiotics .....	15
1.4. Macrolides' Action .....	17
1.5. Macrolide Resistance.....	21
1.5.1. Methylation of rRNA .....	21
1.5.2. Macrolide Resistance Conferred by Base Substitutions in 23S rRNA.....	24
1.5.3. Macrolide Resistance Mutations in Ribosomal Proteins L22 and L4 .....	25
1.5.4. Macrolide Resistance Conferred by Drug-Efflux Transporters.....	26
1.6. Resistance Conferred by Structural Modification of Macrolides .....	28
1.7. Peptide Mediated Macrolide Resistance.....	29
1.8. The Prevalence of Mechanisms of Macrolide Resistance in Clinical Isolates .....	30
2. RESULTS AND DISCUSSION .....	31
2.1. Translation Initiation Region Sequence Preferences in <i>Escherichia Coli</i> .....	31
2.1.1. Effect of the Translation Initiation Region on the Level of Protein Synthesis.....	31
2.2. Peptide Mediated Macrolide Resistance.....	33
2.2.1. Josamycin Resistance Peptides .....	33
2.2.2. Peptide Mediated Resistance is Macrolide Specific .....	34
2.2.3. Classification of Resistance Peptides.....	34
2.2.4. Mechanism of Macrolide Displacement from Ribosome .....	39
2.2.5. Mechanism of Peptide Mediated Erythromycin Resistance ...	40
2.2.6. Clinical Significance of Peptide Mediated Resistance.....	41
2.2.7. The Mechanisms of Peptide Mediated Erythromycin and Josamycin Resistance Differ .....	43
2.2.8. Antibiotic Efflux in Peptide Mediated Resistance .....	45
2.2.9. Antibiotic Efflux in Erythromycin Resistance Conferred by L22 and L4 Mutations .....	45
2.2.10. Interplay Between Antibiotic Efflux and Resistance Described in Other Studies.....	47

CONCLUSIONS .....	48
REFERENCES .....	49
KOKKUVÕTE (Summary in Estonian).....	62
ACKNOWLEDGEMENTS .....	64
PUBLICATIONS .....	65

## LIST OF ORIGINAL PUBLICATIONS

Current thesis is based on the following original publications which will be referred by their Roman numerals:

- I.** **Vimberg, V.**, Tats, A., Remm, M., Tenson, T. 2007. Translation initiation region sequence preferences in *Escherichia coli*. *BMC Mol Biol.* 8:100.
- II.** **Vimberg, V.**, Xiong, L., Bailey, M., Tenson, T., Mankin, A. 2000. Peptide-mediated macrolide resistance reveals possible specific interactions in the nascent peptide exit tunnel. *Mol Microbiol.* 54(2):376–85.
- III.** Lovmar, M., Nilsson, K., **Vimberg, V.**, Tenson, T., Nervall, M., Ehrenberg, M. 2006. The molecular mechanism of peptide-mediated erythromycin resistance. *J Biol Chem.* 281(10):6742–50.
- IV.** Nilsson, K., Lovmar, M. , **Vimberg, V.**, Tenson, T., Ehrenberg, M. 2006. Mechanisms and Requirements of Peptide Mediated Macrolide Resistance. Manuscript.
- V.** Lovmar, M., Nilsson, K., Lukk, E., **Vimberg, V.**, Tenson, T., Ehrenberg, M. 2008. Kinetic Coupling Between Target Binding and Efflux Pump Efficiency – the Case of Erythromycin Resistance. Manuscript.

## LIST OF ABBREVIATIONS

ABC	ATP binding cassette
Arg	arginine
aSD	anti Shine-Dalgarno
A site	ribosomal site for aminoacyl-tRNA
AZI	azithromycin
DB	downstream box
<i>E. coli</i>	<i>Escherichia coli</i>
EF-G	elongation factor-G
EF-Ts	elongation factor-Ts
EF-Tu	elongation factor-Tu
ERY	erythromycin
E site	ribosomal site for tRNA exit
fMet	N-formyl-methionine
GFP	green fluorescent protein
IF	initiation factor
Ile	Isoleucine
IPTG	isopropyl- $\beta$ -galactoside
JOS	josamycin
KET	ketolide
Leu	leucine
Lys	lyzine
MATE	multidrug and toxic compound efflux
Met	methionine
MF	major facilitator
mRNA	messenger RNA
OLE	oleandomycin
ORF	open reading frame
Phe	phenylalanine
P site	ribosomal site for peptidyl-tRNA
$P_{tac}$	tac promoter
RF	release factor
RND	resistance/nodulation/cell division
rRNA	ribosomal RNA
SD	Shine-Dalgarno
SMR	small multidrug resistance
TIR	translation initiation region
tRNA	transport RNA
Tyr	tyrosine
Val	valine

## INTRODUCTION

For over 50 years researchers have been trying to understand the peculiarities of translation mechanism. For the present moment we have enormous information about ribosome structure, formation and translation regulation. But continuing discoveries of new and suprising mechanisms of translation regulation suggest that our understanding of this complex biological process remains incomplete.

The main step of translation regulation in bacteria occurs during initiation. The rate-limiting step in this process is binding of the small ribosomal subunit to the translation initiation region on mRNA. The mRNA translation initiation region comprises the initiator codon, Shine-Dalgarno sequence and translational enhancers. We have tested the influence of Shine-Dalgarno sequence length and the presence of enhancers on the efficiency of translation initiation.

The ribosome is one of the main antibiotic targets in the cell. Studies on the ribosome targeted antibiotics are interesting from two viewpoints: characterization of the antibiotic mechanisms of action and resistance mechanisms can help in designing better drugs; as the antibiotics bind to functionally essential parts of the ribosome, studies on ribosome targeted antibiotics have often provided information essential for understanding the basic mechanisms of protein synthesis.

Macrolides are a group of clinically useful antibiotics containing a 14-, 15- or 16- member lactone ring. The macrolides bind to the large ribosomal subunit in the vicinity of the peptidyl transferase centre, where tight contacts with 23S rRNA are formed. The primary mode of action of the macrolides is inhibition of protein synthesis, although they can also interfere with ribosome assembly.

The therapeutical utility of macrolides has been compromised by the emergence of drug resistance in many pathogenic bacteria. The known mechanisms of macrolide resistance include modification of 23S ribosomal RNA (methylation or mutation of 23S rRNA bases) and ribosomal protein mutations, active efflux of the drug from the cell, structural modification of macrolides.

In the present work we determine the mechanism of macrolide resistance conferred by expression of specific short peptides. We argue that broad-specific multi-drug pumps located in the inner membrane may account for the required rapid outflow rate of the antibiotic to confer peptide-mediated resistance.

# I. REVIEW OF LITERATURE

## I.1. Protein Biosynthesis in Bacteria

Protein synthesis is a final step in gene expression. During this process genetic information, encoded within mRNA, is translated into protein. Pivotal for protein biosynthesis is a multifunctional ribonucleoprotein complex, termed ribosome.

Ribosomes of bacteria consist of two unequal subunits containing 3 RNA molecules and a number of different ribosomal proteins. In prokaryotes, the larger subunit sediments at 50S, is ~1.5MDa in molecular weight and contains ~3000 nucleotides of ribosomal RNA (termed 23S rRNA) and 34 proteins. The smaller subunit sediments at 30S, has a molecular weight of 0.8MDa and comprises 1500 nucleotides of ribosomal RNA (termed 16S rRNA) and 21 proteins (Schuwirth et al., 2005; Selmer et al., 2006). The small ribosomal subunit is engaged in decoding of genetic information, while the large subunit assembles amino acids into a polypeptide chain. Catalysis of peptide bond formation and amino acid polymerization occurs in the peptidyl transferase centre located on the large subunit (reviewed in Steitz, 2008). The ribosome has three separate tRNA binding sites, each spanning the two subunits (Yusupov et al., 2001; Marquez et al., 2002). The A site binds aminoacyl-tRNA, the P site binds peptidyl-tRNA or deacylated tRNA, and the E site binds deacylated tRNA (Rheinberger, 1991).

Translation is viewed conceptually as a three-step process: initiation, in which the translation machinery is assembled; elongation, in which amino acids are added to the growing peptide; and termination, in which the nascent peptide synthesis is terminated and the translation machinery is disassembled (reviewed in Ramakrishnan, 2002).

The efficiency of initiation is the most important determinant of mRNA translation efficiency (Boelens and Gualerzi, 2002). In bacteria the 30S small ribosomal subunit, assisted by initiation factors 1, 2 and 3 and fMet-tRNA<sup>fMet</sup> recognizes the translation initiation region (TIR) of the mRNA. This event is followed by binding of the 50S large ribosomal subunit and release of the initiation factors. The rate-limiting step of this process is 30S subunit binding to the TIR (Gualerzi and Pon, 1990).

TIR consists of several sequence elements (Figure 1) that contribute to its efficiency: (1) the initiation codon, that is most commonly AUG but sometimes also GUG and very rarely UUG or AUU (Gren 1984; Schneider et al., 1986); (2) Shine-Dalgarno (SD) sequence (Shine and Dalgarno, 1974; Shultzaberger et al., 2001); (3) regions upstream of the SD sequence and downstream of the initiation codon that are often described as enhancers of translation (Stormo et al., 1982; Stenstrom and Isaksson, 2002 ). In addition, spacing between these sequence elements is often critical. For example, the distance between the SD

sequence and the initiation triplet has large effect on the efficiency of translation (Chen et al., 1994).

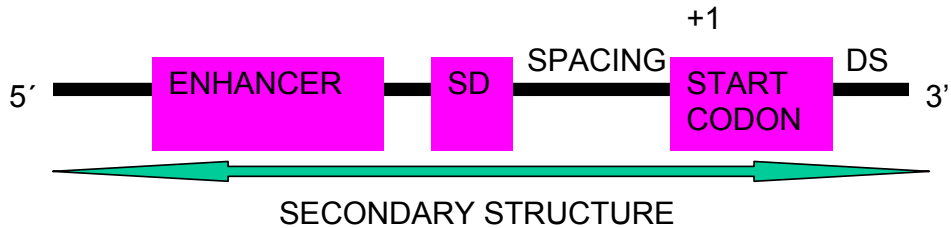


**Figure 1.** Elements of mRNA translation initiation region, that contribute to the efficiency of translation initiation. Secondary structure of TIR, indicated by green arrow, is an important determinant of TIR effectiveness.

The SD sequence base pairs directly with the anti Shine-Dalgarno (aSD) sequence on the 16S rRNA 3' terminal end (Shine and Dalgarno, 1974). The maximal length of the SD:aSD duplex is 12 or 13 nucleotides (Yusupova et al., 2006). In most *E. coli* genes the SD sequence is shorter. The calculation of the free energies for all possible duplexes between the 16S rRNA 3' end and a region of 21 nucleotides upstream from the start codon in 1159 *E. coli* genes has revealed that the average number of paired mRNA:rRNA nucleotides is 6.3 (Schurr et al., 1993). A similar calculation has been made for the ribosomal protein genes. This study suggests that the average SD length is 4.4 nucleotides (Komarova et al., 2002). It was also observed that long SD sequences are not very efficient, probably because of increased time for clearance of the TIR. On the other hand, there are studies where the importance of the SD for the initiation of translation has been argued: Lee et al. (1996) reported that translational efficiency correlates very poorly with the strength SD:aSD interaction. Unfortunately, we are currently lacking a systematic study that could reveal the correlation between the strength of SD:aSD interaction and the efficiency of translation.

It has been recently described that before the SD:aSD interaction occurs, the 30S ribosomal subunit can bind to a standby site in the vicinity of SD (de Smit and van Duin, 2003; Studer and Joseph, 2006). Binding to the standby site might increase the local concentration of 30S subunits at the TIR. In addition, the ribosome attached to the standby site might wait for the moment when the SD sequence will be in appropriate conformation able to bind the aSD. Through this mechanism the standby site could stimulate translation of mRNAs where the SD can be trapped in secondary structures. Attachment to the standby site could be mediated by ribosomal S1 protein, the largest protein of the small ribosomal subunit. S1 consists of two major domains with a freely rotatable region in between (Subramanian, 1983). One domain is attached to the 30S; the second domain is exposed outside the small subunit, scanning the space around

the ribosome and searching for A and U nucleotide (A/U) rich sequences that are recognized with the help of four RNA-binding motifs. It has been shown that S1 can act as a RNA chaperone, destabilizing RNA secondary structures (Thomas and Szer, 1982). Cross-linking studies have aligned the nucleic acid-binding domain of S1 with a region of the mRNA upstream of the SD, suggesting that S1 may interact with 5' parts of the TIR (Boni et al., 1991; Zhang and Deutscher, 1992). Consistent with this observation, A/U rich sequences in front of SD enhance protein synthesis (Komarova et al., 2002). Currently, there are nine sequences that have been shown experimentally to act as translational enhancers. They are all rich in A and U nucleotides and contain very few Gs (Komarova et al., 2002). The disruption of the *E. coli* gene coding for S1 protein has been previously reported to be lethal (Kitakawa and Isono, 1982). The decrease in the level of S1 protein in the cells leads to the fast decrease in the whole protein synthesis (Sorensen et al., 1998). Thus it could be speculated that the SD sequence alone cannot mediate efficient initiation of translation but has to be complemented with an enhancer sequence. Unfortunately, there are no experimental reports describing the effects of combining the enhancers with different SD sequences.

Once an initiation complex has been formed translation elongation starts. During this process the ribosome with the help of tRNAs, charged with specific amino acids, and elongation factors Tu, Ts and G (EF-Tu, EF-G, EF-TS), decodes mRNA and synthesizes protein. Elongation is activated when amino acid enters the ribosome acceptor site (A site) as aminoacyl-tRNA together with EF-Tu and GTP, ternary complex. When the correct base pairing between mRNA codon and the tRNA anticodon occurs GTP is hydrolysed and EF-Tu leaves the ribosome (Daviter et al., 2006; Steitz, 2008). Aminoacyl-tRNA, released from the EF-Tu moves through the ribosome into the peptidyl transferase centre (Beringer and Rodnina, 2007). In the peptidyl transferase centre the nascent peptide from the peptidyl-tRNA is transferred to the amino acid on the A-site tRNA, and thus the peptide grows by one amino acid (reviewed in Steitz, 2008). Completion of the elongation cycle involves EF-G dependent translocation event, resulting in the moving of the peptidyl-tRNA from the A to the P site, and EF-G is released upon GTP hydrolysis (Frank et al., 2007).

The final step in protein synthesis is hydrolysis of the ester bond in peptidyl-tRNA and release of the finished protein. The reaction is induced in prokaryotes by one of the two class I release factors, RF1 or RF2 (Scolnick et al., 1968). Termination of translation is triggered by the class I factors following a translocation step that places a stop codon in the ribosomal A site and peptidyl-tRNA in the P-site. In prokaryotes, RF1 recognizes stop codons UAA and UAG, while RF2 recognizes UAA and UGA (Kisselev and Buckingham, 2000). After the protein has been released from the ribosome a class II factor, RF3, promotes rapid dissociation of RF1 or RF2 from the posttermination complex

(Zavialov et al., 2001). And finally, ribosome recycling factor with the help of EF-G and IF3 dissociates ribosome into two subunits (Karimi et al., 1999).

## I.2. Antibiotics and the Ribosome

The ribosome is essential to all living cells and is one of the major targets for antibiotics (Spahn and Prescott, 1996; Tenson and Mankin, 2006). In the Table 1 antibiotics, implicated in inhibition of the protein synthesis, are described.

**Table 1.** Antibiotics that inhibit protein synthesis.

Antibiotic	Mode of action	Reference
Paromomycin type aminoglycosides: Kanamycin Neomycin Paromomycin Tobramycin Amikacin Gentamicin Spectinomycin	Bind to 30S subunit. Affect ribosome accuracy at the initial step of aminoacyl-tRNA selection that leads to increased frequency of amino acid misincorporation into nascent protein. Increase the rate of GTP hydrolysis in case of the near cognate tRNA to be closer to the cognate value. Inhibit translocation.	Reviewed in Spahn and Prescott, 1996; Recht et al., 1999; Ogle and Ramakrishnan, 2005; Tenson and Mankin, 2006
Streptomycin type aminoglycosides: Streptomycin	Bind to 30S subunit. Affect ribosome accuracy at the initial step of aminoacyl-tRNA selection by reducing the conformational flexibility of the small ribosomal subunit, lowering the rate of GTPase activation for cognate tRNA but increasing it for near cognate tRNA.	Reviewed in Tenson and Mankin, 2006
Tetracyclines: Tetracycline Chlortetracycline Doxycycline Minocycline Rolitetracycline	Bind to 30S subunit. Prevent aminoacyl-tRNA binding to A site. Inhibit fMet-tRNA binding to P site. Block tRNA selection after codon recognition, by slowing GTP hydrolysis occurring.	Geigenmüller and Nierhaus, 1986; Moazed and Noller, 1987; Blanchard et al., 2004.
Chloramphenicol	Binds 50S subunit. Blocks peptidyl transferase activity by interfering with the positioning of the amino acyl moiety of aminoacyl-tRNA in the A site. Causes translational inaccuracy.	Kirillov et al., 1997; Thompson et al., 2002.

**Table 1.** Continuation

Antibiotic	Mode of action	Reference
Lincosamides: Clindamycin Lincomycin Celesticetin	Bind 50S subunit. Block peptidyl-transferase reaction. Directly interfere with the positioning of the aminoacyl group at the A site and the peptidyl group at the P site while also sterically blocking the progression of the nascent peptide toward the tunnel.	Douthwaite, 1992; Kallia-Raftopoulos et al., 1994
Macrolides: Methymycin Erythromycin Clarithromycin Dirithromycin Flurithromycin Roxithromycin Azithromycin Josamycin Carbomycin Tylosin Spiramycin	Bind to 50S subunit. Block progression of the nascent peptide.	Tenson and Mankin, 2006
Oxazolidinones: Linezolid Eperzolid	Bind to 50S subunit. Hamper mRNA and/or tRNA binding. Inhibit formation of the first peptide bond. Interfere translocation. Cause translational inaccuracy.	Shinabarger et al., 1997; Xiong et al., 2000; Thompson et al., 2002
Streptogramin A: Virginiamycin M.	Binds to 50S subunit. Blocks peptidyl-transferase reaction.	Reviewed in Spahn and Prescott, 1996; Cocito et al., 1997
Streptogramin B: Virginiamycin S Vernamycin B	Bind to 50S subunit. Do not block peptidyl-transferase reaction. Prevent the extension of nascent peptide, inducing peptidyl-tRNA drop off.	Reviewed in Spahn and Prescott, 1996; Cocito et al., 1997
Puromycin	Binds to 50S subunit. Structural analogue of the 3'-end of aminoacyl-tRNA. Binds to A site and peptidyl transferase links the peptidyl residue covalently to the drug.	Pestka, 1977

**Table 1.** Continuation

Antibiotic	Mode of action	Reference
Thiostrepton	Binds to 50S subunit. Inhibits GTP hydrolysis during translocation.	Reviewed in Spahn and Prescott, 1996
Kirromycin	Binds to EF-Tu-GTP-aminoacyl-tRNA at 50S subunit, inhibiting the structural transition of EF-Tu to the GDP bound conformation.	Parmeggiani and Swart, 1985. Vogeley et al., 2001.
Fusidic acid	Binds to 50S subunit. Stalls the ribosome in the complex with EF-G and GDP.	Rodnina et al., 2000

### 1.3. Macrolide Antibiotics

#### *Macrolides*

Macrolides are important antibacterial antibiotics, commonly used in clinical practice to treat infections such as respiratory tract and soft tissue infections (Ōmura, 2002). The structures of all macrolides are based on a lactone ring. The therapeutically most relevant macrolides comprise a 14-, 15- or 16- membered lactone ring (Figure 2).

#### *Erythromycin*

Erythromycin, derived in 1949 from *Saccharopolyspora erythraea*, was the first macrolide to be used clinically (Blondeau et al., 2002).

#### *Erythromycin structure*

Erythromycin consists of a 14-membered lactone ring with two attached sugar groups: L-cladinose at position 3 and desosamine at position 5 of the lactone ring (Figure 2).

#### *Erythromycin disadvantages*

Although erythromycin is an important antimicrobial agent, it has some negative features that impair its clinical use:

- poor oral bioavailability
- inactivation in acidic environment
- gastrointestinal side effects – nausea, cramping, diarrhoea
- short half-life – multiple daily dosing
- poor activity against gram-negative bacteria

Erythromycin properties were improved by chemical modifications of the lactone ring and/or sugar moiety.

### *Josamycin – macrolide with 16-membered lactone ring*

Josamycin is a macrolide with 16-membered lactone ring with mycaminose-mycarose-isobutyrate side chain attached at carbon 5 of the lactone ring produced by *Streptomyces narbonensis* (Figure 2). Its spectrum of activity is similar to that of erythromycin; at the same time, josamycin is better tolerated by patients than erythromycin (Strausbaugh et al., 1976; Periti et al., 1993; von Rosensteil and Adam, 1995). The main disadvantage of the josamycin is short half life in comparence with that of next generation of macrolides (Fraschini, 1990; Aprim et al., 1990).

### *Second generation of macrolides*

Semisynthetic derivatives of erythromycin, such as clarithromycin, roxithromycin, azithromycin and oleandomycin represented the second generation of macrolides (Figure 2).

Clarithromycin has been synthesized by methylation of the C6-OH group of erythromycin, whereas roxithromycin has been produced by the insertion of an etheroxime chain at the C9 position (Figure 2).

Azithromycin is a derivative of erythromycin with a 15-membered lactone ring possessing an additional nitrogen (Figure 2).

Oleandomycin differs from erythromycin by the presence of an 8-oxirane cycle, a methyl attached at carbon 13 of the lactone ring and the lack of a 12-hydroxyl (Figure 2).

These antibiotics have higher activity against gram-negative bacteria, as with that of erythromycin. Modifications increase drugs' stability in acidic environment and reduce gastrointestinal side effects (Blondeau et al., 2002; Asaka et al., 2003).

### *Third generation of macrolides*

Increasing macrolide resistance among respiratory tract pathogens, particularly *Streptococcus pneumoniae*, has led to a search for new agents that are more effective against macrolide resistant strains. Ketolides represent a new family of antibiotics that are derived chemically from the macrolides. Ketolides contain a keto group instead of the cladinose residue at position three of the lactone ring and carry alkyl-aryl or quinolylallyl side chains (Figure 2). These modifications increase macrolide stability in acidic environment and help to overcome erythromycin resistance (Bryskier, 2000; Douthwaite, 2001).

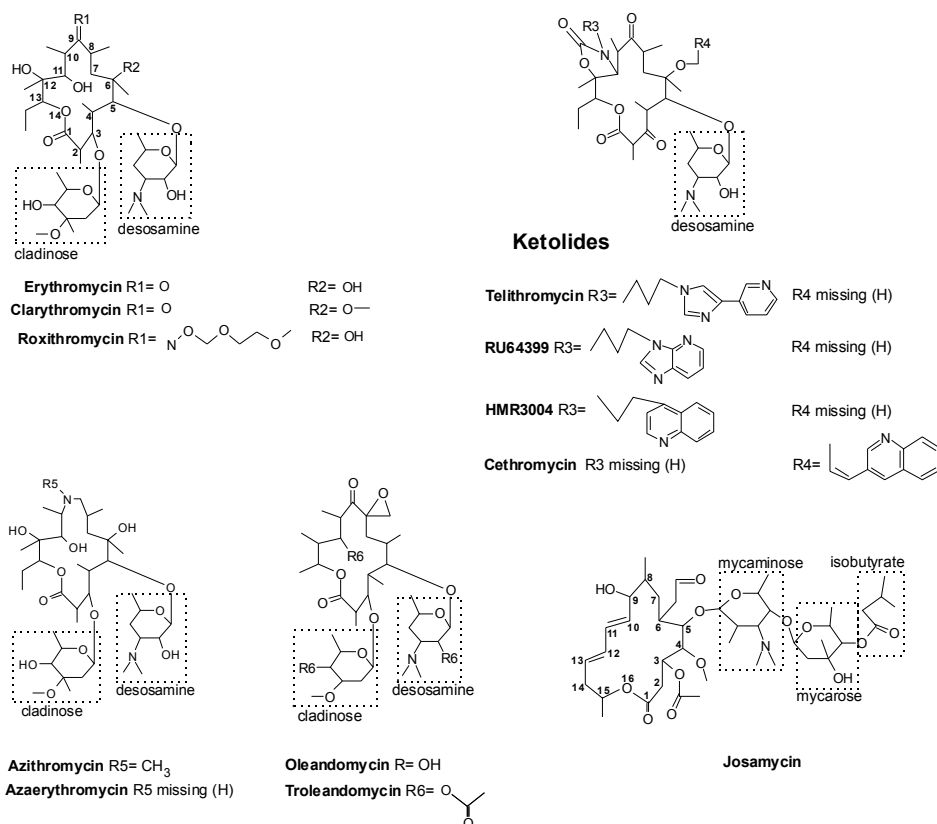


**Figure 2.** Chemical structures of the representative macrolide antibiotics (Adapted from Vimberg et al., 2004).

## I.4. Macrolides' Action

Macrolides inhibit protein synthesis in prokaryotes (Pestka, 1977).

### *Macrolides' target*

Macrolides bind to either the vacant ribosome or a translating ribosome carrying a very short nascent peptide, the ribosomes that contain longer nascent peptide are resistant to the drug (Andersson and Kurland, 1987; Tenson et al., 2003). All macrolides bind to the large ribosomal subunit of the ribosome (Vazquez, 1979). The macrolides' binding site is located between the peptidyl transferase centre and the entrance of the nascent polypeptide exit tunnel (Nissen et al., 2000; Schlünzen et al., 2001, 2003; Hansen et al., 2002, 2003; Berisio et al., 2003a, b; Tu et al., 2005).

### Macrolide's interactions with the ribosome

Different macrolide compounds bind to the ribosome with a similar orientation of the lactone ring. Binding of the macrolide is achieved through hydrogen bonding of the macrolide sugar residues to 23S rRNA as well as hydrophobic and van der Waals interactions of the lactone ring with the RNA-based surface of the ribosome (Figure 3) (Schlünzen et al., 2001; Hansen et al., 2002).

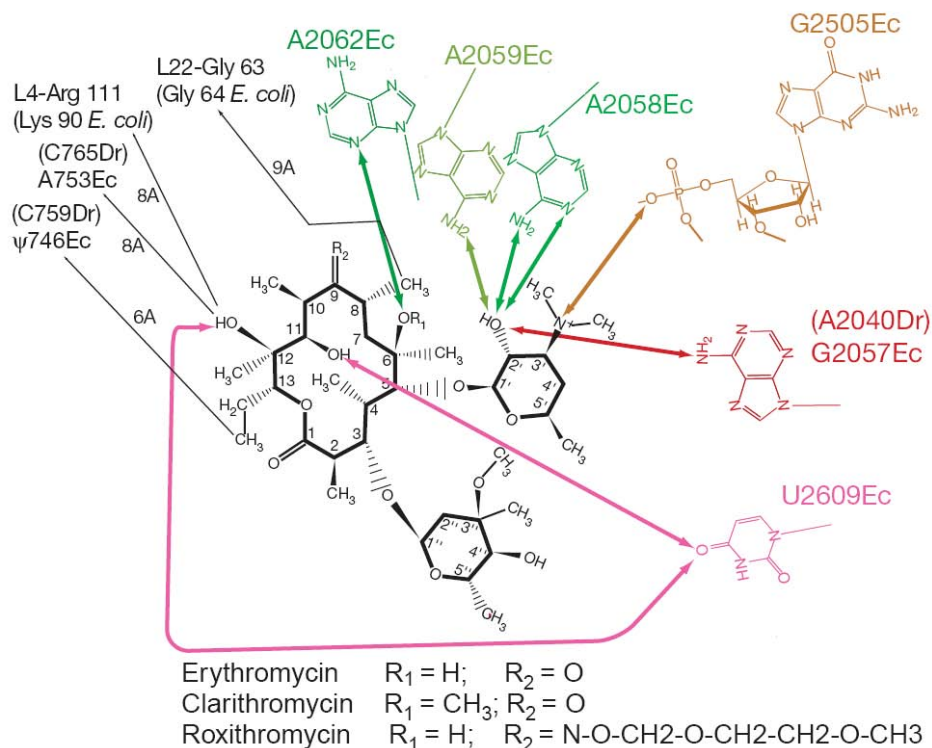


**Figure 3.** Interaction of macrolides with the ribosome (Adapted from Schlünzen et al., 2001). Chemical structure diagram of the macrolides (erythromycin, clarithromycin and roxithromycin) showing the interactions (coloured arrows) of the reactive groups of the macrolides with the nucleotides of the peptidyl transferase cavity (coloured). Coloured arrows between two chemical moieties indicate that the two groups are less than 4.4Å apart. Distance of macrolide moieties to groups implicated previously in antibiotic interaction (L4, L22 and domain II of the 23S rRNA) are shown. Nucleotides of 23S rRNA of *Deinococcus radiodurance* (Dr) that correspond to the *Escherichia coli* (Ec) 23S rRNA nucleotides and interact with the macrolides are marked. L4-Arg111 of *Deinococcus radiodurance* corresponds to Lys90 of *Escherichia coli* L4. L22-Gly63 of *Deinococcus radiodurance* corresponds to Gly64 of *Escherichia coli* L22.

### *23S rRNA V domain*

The main component of the macrolide binding site on the ribosome is the central loop of domain V of the 23S rRNA, where adenosine 2058 (A2058) and adjacent nucleotides interact with desosamine sugar of the macrolide. The 2'OH group of the desosamine sugar forms hydrogen bonds with N6 and N1 of A2058 and N6 of A2059 (Schlünzen et al., 2001).

### *Macrolides' universal interactions*

Various side chains attached to the lactone ring confer universal interactions of macrolides with the 23S rRNA (Poulsen et al., 2000; Schlünzen et al., 2001; Hansen et al., 2002; Tu et al., 2005).

Alkyl-aryl side chains of ketolides protube in the direction of the peptide chain exit channel and form likely direct contacts with domain II of 23S rRNA (Xiong et al., 1999; Hansen et al., 1999; Douthwaite et al., 2000; Hansen et al., 2002; Liu and Douthwaite 2002; Schlünzen et al., 2003).

Josamycin mycaminoso-mycarose-isobutyrate moiety attached to position 5 of the lactone ring approaches the peptidyl transferase centre where it interacts with the A2451 and A2452 nucleotides of 23S rRNA (Hansen et al., 2002).

### *Mechanism of macrolide action*

Macrolide bound in the vicinity of the narrowest point of the peptide exit channel perturbs nascent peptide penetration into the exit tunnel, leading to arrest of protein synthesis during early rounds of translation.

Inhibition of translation elongation leads to the dissociation of peptidyl-tRNA from the ribosome (Menninger and Otto, 1982; Tenson et al., 2003). This might cause the depletion of free tRNA pools, that might be important factor contributing to the inhibition of protein synthesis (Menninger 1979., Heurgue-Hamard et al., 1996; 2000).

There is a correlation between the space available for the nascent peptide within the drug-bound ribosome and the average length of peptides on the peptidyl-tRNAs that dissociate from ribosomes under the influence of various macrolides (Figure 4) (Tenson et al., 2003). Translation of the protein results in drop off of di- or tripeptidyl-tRNA in the case of josamycin, di- and tetrapeptidyl-tRNA in the case of clindamycin, di-, tri- or tetrapeptidyl-tRNA in the case of spiramycin and hexa-, hepta- or octapeptidyl-tRNAs for erythromycin. The ketolides, due to the absence of the cladinose sugar residue, leave more space for the growing peptide than erythromycin. Thus telithromycin causes drop off of peptidyl-tRNAs with peptides ranging from 9 to 12 amino acid residues (Tenson et al., 2003).

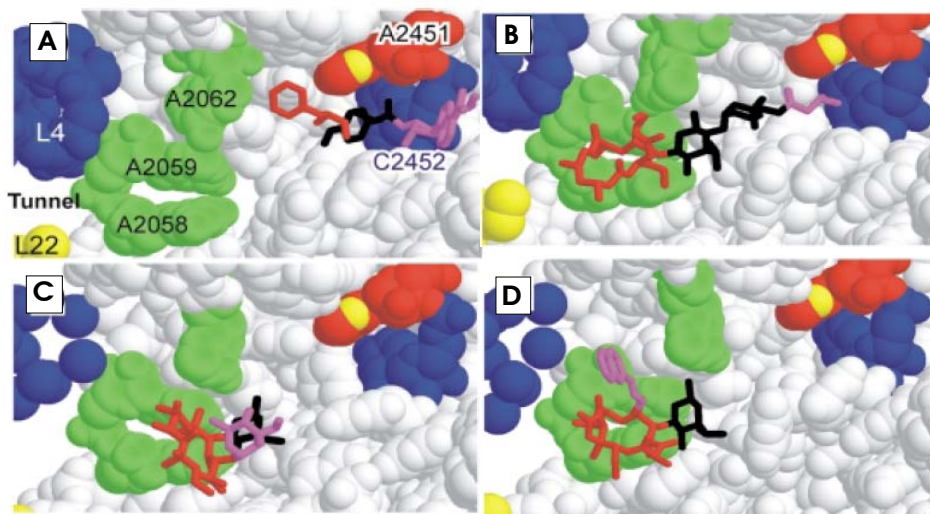


**Figure 4.** The Figure shows the crystal structure of 50S subunits in complex with a peptidyl-tRNA analogue and different MLS antibiotics as well as N3 of A2451, an atom located very close to the catalytic site of the peptidyl transferase. (Adapted from Tenson et al., 2003)

**A.** *Haloarcula marismortui* 50S subunit with a dipeptidyl-tRNA analogue in the A site. For clarity, parts of the analogue (caproic acid and biotin residues) are not shown. The N-terminal phenylalanine residue is shown in red, the next, tyrosine residue in black and A76 of tRNA is shown in magenta. Nucleotides A2058, A2059, A2062 (*E. coli* numbering) of the 23 S ribosomal RNA, essential for macrolide binding, are shown in green, A2451, an important component of the peptidyl transferase centre, is shown in red and C2452 is shown in blue. N3 of A2451 of 23 S RNA is shown in yellow and the proteins L4 and L22 that form part of the tunnel wall are shown in blue and yellow, respectively.

**B.** Josamycin (carbomycin) bound to the *H. marismortui* 50S ribosomal subunit. Carbomycin has been used as a guide for josamycin-ribosome interactions. These compounds have very similar chemical structures and have the same groups (mycaminose, mycarose and isobutyrate residues) approaching the peptidyl transferase centre. The lactone ring is shown in red, the mycaminose and mycarose residues in black and the isobutyrate residue, which approaches the peptidyl transferase center, is shown in magenta.

**C.** Erythromycin, bound to the *D. radiodurans* 50S ribosomal subunit. The desosamine residue of erythromycin is shown in black and the cladinose moiety (not present in ketolides) is shown in magenta.

**D.** ABT 773 in the *D. radiodurans* 50S ribosomal subunit, as a guide to the binding of telithromycin to the ribosome. The desosamine residue of ABT 773 is shown in black and the quinolylallyl group in magenta.

Macrolides prevent ribosomal large subunit formation (Champney and Tober, 1998; Usary and Champney, 2001). According to Champney and Tober, 1998., macrolides bind to the precursors of the large ribosomal subunit and stall ribosome assembly. These stalled assembly intermediates then become substrates for ribonucleases (Usary and Champney, 2001). However, the effect of erythromycin on ribosome assembly might be indirect. Observations made by Siibak et al. (unpublished results) suggest that ribosome can become fully assembled in the presence of the macrolide.

## **1.5. Macrolide Resistance**

The therapeutical utility of macrolides has been severely compromised by the emergence of drug resistance in many pathogenic bacteria (Blondeau et al., 2002; Katz and Klausner, 2008; Richter et al., 2008; Wang et al., 2008).

The known mechanisms of macrolide resistance include modification of 23S ribosomal RNA (methylation or mutation of 23S rRNA bases) (Weisblum, 1995; Vester and Douthwaite, 2001), ribosomal protein mutations (Wittmann et al., 1973; Chittum and Champney, 1994), active efflux of the drug from the cell (Borges-Walmsley et al., 2003), structural modification of macrolides (Ounissi and Courvalin, 1985; Jenkins and Cundliffe, 1991; Chesneau et al., 2007), peptide mediated macrolide resistance (Tenson et al., 1996; Tripathi et al., 1998; Tenson and Mankin, 2001).

### **1.5.1 Methylation of rRNA**

#### *Erm ribosomal RNA methylases*

The synthesis of ribosomal RNA methyltransferases, encoded by *erm* genes, leads to the macrolide resistance (Weisblum et al., 1995a, b).

*Erm* genes are found in a diverse range of pathogenic and drug-producing bacteria (Shivakumar and Dubnau, 1981; Rasmussen et al., 1986; Weisblum et al., 1995a; Douthwaite et al., 2005; Madsen et al., 2005).

All *erm* genes encode methyltransferases that specifically target nucleotide A2058 in 23S rRNA but differ as to whether they monomethylate or dimethylate this nucleotide (Skinner et al., 1983; Weisblum, 1995a). Monomethylation of A2058 confers resistance to erythromycin, but cells remain sensitive to ketolides (telithromycin); dimethylation renders cell resistant to macrolides and ketolides (Douthwaite et al., 2005).

Methylation of A2058 sterically hinders the binding of macrolides to the ribosome (Schlunzen et al., 2001; Tu et al., 2005).

### *Substrate for methylation*

It has been found that fully assembled 50S subunits cannot be methylated (Skinner et al., 1983; Weisblum, 1995a). In the presence of the methyltransferase, the 50S ribosomal subunit precursors serve as a substrate for methylation (Pokkunuri and Champney, 2007).

### *Erm expression*

Expression of Erm methyltransferases can be either constitutive or inducible by low concentrations of macrolides (Weisblum, 1995a, b; Liu and Douthwaite, 2002).

The mechanism of inducible Erm resistance regulation came from the study of ErmC methyltransferase (Weisblum et al., 1971; Dubnau et al., 1984; Mayford and Weisblum, 1989; Weisblum, 1995a). *ErmC* expression is induced by the low concentration of erythromycin. Erythromycin binds to the ribosome and inhibits translation of 19 amino acid peptide encoded by the 141 nucleotide leader sequence of the *ermC* mRNA extending from the transcription initiation site to the methylase initiator methionine codon (Mayford and Weisblum, 1989; Weisblum, 1995b).

The 141 nucleotide *ermC* mRNA leader can take three alternative conformations (Figure 5). When no erythromycin is present the ErmC protein synthesis occurs with a low efficiency because the first two codons of ErmC ORF, as well as ErmC ribosome binding site, are sequestered in the secondary structure, only the leader peptide being synthesized (Figure 5A). When the erythromycin binds to the ribosome, translating ribosome stalls on the *ermC* upstream ORF and induces conformational change in *ermC* mRNA secondary structure. This opens translation initiation region of the ErmC protein coding ORF, allowing the ribosome, free from the macrolide, to start methyltransferase synthesis (Figure 5B). After the concentration of erythromycin decreases and can no longer support induction, the leader region can refold into an inactive conformation, shown in figure 5C. The conformational transition 4B to 5A would also repress *ermC*, but the conformational transition 5B to 5C would be energetically more favored (Mayford and Weisblum, 1989, Weisblum, 1995b). This mechanism has been known as translational attenuation. Although the leader peptide is 19 amino acids long, only the first 9 amino acids (fMGIFSIFVI-) are necessary for induction. Whereas SIFVI amino acids are crucial for the ribosome stalling on the mRNA during leader peptide synthesis in the presence of the erythromycin (Mayford and Weisblum, 1989).

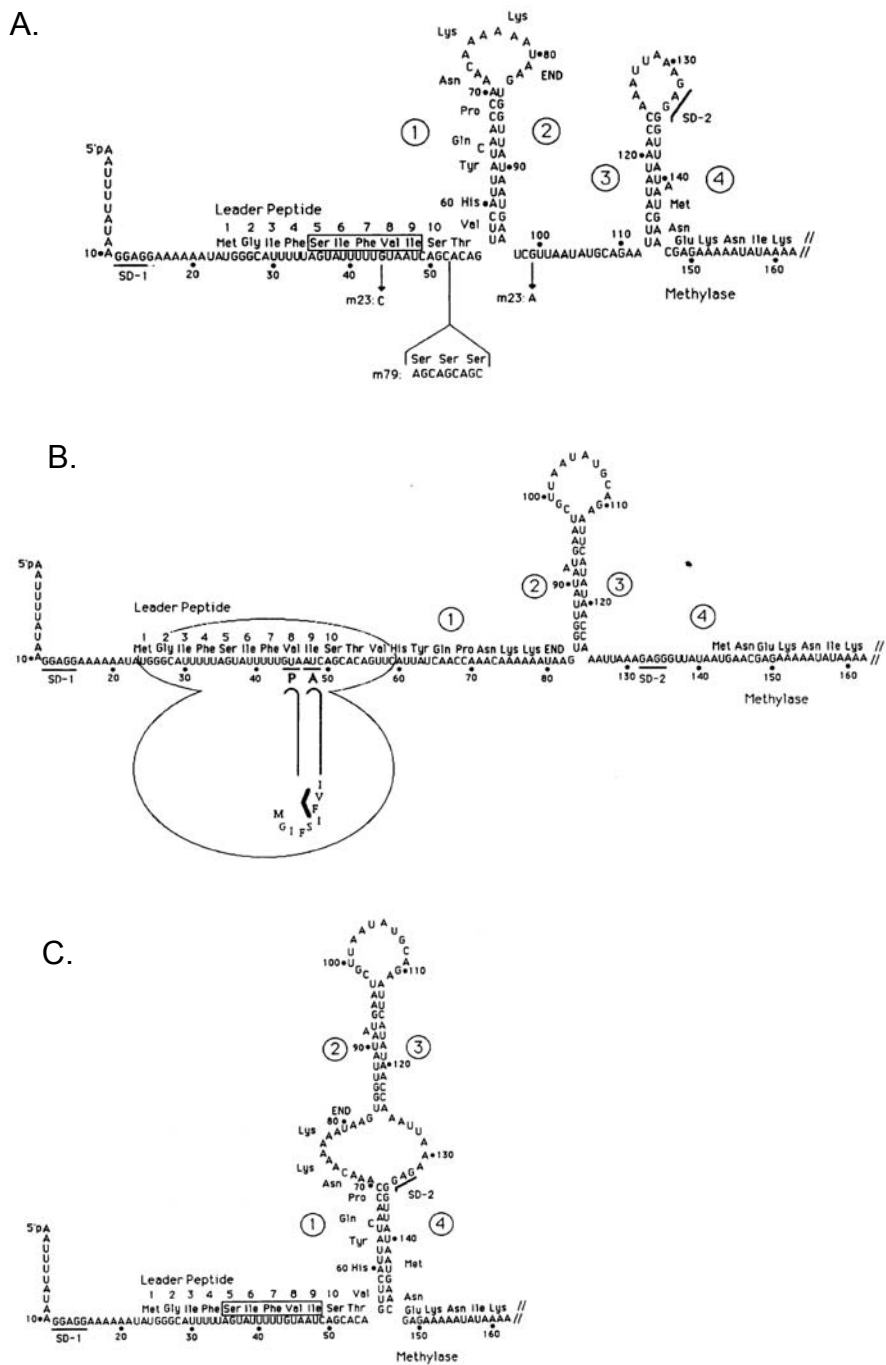


**Figure 5.** Structure of the 5' end of the *ermC* transcript (Adapted from Mayford and Weisblum, 1989)

### *Spread of erm coded resistance*

In Europe and the Far East *erm* genes are responsible for most of the macrolide resistance (Farrell et al., 2004). The resistance caused by rRNA methylation is a more serious threat to human health than other resistance mechanisms. Methylation of the rRNA not only confers higher level erythromycin resistance but simultaneously confers cross-resistance to all other macrolide, lincosamide and streptogramin B classes of antibiotics (Weisblum, 1995b).

### *Methylation of rRNA hairpin 35 in domain II*

Methylation of the nucleotide G745 in gram-negative bacteria 23S rRNA by methyltransferase enzyme RrmA (Rlm<sup>I</sup>) and methylation of the nucleotide G748 in gram-positive bacteria by the methyltransferase enzyme TlrB (Rlm<sup>II</sup>) has been described (Gustafsson and Persson, 1998; Liu et al., 2000; Liu and Douthwaite, 2002a, b). Both G745 and G748 nucleotides are integral components of the narrowest region of the ribosome tunnel, which is the binding site for the macrolides (Schlünzen et al., 2001). Methylation of G745 or G748 nucleotide alone confer very low resistance to the macrolides (Liu and Douthwaite, 2002b).

However, acting together with methylation of A2058, G745 (gram-negative bacteria) or G748 (gram-positive bacteria) methylation confer high resistance to macrolides, especially tylosin and mycinamycin (Liu and Douthwaite, 2002b).

## **1.5.2. Macrolide Resistance Conferred by Base Substitutions in 23S rRNA**

23S rRNA mutations confer macrolide resistance (Vester and Douthwaite, 2001; and references therein). Mutations at A2058, or at A2059 confer the highest levels of resistance. Lower level drug resistance is provided by mutations at positions 2057, 2452, and 2611, which are close in the secondary structure although outside the focal point of macrolide interaction (Douthwaite and Aagaard, 1993). Low-level macrolide resistance is conferred in an *E. coli* laboratory strain by a mutation at position 754 (Xiong et al., 1999).

### *Resistance in pathogenic strains*

This type of resistance is not widely spread in clinical pathogenic bacterial isolates (Farrell et al., 2003; Wierzbowski et al., 2007). Multiplicity of rRNA genes in most microorganisms slows development of this type of resistance (Cundliffe, 1990). rRNA mutations, conferring macrolide resistance, has been usually identified in clinical pathogens possessing only one or two *rrn* operons: *Brachyspira hyodysenteriae*, *Mycoplasma pneumoniae*, *Mycobacterium abscessus*, *Helicobacter pylori*, *Treponema pallidum*, *Chlamydia trachomatis* (Lucier et al., 1995; Versalovic et al., 1996; Vester and Douthwaite, 2001; Misyurina et

al., 2004). However, rRNA mutations, conferring macrolide resistance, have been also reported for clinical pathogenic bacteria isolates with 3 and 4 *rrn* operons: *Streptococcus pneumoniae*, *Streptococcus pyogenes*, *Propionibacterium pneumoniae* (Vester and Douthwaite, 2001; Farrell et al., 2003; Doktor et al., 2004; Wierzbowski et al., 2007).

In bacteria with several copies of the *rrn* operons mutations can be in one or more copies of the gene (Tait-Kramradt et al., 2000; Doktor et al., 2004). The resistance to macrolides when all copies of rRNA genes are mutated is higher (Doktor et al., 2004).

### **1.5.3. Macrolide Resistance Mutations in Ribosomal Proteins L22 and L4**

#### *Characteristics of L4 and L22 proteins*

L4 and L22 proteins are the early assembly proteins of the large subunit and their modifications perturb the assembly of the 50S subunit (Rohl and Nierhaus, 1982; Herold and Nierhaus, 1987; Stelzl et al., 2000). L4 and L22 proteins have globular domains on the surface of the ribosome and long tentacles that extend into the core of the ribosome. L4 and L22 proteins reach the nascent polypeptide chain exit tunnel and form the narrowest cross-section of the exit tunnel entrance.

#### *Role of the exit tunnel gate formed by L4, L22 proteins*

The role of this narrowest cross-section of the exit tunnel (exit tunnel gate) is not understood. It might function as a sensor, recognizing special features of the nascent peptide chain and transmitting message to the peptidyl transferase centre (Nissen et al., 2000), it might provide alternative exits for the nascent peptides (Gabashvili et al., 2001), or it might regulate the protein elongation by stopping or modulating the traffic (Nakatogawa and Ito, 2002; Tenson and Ehrenberg, 2002).

#### *Resistance mutations*

The first isolated *E. coli* L22 mutation is a deletion of three amino acid residues, Met82, Lys83 and Arg84 (Chittum and Champney, 1994). The first isolated *E. coli* L4 mutation is a single amino acid substitution, Lys63Glu (Chittum and Champney, 1994). Mutated amino acid residues are located in the tunnel entrance (Gabashvili et al., 2001; Tu et al., 2005).

Recently, new mutations in *E. coli* L4 and L22 ribosomal proteins, conferring resistance to erythromycin, have been isolated (Zaman et al., 2007). In L4, all mutations mapped within the tentacle. Of the five new missense mutations, four were in the glycine at position 66 and one was in 62th amino acid. Three large insertion mutations after codons 56, 63 and 72 were also identified. Of the L22 mutations, one was in the extended loop of the tentacle (45 bp insertion

after codon 99), while one (6 bp insertion after codon 105) was in the globular domain (Zaman et al., 2007).

#### *Erythromycin sensitive mutation in L4*

It has been reported that heterologous overproduction of L4 protein from *Thermus thermophilus* with Gly55Ser mutation in *E. coli* make bacteria more sensitive to erythromycin (Tsagkalia et al., 2005).

#### *Mechanism of resistance*

Mutations in L4 and L22 confer macrolide resistance due to conformational changes in the structure of the ribosome rather than any direct interaction of the ribosomal proteins with the macrolide (Schlunzen et al., 2001).

Biochemical studies have shown that ribosomes containing the mutant L4 protein no longer bind erythromycin. In contrast, ribosomes carrying the altered L22 protein still bind the antibiotic (Wittmann et al., 1973; Zaman et al., 2007). Cryo-EM reconstructions indicated that the L4 mutant protein causes a narrowing of the entry of the exit tunnel that apparently prevented erythromycin binding while the altered L22 caused a widening of the tunnel that allowed drug binding without inhibiting entry of the nascent peptide into the enlarged tunnel. (Gabashvili et al., 2001; Tu et al., 2005).

#### *Resistance in pathogenic strains*

L4 and L22 mutations conferring resistance to the macrolides have been identified in clinical isolates of bacteria, including *Haemophilus influenzae*, *Streptococcus pyogenes*, *Streptococcus pneumoniae*, *Staphylococcus aureus*. Most of the mutations map to the nascent peptide exit tunnel entrance (Peric et al., 2003; Doktor et al., 2004; Franceschi et al., 2004; Berisio et al., 2006).

### **1.5.4. Macrolide Resistance Conferred by Drug-Efflux Transporters**

One strategy in biological systems that provide resistance to cytotoxic drugs is efflux of these compounds from the cell via membrane proteins, decreasing the intracellular concentration of the drug to subtoxic levels (Piddock, 2006).

The resistance pumps are categorized into families: MF (major facilitator) superfamily, SMR (small multidrug resistance) family, RND (resistance/nodulation/cell division) family, MATE (multidrug and toxic compound efflux) family, ABC (ATP binding cassette) superfamily (Piddock, 2006).

Macrolide resistance is conferred by pumps belonging to MF superfamily, RND family and ABC superfamily (Borges-Walmsley et al., 2003).

### *RND family macrolide efflux pumps*

RND family macrolide efflux pumps include AcrAB-TolC in *Haemophilus influenzae* and *E. coli*, MexAB-OprM in *Pseudomonas aeruginosa*, MtrCDE in *Neisseria gonorrhoeae*, and AmrAB-OprA in *Burkholderia pseudomallei* (Zhong and Shortridge, 2000). In addition to the macrolides these drug resistance pumps can transport a variety of structurally different drugs (Borges-Walmsley et al., 2003).

RND family pumps share a common three-component organization: a transporter located in the inner membrane functions with an outer membrane channel and a periplasmic accessory protein.

### *AcrAB-TolC*

Knowledge about function and structure of RND family pumps comes from the studies on *E. coli* multidrug AcrAB-TolC pump. This pump can eliminate from the cell not only macrolides, but also acriflavin, bile salts, ethidium bromide, fusidic acid and other compounds (reviewed in Borges-Walmsley et al., 2003).

AcrB is an inner membrane protein that interacts with the outer membrane protein TolC. This interaction is transiently coupled by the periplasmic protein AcrA, which anchors to the inner-membrane by a lipid moiety.

All three components are required for efficient transport, because disruption of any of the three genes results in hypersusceptibility of *E. coli* to antibiotics (Okusu et al., 1996; Chollet et al., 2004).

AcrAB-TolC complex is assembled in the absence of known substrates of this pump and no energy is required for the assembly, however, the substrates of the AcrAB-TolC stabilize interactions within the complex (Tikhonova and Zgurskaya, 2004).

AcrB recognizes the substrate and transports drugs by a three-step binding mechanism involving substrate entry, binding and extrusion. This cycling peristaltic-like mechanism pumps drug into the central TolC exit duct (Murakami et al., 2006; Seeger et al., 2006; Sennhauser et al., 2007; Törnroth-Horsefield et al., 2007).

TolC can function as the protein channel for different efflux pumps and can interact with a variety of transporters, only some of which transport antibiotics (for example ErmAB and MacAB of *E. coli*) (Zgurskaya and Nikaido, 2000; Piddock et al., 2006).

### *Macrolide resistance encoded by MF family efflux transporters*

*Mef(A)* and *mef(E)* coded proteins belong to the MF superfamily of efflux pumps (van Bambeke et al., 2000). The macrolide specific efflux system, coded by *mef(A)* and *mef(E)* gene was first described and firmly established in 1996 (Clancy et al., 1996; Sutcliffe et al., 1996). No substrates other than 14- and 15-membered macrolides were identified for efflux pumps coded by these genes (Tait-Kamradt et al., 1997). The coding sequences of these two genes appeared to share 90% identity at the DNA level. The encoded proteins are strongly

hydrophobic, apparent integral membrane proteins with 12 transmembrane segments (Klaassen and Mouton, 2005 and references therein).

Because of the high degree of similarity between the *mef(A)* and the *mef(E)* genes, Roberts et al. (1999) suggested that both genes be referred to as just a single class, *mef(A)*.

The *mef* genes, originally described for gram-positive bacteria, have recently been identified in clinical isolates of gram-negative bacteria (Luna et al., 2000; Ojo et al., 2004; Klaassen and Mouton, 2005). Moreover, *mef(A)* gene was found to be the most frequent gene among macrolide resistance genes identified in gram-negative strains, isolated from healthy children in Portugal (Ojo et al., 2004).

#### *ABC superfamily macrolide efflux pumps*

*Msr(A)* gene expression confers resistance to macrolides: azithromycin, clarithromycin, erythromycin, oleandomycin, as well as doxorubicin. *Msr(A)* gene codes for an ATP transporter that transports erythromycin from the cell using energy from ATP hydrolysis and has been identified in *Staphylococcus*, *Streptococcus*, *Enterococcus*, *Corynebacterium* and *Pseudomonas* isolates (Ojo et al., 2006).

*Msr(A)* homolog *Mel* that confers resistance to macrolides has been recently identified in *Staphylococcus pneumoniae* (Ambrose et al., 2005; Piddock, 2006).

*MacB* gene in *E. coli* codes for ABC superfamily drug efflux pump. *MacB* gene coexpression with peripheral membrane protein MacA and outer membrane channel forming protein TolC confers *E. coli* resistance to macrolides composed of 14- and 15-membered lactones but no or weak resistance against 16-membered ones (Kobayashi et al., 2001).

## **I.6. Resistance Conferred by Structural Modification of Macrolide**

#### *Macrolide phosphorylation*

Resistance by macrolide phosphorylation has been found in *Stenotrophomonas maltophilia*, *Aeromonas hydrophila*, *Pseudomonas aeruginosa* (Alonso et al., 2000; Nakamura et al., 2000; Poole et al., 2006) and in *Staphylococcus aureus* (Matsuoka et al., 1998). Phosphorylation, catalyzed by macrolide 2'-phosphotransferases, is coded by *mph* genes, which phosphorylate 2'OH group of the desosamine sugar of the macrolides (O'Hara et al., 1989).

#### *Macrolide glycosylation*

Macrolides can be modified by glycosylation. *Mgt* gene coding for glycosyltransferase has been found in *Streptomyces* species. Glycosyltransferase

glycosylates 2'OH group of the desosamine sugar of the macrolide (Cundliffe, 1992).

#### *Macrolide esterase*

*E. coli*, *Enterobacter*, *Klebsiella*, *Citrobacter*, *Proteus* species and *Providencia stuartii* can resist macrolides by the production of an erythromycin esterases, coded by *ere* genes, which hydrolyze the lactone ring of the antibiotic (Ounissi and Courvalin, 1985; Arthur et al., 1987; Plante et al., 2003; Ojo et al., 2004)

## **1.7. Peptide Mediated Macrolide Resistance**

The discovery of peptide mediated resistance mechanism came from an observation that overexpression of a short segment of *E. coli* 23S rRNA (positions 1235–1268) rendered cells resistant to erythromycin (Tenson et al., 1996). Mutational and biochemical analyses demonstrated that resistance is caused by translation of a pentapeptide open reading frame, encoded in *E. coli* 23S rRNA. The rRNA encoded pentapeptide is not normally expressed, because the Shine-Dalgarno region of the peptide ORF is sequestered in the 23S rRNA secondary structure. However, peptide expression can be activated by site-specific fragmentation of rRNA or by rRNA mutations that increase accessibility of the Shine-Dalgarno region of the erythromycin resistance peptide ORF (Dam et al., 1996).

The peptide enters the site of its action cotranslationally and acts *in cis*, affecting properties of only that ribosome on which it has been translated (Tenson et al., 1996). Analysis of more than 70 pentapeptides that can confer resistance to erythromycin (E-peptides) revealed a consensus sequence (MXLXV), which could be recognized in the majority of erythromycin resistance peptides and was especially pronounced in the most active erythromycin resistance peptides that could confer very high levels of erythromycin resistance (Tenson et al., 1997).

Peptides that confer resistance to other macrolides have been also described (Tripathi et al., 1998; Tenson and Mankin, 2001).

A mechanism for peptide mediated resistance has been proposed (Tenson et al., 1996; Tripathi et al., 1998; Verdier et al., 2002). A nascent resistance peptide is suggested to remove the macrolide from the ribosome by which it has been synthesized. These peptides act probably as a “bottle brush” that “clean” the ribosome from the bound antibiotic (Tenson et al., 1996; Tripathi et al., 1998; Verdier et al., 2002).

## I.8. The Prevalence of Mechanisms of Macrolide Resistance in Clinical Isolates

The usage of macrolides has led to increased macrolide resistance in clinical isolates. Main mechanisms of the macrolide resistance found in clinical isolates are ribosomal RNA modification and efflux of macrolide. The prevalence of resistance mechanisms in some bacteria has been summarized in tabel 2.

**Table 2.** The prevalence of types of macrolide resistance in clinical isolates.

Bacteria	Rank of prevalence of macrolide resistance mechanisms				Reference
	I	II	III	IV	
<i>Staphylococcus aureus</i>	23S rRNA methylation	Macrolide efflux	Macrolide inactivation		Wang et al., 2008
<i>Streptococcus pneumoniae</i> (Canada, USA)	Macrolide efflux	23S rRNA methylation	Mutations in 23S rRNA	Mutations in L4 and L22	Depardieu and Courvalin, 2001; Blondeau et al., 2002; Doktor et al., 2004; Wierzbowski et al., 2007;
<i>Streptococcus pneumoniae</i> (Europe, Africa)	23S rRNA methylation	Macrolide efflux	Mutations in 23S rRNA	Mutations in L4 and L22	Depardieu and Courvalin, 2001; Blondeau et al., 2002; Doktor et al., 2004; Wolter et al., 2008;
<i>Streptococcus pyogenes</i>	23S rRNA methylation	Macrolide efflux	Mutations in L4 and L22	Mutations in 23S rRNA	Malbruny et al., 2002
<i>Helicobacter pylori</i>	Mutations in 23S rRNA				Furuta et al., 2007
<i>Haemophilus influenzae</i>	Macrolide efflux	Mutations in 23S rRNA	Mutations in L4 and L22		Peric et al., 2004
<i>Neisseria</i> spp.	23S rRNA methylation	Macrolide efflux			Luna et al., 2000; Cousin et al., 2003
<i>Acinetobacter junii</i>	Macrolide efflux				Luna et al., 2000

## 2. RESULTS AND DISCUSSION

### 2.1. Translation Initiation Region Sequence Preferences in *Escherichia Coli*

The mRNA translation initiation region (TIR) comprises the initiator codon, Shine-Dalgarno sequence and translation enhancer. Probably the most abundant class of enhancers contains A/U-rich sequences. We have tested the influence of SD sequence length and the presence of enhancers on the efficiency of translation initiation.

#### 2.1.1. Effect of the Translation Initiation Region on the Level of Protein Synthesis (Reference I)

##### *Design of the model constructs*

Three sets of TIRs were designed and cloned in front of GFP coding reporter gene. Each set contained 10 variants of the SD sequence. The SD variants were constructed by mutating the sequence, forming an 8 base pair duplex with the complementary aSD, and reducing its length from 8 nucleotides to 1. Each set contained a unique sequence upstream of the SD: one contained no translational enhancer, one with a previously described strong A/U rich enhancer, and one with a weak enhancer (Komarova et al., 2002; Reference I).

##### *SD and enhancer*

Irrespective of the enhancer context, protein expression was highest for the 6-nucleotide SD AGGAGG (Reference I). Both shorter and longer SD sequences were less efficient. Shorter SD sequences may be less efficient because binding to ribosome is weaker. Longer SDs, probably, make ribosome mRNA interaction too strong, therefore, it might take more time for the ribosome to leave translation initiation site and proceed with protein elongation (Komarova et al., 2002).

In the absence of enhancer, there were only slight differences between weak and strong SD sequences. When strong enhancer was introduced into the TIR, the differences between the SD sequences were increased greatly. A/U-rich enhancer worked in positive cooperativity with the SD sequence, enhancing the efficiency of selection of the strongest SD sequence and having only a minor effect on the weakest one (Reference I).

##### *Importance of enhancer in translation*

mRNA conformation, not stabilized by interactions with proteins, is labile. The time window when SD is exposed to the ribosome attachment is very short, especially, when TIRs are buried in the stable hairpin structures (de Smit and

van Duin, 2003; Studer and Joseph, 2006). In order to increase the probability of the 30S ribosomal subunit attachment and the initiation of the translation bacterial mRNAs contain standby sites that are used for the primary binding of the small ribosomal subunits in the vicinity of the SD and start codon sequences (de Smit and van Duin, 2003; Studer and Joseph, 2006). This interaction is mediated by the S1 protein on the ribosome and A/U rich sequence on the mRNA (Subramanian, 1983). It was previously speculated that all highly expressed proteins in bacteria possess the A/U rich sequences upstream of the SDs (Komarova et al., 2002). The fact that nearly all protein synthesis in bacteria is S1 protein dependent assists to that proposal (Sorensen et al., 1998).

#### *TIR efficiency in different media*

The efficiency of the TIRs was determined solely by the strength of TIR interaction with the 30S ribosomal subunit and were not influenced by different media, growth rate (Reference I), and overexpression of translation initiation factors (data not shown).

Although, there were quantitative differences in the TIR selection pattern, the ranking order did not change.

#### *Effect of temperature on TIR selection*

The energy of base pairing between two RNA strands depends on the temperature. Therefore, the strength of SD:aSD interaction is temperature dependent. If the free energy of this interaction determines the efficiency of translation then at lower temperature shorter SD:aSD duplexes would be preferred. Alternatively, the SD:aSD interaction might be a trigger for conformational changes in the ribosome. This trigger effect might be temperature independent and it would be rather the helix length that determines the efficiency. In this case it could be similar to the way a codon:anticodon helix is recognized in the A site of the ribosome. To test these possibilities, we measured the TIR preference pattern at 20°C and compared to the data collected at 37°C (Reference I). At 37°C the most efficient SD sequence was AGGAGG ( $\Delta G$  7.7 kcal/mol); at 20°C the GGAGG sequence ( $\Delta G$  9.4 kcal/mol) – with decrease in temperature the optimum shifted to a shorter sequence. This result indicated that the strength of SD:aSD interaction determines the SD efficiency. It also suggested that the length of SD sequence could be used for temperature dependent regulation of gene expression. Unfortunately, we were not able to analyze the length of SD sequences in the known cold shock genes of *E. coli* as the dataset is too small for statistically meaningful conclusions.

#### *Correlation between SD length and predicted expression level*

We have looked for the relationship between the levels of the predicted protein expression by CAI (codon adaptation index) and the free energy changes of the SDs in the *Escherichia coli* (Reference I). The base pairing potential of the SD

sequences did not correlate with the codon adaptation index, which is used as an estimate of gene expression level (Sharp and Li, 1987).

Why do most *E. coli* mRNAs, including those coding for highly expressed genes, have SDs that are not expected to direct the highest level of translation at 37°C? We suggest two possibilities. First, *E. coli* has to grow in the mammalian gut but also to survive at lower temperatures outside the host. The temperatures of both environments may have contributed to the selection of SD sequences. Second, the noise in gene expression levels may be involved. A particular expression level could be achieved by different contributions from transcription and translation. The theoretical calculations have suggested and experimental data confirmed that high level of transcription combined with low level of translation creates considerably smaller fluctuations in gene expression as compared to the situation when the same expression level is achieved by combining low level of transcription with highly efficient translation (Ozdubak et al., 2002; Swain et al., 2002; Raser and O'Shea, 2005). Therefore, using suboptimal TIRs might reduce noise in gene expression.

## **2.2. Peptide Mediated Macrolide Resistance**

Peptide mediated macrolide resistance is a phenomenon where correlations between the structures of nascent peptides and macrolide antibiotics are observed (Tenson et al., 1996; Tenson et al., 1997; Tripathi et al., 1998; Tenson and Mankin, 2001; Reference I).

Purposes of the present studies are

1. to select josamycin resistance peptides
2. to establish spectrum of resistance afforded by resistance peptides
3. to clarify molecular mechanism of peptide mediated resistance
4. to determine role of macrolide efflux in antibiotic resistance

### **2.2.1 Josamycin Resistance Peptides (Reference II)**

Josamycin resistance (JOS) peptides were selected from a five-codon random mini-gene expression library (Tenson et al., 1997). In this library, the plasmid-encoded mini-genes are composed of an initiation codon, four randomized codons and a termination codon. The mini-genes are equipped with a translation initiation sequence and are expressed under the control of the isopropyl-β-D-thiogalactopyranoside inducible  $P_{tac}$  promoter.

All JOS peptides contained an aromatic amino acid, phenylalanine or tyrosine, in the second amino acid position. Amino acid conservation in other positions of josamycin resistance peptides was not observed.

The property of the second amino acid in the JOS peptides appears to be crucial for peptide activity.

### **2.2.2. Peptide Mediated Resistance is Macrolide Specific (Reference II)**

Peptides, conferring resistance to telithromycin, erythromycin, oleandomycin have been described (Tripathi et al., 1998; Tenson and Mankin, 2001; Reference II). The spectrum of resistance caused by KET, ERY, OLE, JOS peptides was examined.

The experimental data showed that peptide mediated resistance is specific. Peptides selected on a particular antibiotic provided the highest level of resistance to this drug. In most cases peptides conferred little or no cross-resistance to other types of macrolides.

### **2.2.3. Classification of Resistance Peptides (Reference II)**

Comparison of all known resistance peptides gives a clear evidence for correlation between the amino acid sequences and the structures of antibiotics they confer resistance (Figure 6).

Peptides with similar consensus amino acid sequences confer resistance to macrolides with similar structure. Significant changes in the structure of macrolide are reflected in significant changes in resistance peptide sequences. If the structural differences between macrolides are only slight then resistance peptides' consensus sequences are identical or very similar.

We classified all known resistance peptides into five structural classes (Table 3).

#### *ERY group peptides*

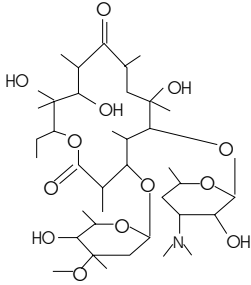
The resistance peptides of the ERY group include those that confer resistance to the erythromycin type macrolides (erythromycin, clarithromycin, roxithromycin and RU69874) (Tenson and Mankin, 2001). Erythromycin type macrolides are 14-membered lactone ring macrolides with L-cladinose at position 3 and desosamine at position 5 of the lactone ring. The peptides are characterized by the presence of Leu or Ile in the third position, the preference of bulky hydrophobic amino acid in the second position and Val in the end of the peptide.

**Table 3.** Classification of resistance peptides into structural groups.

class	representative antibiotics	reference	amino acid position				
			1	2	3	4	5
ERY	erythromycin clarithromycin roxithromycin RU69874	Tenson et al., 1997 Tenson, Mankin, 2001 Tenson, Mankin, 2001 Tenson, Mankin, 2001	Met	bulky hydrophobic	<u>Leu or Ile</u>	hydrophobic	Val
AZI	azithromycin azaerythromycin	Vimberg et al., 2004 Vimberg et al., 2004	Met	bulky hydrophobic	<u>Leu or Ile</u>	<u>Arg or Lys</u>	X
KET	telithromycin RU64399 HMR3004 ABT377	Tenson, Mankin, 2001 Tenson, Mankin, 2001 Tripathi et al., 1998 Vimberg et al., 2004	Met	<u>Arg or Lys</u>	hydrophobic or Arg	hydrophobic or Lys	X
OLE	oleandomycin	Vimberg et al., 2004	Met	X	<u>Arg or Lys</u>	<u>Arg or Lys</u>	Tyr or Ile
JOS	josamycin	this study	Met	<u>Phe or Tyr</u>	X	X	Leu

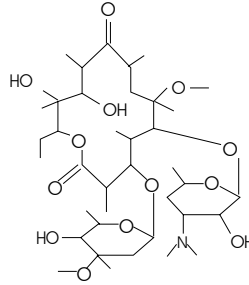
X – no obvious amino acid preference.

**ERYTHROMYCIN**



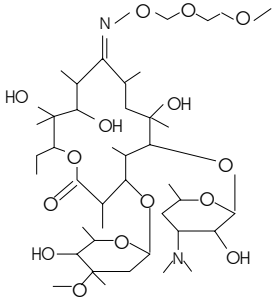
**MLLLV  
MTRLV  
MRLFV  
MVLfV  
MTLKV**

**CLARITHROMYCIN**



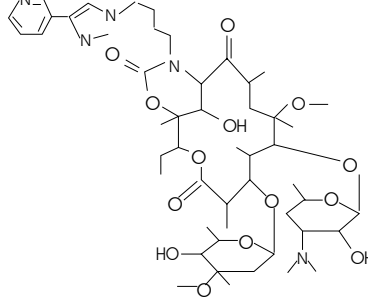
**MLLLV  
MFLWV  
MILRV  
MTLKV  
MLLWV**

**ROXITHROMYCIN**



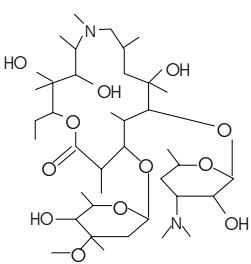
**MVLIV  
MLLIV  
MRLFV  
MPLFV  
MMILV**

**Ru69874**



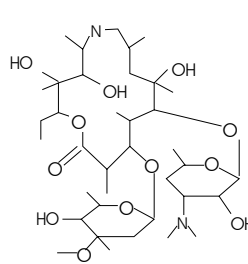
**MVLTV  
MVLmV  
MVLRT  
MVLTT**

**AZITHROMYCIN**



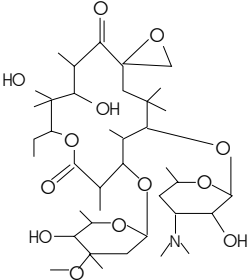
**MLLRV  
MFLKV  
MILMV  
MFLKL  
MLLRT**

**AZAERYTHROMYCIN**



**MLLLV  
MLLFV  
MVLRV  
MTLKV  
MVLWV**

**OLEANDOMYCIN**



**MRKKY  
MPKKN  
MVKL  
MIKRY  
MVRKY**

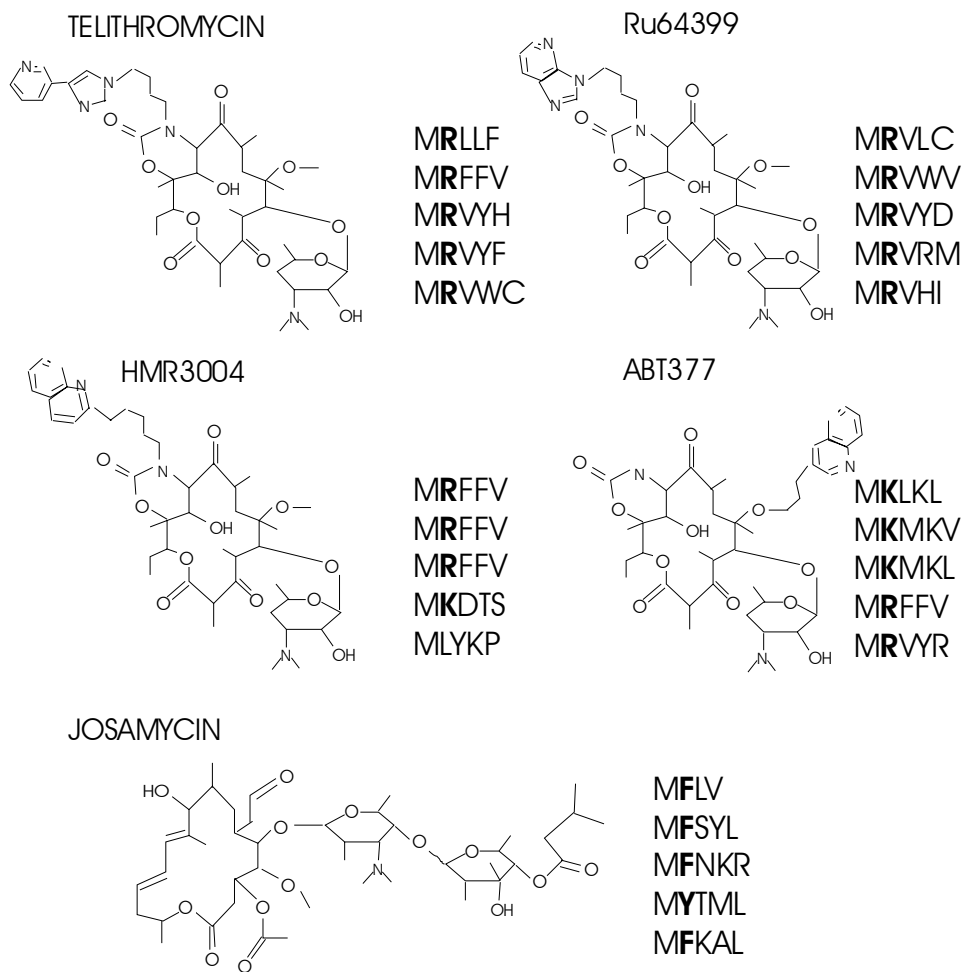


**Figure 6.** Amino acid sequences of the peptides conferring resistance to different macrolides.

### *AZI group peptides*

AZI group peptides confer bacteria resistance to azithromycin and azaerythromycin.

Azithromycin and azaerythromycin are 15-member ring macrolides. Extending the 14-atom lactone ring by an additional nitrogen atom alters the ring conformation resulting in a novel interaction with 23S rRNA base 2586 as seen in the crystallographic complexes of azithromycin with the *Deinococcus radiodurans* ribosome (Schlünzen et al., 2003).

AZI peptides, which include azithromycin and azaerythromycin resistance peptides, are generally similar to ERY peptides. As with the ERY peptides the

AZI peptides contain Leu in the third amino acid position and show preference for a bulky hydrophobic amino acid in the second position (Leu, Ile, Phe, Val). However, in contrast to the ERY peptides, the peptides selected with azithromycin show a strong preference for a positively charged amino acid (Lys or Arg) in the fourth position.

The structural differences between azaerythromycin and azithromycin are minute. Azaerythromycin lacks a single methyl group at the nitrogen atom of the azithromycin azalide ring. This small alteration in drug structure appears to result in reduced requirements for Leu in the third peptide position and for the positively charged amino acid in the fourth position (Reference II).

#### *KET group peptides*

KET group peptides confer resistance to ketolides (telithromycin, RU64399, HMR3004, ABT377).

Ketolides contain keto group at position 3 of the lactone ring and alkyl-aryl side chain, attached to the 11,12-carbamate group on the opposite side of the lactone ring. In the ribosome-bound form of the drugs, the side chain extends towards helix 35 in domain II of 23S rRNA and establishes interactions, which are important both for the high affinity of the ketolide as well as the positioning of the drug molecule in the ribosome (Schlünzen et al., 2003).

The second position in KET peptides is represented predominantly by positively charged amino acids.

The KET peptides show amino acid preference in positions 3 and 4, which are commonly represented by either hydrophobic or positively charged amino acids. It is not clear whether the amino acid preference in third and fourth positions of the peptide is determined by the nature of alkyl-aryl and quinolyl side chains.

#### *OLE group peptides*

Surprisingly, the peptides conferring resistance to oleandomycin, another 14-member ring cladinose-containing macrolide, were substantially different from the ERY peptides. Oleandomycin structurally is similar to erythromycin. None of the oleandomycin resistance peptides had Leu or Ile in the third position; instead a positively charged amino acid was frequently present at position 3 and/or 4 of the peptide. Because of the high content of positively charged amino acids, OLE peptides appear to more closely resemble the KET peptides than the peptides conferring resistance to other 14-member cladinose-containing macrolides.

Oleandomycin differs from erythromycin and related compounds by the presence of an 8-oxirane cycle, a methyl instead of an ethyl group attached at C13 of the lactone ring and the lack of a 12-hydroxyl. Variations in substitutions at C12 and C13 may directly contribute to the unusual binding of oleandomycin. The C13 ethyl of erythromycin reaches towards the loop of helix 35 in domain II of 23S rRNA (Schlünzen et al., 2001). Shortening this side

chain by one carbon atom in oleandomycin may affect possible interaction with this rRNA region. The C12 hydroxyl of erythromycin forms a hydrogen bond with O4 of rRNA residue U2609 (Schlünzen et al., 2001). The lack of this hydroxyl in oleandomycin should destabilize this contact. Interestingly, both helix 35 and U2609 are implicated in specific interactions with ketolides (Hansen et al., 1999; Xiong et al., 1999; Schlünzen et al., 2001; Garza-Ramos et al., 2002; Hansen et al., 2002).

Thus, some of the peculiar contacts of oleandomycin with the ribosome affect the ribosome-drug interactions and make them different in comparison with erythromycin. It is conceivable that the position of oleandomycin in the ribosome may structurally resemble more closely the binding of ketolides than that of the erythromycin-type antibiotics, which can account for the similarity of oleandomycin and ketolide resistance peptides.

#### *JOS group peptides*

Josamycin, a 16-member lactone ring macrolide, contains a mycaminose-mycarose-isobutyrate side chain that, by analogy with carbomycin, is likely to reach into the ribosomal peptidyl transferase centre (Hansen et al., 2002). The drug leaves a fairly small space for the nascent peptide and allows synthesis of di- or tripeptides (Hansen et al., 2002; Lovmar et al., 2004).

JOS peptides' consensus sequence is drastically different from that seen with other macrolides. The second amino acid position in all JOS peptides is occupied by an aromatic amino acid, phenylalanine or tyrosine.

### **2.2.4. Mechanism of Macrolide Displacement from Ribosome**

Drawing clues from the correlation between the amino acid sequences of resistance peptides and the chemical structures of the drugs, one can envision a possible mechanism of drug displacement based on a direct interaction between the macrolide molecule and the peptide.

Structure-specific interaction with the nascent resistance peptide may alter drug conformation resulting in reduced affinity to the ribosome. Although no high-affinity binding between synthetic resistance peptides and antibiotics was observed in solution (Tenson et al., 1996) such interaction may be possible in the ribosome where peptide structure is expected to be constrained by its contacts with the exit tunnel.

#### *ermC leader peptide interaction with erythromycin*

Tu et al. (2005) modelled eight N-terminal amino acids of the *ermC* operon leader peptide bound at the peptidyl transferase centre end of the peptide exit tunnel in the presence of erythromycin. The tunnel is not so occluded by erythromycin that a peptide cannot get past it. The N-terminal residue of an eight

residue long peptide reaches a point in the tunnel that essentially pasts the drug. *ErmC* leader peptide interacts with the erythromycin (Tu et al., 2005). Interaction between SIFV amino acid residues of the *ErmC* leader peptide and the erythromycin occurs (Tu et al., 2005). This is consistent with the fact that SIFVI amino acids are crucial for the ribosome stalling during induction of *ErmC* synthesis by erythromycin (Weisblum, 1995a, b).

#### *ermC leader peptide and ERY peptides*

It is obvious that *ermC* leader peptide's amino acid sequence is quite similar to the amino acid sequence of the ERY peptides, characterized by the presence of valine and isoleucine, and bulky hydrophobic amino acids.

According to the structural model for the mechanism of resistance peptide action proposed by Lovmar et al. (2006), ERY peptides interact with the erythromycin molecule through conserved valine – third amino acid residue of the peptide (Reference III).

#### *Resistance peptides and macrolides*

Alterations in the amino acid sequence of resistance peptides change the spectrum of antibiotics to which the peptide confers resistance. This occurs due to the change in spectrum of interactions the resistance peptides can make with the macrolides.

Based on the correspondence between resistance peptides' sequences and the chemical structures of the macrolides Tripathi et al. (1998) proposed a "bottlebrush" model.

### **2.2.5. Mechanism of Peptide Mediated Erythromycin Resistance (Reference III)**

#### *Erythromycin dissociation*

The length of peptide conferring resistance to erythromycin is of great importance for the erythromycin dissociation from the ribosome.

In a cell free system the rate constant for erythromycin dissociation increases gradually by a factor of six as the peptide grows from fMet to di- and then to penta-peptide. In addition, when translation termination factor is added, the rate constant for erythromycin release is further enhanced by a factor of two (Reference III).

The resistance peptide shortening or lengthening abolishes erythromycin resistance *in vivo* (Reference IV).

#### *Model of peptide mediated resistance*

Based on the "bottlebrush" model for the erythromycin ejection from the ribosome and biochemical data, the mathematical model for the erythromycin resistance has been constructed (Reference III).

The nascent resistance peptide removes the macrolide from the ribosome by which it has been synthesised. The effect is only contemporary, since the macrolide molecule may bind to the ribosome again. Translation of the resistance peptide increases the pool of the ribosomes free of antibiotic. Consequently, this increases the probability that translating ribosomes pass the critical length of the nascent protein after which the ribosomes become inaccessible to the drug and finish protein synthesis (Andersson and Kurland, 1987; Reference III).

The model accounts for dilution of all compounds due to cell volume growth and for a finite rate of diffusion across the cell membrane and takes into account the efflux pumps, used by *E. coli* to actively transport erythromycin from the membrane and cytoplasm to the growth medium (Figure 7).

The validity of the model simulations has been confirmed by observations from experiments in which the expression level of resistance peptide was varied for bacteria growing in media containing varying concentrations of erythromycin. The increasing expression level of resistance peptide in a bacterial population led to increasing erythromycin resistance until a plateau, specific for each concentration of the erythromycin, was reached.

#### *Resistance peptide coding mRNA concentration*

As measured by real-time PCR, there should be approximately 20 times more copies of resistance peptide coding mRNAs than EF-Tu mRNA to confer the highest level of resistance to the macrolide (Reference III).

The copy number of EF-Tu mRNA, one of the most abundant mRNA in the *Escherichia coli* cells, is approximately 2000 copies per cell (Vimberg and Tenson, unpublished results). This means that it is impossible to confer erythromycin resistance by expressing resistance peptide at the level of bacterial mRNA. The only suitable source for the adequate copy number of ERY peptide coding mRNAs are ribosomal RNA (approximately 17000 molecules per cell) or transcription from a high copy number plasmid (Dennis and Bremer, 1974; Reference III).

This is in a good agreement with the fact that the peptide mediated resistance was first demonstrated for a pentapeptide encoded in *Escherichia coli* 23S rRNA (Tenson et al., 1996).

### **2.2.6. Clinical Significance of Peptide Mediated Resistance**

In the absence of direct evidence for expression of the macrolide resistance peptides in wild-type cells, we can only speculate about their clinical significance.

### *Resistance peptide expression*

Although the expression of erythromycin resistant peptide, coded by 23S rRNA, is impaired, because its' ribosome binding site is sequestered in the rRNA secondary structure (Tenson et al., 1996), expression can be activated by a specific rRNA fragmentation (Tenson et al., 1996). For example, a spontaneous deletion of 12 nucleotides (positions 1219–1230) from the 23S rRNA gene has been described as causing resistance to erythromycin (Douthwaite et al., 1985). The 12 nucleotide deletion could destabilize the rRNA secondary structure that masks ribosome binding site, thus activating peptide's expression and resistance to erythromycin.

It is not clear whether the presence of a functional peptide coding gene in *E. coli* rRNA is a coincidence or a result of evolutionary selection. Nevertheless, many, but not all, prokaryotic 23S rRNA sequences contain a pentapeptide mini-gene at the junction of domains II and III.

### *Resistance mediated by resistance peptide expression in clinical bacteria isolates*

Is it possible that macrolide resistance peptide expression would confer macrolide resistance in clinical isolates?

Maximum observed erythromycin concentration in serum after a single 500 milligram oral dose is 2.37 microgrammes per milliliter (Kroboth et al., 1982).

This concentration is sufficient for inhibition of gram-positive bacteria (Lin et al., 2005; Sunakawa and Farrell, 2007) and some gram-negative bacteria (Blondeau et al., 2002). Macrolides cannot be used for the treatment of an infection with some species of gram-negative bacteria, because bacteria have intrinsic resistance, due to the cell permeability barrier and due to the active macrolide efflux (Walsh, 2003; Piddock, 2006; Reference III).

The only evidence of peptide mediated resistance in bacteria that can be inhibited by erythromycin at concentration present in serum comes from the work of Novikova et al. (2000). Novikova et al. (2000) studied peptide mediated resistance in *Bacillus subtilis*, the model organism to study gram-positive bacteria. For *Bacillus subtilis* the minimal inhibitory concentration of the erythromycin is 0.125 µg/ml (Lin et al., 2005), the concentration 20 times lower than erythromycin concentration in serum after macrolide oral administration (Kroboth et al., 1982). However, erythromycin concentration in the serum is 12 times lower than the erythromycin concentration tolerated by *Bacillus subtilis*, expressing erythromycin resistance peptide (Novikova et al., 2000).

Therefore, it is quite probable that macrolide resistance observed in clinical isolates could be conferred by the macrolide resistance peptide expression.

## 2.2.7. The Mechanisms of Peptide Mediated Erythromycin and Josamycin Resistance Differ (Reference IV)

### *Josamycin resistance dependency on the length of the resistance peptide*

Change in the length of JOS peptides did not affect the peptide's activity. It was enough to code for dipeptide MF in order to provide resistance against josamycin. Termination of translation was not required for the JOS peptide mediated resistance as well (Reference IV).

### *Mechanism of josamycin resistance peptide action*

We propose that expression of the JOS peptides containing phenylalanine in the second position transfer ribosomes containing josamycin into translationally inactive complexes, thus taking those ribosomes away from the protein synthesis system.

There are two arguments that support this hypothesis. First, the main difference between josamycin and erythromycin is that the former has much slower binding and dissociation kinetics than the latter. The rate constant for association of erythromycin to the ribosome is about 30 times larger than the association rate constant for josamycin. The dissociation rate constant for the complex between erythromycin and the ribosome is about 60 times faster than the corresponding parameter for josamycin. These differences in rate constants determine that the average lifetime on the ribosome is 3 hours for josamycin and less than 2 minutes for erythromycin (Lovmar et al., 2004).

Second, josamycin slows down formation of a first peptide bond of a nascent peptide in an amino acid-dependent way and completely inhibits formation of the second or third peptide bond (Lovmar et al., 2004). The formation of fMet-Val-tRNA<sup>Val</sup> in the presence of josamycin is decreased 5-fold. At the same conditions synthesis of fMet-Phe-tRNA<sup>Phe</sup> is decreased 1000-fold (Lovmar et al., 2004).

Taking into consideration these two arguments it is more simple for the cell to remove josamycin containing ribosomes from the translation than to try to brake the very stable ribosome-josamycin complex.

### *Consequences of josamycin binding to ribosome*

Josamycin bound to the ribosome causes the dissociation of di- or tripeptidyl-tRNAs (Lovmar et al., 2004). Increased drop off of the dipeptidyl-tRNAs might decrease the pool of free tRNAs, thus inhibiting bacterial growth (Dincbas et al., 1999). Overexpression of peptidyl-tRNA hydrolase enzyme in *E. coli* conferred low resistance against josamycin, probably, by relieving the effect of free tRNA depletion (Soosar et al., unpublished results). Transferring the ribosomes, containing josamycin, into translationally inactive complexes by translating JOS peptide coding mRNAs would not allow the ribosomes, containing josamycin, to accumulate dipeptidyl-tRNAs in the cell and deplete the pool of the free tRNAs.

In addition to the increased peptidyl-tRNA accumulation, josamycin might impair translation of proteins with phenylalanine in the second position (Table 4). If second codon of mRNA's open reading frame codes for phenylalanine amino acid, ribosome in complex with josamycin stops this mRNA translation and turns into translationally inactive complexes. Impairing of translation of proteins, involved in cell division process (FtsZ), in ribosome formation (L25), in regulation of gene expression (Fis) would stop growth of bacteria (Table 4).

Transferring the ribosomes, containing josamycin, into translationally inactive complexes by translating JOS peptide coding mRNAs would take ribosome-josamycin complexes away from the protein synthesis system and allow translation of proteins with the phenylalanine in the second codon.

**Table 4.** List of *E. coli* genes coding proteins, that contain phenylalanine in the second position of the amino acid sequence.

GENE	FUNCTION	N-SEQUENCE
FtsZ	Cell division GTPase	MFEPMELTND..
Hypothetical protein Z0091		MFRGATLVNL...
SbmA	Possibly envelope protein (fuses permease and ATPase components)	MFKSFFPKPG...
CyoB	Cytochrome O ubiquinol oxidase subunit I (aerobic respiration)	MF GKLSLDAV...
LysR	Putative transcriptional regulator LYSR-type	MFDPETLRTF...
Fes	Enterocholin esterase (transport of cations)	MFEVTFWWRD...
Mip	Aquaporin Z (transport of small molecules)	MFRKLAACEF...
TyrB	Aspartate aminotransferase	MFENITAAPA...
Fis	DNA-binding protein	MFEQRVNSDV...
UmuC	DNA Polymerase IV	MFALCD...
Rnb	Exoribonuclease II (3'-5' degradation)	MFQDNPLLAQ..
RibE	Riboflavin synthase subunit alpha	MFTGIVQGTA...
RplY	50S ribosomal protein L25	MFTINAEVR...
Ffh	GTP-binding export factor (binds to signal sequence, GTP, RNA; transport of large molecules)	MFDNLTDRLS...
EscV	Type III secretion apparatus protein	MFNKVLVGLR...
PrfB	Peptide chain release factor 2	MFEINPVNNR...

### **2.2.8. Antibiotic Efflux in Peptide Mediated Resistance (Reference IV)**

Mathematical modelling of peptide mediated erythromycin resistance predicted the requirement of a fast outflow rate of the drug over the cell membrane to confer resistance (Reference III).

The AcrAB-TolC pump system is the major contributor of erythromycin resistance in gram-negative bacteria (Zhong and Shortridge, 2000).

To validate the model's prediction we have done experiments with wild-type and *tolC* mutant *E. coli* cells, expressing resistance peptide. No resistance was observed in the *tolC* mutant bacteria (Reference IV).

#### *Resistance and erythromycin efflux*

In the case of erythromycin, where expression of a resistance peptide actively removes a bound drug molecule from the ribosome (Reference III), resistance is a consequence of an increased dissociation of erythromycin. According to the mathematical model, such a resistance mechanism is sensitive to the fate of the drug molecule after ejection. It either leaves the cell by passive diffusion over the membrane or is actively transported by efflux pumps or it reassociates to another ribosome (Figure 7).

The value of the rate constant for leaving the cell in relation to the association rate constant of the antibiotic becomes very important. The fast outflow rate for erythromycin resistance mechanism to work is then a requirement. The AcrAB-TolC efflux pump system provides the required high efflux rate.

#### *Josamycin*

Results of the experiment have shown no josamycin resistance in the *tolC* mutant cells, expressing JOS peptide, which resistance mechanism clearly differs from that of erythromycin.

The details of josamycin resistance need to be further clarified experimentally. Since the antibiotic is not actively removed from the ribosome (Lovmar et al., 2004) there is most likely another reason for the absence of resistance in the TolC mutant.

### **2.2.9. Antibiotic Efflux in Erythromycin Resistance Conferred by L22 and L4 Mutations (Reference V)**

The restoration of erythromycin susceptibility in the absence of drug's efflux has been described in *Haemophilus influenzae*, *Campylobacter jejuni* and *Campylobacter coli* L4, L22 erythromycin resistance mutants (Peric et al., 2004; Cagliero et al., 2006). In addition, *Campylobacter jejuni* and *Campy-*

*lobacter coli*, inactivation of CmeABC efflux pump lead to restoration of the susceptibility in 23S rRNA A2057G erythromycin resistance mutants (Cagliero et al., 2005).

We checked if the fast outflow rate of the drug over the cell membrane is important for *E.coli* erythromycin resistance, conferred by L22 and L4 mutations. The erythromycin resistance in *E. coli*, conferred by the L22 and L4 mutations, dissappeared in the  $\Delta tolC$  and  $\Delta acrB$  genetic background (Reference V).

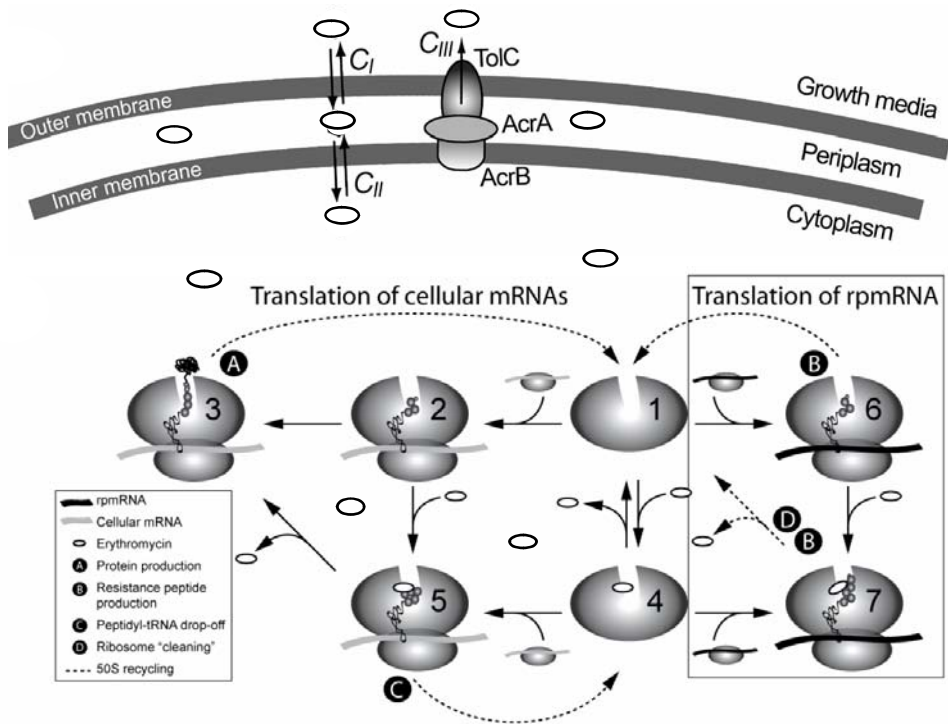


**Figure 7.** Cartoon illustrating the fate of erythromycin

The erythromycin sensitivity for the ribosomal wild-type was greatly increased by  $\Delta acrB$  deletion, but the largest sensitivity was conferred by the  $\Delta tolC$  deletion. We suggest that the erythromycin efflux pump activity is insignificant for the  $\Delta tolC$  strain, and the  $\Delta acrB$  strain retains a small but significant efflux pump activity.

We propose that low macrolide efflux efficiency completely masks the effects of a target resistance mutations that would give a clear fitness advantage at high drug efflux efficiency (References IV, V).

There are no experimental evidences that elimination of macrolides efflux out of the cytosol of gram-positive bacteria, resistant to erythromycin, would restore bacteria erythromycin susceptibility. Taking into account the prediction of the mathematical modelling of erythromycin resistance (References IV, V), that fast rate of erythromycin outflow from cell compared to slow rate of antibiotic association to the ribosome is the requirement for erythromycin resistance mechanism to work, gram-positive bacteria should possess very effective erythromycin efflux pumps to provide high antibiotic efflux rate. Macrolide efflux pumps are well known in gram-positive bacteria, for example *mefA* in *Streptococcus* species. These pumps might be capable of efficient macrolide export from the bacterial cell (Masaoka et al., 2000; Walsh, 2003; Piddock, 2006).

### **2.2.10. Interplay Between Antibiotic Efflux and Resistance Described in Other Studies**

It appears to be a general phenomen that low antibiotic efflux efficiency completely masks the effects of a large set of target resistance mutations.

Resistance to fluoroquinolone family drugs (inhibitors of DNA topoisomerase) often occurs as combination of drug efflux and target site mutations. It has been shown that efflux pump inhibitors reverse acquired fluoroquinolone resistance attributable to DNA topoisomerase mutations, conferring fluoroquinolone resistance (Kriengkauykiat et al., 2005).

## CONCLUSIONS

### *Initiation of translation*

1. Shine-Dalgarno selection preferences are influenced by the growth temperature.
2. Shine-Dalgarno selection preferences are not influenced by the growth rate.
3. The A/U rich enhancers stimulate translation considerably by acting cooperatively with the Shine-Dalgarno sequence.

### *Peptide mediated macrolide resistance*

4. Peptide mediated resistance is macrolide specific. Peptides selected on a particular antibiotic provide the highest level of resistance to this drug.
5. Peptides with similar consensus amino acid sequences confer resistance to macrolides with similar structure. Significant changes in the structure of the macrolide are reflected in significant changes in resistance peptide sequences.
6. The peptide mediated resistance mechanisms against josamycin and erythromycin are different.

### *Macrolides' efflux out of the cell*

7. The fast outflow of the erythromycin is required for the peptide mediated erythromycin resistance mechanism to work. The AcrAB-TolC efflux pump system provides the required high efflux rate in *E. coli*.
8. Low macrolide efflux efficiency masks the effects of the erythromycin resistance, conferred by mutations in the ribosomal proteins L22 and L4.

## REFERENCES

1. **Alonso, A.**, Sanchez, P., Martínez, J. 2000. *Stenotrophomonas maltophilia* D457R contains a cluster of genes from gram-positive bacteria involved in antibiotic and heavy metal resistance. *Antimicrob Agents Chemother.* 44(7):1778–82.
2. **Ambrose, K.**, Nisbet, R., Stephens, D. 2005. Macrolide efflux in *Streptococcus pneumoniae* is mediated by a dual efflux pump (mel and mef) and is erythromycin inducible. *Antimicrob Agents Chemother.* 49(10):4203–9.
3. **Andersson, S.**, Kurland, C. 1987. Elongating ribosomes in vivo are refractory to erythromycin. *Biochimie.* 69(8):901–4.
4. **Aprim, Brion, J.**, Sedallian, A., Le Noc, P., Briffod, J., Micoud, M. 1990. Azithromycin versus josamycin: treatment of 89 cases of acute pneumonia. *Pathol Biol (Paris).* 38(5 ( Pt 2)):521–5.
5. **Arthur, M.**, Brisson-Noel, A., Courvalin, P. 1987. Origin and evolution of genes specifying resistance to macrolide, lincosamide and streptogramin antibiotics: data and hypotheses. *J Antimicrob Chemother.* 20(6):783–802.
6. **Asaka, T.**, Manaka, A., Sugiyama, H. 2003. Recent developments in macrolide antimicrobial research. *Curr Top Med Chem.* 3(9):961–89.
7. **Beringer, M.**, Rodnina, M. 2007. The ribosomal peptidyl transferase. *Mol Cell.* 26(3):311–21.
8. **Berisio, R.**, Harms, J., Schluenzen, F., Zarivach, R., Hansen, H., Fucini, P., Yonath, A. 2003a. Structural insight into the antibiotic action of telithromycin against resistant mutants. *J Bacteriol.* 185(14):4276–9.
9. **Berisio, R.**, Schluenzen, F., Harms, J., Bashan, A., Auerbach, T., Baram, D., Yonath, A. 2003b. Structural insight into the role of the ribosomal tunnel in cellular regulation. *Nat Struct Biol.* 10(5):366–70.
10. **Berisio, R.**, Corti, N., Pfister, P., Yonath, A., Böttger, E. 2006. 23S rRNA 2058A→G alteration mediates ketolide resistance in combination with deletion in L22. *Antimicrob Agents Chemother.* 50(11):3816–23.
11. **Bertho, G.**, Gharbi-Benarous, J., Delaforge, M., Lang, C., Parent, A., Girault, P. 1998. Conformational analysis of ketolide, conformations of RU 004 in solution and bound to bacterial ribosomes. *J Med Chem.* 41(18):3373–86.
12. **Blanchard, S.**, Gonzalez, R., Kim, H., Chu, S., Puglisi, J. 2004. tRNA selection and kinetic proofreading in translation. *Nat Struct Mol Biol.* 11(10):1008–14.
13. **Blondeau, J.**, DeCarolis, E., Metzler, K., Hansen, G. 2002. The macrolides. *Expert Opin. Invest. Drugs* 11(2):189–215.
14. **Boelens, R.**, Gualerzi, C. 2002. Structure and function of bacterial initiation factors. *Curr Protein Pept Sci.* 3(1):107–19.
15. **Boni, I.**, Isaeva, D., Musychenko, M., Tzareva, N. 1991. Ribosome-messenger recognition: mRNA target sites for ribosomal protein S1. *Nucleic Acids Res.* 19(1):155–62.
16. **Borges-Walmsley, M.**, McKeegan, K., Walmsley, A. 2003. Structure and function of efflux pumps that confer resistance to drugs. *Biochem J.* 376(Pt 2):313–38.
17. **Bryskier, A.** 2000. Ketolides-telithromycin, an example of a new class of antibacterial agents. *Clin Microbiol Infect.* 6(12):661–9.
18. **Cagliero, C.**, Mouline, C., Payot, S., Cloeckert, A. 2005. Involvement of the CmeABC efflux pump in the macrolide resistance of *Campylobacter coli*. *J Antimicrob Chemother.* 56(5):948–50.

19. **Cagliero, C.**, Mouline, C., Cloeckaert, A., Payot, S. 2006. Synergy between efflux pump CmeABC and modifications in ribosomal proteins L4 and L22 in conferring macrolide resistance in *Campylobacter jejuni* and *Campylobacter coli*. *Antimicrob Agents Chemother.* 50(11):3893–6.
20. **Champney, W.**, Tober, C. 1998. Inhibition of translation and 50S ribosomal subunit formation in *Staphylococcus aureus* cells by 11 different ketolide antibiotics. *Curr Microbiol.* 37(6):418–25.
21. **Chen, H.**, Bjerknes, M., Kumar, R., Jay, E. 1994. Determination of the optimal aligned spacing between the Shine-Dalgarno sequence and the translation initiation codon of *Escherichia coli* mRNAs. *Nucleic Acids Res.* 22(23):4953–7.
22. **Chesneau, O.**, Tsvetkova, K., Courvalin, P. 2007. Resistance phenotypes conferred by macrolide phosphotransferases. *FEMS Microbiol Lett.* 269(2):317–22.
23. **Chollet, R.**, Chevalier, J., Bryskier, A., Pagès, J. 2004. The AcrAB-TolC pump is involved in macrolide resistance but not in telithromycin efflux in *Enterobacter aerogenes* and *Escherichia coli*. *Antimicrob Agents Chemother.* 48(9):3621–4.
24. **Chittum, H.**, Champney, W. 1994. Ribosomal protein gene sequence changes in erythromycin-resistant mutants of *Escherichia coli*. *J Bacteriol.* 176(20):6192–8.
25. **Clancy, J.**, Petitpas, J., Dib-Hajj, F., Yuan, W., Cronan, M., Kamath, A., Bergeron, J., Retsema, J. 1996. Molecular cloning and functional analysis of a novel macrolide-resistance determinant, *mefA*, from *Streptococcus pyogenes*. *Mol Microbiol.* 22(5):867–79.
26. **Cocito, C.**, Di Giambattista, M., Nyssen, E., Vannuffel, P. 1997. Inhibition of protein synthesis by streptogramins and related antibiotics. *J Antimicrob Chemother.* 39 Suppl A:7–13.
27. **Cole, S.**, Bhardwaj, G., Gerlach, J., Mackie, J., Grant, C., Almquist, K., Stewart, A., Kurz, E., Duncan, A., Deeley, R. 1992. Overexpression of a transporter gene in a multidrug-resistant human lung cancer cell line. *Science.* 258(5088):1650–4.
28. **Cousin, S.**, Whittington, W., Roberts, M. 2003. Acquired macrolide resistance genes in pathogenic *Neisseria* spp. isolated between 1940 and 1987. *Antimicrob Agents Chemother.* 47(12):3877–80.
29. **Cundliffe, E.** 1990. Recognition sites for antibiotics within rRNA. *Ribosome: Structure, Function and Evolution.* Washington, DC: American Society for Microbiology.
30. **Cundliffe, E.** 1992. Glycosylation of macrolide antibiotics in extracts of *Streptomyces lividans*. *Antimicrob Agents Chemother.* 36(2):348–52.
31. **Dam, M.**, Douthwaite, S., Tenson, T., Mankin, A. 1996. Mutations in domain II of 23S rRNA facilitate translation of a 23S rRNA-encoded pentapeptide conferring erythromycin resistance. *J Mol Biol.* 259(1):1–6.
32. **Daviter, T.**, Gromadski, K., Rodnina, M. 2006. The ribosome's response to codon-anticodon mismatches. *Biochimie.* 88(8):1001–11.
33. **Dennis, P.**, Bremer, H. 1974. Differential rate of ribosomal protein synthesis in *Escherichia coli* B/r. *J Mol Biol.* 84(3):407–22.
34. **Depardieu, F.**, Courvalin, P. 2001. Mutation in 23S rRNA responsible for resistance to 16-membered macrolides and streptogramins in *Streptococcus pneumoniae*. *Antimicrob Agents Chemother.* 45(1):319–23.
35. **de Smit, M.**, van Duin, J. 2003. Translational standby sites: how ribosomes may deal with the rapid folding kinetics of mRNA. *J Mol Biol.* 331(4):737–43.

36. **Dincbas, V.**, Heurgue-Hamard, V., Buckingham, R.H., Karimi, R., Ehrenberg, M. 1999. Shutdown in protein synthesis due to the expression of mini-genes in bacteria. *J Mol Biol* 291(4):745–59.
37. **Dinos, G.**, Michelinaki, M., Kalpaxis, D. 2001. Insights into the mechanism of azithromycin interaction with an *Escherichia coli* functional ribosomal complex. *Mol. Pharmacol.* 59:1441–45.
38. **Doktor, S.**, Shortridge, V., Beyer, J., Flamm, R. 2004. Epidemiology of macrolide and/or lincosamide resistant *Streptococcus pneumoniae* clinical isolates with ribosomal mutations. *Diagn Microbiol Infect Dis.* 49(1):47–52.
39. **Douthwaite, S.**, Prince, J., Noller, H. 1985. Evidence for functional interaction between domains II and V of 23S ribosomal RNA from an erythromycin-resistant mutant. *Proc Natl Acad Sci U S A.* 82(24):8330–4.
40. **Douthwaite, S.** 1992. Interaction of the antibiotics clindamycin and lincomycin with *Escherichia coli* 23S ribosomal RNA. *Nucleic Acids Res.* 20(18):4717–20.
41. **Douthwaite, S.**, Aagaard, C. 1993. Erythromycin binding is reduced in ribosomes with conformational alterations in the 23 S rRNA peptidyl transferase loop. *J Mol Biol.* 232(3):725–31.
42. **Douthwaite, S.**, Hansen, L., Mauvais, P. 2000. Macrolide-ketolide inhibition of MLS-resistant ribosomes is improved by alternative drug interaction with domain II of 23S rRNA. *Mol Microbiol.* 36(1):183–93.
43. **Douthwaite, S.** 2001. Structure-activity relationships of ketolides vs. macrolides. *Clin Microbiol Infect.* 3:11–7.
44. **Douthwaite, S.**, Crain, P., Liu, M., Poehlsgaard, J. 2004. The tylosin-resistance methyltransferase RlmA(II) (TlrB) modifies the N-1 position of 23S rRNA nucleotide G748. *J Mol Biol.* 337(5):1073–7.
45. **Douthwaite, S.**, Jalava, J., Jakobsen, L. 2005. Ketolide resistance in *Streptococcus pyogenes* correlates with the degree of rRNA dimethylation by Erm. *Mol Microbiol.* 58(2):613–22.
46. **Dubnau, D.** 1984. Translational attenuation: the regulation of bacterial resistance to the macrolide-lincosamide-streptogramin B antibiotics. *CRC Crit Rev Biochem.* 16(2):103–32.
47. **Farrell, D.**, Douthwaite, S., Morrissey, I., Bakker, S., Poehlsgaard, J., Jakobsen, L., Felmingham, D. 2003. Macrolide resistance by ribosomal mutation in clinical isolates of *Streptococcus pneumoniae* from the PROTEKT 1999–2000 study. *Antimicrob Agents Chemother.* 47(6):1777–83.
48. **Farrell, D.**, Morrissey, I., Bakker, S., Morris, L., Buckridge, S., Felmingham, D. 2004. Molecular epidemiology of multiresistant *Streptococcus pneumoniae* with both erm(B)- and mef(A)-mediated macrolide resistance. *J Clin Microbiol.* 42(2):764–8.
49. **Franceschi, F.**, Kanyo, Z., Sherer, E., Sutcliffe, J. 2004. Macrolide resistance from the ribosome perspective. *Curr Drug Targets Infect Disord.* 4(3):177–91.
50. **Frank, J.**, Gao, H., Sengupta, J., Gao, N., Taylor, D. 2007. The process of mRNA-tRNA translocation. *Proc Natl Acad Sci U S A.* 104(50):19671–8.
51. **Fraschini, F.** 1990. Clinical efficacy and tolerance of two new macrolides, clarithromycin and josamycin, in the treatment of patients with acute exacerbations of chronic bronchitis. *J Int Med Res.* 18(2):171–6.
52. **Furuta, T.**, Soya, Y., Sugimoto, M., Shirai, N., Nakamura, A., Kodaira, C., Nishino, M., Okuda, M., Okimoto, T., Murakami, K., Fujioka, T., Hishida, A.

2007. Modified allele-specific primer-polymerase chain reaction method for analysis of susceptibility of *Helicobacter pylori* strains to clarithromycin. *J Gastroenterol Hepatol.* 22(11):1810–5.
53. **Gabashvili, I.**, Gregory, S., Valle, M., Grassucci, R., Worbs, M., Wahl, M., Dahlberg, E., Frank, J. 2001. The polypeptide tunnel system in the ribosome and its gating in erythromycin resistance mutants of L4 and L22. *Mol Cell.* 8(1):181–8.
  54. **Garza-Ramos, G.**, Xiong, L., Zhong, P., Mankin, A. 2002. Binding site of macrolide antibiotics on the ribosome: new resistance mutation identifies a specific interaction of ketolides with rRNA. *J Bacteriol.* 183(23):6898–907.
  55. **Geigenmüller, U.**, Nierhaus, K. 1986. Tetracycline can inhibit tRNA binding to the ribosomal P site as well as to the A site. *Eur J Biochem.* 161(3):723–6.
  56. **Gibreel, A.**, Kos, V., Keelan, M., Trieber, C., Levesque, S., Michaud, S., Taylor, D. 2005. Macrolide resistance in *Campylobacter jejuni* and *Campylobacter coli*: molecular mechanism and stability of the resistance phenotype. *Antimicrob Agents Chemother.* 49(7):2753–9.
  57. **Gottesman, M.**, Ling, V. 2006. The molecular basis of multidrug resistance in cancer: the early years of P-glycoprotein research. *FEBS Lett.* 580(4):998–1009.
  58. **Gustafsson, C.**, Persson, B. 1998. Identification of the *rrmA* gene encoding the 23S rRNA m1G745 methyltransferase in *Escherichia coli* and characterization of an m1G745-deficient mutant. *J Bacteriol.* 180(2):359–65.
  59. **Gualerzi, C.**, Pon, C. 1990. Initiation of mRNA translation in prokaryotes. *Biochemistry.* 29(25):5881–9.
  60. **Gren, E.** 1984. Recognition of messenger RNA during translational initiation in *Escherichia coli*. *Biochimie.* 66(1):1–29.
  61. **Hansen, L.**, Mauvais, P., Douthwaite, S. 1999. The macrolide-ketolide antibiotic binding site is formed by structures in domains II and V of 23S ribosomal RNA. *Mol Microbiol.* 31(2):623–31.
  62. **Hansen, J.**, Ippolito, J., Ban, N., Nissen, P., Moore, P., Steitz, T. 2002. The structures of four macrolide antibiotics bound to the large ribosomal subunit. *Mol Cell* 10:117–128.
  63. **Hansen, J.**, Moore, P., Steitz, T. 2003. Structures of five antibiotics bound at the peptidyl transferase center of the large ribosomal subunit. *J Mol Biol.* 2003 330(5):1061–75.
  64. **Herold, M.**, Nierhaus, K. 1987. Incorporation of six additional proteins to complete the assembly map of the 50S subunit from *Escherichia coli* ribosomes. *J Biol Chem.* 262(18):8826–33.
  65. **Heurgue-Hamard, V.**, Mora, L., Guarneros, G., Buckingham, R. 1996. The growth defect in *Escherichia coli* deficient in peptidyl-tRNA hydrolase is due to starvation for Lys-tRNA(Lys). *EMBO J.* 15(11):2826–33.
  66. **Heurgue-Hamard, V.**, Dincbas, V., Buckingham, R.H., Ehrenberg, M. 2000. Origins of minigene-dependent growth inhibition in bacterial cells. *EMBO J* 19(11):2701–9.
  67. **Jenkins, G.**, Cundliffe, E. 1991. Cloning and characterization of two genes from *Streptomyces lividans* that confer inducible resistance to lincomycin and macrolide antibiotics. *Gene.* 108(1):55–62.
  68. **Kallia-Raftopoulos, S.**, Kalpaxis, D., Coutsogeorgopoulos, C. 1994. New aspects of the kinetics of inhibition by lincomycin of peptide bond formation. *Mol Pharmacol.* 46(5):1009–14.

69. **Karimi, R.**, Pavlov, M., Buckingham, R., Ehrenberg, M. 1999. Novel roles for classical factors at the interface between translation termination and initiation. *Mol Cell.* 3(5):601–9.
70. **Katz, K.**, Klausner, J. 2008. Azithromycin resistance in *Treponema pallidum*. *Curr Opin Infect Dis.* 21(1):83–91.
71. **Kirillov, S.**, Porse, B., Vester, B., Woolley, P., Garrett, R. 1997. Movement of the 3'-end of tRNA through the peptidyl transferase centre and its inhibition by antibiotics. *FEBS Lett.* 406(3):223–33.
72. **Kisselev, L.**, Buckingham, R. 2000. Translational termination comes of age. *Trends Biochem Sci.* 25(11):561–6.
73. **Kitakawa, M.**, Isono, K. 1982. An amber mutation in the gene *rpsA* for ribosomal protein S1 in *Escherichia coli*. *Mol Gen Genet.* 185(3):445–7.
74. **Klaassen, C.**, Mouton, J. 2005. Molecular detection of the macrolide efflux gene: to discriminate or not to discriminate between *mef(A)* and *mef(E)*. *Antimicrob Agents Chemother.* 49(4):1271–8.
75. **Kobayashi, N.**, Nishino, K., Yamaguchi, A. 2001. Novel macrolide-specific ABC-type efflux transporter in *Escherichia coli*. *J Bacteriol.* 183(19):5639–44.
76. **Komarova, A.**, Tchufistova, L., Supina, E., Boni, I. 2002. Protein S1 counteracts the inhibitory effect of the extended Shine-Dalgarno sequence on translation. *RNA.* 8(9):1137–47.
77. **Kriengkauykiat, J.**, Porter, E., Lomovskaya, O., Wong-Beringer, A. 2005. Use of an efflux pump inhibitor to determine the prevalence of efflux pump-mediated fluoroquinolone resistance and multidrug resistance in *Pseudomonas aeruginosa*. *Antimicrob Agents Chemother.* 49(2):565–70.
78. **Kroboth, P.**, Brown, A., Lyon, J., Kroboth, F., Juhl, R. 1982. Pharmacokinetics of single-dose erythromycin in normal and alcoholic liver disease subjects. *Antimicrob Agents Chemother.* 21(1):135–40.
79. **Lee, K.**, Holland-Staley, C., Cunningham, P. 1996. Genetic analysis of the Shine-Dalgarno interaction: selection of alternative functional mRNA-rRNA combinations. *RNA.* 2(12):1270–85.
80. **Leontiou, C.**, Lakey, J., Austin, C. 2004. Mutation E522K in human DNA topoisomerase II $\beta$  confers resistance to methyl N-(4'-(9-acridinylamino)-phenyl)carbamate hydrochloride and methyl N-(4'-(9-acridinylamino)-3-methoxyphenyl) methane sulfonamide but hypersensitivity to etoposide. *Mol Pharmacol.* 66(3):430–9.
81. **Lin, J.**, Connelly, M., Amolo, C., Otani, S., Yaver, D. 2005. Global transcriptional response of *Bacillus subtilis* to treatment with subinhibitory concentrations of antibiotics that inhibit protein synthesis. *Antimicrob Agents Chemother.* 49(5):1915–26.
82. **Liu, M.**, Kirpekar, F., Van Wezel, G., Douthwaite, S. 2000. The tylosin resistance gene *tlrB* of *Streptomyces fradiae* encodes a methyltransferase that targets G748 in 23S rRNA. *Mol Microbiol.* 37(4):811–20.
83. **Liu, M.**, Douthwaite, S. 2002a. Methylation at nucleotide G745 or G748 in 23S rRNA distinguishes Gram-negative from Gram-positive bacteria. *Mol Microbiol.* 44(1):195–204.
84. **Liu, M.**, Douthwaite, S. 2002b. Resistance to the macrolide antibiotic tylosin is conferred by single methylations at 23S rRNA nucleotides G748 and A2058 acting in synergy. *Proc Natl Acad Sci U S A.* 99(23):14658–63.

85. **Lovmar, M.**, Tenson, T., Ehrenberg, M. 2004. Kinetics of macrolide action: the josamycin and erythromycin cases. *J Biol Chem.* 279(51):53506–15.
86. **Lucier, T.**, Heitzman, K., Liu, S., Hu, P. 1995. Transition mutations in the 23S rRNA of erythromycin-resistant isolates of *Mycoplasma pneumoniae*. *Antimicrob Agents Chemother.* 39(12):2770–3.
87. **Luna, V.**, Cousin, S., Whittington, W., Roberts, M. 2000. Identification of the conjugative *mef* gene in clinical *Acinetobacter junii* and *Neisseria gonorrhoeae* isolates. *Antimicrob Agents Chemother.* 44(9):2503–6.
88. **Madsen, C.**, Jakobsen, L., Douthwaite, S. 2005. *Mycobacterium smegmatis* Erm(38) is a reluctant dimethyltransferase. *Antimicrob Agents Chemother.* 49(9):3803–9.
89. **Malbruny, B.**, Nagai, K., Coquemont, M., Bozdogan, B., Andrasevic, A., Hupkova, H., Leclercq, R., Appelbaum, P. 2002. Resistance to macrolides in clinical isolates of *Streptococcus pyogenes* due to ribosomal mutations. *J Antimicrob Chemother.* 49(6):935–9.
90. **Márquez, V.**, Wilson, D., Nierhaus, K. 2002. Functions and interplay of the tRNA-binding sites of the ribosome. *Biochem Soc Trans.* 30(2):133–40.
91. **Masaoka, Y.**, Ueno, Y., Morita, Y., Kuroda, T., Mizushima, T., Tsuchiya, T. 2000. A two-component multidrug efflux pump, EbrAB, in *Bacillus subtilis*. *J Bacteriol.* 182(8):2307–10.
92. **Matsuoka, M.**, Endou, K., Kobayashi, H., Inoue, M., Nakajima, Y. 1998. A plasmid that encodes three genes for resistance to macrolide antibiotics in *Staphylococcus aureus*. *FEMS Microbiol Lett.* 167(2):221–7.
93. **Mayford, M.**, Weisblum, B. 1989. Conformational alterations in the *ermC* transcript in vivo during induction. *EMBO J.* 8(13):4307–14.
94. **Mayford, M.**, Weisblum, B. 1989. *ermC* leader peptide. Amino acid sequence critical for induction by translational attenuation. *J Mol Biol.* 206(1):69–79.
95. **Menninger, J.** 1979. Accumulation of peptidyl tRNA is lethal to *Escherichia coli*. *J Bacteriol.* 137(1):694–6.
96. **Menninger, J.**, Otto, D. 1982. Erythromycin, carbomycin, and spiramycin inhibit protein synthesis by stimulating the dissociation of peptidyl-tRNA from ribosomes. *Antimicrob Agents Chemother.* 21(5):811–8.
97. **Misyurina, O.**, Chipitsyna, E., Finashutina, Y., Lazarev, V., Akopian, T., Savicheva, A., Govorun, V. 2004. Mutations in a 23S rRNA gene of *Chlamydia trachomatis* associated with resistance to macrolides. *Antimicrob Agents Chemother.* 48(4):1347–9.
98. **Moazed, D.**, Noller, H. 1987. Interaction of antibiotics with functional sites in 16S ribosomal RNA. *Nature.* 327(6121):389–94.
99. **Murakami, S.**, Nakashima, R., Yamashita, E., Matsumoto, T., Yamaguchi, A. 2006. Crystal structures of a multidrug transporter reveal a functionally rotating mechanism. *Nature.* 443(7108):173–9.
100. **Nakamura, A.**, Miyakozawa, I., Nakazawa, K., O-Hara, K., Sawai, T. 2000. Detection and characterization of a macrolide 2'-phosphotransferase from a *Pseudomonas aeruginosa* clinical isolate. *Antimicrob Agents Chemother.* 44(11):3241–2.
101. **Nakatogawa, H.**, Ito, K. 2002. The ribosomal exit tunnel functions as a discriminating gate. *Cell.* 108(5):629–36.

102. **Nascimento, A.**, Goldman, G., Park, S., Marras, S., Delmas, G., Oza, U., Lolans, K., Dudley, M., Mann, P., Perlin, D. 2003. Multiple resistance mechanisms among *Aspergillus fumigatus* mutants with high-level resistance to itraconazole. *Antimicrob Agents Chemother.* 47(5):1719–26.
103. **Nissen, P.**, Hansen, J., Ban, N., Moore, P., Steitz, T. 2000. The structural basis of ribosome activity in peptide bond synthesis. *Science.* 289:920–930.
104. **Novikova, S.**, Bushueva, A., Trachuk, L., Konstantinova, G., Serkina, A., Hoischen, C., Gumpert, J., Chestukhina, G., Mankin, A., Shevelev, A. 2000. Introduction of a mini-gene encoding a five-amino acid peptide confers erythromycin resistance on *Bacillus subtilis* and provides temporary erythromycin protection in *Proteus mirabilis*. *FEMS Microbiol Lett.* 182(2):213–8.
105. **Ogle, J.**, Ramakrishnan, V. 2005. Structural insights into translational fidelity. *Annu Rev Biochem.* 74:129–77.
106. **O'Hara, K.**, Kanda, T., Ohmiya, K., Ebisu, T., Kono, M. 1989. Purification and characterization of macrolide 2'-phosphotransferase from a strain of *Escherichia coli* that is highly resistant to erythromycin. *Antimicrob Agents Chemother.* 33(8):1354–7.
107. **Ojo, K.**, Ulep, C., Van Kirk, N., Luis, H., Bernardo, M., Leitao, J., Roberts, M. 2004. The *mef(A)* gene predominates among seven macrolide resistance genes identified in gram-negative strains representing 13 genera, isolated from healthy Portuguese children. *Antimicrob Agents Chemother.* 48(9):3451–6.
108. **Ojo, K.**, Striplin, M., Ulep, C., Close, N., Zittle, J., Luis, H., Bernardo, M., Leitao, J., Roberts, M. 2006. *Staphylococcus* efflux *msr(A)* gene characterized in *Streptococcus*, *Enterococcus*, *Corynebacterium*, and *Pseudomonas* isolates. *Antimicrob Agents Chemother.* 50(3):1089–91.
109. **Okusu, H.**, Ma, D., Nikaido, H. 1996. AcrAB efflux pump plays a major role in the antibiotic resistance phenotype of *Escherichia coli* multiple-antibiotic-resistance (Mar) mutants. *J Bacteriol.* 178(1):306–8.
110. **Ounissi, H.**, Courvalin, P. 1985. Nucleotide sequence of the gene *ereA* encoding the erythromycin esterase in *Escherichia coli*. *Gene.* 35(3):271–8.
111. **Ozubudak, E.**, Thattai, M., Kurtser, I., Grossman, A., van Oudenaarden, A. 2002. Regulation of noise in the expression of a single gene. *Nat Genet.* 31(1):69–73.
112. **Parmeggiani, A.**, Swart, G. 1985. Mechanism of action of kirromycin-like antibiotics. *Annu Rev Microbiol.* 39:557–77.
113. **Peric, M.**, Bozdogan, B., Jacobs, M., Appelbaum, P. 2003. Effects of an efflux mechanism and ribosomal mutations on macrolide susceptibility of *Haemophilus influenzae* clinical isolates. *Antimicrob Agents Chemother.* 47(3):1017–22.
114. **Peric, M.**, Bozdogan, B., Galderisi, C., Krissinger, D., Rager, T., Appelbaum, P. 2004. Inability of L22 ribosomal protein alteration to increase macrolide MICs in the absence of efflux mechanism in *Haemophilus influenzae* HMC-S. *J Antimicrob Chemother.* 54(2):393–400.
115. **Periti, P.**, Mazzei, T., Mini, E., Novelli, A. 1993. Adverse effects of macrolide antibacterials. *Drug Saf.* 9(5):346–64.
116. **Pestka, S.** 1977. Inhibitors of Protein Synthesis. *Molecular Mechanisms of Protein Biosynthesis.* Academic Press, New York, San Francisco, London.
117. **Piddock, L.** 2006. Multidrug-resistance efflux pumps – not just for resistance. *Nat Rev Microbiol.* 4(8):629–36.

118. **Plante, I.,** Centrón, D., Roy, PH. 2003. An integron cassette encoding erythromycin esterase, *ere(A)*, from *Providencia stuartii*. *J Antimicrob Chemother.* 51(4):787–90.
119. **Pokkunuri, I.,** Champney, W. 2007. Characteristics of a 50S Ribosomal Subunit Precursor Particle as a Substrate for *ermE* Methyltransferase Activity and Erythromycin Binding in *Staphylococcus aureus*. *RNA Biol.* 4(3).
120. **Poole, T.,** Callaway, T., Bischoff, K., Warnes, C., Nisbet, D. 2006. Macrolide inactivation gene cluster *mphA-mrx-mphR* adjacent to a class I integron in *Aeromonas hydrophila* isolated from a diarrhoeic pig in Oklahoma. *J Antimicrob Chemother.* 57(1):31–8.
121. **Poulsen, S.M.,** Kofoed, C., Vester, B. 2000. Inhibition of the ribosomal peptidyl transferase reaction by the mycarose moiety of the antibiotics carbomycin, spiramycin and tylosin. *J Mol Biol.* 304(3):471–81.
122. **Ramakrishnan, V.** 2002. Ribosome structure and the mechanism of translation. *Cell.* 108(4):557–572.
123. **Raser, J.,** O'Shea, E. 2005. Noise in gene expression: origins, consequences, and control. *Science.* 309(5743):2010–3.
124. **Rasmussen, J., Odelson, D., Macrina, F.** 1986. Complete nucleotide sequence and transcription of *ermF*, a macrolide-lincosamide-streptogramin B resistance determinant from *Bacteroides fragilis*. *J Bacteriol.* 168(2):523–33.
125. **Recht, M.,** Douthwaite, S., Puglisi, J. 1999. Basis for prokaryotic specificity of action of aminoglycoside antibiotics. *EMBO J.* 18(11):3133–8.
126. **Rheinberger, H.** 1991. The function of the translating ribosome: allosteric three-site model of elongation. *Biochimie.* 73(7–8):1067–88.
127. **Richter, S.,** Heilmann, K., Dohrn, C., Beekmann, S., Riahi, F., Garcia-de-Lomas, J., Ferech, M., Goossens, H., Doern, G. 2008. Increasing telithromycin resistance among *Streptococcus pyogenes* in Europe. *J Antimicrob Chemother.* 61(3):603–11.
128. **Riska, P.,** Kutlin, A., Ajiboye, P., Cua, A., Roblin, P., Hammerschlag, M. 2004. Genetic and culture-based approaches for detecting macrolide resistance in *Chlamydia pneumoniae*. *Antimicrob Agents Chemother.* 48(9):3586–90.
129. **Roberts, M.,** Sutcliffe, J., Courvalin, P., Jensen, L., Rood, J., Seppala, H. 1999. Nomenclature for macrolide and macrolide-lincosamide-streptogramin B resistance determinants. *Antimicrob Agents Chemother.* 43(12):2823–30.
130. **Rodnina, M.,** Stark, H., Savelsbergh, A., Wieden, H., Mohr, D., Matassova, N., Peske, F., Daviter, T., Gualerzi, C., Wintermeyer, W. 2000. GTPases mechanisms and functions of translation factors on the ribosome. *Biol Chem.* 381(5–6):377–87.
131. **Röhl, R.,** Nierhaus, K. 1982. Assembly map of the large subunit (50S) of *Escherichia coli* ribosomes. *Proc Natl Acad Sci U S A.* 79(3):729–33.
132. **Schlünzen, F.,** Zarivach, R., Harms, J., Bashan, A., Tocilj, A., Albrecht, R., Yonath, A., Franceschi, F. 2001. Structural basis for the interaction of antibiotics with the peptidyl transferase centre in eubacteria. *Nature* 413:814–821.
133. **Schlünzen, F.,** Harms, J., Franceschi, F., Hansen, H., Bartels, H., Zarivach, R., Yonath, A. 2003. Structural basis for the antibiotic activity of ketolides and azalides. *Structure (Camb)* 11:329–338.
134. **Schneider, T.,** Stormo, G., Gold, L., Ehrenfeucht, A. 1986. Information content of binding sites on nucleotide sequences. *J Mol Biol.* 188(3):415–31.

135. **Schurr, T.**, Nadir, E., Margalit, H. 1993. Identification and characterization of *E. coli* ribosomal binding sites by free energy computation. *Nucleic Acids Res.* 21(17):4019–23.
136. **Schuwirth, B.**, Borovinskaya, M., Hau, C., Zhang, W., Vila-Sanjurjo, A., Holton, J., Cate, J. 2005. Structures of the bacterial ribosome at 3.5 Å resolution. *Science.* 310(5749):827–34.
137. **Scolnick, E.**, Tompkins, R., Caskey, T., Nirenberg, M. 1968. Release factors differing in specificity for terminator codons. *Proc Natl Acad Sci U S A.* 61(2):768–74.
138. **Seeger, M.**, Schiefner, A., Eicher, T., Verrey, F., Diederichs, K., Pos, K. 2006. Structural asymmetry of AcrB trimer suggests a peristaltic pump mechanism. *Science.* 313(5791):1295–8.
139. **Selmer, M.**, Dunham, C., Murphy, F. 4th, Weixlbaumer, A., Petry, S., Kelley, A., Weir, J., Ramakrishnan, V. 2006. Structure of the 70S ribosome complexed with mRNA and tRNA. *Science.* 313(5795):1935–42.
140. **Sennhauser, G.**, Amstutz, P., Briand, C., Storchenegger, O., Grütter, M. Drug export pathway of multidrug exporter AcrB revealed by DARPIn inhibitors. *PLoS Biol.* 5(1):e7.
141. **Sharp, P.**, Li, W. 1987. The codon Adaptation Index – a measure of directional synonymous codon usage bias, and its potential applications. *Nucleic Acids Res.* 15(3):1281–95.
142. **Shinabarger, D.**, Marotti, K., Murray, R., Lin, A., Melchior, E., Swaney, S., Donyak, D., Demyan, W., Buysse, J. 1997. Mechanism of action of oxazolidinones: effects of linezolid and eperzolid on translation reactions. *Antimicrob Agents Chemother.* 41(10):2132–6.
143. **Shine, J.**, Dalgarno, L. 1974. The 3'-terminal sequence of *Escherichia coli* 16S ribosomal RNA: complementarity to nonsense triplets and ribosome binding sites. *Proc Natl Acad Sci U S A.* 71(4):1342–6.
144. **Shivakumar, A.**, Dubnau, D. 1981. Characterization of a plasmid-specified ribosome methylase associated with macrolide resistance. *Nucleic Acids Res.* 9(11):2549–62.
145. **Shultzaberger, R.**, Bucheimer, R., Rudd, K., Schneider, T. 2001. Anatomy of *Escherichia coli* ribosome binding sites. *J Mol Biol.* 313(1):215–28.
146. **Skinner, R.**, Cundliffe, E., Schmidt, F. 1983. Site of action of a ribosomal RNA methylase responsible for resistance to erythromycin and other antibiotics. *J Biol Chem.* 258(20):12702–6.
147. **Sørensen, M.**, Fricke, J., Pedersen, S. 1998. Ribosomal protein S1 is required for translation of most, if not all, natural mRNAs in *Escherichia coli* in vivo. *J Mol Biol.* 280(4):561–9.
148. **Spahn, C.**, Prescott, C. 1996. Throwing a spanner in the works: antibiotics and the translation apparatus. *J Mol Med.* 74(8):423–39.
149. **Steitz, T.** 2008. A structural understanding of the dynamic ribosome machine. *Nat Rev Mol Cell Biol.* 9(3):242–53.
150. **Stelzl, U.**, Spahn, C., Nierhaus, K. 2000. Selecting rRNA binding sites for the ribosomal proteins L4 and L6 from randomly fragmented rRNA: application of a method called SERF. *Proc Natl Acad Sci U S A.* 97(9):4597–602.

151. **Stenström, C.**, Isaksson, L. 2002. Influences on translation initiation and early elongation by the messenger RNA region flanking the initiation codon at the 3' side. *Gene*. 288(1–2):1–8.
152. **Stormo, G.**, Schneider, T., Gold, L. 1982. Characterization of translational initiation sites in *E. coli*. *Nucleic Acids Res*. 10(9):2971–96.
153. **Strausbaugh, L.**, Bolton, W., Dilworth, J., Guerrant, R., Sande, M. 1976. Comparative pharmacology of josamycin and erythromycin stearate. *Antimicrob Agents Chemother*. 10(3):450–6.
154. **Studer, S.**, Joseph, S. 2006. Unfolding of mRNA secondary structure by the bacterial translation initiation complex. *Mol Cell*. 22(1):105–15.
155. **Subramanian, A.** 1983. Structure and functions of ribosomal protein S1. *Prog Nucleic Acid Res Mol Biol*. 28:101–42.
156. **Sunakawa, K.**, Farrell, D. 2007. Mechanisms, molecular and sero-epidemiology of antimicrobial resistance in bacterial respiratory pathogens isolated from Japanese children. *Ann Clin Microbiol Antimicrob*. 6:7.
157. **Sutcliffe, J.**, Tait-Kamradt, A., Wondrack, L. 1996. *Streptococcus pneumoniae* and *Streptococcus pyogenes* resistant to macrolides but sensitive to clindamycin: a common resistance pattern mediated by an efflux system. *Antimicrob Agents Chemother*. 40(8):1817–24.
158. **Swain, P.**, Elowitz, M., Siggia, E. 2002. Intrinsic and extrinsic contributions to stochasticity in gene expression. *Proc Natl Acad Sci U S A*. 99(20):12795–800.
159. **Tait-Kamradt, A.**, Clancy, J., Cronan, M., Dib-Hajj, F., Wondrack, L., Yuan, W., Sutcliffe, J. 1997. *mefE* is necessary for the erythromycin-resistant M phenotype in *Streptococcus pneumoniae*. *Antimicrob Agents Chemother*. 41(10):2251–5.
160. **Tait-Kamradt, A.**, Davies, T., Cronan, M., Jacobs, M., Appelbaum, P., Sutcliffe, J. 2000. Mutations in 23S rRNA and ribosomal protein L4 account for resistance in pneumococcal strains selected in vitro by macrolide passage. *Antimicrob Agents Chemother*. 44(8):2118–25.
161. **Tenson, T.**, DeBlasio, A., Mankin, A. 1996. A functional peptide encoded in the *Escherichia coli* 23S rRNA. *Proc Natl Acad Sci U S A*. 93(11):5641–6.
162. **Tenson, T.**, Ehrenberg, M. 2002. Regulatory nascent peptides in the ribosomal tunnel. *Cell* 108:591–4.
163. **Tenson, T.**, Herrera, J. V., Kloss, P., Guarneros, G., Mankin, A. S. 1999. Inhibition of translation and cell growth by minigene expression. *J Bacteriol* 181:1617–22.
164. **Tenson, T.**, Mankin, A. 2001. Short peptides conferring resistance to macrolide antibiotics. *Peptides*. 22(10):1661–8.
165. **Tenson, T.**, Lovmar, M., Ehrenberg, M. 2003. The mechanism of action of macrolides, lincosamides and streptogramin B reveals the nascent peptide exit path in the ribosome. *J Mol Biol*. 330(5):1005–14.
166. **Tenson, T.**, Mankin, A. 2006. Antibiotics and the ribosome. *Mol Microbiol*. 59(6):1664–77.
167. **Tenson, T.**, Xiong, L., Kloss, P., Mankin, A. 1997. Erythromycin resistance peptides selected from random peptide libraries. *J Biol Chem*. 272(28):17425–30.
168. **Thomas, J.**, Szer, W. 1982. RNA-helix-destabilizing proteins. *Prog Nucleic Acid Res Mol Biol*. 27:157–87.

169. **Thompson, J.**, O'Connor, M., Mills, J., Dahlberg, A. 2002. The protein synthesis inhibitors, oxazolidinones and chloramphenicol, cause extensive translational inaccuracy in vivo. *J Mol Biol.* 322(2):273–9.
170. **Tikhonova, E.**, Zgurskaya, H. 2004. AcrA, AcrB, and TolC of *Escherichia coli* Form a Stable Intermembrane Multidrug Efflux Complex. *J Biol Chem.* 279(31):32116–24.
171. **Tipper, D.**, Johnson, C., Ginther, C., Leighton, T., Wittmann, H. 1977. Erythromycin resistant mutations in *Bacillus subtilis* cause temperature sensitive sporulation. *Mol Gen Genet.* 150(2):147–59.
172. **Tripathi, S.**, Kloss, P., Mankin, A. 1998. Ketolide resistance conferred by short peptides. *J Biol Chem.* 273(32):20073–7.
173. **Tsagakalia, A.**, Leontiadou, F., Xaplanteri, M., Papadopoulos, G., Kalpaxis, D., Choli-Papadopoulou, T. 2005. Ribosomes containing mutants of L4 ribosomal protein from *Thermus thermophilus* display multiple defects in ribosomal functions and sensitivity against erythromycin. *RNA.* 11(11):1633–9.
174. **Tu, D.**, Blaha, G., Moore, P., Steitz, T. 2005. Structures of MLSBK antibiotics bound to mutated large ribosomal subunits provide a structural explanation for resistance. *Cell.* 121(2):257–70.
175. **Törnroth-Horsefield, S.**, Gourdon, P., Horsefield, R., Brive, L., Yamamoto, N., Mori, H., Snijder, A., Neutze, R. 2007. Crystal structure of AcrB in complex with a single transmembrane subunit reveals another twist. *Structure.* 15(12):1663–73.
176. **Usary, J.**, Champney, W. 2001. Erythromycin inhibition of 50S ribosomal subunit formation in *Escherichia coli* cells. *Mol Microbiol.* 40(4):951–62.
177. **van Bambeke, F.**, Balzi, E., Tulkens, P. 2000. Antibiotic efflux pumps. *Biochem Pharmacol.* 60(4):457–70.
178. **Vazquez, D.** 1979. Inhibitors of protein biosynthesis. *Mol Biol Biochem Biophys.* 30:i–x, 1–312.
179. **Verdier, L.**, Gharbi-Benarous, J., Bertho, G., Mauvais, P., and Girault, J.P. 2002. Antibiotic resistance peptides: interaction of peptides conferring macrolide and ketolide resistance with *Staphylococcus aureus* ribosomes: conformation of bound peptides as determined by transferred NOE experiments. *Biochemistry.* 13: 4218–4229.
180. **Versalovic, J.**, Shortridge, D., Kibler, K., Griffy, M., Beyer, J., Flamm, R., Tanaka, S., Graham, D., Go, M. 1996. Mutations in 23S rRNA are associated with clarithromycin resistance in *Helicobacter pylori*. *Antimicrob Agents Chemother.* 40(2):477–80.
181. **Vester, B.**, Douthwaite, S. 2001. Macrolide resistance conferred by base substitutions in 23S rRNA. *Antimicrob Agents Chemother.* 45(1):1–12.
182. **Vimberg, V.**, Tats, A., Remm, M., Tenson, T. 2007. Translation initiation region sequence preferences in *Escherichia coli*. *BMC Mol Biol.* 8:100.
183. **Vimberg, V.**, Xiong, L., Bailey, M., Tenson, T., Mankin, A. 2004. Peptide-mediated macrolide resistance reveals possible specific interactions in the nascent peptide exit tunnel. *Mol Microbiol.* 54(2):376–85.
184. **Vogelely, L.**, Palm, G., Mesters, J., Hilgenfeld, R. 2001. Conformational change of elongation factor Tu (EF-Tu) induced by antibiotic binding. Crystal structure of the complex between EF-Tu GDP and aurodox. *J Biol Chem.* 276(20):17149–55.
185. **von Rosensteil, N.**, Adam, D. 1995. Macrolide antibacterials. Drug interactions of clinical significance. *Drug Saf.* 13(2):105–22.

186. **Xiong, L.**, Kloss, P., Douthwaite, S., Andersen, N., Swaney, S., Shinabarger, D., Mankin, A. 2000. Oxazolidinone resistance mutations in 23S rRNA of *Escherichia coli* reveal the central region of domain V as the primary site of drug action. *J Bacteriol.* 182(19):5325–31.
187. **Xiong, L.**, Shah, S., Mauvais, P., Mankin, A. 1999. A ketolide resistance mutation in domain II of 23S rRNA reveals the proximity of hairpin 35 to the peptidyl transferase centre. *Mol Microbiol.* 31(2):633–9.
188. **Walsh, C.** 2003. Antibiotics: actions, origins, resistance. American Society for Microbiology.
189. **Wang, Y.**, Wu CM, Lu LM, Ren GW, Cao XY, Shen JZ. 2008. Macrolide-lincosamide-resistant phenotypes and genotypes of *Staphylococcus aureus* isolated from bovine clinical mastitis. *Vet Microbiol.*
190. **Weisblum, B.** 1995a. Erythromycin resistance by ribosome modification. *Antimicrob Agents Chemother.* 39(3):577–85.
191. **Weisblum, B.** 1995b. Insights into erythromycin action from studies of its activity as inducer of resistance. *Antimicrob Agents Chemother.* 39(4):797–805.
192. **Weisblum, B.**, Siddhikol, C., Lai, C., Demohn, V. 1971. Erythromycin-inducible resistance in *Staphylococcus aureus*: requirements for induction. *J Bacteriol.* 106(3):835–47.
193. **Wierzbowski, A.**, Nichol, K., Laing, N., Hisanaga, T., Nikulin, A., Karlowsky, J., Hoban, D., Zhanel, G. 2007. Macrolide resistance mechanisms among *Streptococcus pneumoniae* isolated over 6 years of Canadian Respiratory Organism Susceptibility Study (CROSS) (1998–2004). *J Antimicrob Chemother.* 60(4):733–40.
194. **Wittmann, H.**, Stöffler, G., Apirion, D., Rosen, L., Tanaka, K., Tamaki, M., Takata, R., Dekio, S., Otaka, E. 1973. Biochemical and genetic studies on two different types of erythromycin resistant mutants of *Escherichia coli* with altered ribosomal proteins. *Mol Gen Genet.* 127(2):175–89.
195. **Wolter, N.**, von Gottberg, A., du Plessis, M., de Gouveia, L., Klugman, K.; for the Group for Enteric, Respiratory and Meningeal Disease Surveillance in South Africa (GERMS-SA). 2008. Molecular basis and clonal nature of increasing pneumococcal macrolide resistance in South Africa, 2000–2005. *Int J Antimicrob Agents.*
196. **Yusupov, M.**, Yusupova, G., Baucom, A., Lieberman, K., Earnest, T., Cate, J., Noller, H. 2001. Crystal structure of the ribosome at 5.5 Å resolution. *Science.* 292(5518):883–96.
197. **Yusupova, G.**, Jenner, L., Rees, B., Moras, D., Yusupov, M. 2006. Structural basis for messenger RNA movement on the ribosome. *Nature.* 444(7117):391–4.
198. **Zaman, S.**, Fitzpatrick, M., Lindahl, L., Zengel, J. 2007. Novel mutations in ribosomal proteins L4 and L22 that confer erythromycin resistance in *Escherichia coli*. *Mol Microbiol.* 66(4):1039–50.
199. **Zavialov, A.**, Buckingham, R., Ehrenberg, M. 2001. A posttermination ribosomal complex is the guanine nucleotide exchange factor for peptide release factor RF3. *Cell.* 107(1):115–24.
200. **Zgurskaya, H.**, Nikaido, H. 2000. Multidrug resistance mechanisms: drug efflux across two membranes. *Mol Microbiol.* 37(2):219–25.
201. **Zhang, J.**, Deutscher, M. 1992. A uridine-rich sequence required for translation of prokaryotic mRNA. *Proc Natl Acad Sci U S A.* 89(7):2605–9.

202. **Zhong, P.**, Shortridge, V. 2000. The role of efflux in macrolide resistance. *Drug Resist Updat.* 3(6):325–329.
203. **Ōmura, S.** 2002. *Macrolide antibiotics: chemistry, biology, and practice.* Elsevier Science.

## SUMMARY IN ESTONIAN

### Kokkuvõte

Ribosoom on oluline valgusünteesi läbi viiv makromolekulaarne kompleks. Ribosoom koosneb suurest ja väikesest subühikust. Väike subühik osaleb geneetilise informatsiooni dekodeerimises, samal ajal kui suur subühik assambleerib aminohapped polüpeptiidi ahelasse.

Väikese subühiku seondumine mRNA translatsiooni initsiatsiooni regiooni on translatsiooni efektiivsuse peamine determinant. Me avastasime, et kuuest nukleotiidist koosnev „Shine-Dalgarno” järjestus (AGGAGG) on efektiivsem võrreldes lühemate ja pikemate järjestustega, kui *Escherichi coli* kasvab 37°C juures. A/U rikas tugevdaja soodustab initsiatsiooni efektiivsust, avaldades kõige suurema efekti bakterite eksponentsiaalse kasvufaasi ajal. Bakterite kasvukiirus ei mõjuta translatsiooni initsiatsiooni regiooni selekteerimismustrit. Teisest küljest kasvutemperatuur mõjutab translatsiooni initsiatsiooni regiooni valikut: lühemad SD järjestused on eelistatud madalama kasvutemperatuuri juures. See tulemus näitab, et SD:aSD interaktsiooni tugevus on peamine translatsiooni efektiivsuse determinant.

Suur ribosomaalne subühik on paljude antibiootikumide sihtmärk. Antibiootikumide seondumine peatub valkude sünteesi. Makroliidid on antibiootikumid, mis seonduvad suure ribosomaalse subühikuga peptidültransferaasentri ja kasvava peptiidi väljumistunneli vahele, seega häirivad translatsiooni. Spetsiifiliste peptiidide ekspressioon tagab bakteriraku resistsust makroliidide vastu.

Antud uuringus me selekteerisime peptiidid, mis tagavad resistsuse josamütsiini, 16-aatomilise laktoonringiga makroliidi, vastu. Kõigil josamütsiini resistsuspeptiididel oli teises positsioonis fenüülalaniini või türosiini jääk.

Spetsiifilised resistsuspeptiidid tagavad bakterite resistsust ainult makroliididele millega nemad olid selekteeritud ja ei põhjusta ristresistsust struktuurselt erinevatele makroliididele. Vastavalt resistsuspeptiidide aminohappeliste jätjestustele ja makroliidide struktuuridele, mille vastu resistsus tekib, me klassifitseerisime kõik teadaolevad resistsuspeptiidid 5-ks klassiks.

Resistsuspeptiidide poolt vahendatud resistsuse tekkeks peab resistsuspeptiidi kodeeriva mRNA hulk olema 20 korda suurem kui EF-Tu'd kodeeriva mRNA hulk. Järelikult peab resistsuspeptiidi kodeeriva mRNA tase olema võrdeline ribosomaalse RNA tasemega rakus.

Josamütsiini ja erütromütsiini resistsuspeptiidide pikkuse muutmine omas erinevaid efekte resistsusele. Josamütsiini resistsuspeptiidi pikendamine või lühendamine ei mõjutanud resistsust. Seevastu erütromütsiini resistsuspeptiidi pikendamine või lühendamine täiesti elimineeris aktiivsuse. Arvestades erütromütsiini ja josamütsiini aktiivsuse kineetikat me oletame, et nende kahe peptiidi klassi toimemehhanismid on erinevad.

Makroliidresistentsus on tundlik antibiootikumsaatusele pärast makroliidi dissotsieerumist ribosoomist. Peptiidide poolt vahendatud makroliidresistentsuse matemaatiline modelleerimine ennustas, et resistentsuse tekkeks rakk peab antibiootikumi efektiivselt välja pumpama. *Escherichia coli* AcrAB-TolC pump tagab makroliidide välja pumpamist rakust. Makroliidresistentsus oli elimineeritud *tolC* mutantsetes bakterites.

AcrAB-TolC pumba inaktiveerimine elimineerib mitte ainult resistentsuspeptiidi poolt tagatud erütromütsiini resistentsust aga samuti resistentsust, mis on tagatud L22 ja L4 valkude mutatsiooniga.

Tundub, et madal antibiootikumi äravool varjab antibiootikumi sihtmärgi resistentsusmutatsiooni, on üldine fenomeen. See fenomeen võib olla rakendatud antibakteriaalsete antibiootikumide kliinilises kasutuses, aga samuti eukarüootsete parasiitide ravis ja vähi kemoterapias.

## ACKNOWLEDGEMENTS

A lot of people have contributed to this work and the papers presented here in different ways, and without them this thesis wouldn't have been possible.

First of all I would like to thank **my supervisor Tanel Tenson**, who was always available for help and discussion. I am grateful that you gave me the opportunity to do my research in your lab and provided me with everything I needed.

I would like to thank all people, presently or previously in the lab who contributed to a pleasant atmosphere and a wonderful surrounding to do science: Aksel Soosar, Arvi Jõers, Eliisa Lukk, Age Tats, Hannes Luidalepp, Johanna Kase, Kristi Kurg, Liina Kosenkranius, Niilo Kaldalu, Vallo Varik, Veljo Kisand, Villu Kasari, Ülar Allas.

A big thanks to the molecular biology group for being so hospitable and giving the opportunity to visit you and work in your lab.

My special thanks to my wife and my sons Christian and Edvard for their love and support.

Спасибо моим папе, маме и брату за то, что верили и поддерживали меня.

Особо хочу поблагодарить учителя биологии, Юрия Валентиновича. Ваши уроки открыли для меня удивительный мир живых организмов. Спасибо учителю математики, Александру Васильевичу. Ваша фраза о том, что важна идея, а всё остальное – дело техники, стала для меня лозунгом, под которым была проделана вся научная работа.

Finally thanks to all the people that i have forgotten, believe me, it was not intentional, just the lack of brain and time.

## **PUBLICATIONS**





**Vimberg, V.**, Tats, A., Remm, M., Tenson, T. 2007.  
Translation initiation region sequence preferences  
in *Escherichia coli*. *BMC Mol Biol.* 8:100.

Research article

Open Access

## Translation initiation region sequence preferences in *Escherichia coli*

Vladimir Vimberg<sup>1</sup>, Age Tats<sup>2</sup>, Maido Remm<sup>2</sup> and Tanel Tenson<sup>\*1</sup>

Address: <sup>1</sup>Institute of Technology, University of Tartu, Nooruse 1, Tartu 50411, Estonia and <sup>2</sup>Department of Bioinformatics, Institute of Molecular and Cell Biology, University of Tartu, Riia 23, Tartu 51010, Estonia

Email: Vladimir Vimberg - ribloom@hot.ee; Age Tats - age.tats@ut.ee; Maido Remm - maido.remm@ut.ee; Tanel Tenson\* - tanel.tenson@ut.ee

\* Corresponding author

Published: 31 October 2007

Received: 2 July 2007

BMC Molecular Biology 2007, 8:100 doi:10.1186/1471-2199-8-100

Accepted: 31 October 2007

This article is available from: <http://www.biomedcentral.com/1471-2199/8/100>

© 2007 Vimberg et al; licensee BioMed Central Ltd.

This is an Open Access article distributed under the terms of the Creative Commons Attribution License (<http://creativecommons.org/licenses/by/2.0>), which permits unrestricted use, distribution, and reproduction in any medium, provided the original work is properly cited.

### Abstract

**Background:** The mRNA translation initiation region (TIR) comprises the initiator codon, Shine-Dalgarno (SD) sequence and translational enhancers. Probably the most abundant class of enhancers contains A/U-rich sequences. We have tested the influence of SD sequence length and the presence of enhancers on the efficiency of translation initiation.

**Results:** We found that during bacterial growth at 37°C, a six-nucleotide SD (AGGAGG) is more efficient than shorter or longer sequences. The A/U-rich enhancer contributes strongly to the efficiency of initiation, having the greatest stimulatory effect in the exponential growth phase of the bacteria. The SD sequences and the A/U-rich enhancer stimulate translation co-operatively: strong SDs are stimulated by the enhancer much more than weak SDs. The bacterial growth rate does not have a major influence on the TIR selection pattern. On the other hand, temperature affects the TIR preference pattern: shorter SD sequences are preferred at lower growth temperatures. We also performed an *in silico* analysis of the TIRs in all *E. coli* mRNAs. The base pairing potential of the SD sequences does not correlate with the codon adaptation index, which is used as an estimate of gene expression level.

**Conclusion:** In *E. coli* the SD selection preferences are influenced by the growth temperature and not influenced by the growth rate. The A/U rich enhancers stimulate translation considerably by acting co-operatively with the SD sequences.

### Background

The efficiency of initiation is the most important determinant of translation efficiency [1]. In bacteria, the 30S ribosomal subunit, assisted by initiation factors (IF) 1, 2 and 3 and fMet-tRNA<sup>fMet</sup>, recognizes the translation initiation region (TIR) of the mRNA. This event is followed by binding of the 50S ribosomal subunit and release of the initiation factors [1]. The rate-limiting step in this process is binding of the 30S subunit to the TIR [2]. There are two alternative pathways for mRNA recognition by 30S sub-

units. In the first, the 30S subunit complexed with IF1 and IF3 binds to the mRNA, followed by IF2 and GTP-dependent binding of fMet-tRNA<sup>fMet</sup> [2]. In the second, the IF2:GTP:fMet-tRNA<sup>fMet</sup> complex binds to the 30S subunit followed by mRNA recognition [3]. The relative frequencies with which these pathways are used in bacterial cells are currently not clear.

The following sequence elements of the TIR contribute to its efficiency: (a) the initiation codon, which is most com-

monly AUG but sometimes GUG and very rarely UUG, AUU or CUG [4-7]; (b) the Shine-Dalgarno (SD) sequence [8,9]; (c) regions upstream of the SD sequence and downstream of the initiation codon, which are often described as enhancers of translation [10-15]. In addition, the spacing between these sequence elements is often critical. For example, the distance between the SD sequence and the initiation triplet has a marked effect on the efficiency of translation [16].

The SD sequence base-pairs directly with the anti-Shine-Dalgarno (aSD) sequence on the 3' end of the 16S rRNA [8]. The maximum known length of the SD:aSD duplex is 12 or 13 nucleotides [17]; in most *E. coli* genes the SD sequence is shorter. Free energy calculations for all possible duplexes between the 16S rRNA 3' end and a region 21 nucleotides upstream from the start codon in 1159 *E. coli* genes show that the average number of paired mRNA:rRNA nucleotides is 6.3 [18]. A similar calculation has been made for the ribosomal protein genes and indicates that the average SD length is 4.4 nucleotides [19]. Studies have shown that mRNAs lacking an SD sequence cannot bind the 30S subunit efficiently without the contribution of translational enhancers, additional sequences in the TIR able to increase the efficiency of translation [20]. Also, SD sequences longer than six nucleotides are not very efficient, probably because more time is needed for clearance of the TIR [19,21]. On the other hand, other studies have questioned the importance of the SD for the initiation of translation: Lee et al. [22] report that translation efficiency correlates very poorly with the strength of the SD:aSD interaction. Unfortunately, no systematic study to date has established the correlation between the SD:aSD interaction strength and the efficiency of translation.

Recently, it has been shown that before the SD:aSD interaction occurs, the 30S ribosomal subunit can bind to a standby site in the vicinity of the SD [23,24]. Binding to this standby site might increase the local concentration of 30S subunits at the TIR. The ribosome may remain attached to the standby site until the SD sequence is in a conformation appropriate for binding the aSD. Through this mechanism, the standby site could stimulate translation of mRNAs in which the SD can be trapped by secondary structures. One possible way in which a standby site in mRNA could be created is by binding to S1, the largest protein component of the small ribosomal subunit. S1 consists of two major domains with a freely rotatable region between them [25]. One domain is attached to the 30S; the second is exposed on the surface of the small subunit, scanning the space around the ribosome and searching for A/U-rich sequences [14,19,26] that are recognized with the help of four RNA-binding motifs [27]. It has been shown that S1 can destabilize RNA secondary structures

[28]. Cross-linking studies have shown that the nucleic acid-binding domain of S1 is aligned with a region of the mRNA upstream of the SD, suggesting that S1 may interact with 5' parts of the TIR [29,30]. Consistent with this observation, A/U-rich sequences in front of the SD or downstream of the initiator codon enhance protein synthesis [15,19]. To date, nine sequences have been shown experimentally to act as translational enhancers. They are all A/U-rich and contain very few Gs [19]. Disruption of the *E. coli* gene coding for S1 has been reported to be lethal [31]. A decreased level of S1 protein in the cell leads to a rapid decrease in total protein synthesis [32]. Thus it can be speculated that the SD sequence alone cannot mediate efficient initiation of translation but has to be complemented with an enhancer sequence. Unfortunately, information about the effects of combining the enhancers with different SD sequences is very limited [19].

In the current study we have constructed a set of SD sequences, ranging between 1 and 8 nucleotides, and tested their efficiency with a reporter gene. This allowed the most efficient SD sequences in *E. coli* to be defined. In addition, we have combined all the SD sequences with translational enhancers and determined the effects on reporter gene expression. We have tested all the TIR variants at different bacterial growth phases, growth rates and temperatures.

## Results

### Design of the model constructs

Three sets of TIRs were designed and cloned in front of the GFP coding reporter gene (Figure 1, Additional file 1). Each set contained 10 variants of the SD sequence. The SD variants were constructed by mutating the sequence, forming an 8 base pair duplex with the complementary aSD, and reducing its length from 8 nucleotides to 1. Each set contained a unique sequence upstream of the SD: one containing no translational enhancer ("no enhancer"), one containing a previously-described strong A/U rich enhancer, and one with a weak enhancer [19,33]. Transcription of the reporter genes was controlled by the IPTG inducible *tac* promoter [34]. The mRNAs synthesized from the *tac* promoter contained a *lacO* operator sequence in front of the TIRs. We suspected that the *lacO* sequence might influence the activity of the TIR. Therefore a fourth set of SD sequences was cloned under a different promoter, the arabinose-inducible *araBAD* promoter [35].

In our constructs, a 6-nucleotide spacer sequence separated the SD from the initiation codon (Additional file 1). The particular sequence used has been reported to direct translation efficiently [36]. This spacing between the SD and the AUG codon has been shown to be optimal for efficient gene expression [16]. The spacer sequence (5'-

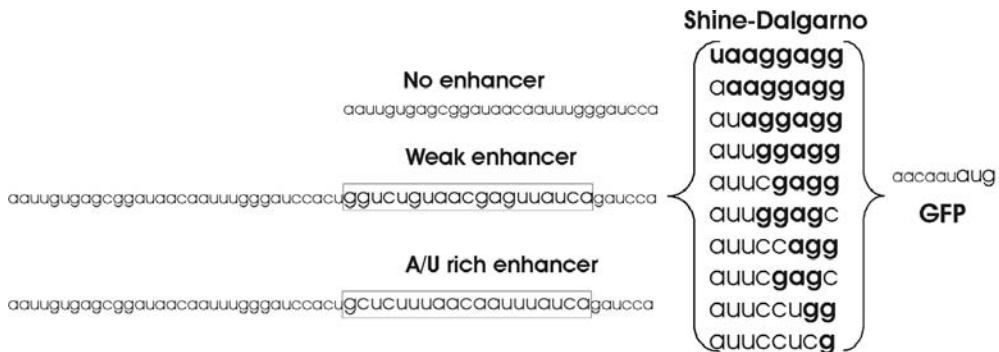


**Figure 1**

Sequences used in the current study. The SD sequences and enhancers were inserted in front of the ORF coding for green fluorescent protein (GFP). Different SD variants were constructed by mutating the sequence into complementary nucleotides. The enhancers used were the "A/U-rich enhancer" (the boxA sequence of *rrnB* [19, 33]) and its mutant with decreased activity ("weak enhancer") [19]. All SD variants in combination with the enhancers were inserted under control of the *tac* promoter regulated by IPTG.

AACAAU-3') provides no opportunities for forming strong alternative SD:aSD interactions, although the "AGG", "GG" and "G" SD sequences could possibly give alternative interactions, which would create AGGA, GGA and GA SD sequences closer to the initiation codon. However, this alternative interpretation of the results concerns only the weakest SD sequences and therefore would not influence the conclusions of the current work.

It is known that RNA secondary structure involving the TIR can influence the efficiency of initiation [37-39]. Therefore we have used the Mfold RNA folding program [40,41] to study the possible secondary structures in the 5' untranslated leader regions of our mRNAs. This modeling suggests that in all our constructs the SD region is not involved in strong secondary structure interactions.

Our aim was to determine the translational activities of the different TIR sequences. It has been reported that sequences in the 5' part of mRNA could influence mRNA stability in the cell [42]. We therefore used quantitative RT-PCR to detect any differences in the levels of mRNAs expressed from our constructs. The results (Additional file 2) indicate that all our constructs expressed mRNA at very similar levels, the differences among them being less than 13%.

#### Effects of the TIR variations on the level of protein synthesis

The plasmids coding for mRNAs with different TIRs were transformed into *E. coli* MG1655 cells and the levels of protein synthesis were measured by the fluorescence of

the GFP reporter gene. The bacterial cultures were inoculated and aliquots were taken after every hour. GFP expression was induced in these aliquots for one hour and the fluorescence was measured. Bacterial growth was monitored by optical density. In addition, mRNA levels were monitored by real time PCR. To eliminate errors that occurred during mRNA preparation, the levels of both GFP and EF-Tu mRNAs were measured; the "normalized mRNA level" is defined as the molar amount of GFP mRNA divided by the molar amount of EF-Tu mRNA. The "expression level" (Figure 2) is calculated by dividing the fluorescence signal by the "normalized mRNA level". Thus, the "expression level" indicates the amount of GFP that is produced per mRNA. We also present the ratios of the fluorescence values to the optical density values, reflecting the amount of the protein synthesized per cell (Additional file 3). As the particular GFP variant matures in considerably less than 1 hour [43] and no degradation of the protein occurs during this time [44], our data show the total accumulation of the protein during the induction period.

When the different sets of constructs with and without enhancers were compared, the expected pattern [19] was observed: the weak enhancer caused a small increase in reporter gene expression while the strong enhancer caused the greatest increase (Figure 2). The two sets of constructs that lacked an enhancer, expressed from the *tac* (Figure 2) or the *araBAD* promoter (Additional file 3), produced the lowest amounts of GFP. The results with the *tac* and *araBAD* promoters were nearly identical (Additional file 3), showing that the operator sequences have no specific

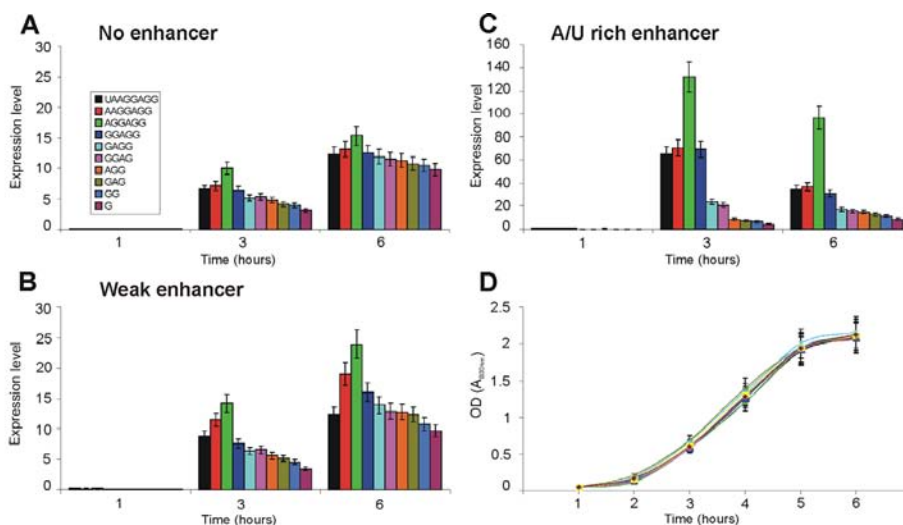


**Figure 2**

The effect of the TIR on GFP synthesis. GFP synthesis directed by mRNAs lacking enhancer (A). GFP synthesis directed by mRNAs containing weak enhancers (B). GFP synthesis directed by mRNAs containing A/U-rich enhancers (C). Growth curve of the cultures shown on panel C (D). The bacterial cultures were inoculated and aliquots were taken at the indicated time points. GFP expression was induced in these aliquots for one hour and the fluorescence was measured. In addition, mRNA levels were monitored by real time PCR. The expression level was calculated according to the following formula: expression level = fluorescence/(molar amount of GFP mRNA/molar amount of EF-Tu mRNA).

influence on the TIR activity. In addition, we have tested the different SD sequences in front of *lacZ* gene (data not shown). Also in this case the relative differences between the efficiencies of TIRs are similar to the results obtained in the context of the GFP gene. Thus, in our different sets of constructs the sequences upstream (*tac* or *araBAD* operator) or downstream (*lacZ* or GFP coding gene) of the TIR have been replaced causing no changes in the relative efficiencies. These results suggest that our conclusions are valid for TIRs in different sequence context although we cannot exclude that certain contexts might have major effects on the relative order of SD efficiencies.

Irrespective of the enhancer context, protein expression was highest for the 6-nucleotide SD AGGAGG (Figure 2). In the absence of enhancer, there are only small differences between weak and strong SD sequences (Figure 2A). When a strong enhancer is introduced into the TIR (Figure 2C), the differences between the SD sequences are greatly increased: the A/U-rich enhancer works cooperatively with the SD sequence, enhancing the efficiency of selec-

tion of the strongest SD sequence and having only a minor effect on the weakest one.

The growth phase of the bacterial culture has a considerable effect on reporter gene expression (Figure 2). During the lag phase (1 hour time point) the mRNA is rapidly induced (Additional file 2) but the amount of protein per mRNA is very small. The efficiency of mRNA translation increases in both the exponential (3 hour time point) and stationary (6 hour time point) phases. There is also an enhancer-specific effect: the A/U rich enhancer has a greater stimulatory effect in the exponential phase than in the stationary phase (Additional file 3).

#### Effect of temperature on TIR selection

The differences in SD length lead to differences in the strength of the SD:aSD interaction. We calculated the change of free energy of these interactions for all SD variants tested (Table 1) using a previously-described method [18]. At 37 °C the optimal SD:aSD base pairing free energy value is around -7.7 kcal/mol. Translation is less efficient

when the strength of the interaction is greater or less than this (Table 1; Figure 2). TIRs containing the A/U-rich enhancer are especially sensitive to the strength of the SD:aSD interaction (Figure 2, Table 1).

The binding of SD to the aSD sequence in the 3' end of the 16S rRNA is mediated by base-pairing, which is temperature-dependent. Therefore, temperature change should influence the strength of the SD:aSD interaction. This change in interaction strength could lead to changes in the SD preference pattern. We decided to repeat the measurements of TIR efficiency at a lower growth temperature, 20°C. To visualize the results, all GFP fluorescence values were divided by the fluorescence measured for GAGG SD and plotted against time (Figure 3). A similar calculation was made from the data collected at 37°C (Figure 3). The differences in SD preference were smaller at 20°C than at 37°C (Additional files 3, 4): in constructs without enhancer or with weak enhancer the differences were hardly detectable. When the A/U-rich enhancer was incorporated into the TIR, the 5-nucleotide SD GGAGG gave the highest level of protein synthesis at 20°C (Figure 3). In contrast, the 6-nucleotide SD gave the highest level of translation at 37°C.

We calculated the Gibbs energy values of the SD:aSD interactions at 20°C and 37°C using *hybrid-min* software [45] (Table 1). The  $\Delta G$  value for the 5-nucleotide SD interaction with the aSD sequence is -9.4 kcal/mol at 20°C; at 37°C the  $\Delta G$  of interaction between the optimal 6-nucleotide SD AGGAGG with aSD is -7.7 kcal/mol. This indicates that the optimal free energy of the interaction is between -7.5 and -9.5 kcal/mol.

#### TIR efficiency in different media

It has been shown that the concentrations of cellular components responsible for protein synthesis (ribosomes, tRNA) vary with growth rate [46,47]. Therefore, the

growth rate-dependent regulation might influence the TIR preference pattern. Therefore we measured the efficiency of different TIRs during growth in different media. Bacteria were grown at 37°C in LB or MOPS medium [48] containing either glucose or sodium acetate as a carbon source. The doubling time of the bacteria grown in LB medium is 26 minutes (Figure 4D), in MOPS medium with glucose as energy source 30 minutes (Figure 4H), and in MOPS medium with sodium acetate 340 minutes (Figure 4I). To visualize the results, the GFP fluorescence values were divided by the fluorescence measured for the GAGG SD sequence (Figure 4). The results show that although there are quantitative differences in the TIR selection pattern among the different media, the ranking order does not change.

#### Correlation between SD length and predicted expression level

We showed experimentally that the highest translation level at 37°C is achieved by constructs with 6 paired nucleotides in the SD:aSD region (Figure 2). Which SD sequences are used most often in *E. coli* mRNAs? Are the most efficient sequences used in highly expressed genes? To answer these questions, we analyzed the SD sequences of 4243 *E. coli* genes. We calculated the number of paired nucleotides for the strongest possible base pairing between the 13 3' terminal nucleotides of 16S RNA and the 21-nucleotide sequence upstream of the mRNA initiation codon. Our analysis gave results similar to the conclusions of a study by Schurr et al. [18] in which a smaller dataset was used. The average number of paired nucleotides in genomic SD is 5.8 and the median number is 6 (Figure 5). This result is in good agreement with our observation that a 6-nucleotide SD is optimal at 37°C. In our experimental constructs the optimal 6-nucleotide base pairing between SD and aSD has free energy of -7.7 kcal/mol at 37°C (Table 1). On the other hand, the SD:aSD interaction in the genomic sequences is often shifted to more A/U-rich regions and contains mismatches. (The antiSD sequence is GAUCACCUCCUUA. Different regions of this sequence can be involved in the base pairing interaction. For example, 5 base pair long helix containing the AUCAC sequence is weaker than the similarly 5 base pair long helix containing antiSD sequence CCUCC.) Therefore the average  $\Delta G$  of this interaction in the *E. coli* genomic sequences is lower (only -6 kcal/mol) than in the optimal experimental construct. The reason for this difference is not clear. It might indicate that genomic SD sequences are suboptimal, but it could also be caused by biases in the free energy calculation algorithm (see Discussion).

The codon adaptation index (CAI) [49] characterizes the similarity of synonymous codon usage in a given gene to that in the highly expressed genes. CAI values vary

**Table 1:  $\Delta G$  of SD:aSD interactions.**

Shine-Dalgarno	$\Delta G_{37^\circ\text{C}}$ (kcal/mol)	$\Delta G_{20^\circ\text{C}}$ (kcal/mol)
UAAGGAGG	-9.4	-12.6
AAAGGAGG	-9.3	-12.3
AUAGGAGG	-7.7	-10.1
AUUGGAGG	-6.9	-9.4
AUUCGAGG	-3.9	-5.7
AUUGGAGC	-4.7	-6.7
AUUCGAGG	-1.0	-2.1
AUUCGAGC	-1.7	-2.9
AUUCGAGG	-0.1	-1.3
AUUCGAGC	NA	NA

$\Delta G$  of SD:aSD interactions at 37°C and 20°C, including 8 nucleotides from mRNA and 8 nucleotides from 16S rRNA. Free energy was calculated using *hybrid-min* from the UNAFold package [45].

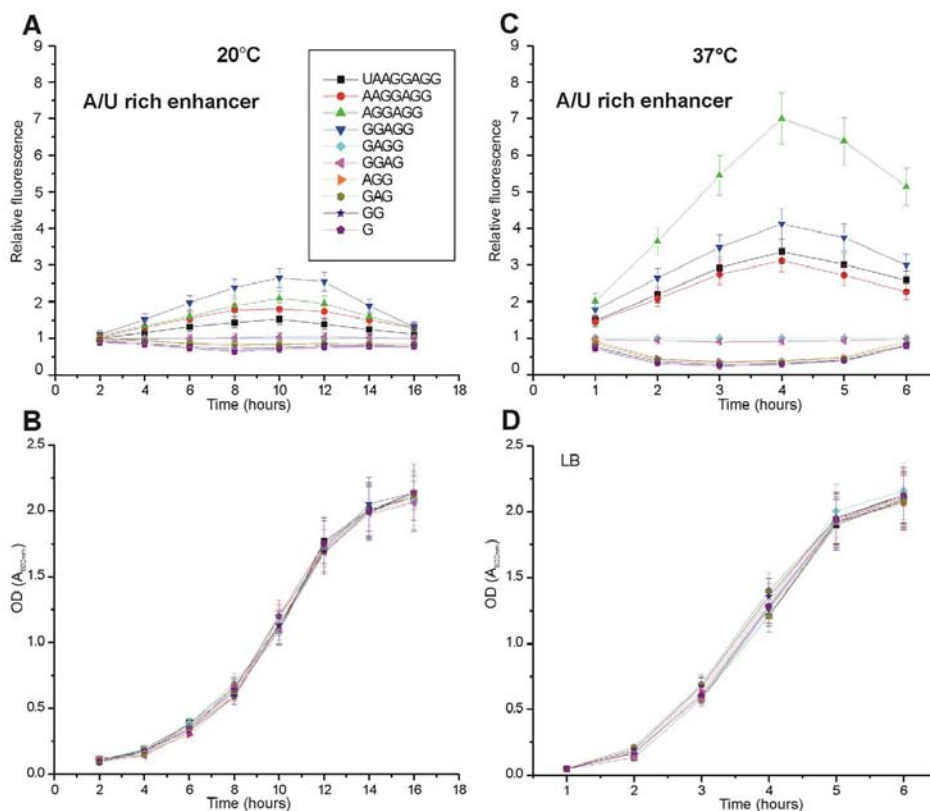


**Figure 3**  
Effect of the growth temperature on TIR selection. The cells were grown either at 20°C (**A**) or at 37°C (**C**). All the TIRs shown contain strong, A/U-rich enhancers. The bacterial cultures were inoculated and aliquots were taken at the indicated time points. GFP expression was induced in these aliquots for one hour and the fluorescence was measured. Relative fluorescence was calculated by dividing the fluorescence values measured for cells containing particular constructs by the fluorescence measured for the GAGG SD sequence. In addition, growth curves at 20°C (**B**) and 37°C (**D**) are shown.

between 0 and 1. A CAI value of 1 is achieved when all amino acids in a given protein are coded by the best codon in each synonymous codon family. The correlation between CAI and gene expression level is well documented [50-52]. Therefore, we used CAI as a measure of gene expression level and plotted it against the number of paired nucleotides in the SD:aSD region. The results indicate that the base pairing potential of the SD sequences does not correlate with CAI: the average CAI is the same for all gene groups with different numbers of base pairs in SD:aSD interactions (Figure 5). Very similar results were

obtained when CAI was plotted against the  $\Delta G$  of the SD:aSD interactions [52], data not shown).

### Discussion

In this study we have investigated the influence of SD sequence length on the efficiency of translation. Variants of the SD sequence were tested with the help of a reporter gene coding for GFP. Shortening of the SD from the 8-nucleotide UAAGGAGG to the single-nucleotide paired G by mutating the sequence into complementary nucleotides reveals an optimal SD length: the 6-nucleotide SD

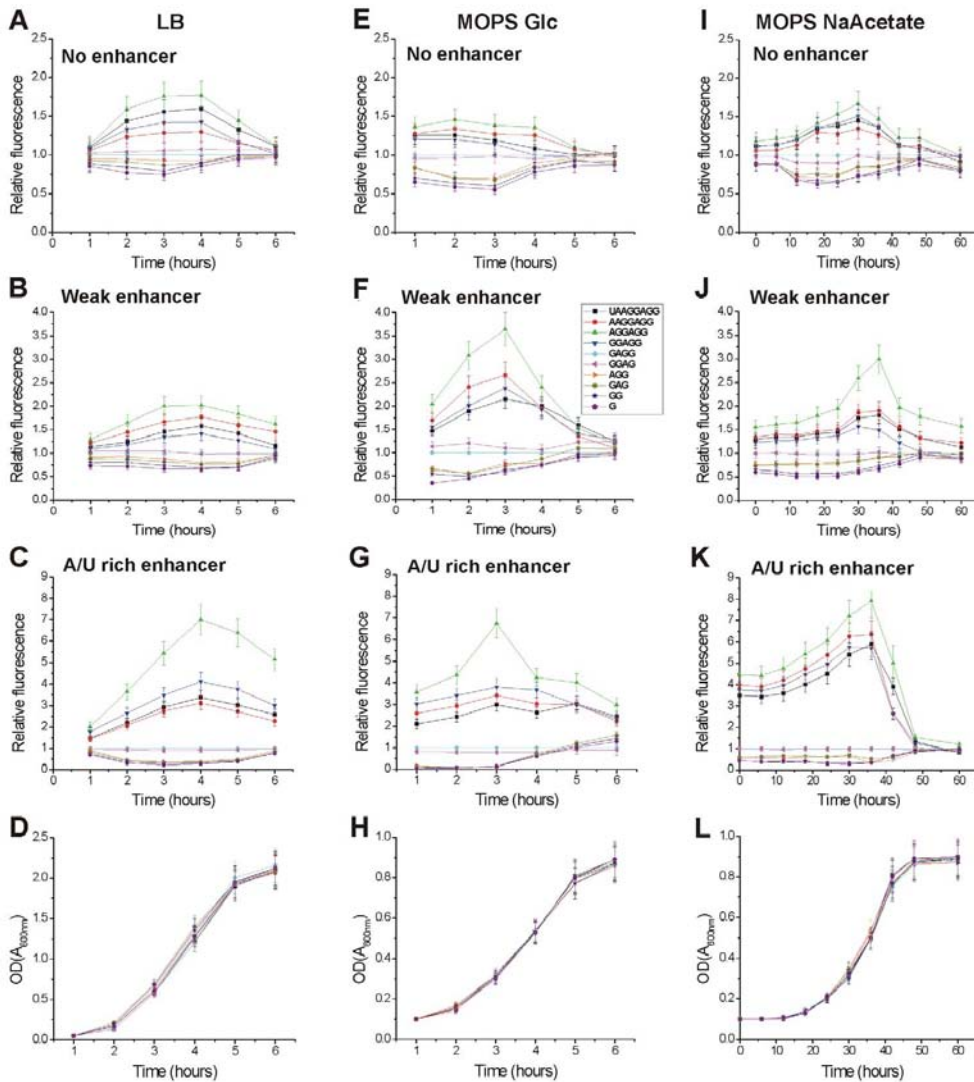


**Figure 4**  
TIR selection in different media. The cells were grown in either LB (**A, B, C, D**), MOPS medium containing glucose, "MOPS Glc" (**E, F, G, H**), or MOPS containing sodium acetate, "MOPS NaAcetate" (**I, J, K, L**) at 37°C. mRNAs lacking enhancer (**A, E, I**), containing the weak enhancer (**B, F, J**) or containing the strong A/U-rich enhancer (**C, G, K**) were tested. The bacterial cultures were inoculated and aliquots were taken at the indicated time points. GFP expression was induced in these aliquots for one hour (LB, MOPS Glc) or 3 hours (MOPS NaAcetate) and the fluorescence was measured. Relative fluorescence was calculated by dividing the fluorescence values measured for cells containing particular constructs by the fluorescence measured for the GAGG SD sequence. In addition, growth curves in different media are shown (**D, H, L**).

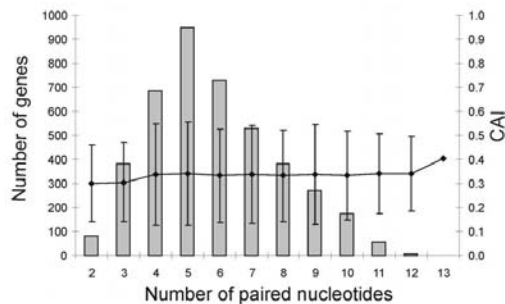


**Figure 5**  
Distribution of the number of paired nucleotides in SD:aSD interactions and the CAI values for 4243 *E. coli* genes. The figure shows the number of genes (grey bars, left axis) and the average CAI with 95% confidence intervals (black dots, right axis).

AGGAGG causes the highest level of protein synthesis (Figure 2). Both shorter and longer SD sequences are less efficient. Shorter SD sequences may be less efficient because binding to the ribosome is weaker. For very long SDs it has been proposed that the interaction of the 30S ribosomal subunit with mRNA is stronger than optimal, increasing the time required for the ribosome to leave the translation initiation site and proceed with protein elongation [19].

Several studies of the influence of SD length on gene expression have been published. According to Rinquist et al. [53] the 8-nucleotide SD UAAGGAGG is 4 times more efficient than the 5-nucleotide AAGGA sequence. Komarova et al. [19] compared the 10-nucleotide AAGGAGGUGA, the 8-nucleotide AAGGAGGU and the 6-nucleotide AAGGAG SD sequences and found that AAGGAG confers the highest expression level of the reporter gene. Chen et al. [16] reported that GAGGU is twice as active as the UAAGG sequence. Although these earlier results are fragmentary and do not allow the most active SD sequence to be defined, the data are consistent with our current finding that the 6-nucleotide SD is the most efficient.

In order to increase the probability of 30S ribosomal subunit attachment and the initiation of translation, bacterial mRNAs contain standby sites that are used for the primary binding of the small ribosomal subunits in the vicinity of the SD and start codon [23,24]. One class of these standby sites contains A/U-rich sequences that can bind the ribosomal protein S1 [26,29] and/or reduce mRNA local secondary structure in the TIR [10]. It has been suggested that all highly expressed mRNAs possess the A/U-rich

sequences upstream of the SDs [19]. The fact that nearly all protein synthesis in *E. coli* is dependent on S1 [32] supports this proposal.

In our study we have investigated the effect of adding enhancers in front of the SDs. The sequences upstream of the SD did not change the SD preference qualitatively: AGGAGG still remained the most efficient SD sequence at 37°C (Figure 2). On the other hand, the A/U-rich enhancer and SD influence the efficiency of protein synthesis cooperatively: a marked increase in protein synthesis was observed for 5- to 8-nucleotide SDs combined with the enhancer; the yield of GFP from 1-, 2- and 3-nucleotide SDs was only slightly increased after the enhancer sequence was added. This result indicates that for efficient initiation of translation both a strong SD and the enhancer sequences are important. Our observations also explain the previous reports that in some cases the strength of the SD:aSD interaction does not determine the efficiency of TIR [22]. Our data show that large differences between the SD sequences are observed only in case the SD is combined with enhancer sequences. What might be the origin of co-operativity between the SD sequences and enhancers? We suggest that the SD sequence determines the maximal rate of initiation; enhancer might increase the local concentration of initiation complexes allowing the strong SD sequences to work most efficiently.

Another sequence element that has been shown to influence the efficiency of TIR is the spacer separating SD from initiation codon. In the current study we have used a spacer sequence that has been reported to direct efficient initiation of translation [36]. It has the optimal length: shorter and longer variants of the spacer are less efficient [16,54]. It has been pointed out previously that the optimal spacing of SD sequences correlates with gene expression level [55]. Therefore it would be interesting to measure experimentally the interaction of suboptimal spacers with SD sequences: does the spacer context influence the SD preference pattern? These experiments remain to be performed in the future.

The concentrations of translation apparatus components depend on the growth phase and growth rate of the bacterial culture [46,47]. As the concentration of ribosomes available for initiation of translation changes, the selection of the TIR may depend on the growth parameters. To investigate this possibility we grew the bacteria in three media that give different growth rates. To detect possible growth phase-dependent variations we followed the induction of the reporter gene throughout the growth curve. The results (Figures 2 and 4) indicate that there are no qualitative differences in the TIR selection pattern, although some quantitative effects were observed. For example, weak enhancer sequences are active only in

media where growth rate is low. Also, the enhancer sequences are more active in the exponential growth phase than in the lag and stationary phases.

The free energy of base pairing between two RNA strands depends on the temperature. Therefore, the strength of the SD:aSD interaction is temperature-dependent. If the optimal free energy of this interaction determines the efficiency of translation, then shorter SD:aSD duplexes should be preferred at lower temperatures. To test this prediction, we measured the TIR preference pattern at 20°C and compared it to the data collected at 37°C (Figure 3). At 37°C the most efficient SD sequence is AGGAGG and at 20°C it is GGAGG; the optimum shifts to a shorter sequence when the temperature is lowered. This result indicates that a certain optimal strength of SD:aSD interaction is required for efficient translation. It also suggests that the length of the SD sequence could be used for temperature-dependent regulation of gene expression. Unfortunately, we cannot analyze the length of SD sequences in the known cold shock genes of *E. coli* as the dataset is too small for a statistically meaningful conclusion.

We found that the most efficient SD at 37°C is AGGAGG, with 6 paired nucleotides. Are the most efficient sequences also commonly used in the *E. coli* genome? To answer this question, we used bioinformatics tools to analyze the SD:aSD interactions in all *E. coli* mRNAs. We found that the average SD length is 5.8 nucleotides, which agrees with the observation that a 6-nucleotide SD is optimal at 37°C. On the other hand, the SD:aSD interaction is often shifted to more A/U-rich regions compared to the AGGAGG sequence and contains one or more mismatches. Therefore the average  $\Delta G$  of this interaction is only -6 kcal/mol rather than -7.7 kcal/mol as achieved with the best experimental SD.

Why do most *E. coli* mRNAs, including those coding for highly expressed genes, have SDs that are not expected to direct the highest level of translation at 37°C? We suggest three possibilities. First, *E. coli* has to grow in the mammalian gut but also to survive at lower temperatures outside the host. The temperatures of both environments may have contributed to the selection of SD sequences. Second, the noise in gene expression levels may be involved. A particular expression level could be achieved by different contributions from transcription and translation. Theoretical calculations have suggested, and experimental data confirmed, that a high level of transcription combined with a low level of translation creates considerably smaller fluctuations in gene expression than a combination of a low level of transcription with highly efficient translation resulting in the same overall expression level [56-58]. Therefore, using weak TIRs might reduce noise in gene expression. Third, the effect may be attributable to

differences in SD structure between the experimental constructs and genes in the *E. coli* genome. Our experimental constructs contain continuous stretches of paired nucleotides without mismatches, whereas *E. coli* genes contain longer paired areas with one or more mismatches. It is not possible to estimate the energetic effect of the mismatches accurately in the context of the ribosome where the SD:aSD helix is stabilized by contacts with ribosomal RNA and proteins [17,59]. Further experiments are needed to evaluate the effect of mismatches in SD sequences.

### Conclusion

In *E. coli* the SD selection preferences are influenced by the growth temperature and not influenced by the growth rate. The A/U-rich enhancer contributes strongly to the efficiency of initiation. The SD sequences and the A/U-rich enhancer stimulate translation co-operatively: strong SDs are stimulated by the enhancer much more than weak SDs. Further experiments are needed to elucidate the biochemical nature of this co-operativity.

### Methods

#### Oligonucleotides

Sequences of the oligonucleotides used are provided in the Appendix.

#### TIR cloning

The gene *gfpmut2* [60] was PCR amplified from the plasmid pMS201 using *Tac* and *Reverse* primers. The PCR product contained the *tac* promoter [34], a BamHI cloning site for TIR insertions and the *trp* terminator (Additional files 1, 5). The *gfpmut2* PCR product was ligated into pGEM-T easy vector (Promega). From pGEM-T easy vector, *gfpmut2* was excised using the restriction enzymes SphI and SacI (Fermentas) and cloned into pET41A vector (Novagene) resulting a plasmid pETGFP (Additional file 5). TIRs generated by PCR with *SD general* (1, 2 or 3) and TIR-specific primers were inserted into the BamHI restriction site in the pETGFP vector.

To express GFP under the *bad* promoter, *gfpmut2* was PCR amplified from pMS201 using *Forward NheI* and *Reverse* primers. The PCR product contained a BamHI cloning site for TIR insertions, *trp* terminator and NheI and SacI restriction sites at the ends. The PCR product was ligated into pGEM-T easy vector. *gfpmut2* was excised from this vector using NheI and SacI (Fermentas) and cloned into pBAD33 vector (Additional file 5) [35] under the control of the *araBAD* promoter. TIRs were generated by PCR as described above and inserted into the BamHI restriction site.

### Growth of bacteria and measurement of GFP expression

Plasmids coding for GFP mRNAs with different TIRs were transformed into *E. coli* MG1655 [61]. Bacteria bearing the plasmids were grown in the presence of 25 µg/ml kanamycin in 2.5 ml LB medium at 37°C or 20°C, MOPS medium supplemented with 0.1% glucose (MOPS Glc), or MOPS medium supplemented with 0.3% sodium acetate (MOPS NaAcetate) [48] at 37°C. Overnight cell cultures were diluted with fresh medium to an optical density of 0.05 ( $A_{600\text{ nm}}$ ). Growth was monitored by the increase in optical densities of the cultures. For bacterial cultures grown at 37°C in LB or MOPS Glc media, samples were taken every hour; in LB medium at 20°C every 2 hours; in MOPS NaAcetate medium at 37°C every 6 hours. Aliquots (50 µl) of each bacterial culture were transferred to black 96-well plates where GFP expression was induced by adding IPTG (final concentration 1 mM) or arabinose (final concentration 10 mM). The 96-well plates were incubated for 1 hour at 37°C (LB, MOPS Glc), for 3 hours at 37°C (MOPS NaAcetate) or for 1 hour at 20°C (LB, 20°C) and GFP fluorescence was measured using a TECAN Fluoroimager. Experiments were repeated at least 3 times and standard deviations of the results were calculated.

### Reverse transcription Real-Time PCR

Sequences coding for GFP (mut2) or *E. coli* EF-Tu were inserted under the control of the T7 promoter (pGEM-T easy, Promega), transcribed *in vitro* and purified. These *in vitro* transcribed mRNAs were used as standards. Bacteria bearing the plasmids coding for GFP mRNAs with different TIRs were grown in 2.5 ml LB medium at 37°C. After 1, 3 or 6 hours of growth, GFP expression was induced by adding IPTG (final concentration 1 mM), followed by incubation for 1 hour. Cells were harvested from 1 ml of the growing cultures and total RNA was isolated using a Macherey-Nagel RNA extraction kit. Reverse transcription was performed in 5 µl volumes containing 0.5 mM of each NTP (Fermentas), 1500 nM GFP Reverse primer, 2 U ribonuclease inhibitor (Fermentas), 10 U Revert-Aid reverse transcriptase (Fermentas) and mRNA in the range 10 fg to 1 ng in Revert-Aid reverse transcription buffer (Fermentas). RNA was reverse transcribed at 42°C for 1 hour and the reverse transcriptase was inactivated by heating at 70°C for 10 minutes. After the reverse transcription reaction, 20 µl PCR reaction components (300 nM GFP Forward primer, 0.0005 µl of SYBR Green I (10,000× concentrate in DMSO; Molecular Probes), 5 mM MgCl<sub>2</sub>, 10 µl 2× PCR Master Mix (Fermentas)) were added, followed by PCR steps: prePCR (95°C for 10 seconds) and 40 PCR cycles (95°C for 5 seconds, 60°C for 10 seconds and 72°C for 10 seconds). Real-time PCR was performed using a SmartCycler (Cepheid). The amount of GFP mRNA was normalized with EF-Tu mRNA, which was determined using the same reverse transcription-PCR pro-

ocol as described above, replacing the primers with EF-Tu Reverse and EF-Tu Forward.

### Calculation of minimal free energy of SD:aSD interaction

The mRNA coding sequences of *Escherichia coli* K-12 [61] were retrieved from the National Center of Biotechnology Information [62]. For each mRNA we used a region of 21 nucleotides upstream from the start codon, as described by Schurr et al. [18]. For anti-SD sequence we used 13 nucleotides from the 3' end of 16S rRNA (GAUACCCUCCUUA). The minimal free energy values for rRNA-mRNA duplexes were calculated by the hybrid-min program from UNAFold package downloaded from the DINAMelt web server [45,63].

### Calculation of codon adaptation index

The codon adaptation index (CAI) was calculated using the program CodonW [64]. This calculation is based on a dataset of highly expressed genes including those encoding ribosomal proteins, outer membrane proteins, elongation factors, heat shock proteins and RNA polymerase subunits [49].

### Authors' contributions

VV constructed the plasmids described in the current study, carried out all molecular biology and microbiology experiments and drafted the first version of the manuscript. AT carried out the *in silico* analysis. MR participated in the design of the study and helped to draft the manuscript. TT participated in the design and coordination of the study and helped to draft the manuscript. All authors read and approved the final manuscript.

### Appendix

#### Sequences of the oligonucleotides

##### Amplification of the GFP coding gene

Tac: tttggtaccttttgacaattaatcatcggctcgtataatgttggaattggagcggataacaatttgggatcc ataaggaggaacaatatgggacccaagggaagaattattcact; Reverse: caacgagctcaaaaaa aagcccgctcattaggcggattattgtacaattcatccatc; Forward Nhel: gctagcggatcctctaaa ggtgaattattcact.

##### Amplification of TIRs without enhancer

SD general 2: tgggggtaccttttgacaattaatcatcggctcgtataatgttggaattgtgagcggataacaatttg ggtatcca; UAAGGAGG 2: caatcgatcctttcatattgttctcttattggatcccaaatgttatcc; AAGGAGG 2: caatcggatcctttcatattgttctcttggatcccaaatgttatcc; AGGAGG 2: caat cggatcctttcatattgttctcttattggatcccaaatgttatcc; GGAGG 2: caatcggatcctttcatattgttctc caattggatcccaaatgttatcc; GAGG 2: caatcggatcctttcatattgttctcgaattggatcccaaatgttatcc;

GGAG 2: caatcggatcctttcatattgttctcgaattggatcccaaatgttatcc; AGG 2: caatcggatcctttc atattgttctcgaattggatcccaaatgttatcc; GAG 2: caatcggatcctttcatattgttctcgaattggatccca

attgttatcc; GG 2: caatcggatcctttcatattgttccaggaattggatccaaattgttatcc; G 2: caatcggatcc ttcatattgttcgaggaattggatccaaattgttatcc.

#### Amplification of TIRs with weak enhancer

*SD general 1:* tggggctacctttgacaattaatcatcggctctgataatgttggaaattgtgagcggataacaatttg ggaatcactggtctgtaacgagttatcagatcca; *UAAGGAGG:* caatcggatcctttcatattgttccctcttgatctgataactcg; *AAGGAGG:* caatcggatcctttcatattgttccctttggatctgataactcg; *AGGAGG:* caatcggatcctttcatattgttccctcttgatctgataactcg; *GGAGG:* caatcggatcctttcatattgttccctcgaattggatctgataactcg; *GAGG:* caatcggatcctttcatattgttccctcgaattggatctgataactcg; *GGAG:* caatcggatcctttcatattgttcccaattggatctgataactcg; *AGG:* caatcggatcctttcatattgttccctcgaattggatctgataactcg; *GAG:* caatcggatcctttcatattgttcccaattggatctgataactcg;

*GG:* caatcggatcctttcatattgt tccaggaattggatctgataactcg; *G:* caatcggatcctttcatattgttcgagga attgactgataactcg.

#### Amplification of TIRs with A/U-rich enhancer

*SD general 3:* acaatttgggaccactgctctttaacaattatcagatcca; *UAAGGAGG 3:* tgaatcggga tctttcatattgttccctcttgatctgataaaattgttaaag; *AAGGAGG 3:* tgaatcggatcctttcatattgttccctctttggatctgataaaattgttaaag; *AGGAGG 3:* tgaatcggatcctttcatattgttccctctttggatctgataaaattgttaaag; *GGAGG 3:* tgaatcggatcctttcatattgttccctctttggatctgataaaattgttaaag; *GAGG 3:* tgaatcggatcctttcatattgttccctcgaattggatctgataaaattgttaaag; *GGAG 3:* tgaatcggatcctttca tattgttgcctcaattggatctgataaaattgttaaag; *AGG 3:* tgaatcggatcctttcatattgttccctcgaattggatctgataaaattgttaaag; *GAG 3:* tgaatcggatcctttcatattgttgcctcgaattggatctgataaaattgttaaag; *G 3:* tgaatcggatcctttcatattgttcgagaattggatctgataaaattgttaaag.

#### Reverse transcription real-time PCR

*GFP Forward:* gttccatggccaaccttagctactactcttc; *GFP Reverse:* agcaaaa atgaagaccatacgcgaa; *EF-Tu Forward:* gagatggagaatcagctctcga; *EF-Tu Reverse:* accagacgtgctgattg.

#### Additional material

##### Additional file 1

Sequences of the TIRs used in the study. Sequences of the TIRs are provided.

Click here for file

[http://www.biomedcentral.com/content/supplementary/1471-2199-8-100-S1.doc]

##### Additional file 2

Reverse transcription real-time PCR to determine mRNA levels. The file contains information about mRNA levels.

Click here for file

[http://www.biomedcentral.com/content/supplementary/1471-2199-8-100-S2.doc]

##### Additional file 3

The effect of the TIR on GFP synthesis at 37°C. The experimental data used for Figure 2 are provided in fluorescence units. In addition, the data for araBAD promoter are shown.

Click here for file

[http://www.biomedcentral.com/content/supplementary/1471-2199-8-100-S3.doc]

##### Additional file 4

The effect of the TIR on GFP synthesis at 20°C. The data from measurements done at 20°C are provided for all enhancer contexts.

Click here for file

[http://www.biomedcentral.com/content/supplementary/1471-2199-8-100-S4.doc]

##### Additional file 5

Plasmids used for GFP expression. Sequences of the plasmids are provided.

Click here for file

[http://www.biomedcentral.com/content/supplementary/1471-2199-8-100-S5.doc]

#### Acknowledgements

We thank Ülo Maiväli, Alexander Mankin, Niilo Kaldalu, Norbert Polacek and Mäns Ehrenberg for valuable comments on the manuscript. This work was supported by The Wellcome Trust International Senior Fellowship (070210/Z/03/Z) (TT) and by the Estonian Science Foundation grant no. 6768 (TT). The English language was corrected by Biomedes, UK.

#### References

- Boelens R, Gualerzi CO: **Structure and function of bacterial initiation factors.** *Curr Protein Pept Sci* 2002, **3**(1):107-119.
- Gualerzi CO, Pon CL: **Initiation of mRNA translation in prokaryotes.** *Biochemistry* 1990, **29**(25):5881-5889.
- Wu XQ, Iyengar P, RajBhandary UL: **Ribosome-initiator tRNA complex as an intermediate in translation initiation in Escherichia coli revealed by use of mutant initiator tRNAs and specialized ribosomes.** *Embo J* 1996, **15**(17):4734-4739.
- Gren EJ: **Recognition of messenger RNA during translational initiation in Escherichia coli.** *Biochimie* 1984, **66**(1):1-29.
- Schneider TD, Stormo GD, Gold L, Ehrenfeucht A: **Information content of binding sites on nucleotide sequences.** *J Mol Biol* 1986, **188**(3):415-431.
- O'Donnell SM, Janssen GR: **The initiation codon affects ribosome binding and translational efficiency in Escherichia coli of cl mRNA with or without the 5' untranslated leader.** *J Bacteriol* 2001, **183**(4):1277-1283.
- Van Etten WJ, Janssen GR: **An AUG initiation codon, not codon-anticodon complementarity, is required for the translation of unleadered mRNA in Escherichia coli.** *Mol Microbiol* 1998, **27**(5):987-1001.
- Shine J, Dalgarno L: **The 3'-terminal sequence of Escherichia coli 16S ribosomal RNA: complementarity to nonsense triplets and ribosome binding sites.** *Proc Natl Acad Sci U S A* 1974, **71**(4):1342-1346.
- Shultzaberger RK, Bucheimer RE, Rudd KE, Schneider TD: **Anatomy of Escherichia coli ribosome binding sites.** *J Mol Biol* 2001, **313**(1):215-228.
- Stenstrom CM, Isaksson LA: **Influences on translation initiation and early elongation by the messenger RNA region flanking the initiation codon at the 3' side.** *Gene* 2002, **288**(1-2):1-8.
- Stormo GD, Schneider TD, Gold LM: **Characterization of translational initiation sites in E. coli.** *Nucleic Acids Res* 1982, **10**(9):2971-2996.
- Tats A, Remm M, Tenson T: **Highly expressed proteins have an increased frequency of alanine in the second amino acid position.** *BMC Genomics* 2006, **7**:28.

13. Brock JE, Paz RL, Cottle P, Janssen GR: **Naturally Occurring Adenines within mRNA Coding Sequences Affect Ribosome Binding and Expression in Escherichia coli.** *J Bacteriol* 2007, **189(2)**:501-510.
14. Dreyfus M: **What constitutes the signal for the initiation of protein synthesis on Escherichia coli mRNAs?** *J Mol Biol* 1988, **204(1)**:79-94.
15. Qing G, Xia B, Inouye M: **Enhancement of translation initiation by A/T-rich sequences downstream of the initiation codon in Escherichia coli.** *J Mol Microbiol Biotechnol* 2003, **6(3-4)**:133-144.
16. Chen H, Bjerknes M, Kumar R, Jay E: **Determination of the optimal aligned spacing between the Shine-Dalgarno sequence and the translation initiation codon of Escherichia coli mRNAs.** *Nucleic Acids Res* 1994, **22(23)**:4953-4957.
17. Yusupova G, Jenner L, Rees B, Moras D, Yusupov M: **Structural basis for messenger RNA movement on the ribosome.** *Nature* 2006, **444(7117)**:391-394.
18. Schurr T, Nadir E, Margalit H: **Identification and characterization of E.coli ribosomal binding sites by free energy computation.** *Nucleic Acids Res* 1993, **21(17)**:4019-4023.
19. Komarova AV, Tchufistova LS, Supina EV, Boni IV: **Protein S1 counteracts the inhibitory effect of the extended Shine-Dalgarno sequence on translation.** *Rna* 2002, **8(9)**:1137-1147.
20. Tzareva NV, Makhno VI, Boni IV: **Ribosome-messenger recognition in the absence of the Shine-Dalgarno interactions.** *FEBS Lett* 1994, **337(2)**:189-194.
21. De Boer HA, Comstock LJ, Hui A, Wong E, Vasser M: **A hybrid promoter and portable Shine-Dalgarno regions of Escherichia coli.** *Biochem Soc Symp* 1983, **48**:233-244.
22. Lee K, Holland-Staley CA, Cunningham PR: **Genetic analysis of the Shine-Dalgarno interaction: selection of alternative functional mRNA-rRNA combinations.** *Rna* 1996, **2(12)**:1270-1285.
23. de Smit MH, van Duin J: **Translational standby sites: how ribosomes may deal with the rapid folding kinetics of mRNA.** *J Mol Biol* 2003, **331(4)**:737-743.
24. Studer SM, Joseph S: **Unfolding of mRNA secondary structure by the bacterial translation initiation complex.** *Mol Cell* 2006, **22(1)**:105-115.
25. Subramanian AR: **Structure and functions of ribosomal protein S1.** *Prog Nucleic Acid Res Mol Biol* 1983, **28**:101-142.
26. Ringquist S, Jones T, Snyder EE, Gibson T, Boni I, Gold L: **High-affinity RNA ligands to Escherichia coli ribosomes and ribosomal protein S1: comparison of natural and unnatural binding sites.** *Biochemistry* 1995, **34(11)**:3640-3648.
27. Selivanova OM, Shiryaev VM, Tiktopulo EI, Potekhin SA, Spirin AS: **Compact globular structure of Thermus thermophilus ribosomal protein S1 in solution: sedimentation and calorimetric study.** *J Biol Chem* 2003, **278(38)**:36311-36314.
28. Thomas JO, Szer VV: **RNA-helix-destabilizing proteins.** *Prog Nucleic Acid Res Mol Biol* 1982, **27**:157-187.
29. Boni IV, Isaeva DM, Musychenko ML, Tzareva NV: **Ribosome-messenger recognition: mRNA target sites for ribosomal protein S1.** *Nucleic Acids Res* 1991, **19(1)**:155-162.
30. Zhang J, Deutscher MP: **A uridine-rich sequence required for translation of prokaryotic mRNA.** *Proc Natl Acad Sci U S A* 1992, **89(7)**:2605-2609.
31. Kitakawa M, Isono K: **An amber mutation in the gene rpsA for ribosomal protein S1 in Escherichia coli.** *Mol Gen Genet* 1982, **185(3)**:445-447.
32. Sorensen MA, Fricke J, Pedersen S: **Ribosomal protein S1 is required for translation of most, if not all, natural mRNAs in Escherichia coli in vivo.** *J Mol Biol* 1998, **280(4)**:561-569.
33. Mogridge J, Greenblatt J: **Specific binding of Escherichia coli ribosomal protein S1 to boxA transcriptional antiterminator RNA.** *J Bacteriol* 1998, **180(8)**:2248-2252.
34. de Boer HA, Comstock LJ, Vasser M: **The tac promoter: a functional hybrid derived from the trp and lac promoters.** *Proc Natl Acad Sci U S A* 1983, **80(1)**:21-25.
35. Guzman LM, Belin D, Carson MJ, Beckwith J: **Tight regulation, modulation, and high-level expression by vectors containing the arabinose PBAD promoter.** *J Bacteriol* 1995, **177(14)**:4121-4130.
36. Barrick D, Villanueva K, Childs J, Kalil R, Schneider TD, Lawrence CE, Gold L, Stormo GD: **Quantitative analysis of ribosome binding sites in E.coli.** *Nucleic Acids Res* 1994, **22(7)**:1287-1295.
37. de Smit MH, van Duin J: **Control of translation by mRNA secondary structure in Escherichia coli. A quantitative analysis of literature data.** *J Mol Biol* 1994, **244(2)**:144-150.
38. de Smit MH, van Duin J: **Secondary structure of the ribosome binding site determines translational efficiency: a quantitative analysis.** *Proc Natl Acad Sci U S A* 1990, **87(19)**:7668-7672.
39. Ringquist S, MacDonald M, Gibson T, Gold L: **Nature of the ribosomal mRNA track: analysis of ribosome-binding sites containing different sequences and secondary structures.** *Biochemistry* 1993, **32(38)**:10254-10262.
40. Mathews DH, Sabina J, Zuker M, Turner DH: **Expanded sequence dependence of thermodynamic parameters improves prediction of RNA secondary structure.** *J Mol Biol* 1999, **288(5)**:911-940.
41. Zuker M: **Mfold web server for nucleic acid folding and hybridization prediction.** *Nucleic Acids Res* 2003, **31(13)**:3406-3415.
42. Komarova AV, Tchufistova LS, Dreyfus M, Boni IV: **AU-rich sequences within 5' untranslated leaders enhance translation and stabilize mRNA in Escherichia coli.** *J Bacteriol* 2005, **187(4)**:1344-1349.
43. Cluzel P, Surette M, Leibler S: **An ultrasensitive bacterial motor revealed by monitoring signaling proteins in single cells.** *Science* 2000, **287(5458)**:1652-1655.
44. Andersen JB, Sternberg C, Poulsen LK, Bjorn SP, Givskov M, Molin S: **New unstable variants of green fluorescent protein for studies of transient gene expression in bacteria.** *Appl Environ Microbiol* 1998, **64(6)**:2240-2246.
45. Markham NR, Zuker M: **DINAMelt web server for nucleic acid melting prediction.** *Nucleic Acids Res* 2005, **33(Web Server issue)**:W577-81.
46. Dennis PP, Ehrenberg M, Bremer H: **Control of rRNA synthesis in Escherichia coli: a systems biology approach.** *Microbiol Mol Biol Rev* 2004, **68(4)**:639-668.
47. Dong H, Nilsson L, Kurland CG: **Co-variation of tRNA abundance and codon usage in Escherichia coli at different growth rates.** *J Mol Biol* 1996, **260(5)**:649-663.
48. Neidhardt FC, Bloch PL, Smith DF: **Culture medium for enterobacteria.** *J Bacteriol* 1974, **119(3)**:736-747.
49. Sharp PM, Li WH: **The codon Adaptation Index--a measure of directional synonymous codon usage bias, and its potential applications.** *Nucleic Acids Res* 1987, **15(3)**:1281-1295.
50. Gutierrez G, Marquez L, Marin A: **Preference for guanosine at first codon position in highly expressed Escherichia coli genes. A relationship with translational efficiency.** *Nucleic Acids Res* 1996, **24(13)**:2525-2527.
51. Jansen R, Bussemaker HJ, Gerstner M: **Revisiting the codon adaptation index from a whole-genome perspective: analyzing the relationship between gene expression and codon occurrence in yeast using a variety of models.** *Nucleic Acids Res* 2003, **31(8)**:2242-2251.
52. Lithwick G, Margalit H: **Hierarchy of sequence-dependent features associated with prokaryotic translation.** *Genome Res* 2003, **13(12)**:2665-2673.
53. Ringquist S, Shinedling S, Barrick D, Green L, Binkley J, Stormo GD, Gold L: **Translation initiation in Escherichia coli: sequences within the ribosome-binding site.** *Mol Microbiol* 1992, **6(9)**:1219-1229.
54. Hartz D, McPheeters DS, Gold L: **Influence of mRNA determinants on translation initiation in Escherichia coli.** *J Mol Biol* 1991, **218(1)**:83-97.
55. Ma J, Campbell A, Karlin S: **Correlations between Shine-Dalgarno sequences and gene features such as predicted expression levels and operon structures.** *J Bacteriol* 2002, **184(20)**:5733-5745.
56. Ozbudak EM, Thattai M, Kurtser I, Grossman AD, van Oudenaarden A: **Regulation of noise in the expression of a single gene.** *Nat Genet* 2002, **31(1)**:69-73.
57. Raser JM, O'Shea EK: **Noise in gene expression: origins, consequences, and control.** *Science* 2005, **309(5743)**:2010-2013.
58. Swain PS, Elowitz MB, Siggia ED: **Intrinsic and extrinsic contributions to stochasticity in gene expression.** *Proc Natl Acad Sci U S A* 2002, **99(20)**:12795-12800.
59. Kaminishi T, Wilson DN, Takemoto C, Harms JM, Kawazoe M, Schlutzenzen F, Hanawa-Suetsugu K, Shirouzu M, Fucini P, Yokoyama S: **A Snapshot of the 30S Ribosomal Subunit Capturing mRNA**

- via the Shine-Dalgarno Interaction. *Structure* 2007, **15(3)**:289-297.
60. Cormack BP, Valdivia RH, Falkow S: **FACS-optimized mutants of the green fluorescent protein (GFP)**. *Gene* 1996, **173(1 Spec No)**:33-38.
  61. Blattner FR, Plunkett G 3rd, Bloch CA, Perna NT, Burland V, Riley M, Collado-Vides J, Glasner JD, Rode CK, Mayhew GF, Gregor J, Davis NW, Kirkpatrick HA, Goeden MA, Rose DJ, Mau B, Shao Y: **The complete genome sequence of Escherichia coli K-12**. *Science* 1997, **277(5331)**:1453-1474.
  62. Information NCB: **National Center of Biotechnology Information**. [[ftp://ftp.ncbi.nih.gov/genomes/Bacteria/Escherichia\\_coli\\_K12](ftp://ftp.ncbi.nih.gov/genomes/Bacteria/Escherichia_coli_K12)].
  63. server DINAM: **DINAMelt web server**. [<http://www.bioinfo.rpi.edu/applications/hybrid/>].
  64. CodonW: **CodonW**. [<http://www.molbiol.ox.ac.uk/cu/>].

Publish with **BioMed Central** and every scientist can read your work free of charge

*"BioMed Central will be the most significant development for disseminating the results of biomedical research in our lifetime."*

Sir Paul Nurse, Cancer Research UK

Your research papers will be:

- available free of charge to the entire biomedical community
- peer reviewed and published immediately upon acceptance
- cited in PubMed and archived on PubMed Central
- yours — you keep the copyright

Submit your manuscript here:  
[http://www.biomedcentral.com/info/publishing\\_adv.asp](http://www.biomedcentral.com/info/publishing_adv.asp)







**Vimberg, V., Xiong, L., Bailey, M., Tenson, T., Mankin, A. 2000.**  
Peptide-mediated macrolide resistance reveals possible specific  
interactions in the nascent peptide exit tunnel.  
Mol Microbiol. 54(2):376–85.

# Peptide-mediated macrolide resistance reveals possible specific interactions in the nascent peptide exit tunnel

Vladimir Vimberg,<sup>1</sup> Liqun Xiong,<sup>2</sup> Marne Bailey,<sup>2</sup> Tanel Tenson<sup>1</sup> and Alexander Mankin<sup>2\*</sup>

<sup>1</sup>*Institute of Technology, Tartu University, Tartu 51010, Estonia.*

<sup>2</sup>*Center for Pharmaceutical Biotechnology, University of Illinois, Chicago, IL 60607, USA.*

## Summary

**Expression of specific short peptides can render cells resistant to macrolide antibiotics. Peptides conferring resistance to structurally different macrolides including oleandomycin, azithromycin, azaerythromycin, josamycin and a ketolide cethromycin were selected from a random pentapeptide expression library. Analysis of the entire collection of the resistance peptides allowed their classification into five distinct groups according to their sequence similarity and the type of resistance they confer. A strong correlation was observed between the structures of macrolide antibiotics and sequences of the peptides conferring resistance. Such a correlation indicates that sequence-specific interactions between the nascent peptide and the macrolide antibiotic and/or the ribosome can occur in the ribosomal exit tunnel.**

## Introduction

The nascent peptide exit tunnel is one of the most enigmatic regions in the ribosome and was originally viewed as a passive conduit for the growing polypeptide. It is now starting to emerge as a functional entity where specific interactions between the ribosome, the nascent peptides, and sometimes auxiliary molecules, can actively affect ribosomal functions (Gong and Yanofsky, 2002; Nakatogawa and Ito, 2002; Tenson and Ehrenberg, 2002; Jenni and Ban, 2003). The results of such interactions may have profound effects on the expression of specific proteins, or, when it comes to drugs that bind in the exit tunnel, on the overall protein synthesis in the cell. Nevertheless, the molecular details of interactions that occur in the exit tunnel remain obscure.

Macrolides are a large family of clinically important anti-

biotics that inhibit bacterial growth by binding to the exit tunnel of the large ribosomal subunit and interfering with protein synthesis (Vazquez, 1975) and large ribosomal subunit assembly (Chittum and Champney, 1995). The core structure of macrolide drugs is a 14-, 15- or 16-member lactone ring decorated with one or several neutral or amino sugars (Fig. 1). The 14-member ring erythromycin represents the first generation of macrolides and was the first widely used drug of this class. Later on, several derivatives with improved efficacy were developed. These include 14-member ring drugs like clarithromycin and roxithromycin, the 15-member ring azithromycin, as well as some 16-member ring derivatives, such as josamycin (Bryskier, 1995). The continuous spread of macrolide-resistant pathogens prompted a search for new compounds capable of overcoming common resistance mechanisms, especially methylation of the rRNA target site. This quest resulted in the development of ketolides, which exhibit increased affinity to the ribosome as well as apparent lower sensitivity to known mechanisms of resistance. These 14-member ring drugs are characterized by the presence of a keto group instead of the cladinose sugar at the C3 position of the lactone ring, an 11,12-carbamate cycle and an extended alkyl-aryl or quinolylallyl side chains (Alvarez-Elcoro and Enzler, 1999; Bryskier, 2001; Zhong and Shortridge, 2001).

The binding site of macrolides is located just outside the peptidyl transferase centre near the narrowest portion of the nascent polypeptide exit tunnel (Mao and Robishaw, 1971; Nissen *et al.*, 2000; Schlünzen *et al.*, 2001; 2003; Hansen *et al.*, 2002; Tenson and Ehrenberg, 2002; Berisio *et al.*, 2003a,b). Tight binding of the macrolide is achieved through hydrophobic and van der Waals interactions of the lactone ring with the RNA-based tunnel surface as well as hydrogen bonding of the macrolide sugar residues to rRNA (Schlünzen *et al.*, 2001; Hansen *et al.*, 2002). Different macrolide compounds bind to the ribosome with a similar orientation of the lactone ring, sharing a set of contacts with 23S rRNA. The universal interactions of macrolides with the target site are additionally supplemented by drug-specific contacts with RNA. For example, the acetaldehyde group at the C6 position of 16-member ring macrolides may form a covalent bond with N6 of rRNA residue A2062; whereas the extended alkyl-aryl side chains of ketolides and the mucinose sugar of tylosin are likely to form direct contacts with domain II

Accepted 24 June, 2004. \*For correspondence. E-mail shura@uic.edu; Tel. (+1) 312 413 1406; Fax (+1) 312 413 9303.

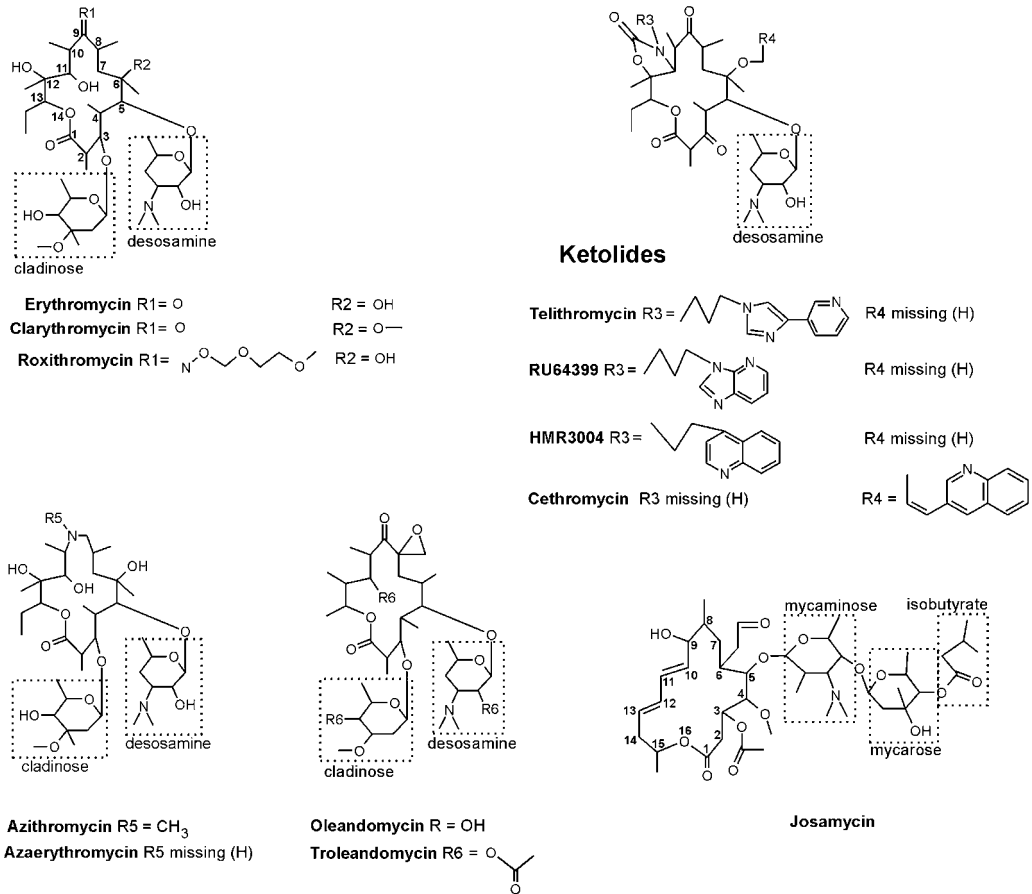


Fig. 1. Chemical structures of representative macrolide antibiotics.

of 23S rRNA (Hansen *et al.*, 1999; 2002; Xiong *et al.*, 1999; Douthwaite *et al.*, 2000; Garza-Ramos *et al.*, 2002; Liu and Douthwaite, 2002; Schlünzen *et al.*, 2003).

The location of the drug binding site, the chemical structure of the antibiotic and the mode of drug–ribosome interactions define the mechanism of macrolide action. Macrolides can bind to either the vacant ribosome or a translating ribosome carrying a very short nascent peptide while ribosomes that carry longer nascent peptide chains are refractory to the drug (Tai *et al.*, 1974; Contreras and Vazquez, 1977; Andersson and Kurland, 1987; Tenson *et al.*, 2003). Binding of macrolides at the exit tunnel constriction jams the tunnel, leading to arrest of protein synthesis during early rounds of translation. Inhibition of translation elongation, at a step when the nascent peptide is only few amino acids long, leads eventually to the dis-

sociation of peptidyl-tRNA from the ribosome (Otaka and Kaji, 1975; Menninger and Otto, 1982; Tenson *et al.*, 2003). Because the dissociated peptidyl-tRNAs are not recycled in the cell efficiently, this ‘drop-off’ causes depletion of free tRNA pools and is apparently another important factor contributing to the inhibition of protein synthesis (Heurgué-Hamard *et al.*, 1996; 2000; Ontiveros *et al.*, 1997; Tenson *et al.*, 1999). A correlation appears to exist between the space available for the nascent peptide within the drug-bound ribosome and the average length of peptides on the peptidyl-tRNAs that dissociate from ribosomes under the influence of different macrolides (Tenson *et al.*, 2003). Josamycin, a 16-member macrolide that has a C5 mycaminose-mycarose sugar moiety that extends towards the peptidyl transferase centre, can hamper formation of even the very first peptide bond, and causes

efficient dissociation of peptidyl-tRNAs containing 2-, 3- or 4-amino acid residues (Mao and Robishaw, 1971; Poulsen *et al.*, 2000; Hansen *et al.*, 2002; Tenson *et al.*, 2003). Erythromycin, which lacks a mycaminose-mycarose sugar, leaves more room and induces dissociation of peptidyl-tRNAs containing 6-, 7- or 8-amino acid residues. Telithromycin, a representative of ketolides that all lack the cladinose sugar, allows polymerization of 9- to 10-amino acid residues before peptidyl-tRNA dissociates. Furthermore, side chain idiosyncrasies among the various macrolide drugs result in the presentation of different functional groups for interaction with the nascent polypeptide synthesized by the ribosome. This suggests that the effect of macrolides on nascent peptide elongation and peptidyl-tRNA dissociation may be protein sequence-specific.

Peptide mediated macrolide resistance is another phenomenon where correlation between the structures of nascent peptides and macrolide antibiotics is observed. Translation of specific short peptides in the bacterial cell was found to render cells resistant to macrolides (in this paper, we will refer to the resistance peptides as 'R-peptides') (Tenson *et al.*, 1996). These *cis*-acting R-peptides are thought to displace the macrolide molecule from its binding site in the ribosome, thus increasing the fraction of drug-free ribosomes in the cell. While hydrophobic pentapeptides containing Leu or Ile in the third amino acid position confer resistance to erythromycin and some of its derivatives, R-peptides conforming to a different consensus sequence (containing a positively charged amino acid in the second position) confer resistance to ketolides (Tenson *et al.*, 1997; Tripathi *et al.*, 1998; Tenson and Mankin, 2001).

In order to gain better understanding of the correlation between the sequences of the resistance pentapeptides and the structures of the macrolide drugs, we extended our study of peptide-mediated resistance. Here, we include drugs that differ substantially in the structure of the lactone ring as well as the nature of the side chains: oleandomycin (a 14-member macrolide), cethromycin (formerly ABT 773, a ketolide), azithromycin and azaerythromycin (15-member macrolides) and josamycin (a 16-membered macrolide). Significantly different peptides were found to confer resistance to diverse macrolide drugs. The results of the current study indicate that not only each macrolide antibiotic forms distinctive contacts with the ribosome, but that they also may establish specific interactions with the growing polypeptide chain.

## Results

Peptides causing resistance to macrolide antibiotics (R-peptides) were selected from a five-codon random mini-gene expression library (Fig. 2) (Tenson *et al.*, 1997). In

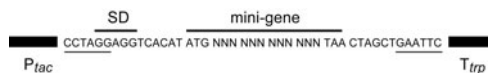


**Fig. 2.** The structure of a random-sequence mini-gene region in the pPOT1AE plasmid used for the selection of R-peptides (Tenson *et al.*, 1997). Positions of the mini-gene, including its start codon, four random codons (12 random nucleotide positions), terminator codon as well as its Shine–Dalgarno translation initiation signal (SD) are marked by horizontal lines above the sequence. Promoter ( $P_{tac}$ ) and terminator ( $T_{trp}$ ) of the mini-gene are shown by black boxes. The *A/II* and *EcoR1* restriction sites used for construction of the random mini-gene library are underlined.

this library, the plasmid-encoded mini-genes are composed of an initiation codon, four randomized codons and a termination codon. The mini-genes are equipped with a Shine–Dalgarno translation initiation sequence (Shine and Dalgarno, 1975) and are expressed under the control of the IPTG-inducible  $P_{tac}$  promoter (de Boer *et al.*, 1983). Macrolide resistant *Escherichia coli* clones expressing R-peptides were selected on LB agar plates containing ampicillin and IPTG that were supplemented with one of the macrolide antibiotics at concentrations corresponding to  $1.5 \times -2 \times$  MIC. A total of 0.1–0.2% of the clones showed resistance. Retransforming the plasmids isolated from the selected resistant clones into fresh *E. coli* cells, and verifying the IPTG dependence of the resistant phenotype established the causative relation between mini-gene expression and macrolide resistance.

Five different macrolide antibiotics were used to select the R-peptides. These include cethromycin (a 14-member ring ketolide), and the following cladinose-containing macrolides: oleandomycin (14-member ring), azithromycin and azaerythromycin (both 15-member ring) and josamycin (16-member ring) (Fig. 1).

### *Cethromycin*

Cethromycin, a ketolide, contains a quinolyallyl side chain, which is attached to C6 of the lactone ring (R4 in Fig. 1). In the ribosome-bound form of the drug, the side chain extends towards helix 35 in domain II of 23S rRNA and establishes interactions, which are important both for the high affinity of the ketolide as well as the positioning of the drug molecule in the ribosome (Garza-Ramos *et al.*, 2002; Schlünzen *et al.*, 2003). Previously we identified peptides that confer resistance to ketolides of the telithromycin group, which all had an alkyl-aryl side chain attached to the 11,12-carbamate group on the opposite side of the lactone ring (R3 in Fig. 1) (Tripathi *et al.*, 1998; Tenson and Mankin, 2001). Those peptides were characterized by the presence of a positively charged amino acid in the second amino acid position and high representation of hydrophobic amino acids throughout the rest of the peptide sequence. It remained unclear whether the nature of ketolide R-peptides would be influenced by the site of

attachment of the functionally important side chain of the ketolide drugs.

The cethromycin R-peptides selected in this study are shown in Fig. 3. All but one of the cethromycin R-peptides contain either Lys or Arg in the second amino acid position. All of the other variable peptide positions (with the

exception of Tyr in the MRVYR peptide) were represented exclusively by either hydrophobic or positively charged amino acids. Thus, cethromycin R-peptides share the major characteristics with R-peptides of the telithromycin group. This similarity indicates that the site of attachment of the alkyl-aryl or quinolylalyl side chain to the lactone

### Cethromycin

ATG AAA TTA AAA CTC MKLKL  
 ATG AAA CTG AAG CTC MKLKL  
 ATG AAA ATG AAA GTT MKMKV  
 ATG AAA ATG AAA CTC MKMKL  
 ATG CGC TTT TTT GTC MRFFV  
 ATG CGG TTC TTT GTT MRFFV  
 ATG CGG TTC TTT GCT MRFFA  
 ATG AAG TTC TTT GTT MKFFV  
 ATG CGA GTA TAC CGA MRVYR  
 ATG AGG CGT TTT ATT MRRFI  
 ATG CTT CGT TGG TGG MLRWW

### Oleandomycin

ATG AGA AAG AAG TAT MRKKY  
 ATG CCG AAG AAA TAC MPKKN  
 ATG ATC AAA AGA TAC MIKRY  
 ATG TAT AAA AGA TAC MYKRY  
 ATG GTA CGA AAA TAC MVRKY  
 ATG GTA GTA AAA CTA MVVKL  
 ATG TCG TGG AAA ATA MSWKI  
 ATG CTT TAC AAA ATC MLYKI  
 ATG AGA TTA AAA ATA MRLKI  
 ATG TAC AGA ATT TGG MYRIW  
 ATG GTC CGT ATA TAT MVRIY  
 ATG AGA ACA CAC ATA MRTHI

### Josamycin

ATG TTC CTA GTA TGA MFLV  
 ATG TTT TCT TAT TTA MFSYL  
 ATG TTC AAC AAG AGA MFNKR  
 ATG TAT ACG ATG TTG MYTML  
 ATG TTT TGT TTG TTT MFCLF  
 ATG TTT AAA GCT CTA MFKAL  
 ATG TAT TAC AAT TTG MYYNL  
 ATG TTC TAC AAA AAA MFYKK  
 ATG TTT TGC GCT TTG MFCAL  
 ATG TTT AGT ATC TTA MFSIL  
 ATG TAT GAG TGT CGA MYECR  
 ATG TTT GTA TCA TTG MFVSL

### Azithromycin

ATG TTG TTG AGG GTT MLLRV  
 ATG TTC TTG AAA GTT MFLKV  
 ATG ATT TTG ATG GTT MILMV  
 ATG GTT TTG TTT GTT MVLFV  
 ATG TTT TTA AAG TTA MFLKL  
 ATG CTT TTA CGT ATC MLLRI  
 ATG TTG CTG CGT ACG MLLRT  
 ATG ATA CTT AAA ACC MILKT  
 ATG ATT TTA CGG TGC MILRC  
 ATG TTT TTA CGT TGT MFLRC  
 ATG GTA CTA CGT ACG MVLRT  
 ATG ATT TTA AAA CAG MILKQ  
 ATG CAG TTA AAA GTA MQLKV  
 ATG ACA TTA AAA GTC MTLKV  
 ATG TAT AAG ATT TAT MYKIY

### Azaerythromycin

ATG TTG TTA TTG GTG MLLLV  
 ATG CTG TTG CTG GTG MLLLV  
 ATG CTA TTG TTT GTG MLLFV  
 ATG GTT CTT CGG GTA MVLRV  
 ATG GTT TTG CGT ATG MVLRM  
 ATG ACA TTA AAA GTC MTLKV  
 ATG GTT TTA CAG CTA MVLQL  
 ATG GTA TTG CTT TGG MVLWV  
 ATG TTT TGG TTG TGG MFWLW  
 ATG GCT TGG TTG GTT MAWLW  
 ATG GTT TGG TTG GTA MVWLW  
 ATG GCG TTT TTT GTT MAFVW  
 ATG TAC ATG TTT ACA MYMFT  
 ATG CCA ATG TTG CTG MPMLL  
 ATG TTG CGA ATG GTG MLRMV  
 ATG CTA CGA CTG TAT MLRLY

A - Alanine      G - Glycine      M - Methionine      S - Serine  
 C - Cysteine    H - Histidine    N - Asparagine    T - Tyrosine  
 D - Aspartic acid    I - Isoleucine    P - Proline        V - Valine  
 E - Glutamic acid    K - Lysine        Q - Glutamine     W - Tryptophan  
 F - Phenylalanine    L - Leucine        R - Arginine        Y - Tyrosine

Fig. 3. Amino acid sequences of the R-peptides conferring resistance to various macrolides. For convenience, the one-letter abbreviations of amino acids are defined at the bottom of the figure.

ring of the ketolide molecule does not significantly affect the binding of ketolides to the ribosome and/or their interaction with the nascent peptide. This conclusion correlates well with the similar protection patterns produced by telithromycin and cethromycin on the rRNA of *E. coli* ribosomes in RNA probing experiments (Hansen *et al.*, 1999; Xiong *et al.*, 1999; Garza-Ramos *et al.*, 2002) and with the generally similar mode of binding of telithromycin and cethromycin to *Deinococcus radiodurans* ribosomes as seen by crystallographic analysis (Berisio *et al.*, 2003a; Schlunzen *et al.*, 2003).

#### Oleandomycin

R-peptides selected previously with 14-member ring, cladinose-containing drugs such as erythromycin and its derivatives (clarithromycin, roxithromycin and RU 69874) were characterized by a well-defined consensus sequence: a bulky hydrophobic amino acid in the second position, Leu or Ile, in the third position, a preference for a hydrophobic amino acid in the fourth position and a prevalence of Val at the C-terminus (Tenson *et al.*, 1997; Tenson and Mankin, 2001). Surprisingly, the peptides conferring resistance to oleandomycin, another 14-member ring cladinose-containing macrolide, were substantially different from the erythromycin R-peptides (Fig. 3). None of the oleandomycin R-peptides had Leu or Ile in the third position; instead a positively charged amino acid was frequently present at position 3 and/or 4 of the peptide. Because of the high content of positively charged amino acids, oleandomycin R-peptides appear to more closely resemble the ketolide R-peptides than the peptides conferring resistance to other 14-member cladinose-containing macrolides.

Oleandomycin differs from erythromycin and related compounds by the presence of an 8-oxirane cycle, a methyl instead of an ethyl group attached at C13 of the lactone ring and the lack of a 12-hydroxyl. Variations in substitutions at C12 and C13 may directly contribute to the unusual binding of oleandomycin. The C13 ethyl of erythromycin reaches towards the loop of helix 35 in domain II of 23S rRNA (Schlunzen *et al.*, 2001). Shortening this side chain by one carbon atom in oleandomycin may affect possible interaction with this rRNA region. The C12 hydroxyl of erythromycin forms a hydrogen bond with O4 of rRNA residue U2609 (Schlunzen *et al.*, 2001). The lack of this hydroxyl in oleandomycin should destabilize this contact. Interestingly, both helix 35 and U2609 are implicated in specific interactions with ketolides (Hansen *et al.*, 1999; Xiong *et al.*, 1999; 2002; Schlunzen *et al.*, 2001; Garza-Ramos *et al.*, 2002). Thus, some of the peculiar contacts of oleandomycin with the ribosome affect the ribosome–drug interactions that distinguish ketolides from cladinose-containing macrolides. It is con-

ceivable therefore, that the position of oleandomycin in the ribosome may structurally resemble more closely the binding of ketolides than that of the erythromycin-type antibiotics, which can account for the similarity of oleandomycin and ketolide R-peptides. Noteworthy, troleandomycin, a drug structurally similar to oleandomycin, binds to the *D. radiodurans* ribosomes in a configuration notably different from that of erythromycin (Berisio *et al.*, 2003b).

#### Azithromycin and azaerythromycin

Azithromycin and azaerythromycin are 15-member ring macrolides. Extending the 14-atom lactone ring by an additional nitrogen atom alters the ring conformation resulting in a novel interaction with rRNA base 2586 as seen in the crystallographic complexes of azithromycin with the *D. radiodurans* ribosome (Schlunzen *et al.*, 2003).

Most of the selected azithromycin R-peptides adhere to a well-defined consensus (Fig. 3). As with the previously studied erythromycin R-peptides, all but one of the azithromycin R-peptides contain Leu in the third amino acid position and show preference for a bulky hydrophobic amino acid in the second position (Leu, Ile, Phe, Val). However, in contrast to the erythromycin R-peptides, the peptides selected with azithromycin show a strong preference for a positively charged amino acid (Lys or Arg) in the fourth position.

In order to verify the importance of a positively charged penultimate amino acid for azithromycin resistance, we compared the ability of an azithromycin R-peptide, MLLRV, and a previously selected erythromycin R-peptide, MLLLV, to confer resistance to these drugs. The erythromycin resistance afforded by both peptides was comparable ( $>1 \text{ mg ml}^{-1}$ ), however, the MLLRV peptide conferred a higher level of resistance to azithromycin ( $\text{MIC} > 200 \text{ } \mu\text{g ml}^{-1}$ ) than the MLLLV peptide ( $\text{MIC} = 120 \text{ } \mu\text{g ml}^{-1}$ ) (data not shown). Thus, the presence of a positively charged amino acid in the fourth position contributes specifically to the R-peptide's ability to confer resistance to azithromycin.

Remarkably, while most of the azithromycin R-peptides conformed to the consensus sequence, one of the selected peptides (MYKIY) was notably different. It lacked both Leu in the third position and a positively charged amino acid in the fourth position. Nevertheless, in spite of the deviation from the consensus, the level of azithromycin resistance conferred by the MYKIY peptide was comparable to that exerted by the 'consensus' peptides (Fig. 4).

The structural differences between azaerythromycin and azithromycin are minute. Azaerythromycin lacks a single methyl group at the nitrogen atom of the azithromycin azalide ring (Fig. 1). However, this small alteration in drug structure appears to result in reduced stringency of the constraints imposed on the R-peptide's structure. The

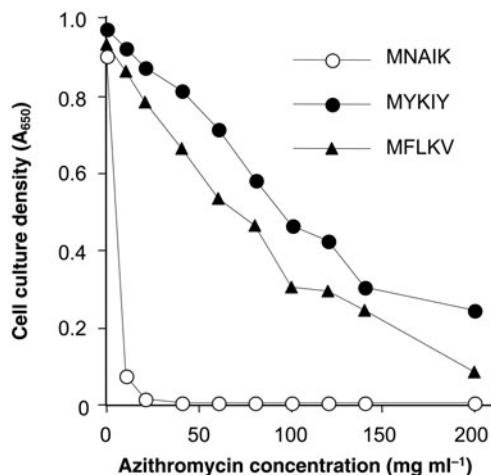


Fig. 4. Effect of azithromycin on growth of cells expressing one of the azithromycin consensus R-peptides, MFLKV, a 'non-consensus' R-peptide, MYKIY, or a control peptide, MNAIK.

requirements for Leu in the third peptide position and for the positively charged amino acid in the fourth position were more relaxed in the case of the azaerythromycin R-peptides (Fig. 3). Because the N-methyl group of azithromycin does not contribute significantly to interactions with the ribosome (Hansen *et al.*, 2002; Schlünzen *et al.*, 2003), it is likely that it affects interactions of the drug with the nascent peptide.

#### Josamycin

Josamycin, a 16-member ring macrolide, contains a mycaminoise-mycarose-isobutyrate side chain that, by analogy with carbomycin, is likely to reach into the ribosomal peptidyl transferase centre (Hansen *et al.*, 2002). The drug leaves a fairly small space for the nascent peptide, and may cause the drop-off of peptidyl-tRNA with a peptidyl moiety as short as 2–3 amino acids (Tenson *et al.*, 2003). However, longer peptides can apparently be synthesized by a ribosome complexed with josamycin, as some of the pentapeptides expressed in the mini-gene library conferred resistance to this macrolide (Fig. 3). The consensus sequence of the josamycin peptides was drastically different from that seen with other macrolides. Leucine, which was frequently seen in position 3 in the erythromycin R-peptides, is often found at the C-terminus of the josamycin pentapeptides. The second amino acid position in all of the josamycin R-peptides was occupied by an aromatic amino acid, phenylalanine or tyrosine. Among these two amino acids, phenylalanine rendered peptides more active as these R-peptides conferred slightly higher levels of josamycin resistance than R-pep-

tides containing tyrosine at the same position (data not shown).

#### High specificity of peptide-mediated resistance

Our previous data (Tenson *et al.*, 1997) indicated that at least some of the erythromycin R-peptides could increase cell resistance to other macrolides. This prompted us to examine the spectrum of resistance afforded by R-peptides, including ketolide-, oleandomycin-, and josamycin R-peptides. The experimental data show that R-peptide resistance is rather specific (Fig. 5). Peptides selected with a particular antibiotic provide the highest level of resistance to this drug. In most cases peptides confer little or no cross-resistance to other types of macrolides. In agreement with our conclusion of the clustering of the oleandomycin- and ketolide R-peptides, a considerable cross-resistance to oleandomycin was conferred by one of the ketolide R-peptides (MRFFV).

#### Discussion

Here, we report the isolation of peptide mini-genes whose expression renders cells resistant to various macrolide antibiotics. Different peptides confer resistance to structurally different macrolides and generally, little cross-resistance is observed.

Strictly speaking, the selection experiments cannot directly distinguish whether the immediate cause of drug resistance is the peptide itself or its mRNA (or even the mini-gene). Previously reported data indicated the importance of mini-gene translation for manifestation of the resistance phenotype (Tenson *et al.*, 1996). Furthermore, examination of the peptide sequences and sequences of their respective mini-genes show an extensive variation in mRNA structure compared to the structure of the encoded peptides (Fig. 3). For example, two of the mini-genes identified in cethromycin-resistant clones code for the same R-peptide, MKLKL, while four out of the 12 random nucleotide positions in the mini-gene are different. Similarly, the MRFFV R-peptide was encoded in two independently isolated mini-genes that differed at three out of 12 random positions. These observations are in agreement with the view that it is the peptide structure and possible interactions of the peptide with the drug and/or ribosome, rather than the mRNA sequence, that are responsible for the resistance.

How does translation of short peptides render cells resistant to ribosome-targeted macrolide antibiotics? A few years ago we proposed a 'bottle-brush' model in which synthesis of an R-peptide on the ribosome leads, through an unknown mechanism, to displacement of the drug from the ribosome. The drug-free ribosome may have enough time to initiate synthesis of one of the cellular proteins and polymerize its first few amino acids before the antibiotic

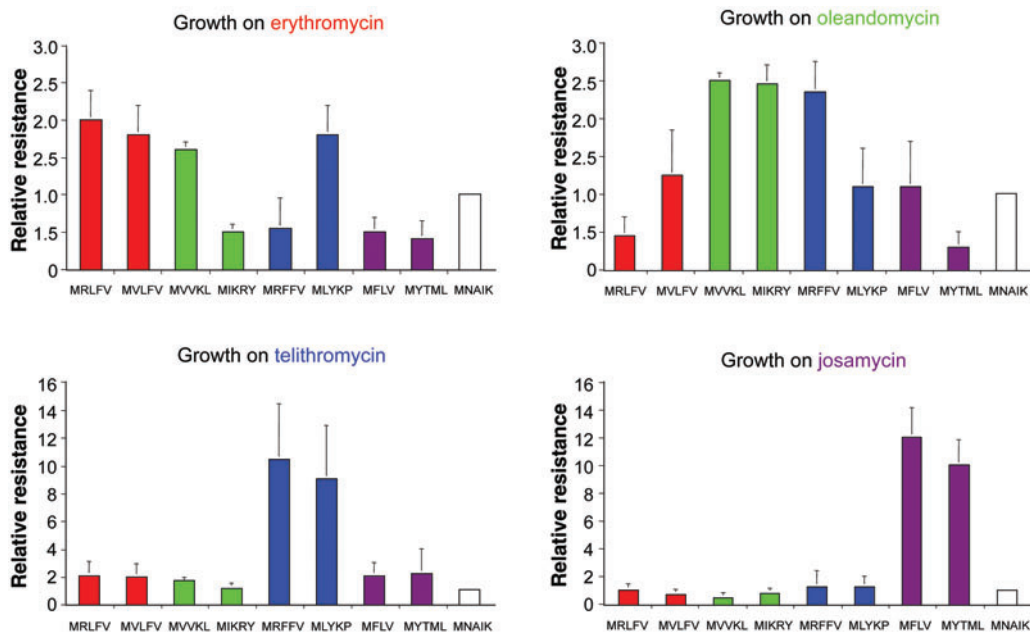


**Fig. 5.** Relative macrolide resistance of cells expressing erythromycin- (red), oleandomycin- (green), ketolide- (blue-) or josamycin- (magenta) R-peptides. Ketolide R-peptides include the MRFFV peptide, which was selected with cethromycin and ketolides HMR3004 as well as the MLYKP peptide, which was selected previously with the ketolides telithromycin and HMR3004 but did not show up in the cethromycin selection (Tenson and Mankin, 2001). The growth of control cells expressing an unselected peptide, MNAIK, is shown by a white bar. Shown resistance values are the average of at least three independent experiments.

binds again. When the nascent peptide chain becomes longer than 5–10 amino acids, it precludes the binding of a macrolide molecule in the nascent peptide exit tunnel, thus allowing the ribosome to finish synthesis of the polypeptide. In this model, active expression of R-peptide mini-genes simply increases the fraction of drug-free ribosomes in the cell, facilitating protein synthesis in the presence of the drug. The model is supported by the previous findings that the peptides work *in cis*, rendering the ribosome on which they were synthesized resistant to macrolides, as well as the inability of exogenously added synthetic R-peptides to cause macrolide resistance in a cell-free translation system (Tenson *et al.*, 1996). The model is in agreement with the recent finding that the translation of R-peptides in a cell-free system leads to displacement of the drug from the ribosome (M. Lovmar, T. Tenson and M. Ehrenberg, in preparation).

A large variety of R-peptides conferring resistance to different classes of macrolides have been isolated in this and previous studies. Comparison of all of the known R-peptides shows a clear correlation between the amino acid sequences of R-peptides and structures of antibiotics to which they confer resistance. Similar peptides confer resistance to similar drugs, while significant changes in the

macrolide structure call for peptides with notably different consensus sequences. Thus, similar, and often the same, peptides were found in selection experiments with cladinose-containing macrolides of the erythromycin group (Tenson *et al.*, 1997; Tenson and Mankin, 2001). However, when the structure of the drug was significantly changed (as in the transition from erythromycin to ketolides), very different peptides were found to render cells drug-resistant. Even smaller variations in the drug structure may affect the sequence of the peptide required to confer resistance. For example, expanding the erythromycin lactone ring by an additional nitrogen atom, as in azithromycin (a relatively small alteration from the structural standpoint) changes the consensus of the resistance peptides.

Analysis of R-peptides selected in this study as well as those characterized previously allows classification of currently known resistance peptides into five structural classes (Table 1). The peptides of the ERY group include those that confer resistance to 14-member ring macrolides of the erythromycin type (erythromycin, clarithromycin, roxithromycin and RU 69874) (Tenson and Mankin, 2001). The most notable feature of these peptides is the presence of Leu or Ile in the third position. AZI peptides, which include azithromycin and azaerythromycin R-

**Table 1.** Classification of R-peptides into structural groups.

Class	Representative antibiotics	Amino acid position					Reference
		1	2	3	4	5	
ERY	Erythromycin Clarithromycin Roxithromycin RU69874	Met	Bulky Hydrophobic	<b>Leu or Ile</b>	Hydrophobic	Val	Tenson <i>et al.</i> (1997) Tenson and Mankin (2001) Tenson and Mankin (2001) Tenson and Mankin (2001)
AZI	Azithromycin Azaerythromycin	Met	Bulky Hydrophobic	<b>Leu or Ile</b>	<b>Arg or Lys</b>	× <sup>a</sup>	This study This study
OLE	Oleandomycin	Met	×	<b>Arg or Lys</b>	<b>Arg or Lys</b>	Tyr or Ile	This study
KET	Telithromycin RU64399 HMR3004 ABT377	Met	<b>Arg or Lys</b>	Hydrophobic or Arg	Hydrophobic or Lys	×	Tenson and Mankin (2001) Tenson and Mankin (2001) Tripathi <i>et al.</i> (1998) This study
JOS	Josamycin	Met	<b>Phe or Tyr</b>	×	×	Leu	This study

a. × – no obvious amino acid preference.

peptides, are generally similar to ERY peptides, but they fall into a separate group because of a strong preference for a positively charged amino acid in the fourth position. Positively charged amino acids are also prevalent in the third and fourth position of the OLE (oleandomycin) R-peptides. The high frequency of occurrence of Arg or Lys in the third peptide position distinguishes OLE peptides from the ERY and AZI R-peptides. KET (ketolide) R-peptides, which include R-peptides conferring resistance to cethromycin, telithromycin, HMR3004 and RU64399 ketolides, show mixed amino acid preference in positions 3 and 4, which are commonly represented by either hydrophobic or positively charged amino acids. However, the second amino acid position in these peptides is represented predominantly by positively charged amino acids. Finally, JOS (josamycin) R-peptides require an aromatic amino acid, phenylalanine or tyrosine, at position 2.

Drawing clues from the correlation between the amino acid sequences of R-peptides and the chemical structures of the drugs, one can envision a possible mechanism of drug displacement based on a direct interaction between the macrolide molecule and the peptide. Structure-specific interaction with the nascent R-peptide may alter drug conformation resulting in reduced affinity for the ribosome. Although no high-affinity binding between synthetic R-peptides and antibiotics was observed in solution (Tenson *et al.*, 1996), such interaction may be possible in the ribosome where peptide structure is expected to be constrained by its contacts with the exit tunnel. Reduced flexibility of the peptide in the tunnel should reduce the entropic cost of the peptide–drug interaction.

Though we favour the model of a direct drug–peptide interaction, an alternative model cannot be excluded in which specific interactions between the peptide and the ribosome may allosterically affect rRNA conformation in the drug binding site resulting in a lower affinity of the drug for the ribosome. Such a view would be in line with the

recent findings of sequence-specific interactions between the ribosome and the nascent peptide observed in other experimental systems (Gong and Yanofsky, 2002; Nakatogawa and Ito, 2002; Fang *et al.*, 2004), reviewed in Tenson and Ehrenberg (2002) and with NMR studies of peptide–ribosome interactions (Verdier *et al.*, 2002). However, this model does not provide a direct explanation of why different drugs are removed by different R-peptides.

Only short peptides, 3- to 6 amino acids long, are able to confer macrolide resistance, while longer peptides are not active (Tenson *et al.*, 1997). What is the reason for such a strict peptide size constraint? One interesting possibility is that termination of translation plays an active role in the dissociation of the drug from the ribosome. Binding of a release factor or other factors involved in translation termination may affect rRNA conformation in the vicinity of the peptidyl transferase centre (Polacek *et al.*, 2003; Rawat *et al.*, 2003) possibly resulting in a reduced affinity for the macrolide molecule. Combined with the direct or an allosteric effect of the R-peptide on drug binding, the structural transitions in rRNA that accompany translation termination might be sufficient to oust a drug from the ribosome.

At the moment, peptide-mediated drug resistance appears to be confined to the macrolide class of ribosome-targeted antibiotics. Even though macrolides have overlapping binding sites with the structurally dissimilar streptogramin-B and lincosamide drugs (Schlünzen *et al.*, 2001; Hansen *et al.*, 2003; Harms *et al.*, 2004), we were unable to select R-peptides that could render cells resistant to either clindamycin (lincosamide) or quinupristin (streptogramin B) (V. Vimberg, T. Tenson, L. Xiong and A. Mankin, unpubl. results). This restriction of the peptide-mediated resistance to macrolide antibiotics could reflect specific structural differences in drug–ribosome interactions or in the kinetics of drug binding.

The recent advances in crystallographic studies of ribo-

some–drug interactions reveal the differences in precise positioning of individual macrolides in the ribosome. However, the poor understanding of peptide placement in the ribosomal exit tunnel precludes direct modelling of the R-peptide–ribosome or R-peptide–drug contacts. The better we understand how the ribosome ‘deals’ with the nascent peptide, the more we will learn about the mode of action of macrolide antibiotics and their mechanisms of resistance. There is hope, however, that studying R-peptides may in turn advance the general knowledge of how the ribosome works and how it interacts with nascent peptides. Suspected specific interactions between R-peptides and ribosome-bound antibiotics may reveal these peptides as favourable candidates for biochemical and crystallographic investigation of ribosome–nascent peptide complexes.

### Experimental procedures

#### Antibiotics, strains and plasmids

Erythromycin, oleandomycin and josamycin were purchased from Sigma, telithromycin was obtained from Aventis Pharma, azithromycin and azaerythromycin were from US Pharmacopeia and cethromycin was from Abbott. *E. coli* strain JM109 [*endA1*, *recA1*, *gyrA96*, *thi*, *hsdR17* ( $r_K^-$ ,  $m_K^+$ ), *relA1*, *supE44*,  $\Delta$ (*lac-proAB*), ( $F'$ , *traD36*, *proAB*, *lacI*<sup>q</sup>  $\Delta$ (*lacZ*)M15] (Yanisch-Perron *et al.*, 1985) was used in the selection experiments. Construction of the random five-codon mini-gene expression plasmid library was described previously (Tenson *et al.*, 1997).

#### Selection of mini-genes conferring macrolide resistance

*E. coli* cells, strain JM109, were transformed with the random five-codon mini-gene expression plasmid library and plated onto LB agar plates containing 100  $\mu\text{g ml}^{-1}$  ampicillin, 1 mM IPTG and either oleandomycin (1.5 mg  $\text{ml}^{-1}$ ), azithromycin (100  $\mu\text{g ml}^{-1}$ ), azaerythromycin (75  $\mu\text{g ml}^{-1}$ ), josamycin (1.2 mg  $\text{ml}^{-1}$ ), or Cethromycin (100  $\mu\text{g ml}^{-1}$ ). Plates were incubated 24–48 h at 37°C. Colonies that appeared were streaked onto a pair of plates (with or without 1 mM IPTG) containing 100  $\mu\text{g ml}^{-1}$  ampicillin and the macrolide that was used in the first step of selection. Plasmids were isolated from the clones that exhibited IPTG-dependent macrolide resistance and the mini-gene was sequenced. In addition, the plasmids were retransformed into fresh cells to confirm that the plasmid markers cause the macrolide resistance phenotype.

#### Testing effects of mini-gene expression on the level of macrolide resistance and cross-resistance

Overnight cultures of cells expressing different R-peptides were grown in YT or LB medium containing 100  $\mu\text{g ml}^{-1}$  ampicillin. Cultures were diluted in the same medium to the final density of  $A_{600} = 0.01$ , followed by the addition of IPTG (1 mM final concentration) and one of the macrolide antibiotics: josa-

mycin (300  $\mu\text{g ml}^{-1}$ ), erythromycin (50  $\mu\text{g ml}^{-1}$ ), oleandomycin (400  $\mu\text{g ml}^{-1}$ ) or telithromycin (50  $\mu\text{g ml}^{-1}$ ). Control cultures lacked the macrolide drug. The optical densities of the cultures were recorded when control culture reached  $A_{600}$  of c. 1. Relative resistance was calculated as a ratio of the optical density of the cultures growing with and without the macrolide. The values were normalized to the control culture expressing the peptide MNAIK. This control clone was randomly picked from the original unselected library; the steady-state level of pentapeptide mRNA in this clone was comparable to levels of peptide mRNAs in macrolide resistant clones (data not shown).

### Acknowledgements

We are grateful to Aventis Pharma and Abbott Laboratories for providing some of the drugs used in this study and to Joerg Harms for assisting in comparison of structures of ribosome-bound antibiotics. This work was supported in part by a Research Grant from Abbott Laboratories (to A.S.M.) and The Wellcome Trust International Senior Fellowship (070210/Z/03/Z) and grant from Estonian Science Foundation (5311) (to T.T.).

### References

- Alvarez-Elcoro, S., and Enzler, M.J. (1999) The macrolides: erythromycin, clarithromycin, and azithromycin. *Mayo Clin Proc* **74**: 613–634.
- Andersson, S., and Kurland, C.G. (1987) Elongating ribosomes *in vivo* are refractory to erythromycin. *Biochimie* **69**: 901–904.
- Berisio, R., Harms, J., Schluenzen, F., Zarivach, R., Hansen, H.A., Fucini, P., and Yonath, A. (2003a) Structural insight into the antibiotic action of telithromycin against resistant mutants. *J Bacteriol* **185**: 4276–4279.
- Berisio, R., Schluenzen, F., Harms, J., Bashan, A., Auerbach, T., Baram, D., and Yonath, A. (2003b) Structural insight into the role of the ribosomal tunnel in cellular regulation. *Nat Struct Biol* **10**: 366–370.
- de Boer, H.A., Comstock, L.J., and Vasser, M. (1983) The *tac* promoter: a functional hybrid derived from the *trp* and *lac* promoters. *Proc Natl Acad Sci USA* **80**: 21–25.
- Bryskier, A. (1995) Antibiotic therapy: past, present and future. *Presse Med* **24**: 55–66.
- Bryskier, A. (2001) Telithromycin – an innovative ketolide antimicrobials. *Jpn J Antibiot* **54** (Suppl. A): 64–69.
- Chittum, H.S., and Champney, W.S. (1995) Erythromycin inhibits the assembly of the large ribosomal subunit in growing *Escherichia coli* cells. *Curr Microbiol* **30**: 273–279.
- Contreras, A., and Vazquez, D. (1977) Cooperative and antagonistic interactions of peptidyl-tRNA and antibiotics with bacterial ribosomes. *Eur J Biochem* **74**: 539–547.
- Douthwaite, S., Hansen, L.H., and Mauvais, P. (2000) Macrolide-ketolide inhibition of MLS-resistant ribosomes is improved by alternative drug interaction with domain II of 23S rRNA. *Mol Microbiol* **36**: 183–193.
- Fang, P., Spevak, C.C., Wu, C., and Sachs, M.S. (2004) A nascent polypeptide domain that can regulate translation elongation. *Proc Natl Acad Sci USA* **101**: 4059–4064.
- Garza-Ramos, G., Xiong, L., Zhong, P., and Mankin, A.

- (2002) Binding site of macrolide antibiotics on the ribosome: new resistance mutation identifies a specific interaction of ketolides with rRNA. *J Bacteriol* **183**: 6898–6907.
- Gong, F., and Yanofsky, C. (2002) Instruction of translating ribosome by nascent peptide. *Science* **297**: 1864–1867.
- Hansen, L.H., Mauvais, P., and Douthwaite, S. (1999) The macrolide-ketolide antibiotic binding site is formed by structures in domains II and V of 23S ribosomal RNA. *Mol Microbiol* **31**: 623–632.
- Hansen, J., Ippolito, J.A., Ban, N., Nissen, P., Moore, P.B., and Steitz, T.A. (2002) The structures of four macrolide antibiotics bound to the large ribosomal subunit. *Mol Cell* **10**: 117–128.
- Hansen, J.L., Moore, P.B., and Steitz, T.A. (2003) Structures of five antibiotics bound at the peptidyl transferase center of the large ribosomal subunit. *J Mol Biol* **330**: 1061–1075.
- Harms, J.M., Schlunzen, F., Fucini, P., Bartels, H., and Yonath, A.E. (2004) Alterations at the peptidyl transferase centre of the ribosome induced by the synergistic action of the streptogramins dalopristin and quinupristin. *BMC Biol* **2**: 4.
- Heurgué-Hamard, V., Mora, L., Guarneros, G., and Buckingham, R.H. (1996) The growth defect in *Escherichia coli* deficient in peptidyl-tRNA hydrolase is due to starvation for Lys-tRNA<sup>Lys</sup>. *EMBO J* **15**: 2826–2833.
- Heurgué-Hamard, V., Dinçbas, V., Buckingham, R.H., and Ehrenberg, M. (2000) Origins of minigene-dependent growth inhibition in bacterial cells. *EMBO J* **19**: 2701–2709.
- Jenni, S., and Ban, N. (2003) The chemistry of protein synthesis and voyage through the ribosomal tunnel. *Curr Opin Struct Biol* **13**: 212–219.
- Liu, M., and Douthwaite, S. (2002) Resistance to the macrolide antibiotic tylosin is conferred by single methylations at 23S rRNA nucleotides G748 and A2058 acting in synergy. *Proc Natl Acad Sci USA* **99**: 14658–14663.
- Mao, J.C.-H., and Robishaw, E.E. (1971) Effects of macrolides on peptide-bond formation and translocation. *Biochemistry* **10**: 2054–2061.
- Menninger, J.R., and Otto, D.P. (1982) Erythromycin, carbomycin, and spiramycin inhibit protein synthesis by stimulating the dissociation of peptidyl-tRNA from ribosomes. *Antimicrob Agents Chemother* **21**: 810–818.
- Nakatogawa, H., and Ito, K. (2002) The ribosomal exit tunnel functions as a discriminating gate. *Cell* **108**: 629–636.
- Nissen, P., Hansen, J., Ban, N., Moore, P.B., and Steitz, T.A. (2000) The structural basis of ribosome activity in peptide bond synthesis. *Science* **289**: 920–930.
- Ontiveros, C., Valadez, J.G., Hernández, J., and Guarneros, G. (1997) Inhibition of *Escherichia coli* protein synthesis by abortive translation of phage lambda minigenes. *J Mol Biol* **269**: 167–175.
- Otaka, T., and Kaji, A. (1975) Release of (oligo) peptidyl-tRNA from ribosomes by erythromycin A. *Proc Natl Acad Sci USA* **72**: 2649–2652.
- Polacek, N., Gomez, M.G., Ito, K., Nakamura, Y., and Mankin, A.S. (2003) The critical role of the universally conserved A2602 of 23S ribosomal RNA in the release of the nascent peptide during translation termination. *Mol Cell* **11**: 103–112.
- Poulsen, S.M., Kofoed, C., and Vester, B. (2000) Inhibition of the ribosomal peptidyl transferase reaction by the mycarose moiety of the antibiotics carbomycin, spiramycin and tylosin. *J Mol Biol* **304**: 471–481.
- Rawat, U.B., Zavialov, A.V., Sengupta, J., Valle, M., Grassucci, R.A., Linde, J., et al. (2003) A cryo-electron microscopic study of ribosome-bound termination factor RF2. *Nature* **421**: 87–90.
- Schlünzen, F., Zarivach, R., Harms, J., Bashan, A., Tocilj, A., Albrecht, R., et al. (2001) Structural basis for the interaction of antibiotics with the peptidyl transferase centre in eubacteria. *Nature* **413**: 814–821.
- Schlünzen, F., Harms, J.M., Franceschi, F., Hansen, H.A., Bartels, H., Zarivach, R., and Yonath, A. (2003) Structural basis for the antibiotic activity of ketolides and azalides. *Structure (Camb)* **11**: 329–338.
- Shine, J., and Dalgarno, L. (1975) Determinant of cistron specificity in bacterial ribosomes. *Nature* **254**: 34–38.
- Tai, P.C., Wallace, B.J., and Davis, B.D. (1974) Selective action of erythromycin on initiating ribosomes. *Biochemistry* **13**: 4653–4659.
- Tenson, T., and Ehrenberg, M. (2002) Regulatory nascent peptides in the ribosomal tunnel. *Cell* **108**: 591–594.
- Tenson, T., and Mankin, A.S. (2001) Short peptides conferring resistance to macrolide antibiotics. *Peptides* **22**: 1661–1668.
- Tenson, T., DeBlasio, A., and Mankin, A. (1996) A functional peptide encoded in the *Escherichia coli* 23S rRNA. *Proc Natl Acad Sci USA* **93**: 5641–5646.
- Tenson, T., Xiong, L., Kloss, P., and Mankin, A.S. (1997) Erythromycin resistance peptides selected from random peptide libraries. *J Biol Chem* **272**: 17425–17430.
- Tenson, T., Herrera, J.V., Kloss, P., Guarneros, G., and Mankin, A.S. (1999) Inhibition of translation and cell growth by minigene expression. *J Bacteriol* **181**: 1617–1622.
- Tenson, T., Lovmar, M., and Ehrenberg, M. (2003) The mechanism of action of macrolides, lincosamides and streptogramin B reveals the nascent peptide exit path in the ribosome. *J Mol Biol* **330**: 1005–1014.
- Tripathi, S., Kloss, P.S., and Mankin, A.S. (1998) Ketolide resistance conferred by short peptides. *J Biol Chem* **273**: 20073–20077.
- Vazquez, D. (1975) The macrolide antibiotics. In *Antibiotics III. Mechanism of Action of Antimicrobial and Antitumor Agents*. Corcoran, J.W., and Hahn, F.E. (eds) New York, Heidelberg, Berlin: Springer-Verlag, pp. 459–479.
- Verdier, L., Gharbi-Benarous, J., Bertho, G., Mauvais, P., and Girault, J.P. (2002) Antibiotic resistance peptides: interaction of peptides conferring macrolide and ketolide resistance with *Staphylococcus aureus* ribosomes: conformation of bound peptides as determined by transferred NOE experiments. *Biochemistry* **41**: 4218–4229.
- Xiong, L., Shah, S., Mauvais, P., and Mankin, A.S. (1999) A ketolide resistance mutation in domain II of 23S rRNA reveals proximity of hairpin 35 to the peptidyl transferase centre. *Mol Microbiol* **31**: 633–639.
- Yanisch-Perron, C., Vieira, J., and Messing, J. (1985) Improved M13 phage cloning vectors and host strains: nucleotide sequences of the M13mp18 and pUC19 vectors. *Gene* **33**: 103–119.
- Zhong, P., and Shortridge, V. (2001) The emerging new generation of antibiotic: ketolides. *Curr Drug Targets Infect Disord* **1**: 125–131.



Lovmar, M., Nilsson, K., **Vimberg, V.**, Tenson, T.,  
Nervall, M., Ehrenberg, M. 2006.  
The molecular mechanism of peptide-mediated  
erythromycin resistance. *J Biol Chem.* 281(10):6742–50.

# The Molecular Mechanism of Peptide-mediated Erythromycin Resistance\*<sup>§</sup>

Received for publication, November 4, 2005, and in revised form, December 21, 2005. Published, JBC Papers in Press, January 12, 2006, DOI 10.1074/jbc.M511918200

Martin Lovmar<sup>#1</sup>, Karin Nilsson<sup>‡§1</sup>, Vladimir Vimberg<sup>¶</sup>, Tanel Tenson<sup>¶</sup>, Martin Nervall<sup>||</sup>, and Måns Ehrenberg<sup>‡2</sup>

From the <sup>‡</sup>Department of Cell and Molecular Biology, Molecular Biology Program, Uppsala University, Uppsala S-75124, Sweden

<sup>§</sup>Department of Biometry and Engineering, Swedish University of Agricultural Sciences, S-75007 Uppsala, Sweden, <sup>¶</sup>Institute of Technology, Tartu University, 51010 Tartu, Estonia, and <sup>||</sup>Department of Cell and Molecular Biology, Structural Biology Program, Uppsala University, S-75124 Uppsala, Sweden

The macrolide antibiotic erythromycin binds at the entrance of the nascent peptide exit tunnel of the large ribosomal subunit and blocks synthesis of peptides longer than between six and eight amino acids. Expression of a short open reading frame in 23 S rRNA encoding five amino acids confers resistance to erythromycin by a mechanism that depends strongly on both the sequence and the length of the peptide. In this work we have used a cell-free system for protein synthesis with components of high purity to clarify the molecular basis of the mechanism. We have found that the nascent resistance peptide interacts with erythromycin and destabilizes its interaction with 23 S rRNA. It is, however, in the termination step when the pentapeptide is removed from the peptidyl-tRNA by a class 1 release factor that erythromycin is ejected from the ribosome with high probability. Synthesis of a hexa- or heptapeptide with the same five N-terminal amino acids neither leads to ejection of erythromycin nor to drug resistance. We propose a structural model for the resistance mechanism, which is supported by docking studies. The rate constants obtained from our biochemical experiments are also used to predict the degree of erythromycin resistance conferred by varying levels of resistance peptide expression in living *Escherichia coli* cells subjected to varying concentrations of erythromycin. These model predictions are compared with experimental observations from growing bacterial cultures, and excellent agreement is found between theoretical prediction and experimental observation.

Erythromycin is a clinically important broad-spectrum antibiotic that belongs to the macrolide class. It binds to a site in 23 S rRNA on the large ribosomal subunit (50 S)<sup>3</sup> close to the peptidyl transferase center, near the entrance to the nascent peptide exit tunnel (1). Erythromycin-bound ribosomes can synthesize peptides with lengths between six and eight amino acids, but further peptide elongation is inhibited, and peptidyl-tRNA dissociates prematurely from the ribosome in the drop-off pathway (2). Different macrolides allow formation of peptides with different lengths depending on the space available between the macrolide

and the peptidyl transferase center. This suggests that macrolides act by preventing the nascent peptide from entering the peptide exit tunnel in the 50 S subunit (2). Once a nascent peptide has passed the erythromycin binding site and entered the peptide exit tunnel of a drug-free ribosome, erythromycin cannot bind to the 50 S subunit, which makes the ribosome refractory to the drug until peptide elongation is terminated by a class 1 release factor (3).

The way nascent peptides interact with the exit tunnel is important both for regulation of messenger RNA (mRNA) translation and protein export (4). For example, expression of the ErmC methyltransferase, which causes erythromycin resistance by methylating base A2058 (*Escherichia coli* numbering) at the erythromycin binding site in 23 S rRNA, is regulated by nascent peptide-erythromycin interactions in the peptide exit tunnel. That is, when there is erythromycin in a cell carrying the *ermC* gene, ribosomes are stalled during translation of an open reading frame present in the leader of the *ermC* mRNA. This causes rearrangements of the secondary structure of the leader mRNA, which make the ribosome binding site available for initiation of translation of the ErmC encoding the open reading frame of the *ermC* mRNA. This regulation requires a special sequence of the leader-encoded peptide, suggesting the existence of specific interactions between the peptide, the peptide exit tunnel, and erythromycin (5).

Another example of such specific interactions is the mechanism by which expression of a small open reading frame buried in the *E. coli* 23 S rRNA and encoding a pentapeptide causes low level resistance to erythromycin. This pentapeptide can only work in *cis*, meaning that resistance is conferred only to a ribosome on which the peptide is synthesized (6). Random libraries have been used to determine a consensus sequence for peptides that cause erythromycin resistance, *i.e.* fMet-(bulky/hydrophobic)-(Leu/Ile)-(hydrophobic)-Val (7). The random library approach has also been used to select resistance peptides to macrolides other than erythromycin. These studies have established correlations between macrolide structures and resistance peptide sequences, suggesting a unique peptide-drug interaction in the ribosomal tunnel for each tested macrolide (8–10). It has been suggested that synthesis of the *cis*-acting peptide that confers resistance to erythromycin removes the drug from the ribosome in an unknown manner (8). However, there has been no direct experimental evidence to support this proposal, and the molecular mechanism by which peptide synthesis could putatively remove erythromycin from the ribosome has remained obscure.

We have used a cell-free translation system with purified components from *E. coli* (11) to study the mechanism of peptide-mediated erythromycin resistance. We have found that, indeed, translation of the resistance peptide mRNA ejects the peptide, and we have identified the very step where this occurs. Based on our biochemical data and with support from docking simulations, we propose a structural model for

\* This work was supported by the Swedish Research Council, the Wellcome Trust International Senior Fellowship (070210/z/03/z), and the Estonian Science Foundation (5311). The costs of publication of this article were defrayed in part by the payment of page charges. This article must therefore be hereby marked "advertisement" in accordance with 18 U.S.C. Section 1734 solely to indicate this fact.

<sup>§</sup> The on-line version of this article (available at <http://www.jbc.org>) contains supplemental material.

<sup>1</sup> These authors are equal contributors.

<sup>2</sup> To whom correspondence should be addressed: Dept. of Cell and Molecular Biology, Molecular Biology Program, BMC, Box 596, Uppsala University, S-75124 Uppsala, Sweden. Tel: 46-18-471-42-13; Fax: 46-18-471-42-62; E-mail: [ehrenberg@xray.bmc.uu.se](mailto:ehrenberg@xray.bmc.uu.se).

<sup>3</sup> The abbreviations used are: 50 S, large ribosomal subunit; IF, initiation factor; RF, release factor; IPTG, isopropyl- $\beta$ -D-thiogalactopyranoside; EF, elongation factor; rpmRNA, resistance peptide mRNA; HPLC, high performance liquid chromatography.

erythromycin ejection by peptide synthesis. We have, furthermore, used our kinetic data in conjunction with mathematical modeling to make quantitative predictions of the degree of resistance conferred by varying levels of resistance peptide expression in living cells subjected to varying external concentrations of erythromycin. These model predictions have been validated by observations from experiments in which the expression of resistance peptide was varied for bacteria growing in media containing varying concentrations of erythromycin.

## EXPERIMENTAL PROCEDURES

### Chemicals and Buffers

GTP, ATP, and [<sup>3</sup>H]Met were from Amersham Biosciences. Putrescine, spermidine, phosphoenolpyruvate, myokinase, inorganic pyrophosphatase, erythromycin, and non-radioactive amino acids were from Sigma-Aldrich. Pyruvate kinase was from Roche Applied Science. [<sup>14</sup>C]Erythromycin was from PerkinElmer Life Sciences, and josamycin was from Alexis Biochemicals (Lausen, Switzerland). All experiments were performed in polymix buffer at working strength containing 5 mM magnesium acetate, 5 mM ammonium chloride, 95 mM potassium chloride, 0.5 mM calcium chloride, 8 mM putrescine, 1 mM spermidine, 5 mM potassium phosphate, and 1 mM dithioerythritol (12).

### mRNA

The template DNAs for *in vitro* transcription were prepared by annealing the following oligonucleotides at the complementary sequences (underlined) and filling the gaps by PCR: forward oligo, CTCTCTGGTACCGAAATTAATACGACTCACTATAGGGAATT-CGGGCCCTTGTAAACAATTAAGGAGG; reverse oligo for MRLFV, TTTTTTTTTTTTTTTTTTTTTTAAACAAACAGACGCATAGT-ATACCTCCTTAATTGTTAACAAGGGCCCG; reverse oligo for MRLFVA, TTTTTTTTTTTTTTTTTTTTTTATGCAACAAA-CAGACGCATAGTATACCTCCTTAATTGTTAACAAGGGCCCG; reverse oligo for MRLFVAN, TTTTTTTTTTTTTTTTTTTTTTAT-ATTTGCAACAAACAGACGCATAGTATACCTCCTTAATTGTTAACAAGGGCCCG; reverse oligo for MNAIK, TTTTTTTTTTTTTTTTTTTTTTAAATTGTTAACAAGGGCCCG. *In vitro* transcription and purification of mRNAs containing a poly(A) tail were as described in Pavlov and Ehrenberg (13).

### The Components of the Purified Translation System

Components of the translation system were purified as described in Tenson *et al.* (2), except for RF1, RF2, and RF3, which were purified as described in Freistroffer *et al.* (11), and RRF, as described in MacDougall *et al.* (14). All experiments were performed at 37 °C in polymix buffer with the addition of ATP (1 mM), GTP (1 mM), and phosphoenolpyruvate (10 mM).

### Recycling Experiments

The initiation mixture contained ribosomes (0.24 μM, ~70% active), [<sup>3</sup>H]Met-tRNA<sup>Met</sup> (5 μM), mRNA (0.5 μM), IF2 (0.5 μM), IF1 (1 μM), IF3 (1 μM), and erythromycin (0.6 μM in the chase and 6 μM in the experiments with only erythromycin). The recycling mixture contained EF-G (2 μM), EF-Tu (40 μM), EF-Ts (1 μM), RF2 (2 μM), RF3 (2 μM), RRF (2 μM), tRNA<sup>bulk</sup> (~0.18 mM), inorganic pyrophosphatase (5 μg/ml), myokinase (3 μg/ml), pyruvate kinase (50 μg/ml), the relevant aminoacyl-tRNA synthetases (0.15 units/μl) (defined in Ehrenberg *et al.* 15), and amino acids (alanine 1.5 mM, leucine 300 μM, and 100 μM concentrations of each of the others). Josamycin (165 μM) was also added to the recycling mix when relevant.

Both initiation mix and recycling mix were preincubated for 10 min at 37 °C to allow for formation of ribosomal initiation complexes and ternary complexes, respectively. After mixing 10 μl of the initiation mix with 10 μl of the recycling mix, reactions were quenched at the specified time points by adding 135 μl of 20% formic acid, and peptide formation was analyzed using reverse phase HPLC as described in Tenson *et al.* (2).

The amount of peptide *P* that is produced per time unit depends on the ribosome recycling rate, *k*<sub>1</sub>, and the amount of active ribosomes, *R*,

$$\frac{dP}{dt} = k_1 R \quad (\text{Eq. 1})$$

Without josamycin, which inhibits formation of these short peptides, the amount of active ribosomes is constant,  $R = R_{\text{tot}}$ , and the recycling rate can be determined from the slope of a curve where the amount of peptides is plotted *versus* time,  $P = R_{\text{tot}} k_1 t$ .

However, if erythromycin is chased with a large excess of josamycin when an erythromycin molecule dissociates from the ribosome, it is immediately replaced by a josamycin molecule, which shuts down protein synthesis. Accordingly, the amount of active ribosomes becomes

$$R = R_{\text{tot}} e^{-k_2 t} \quad (\text{Eq. 2})$$

where *k*<sub>2</sub> is the rate constant for erythromycin dissociation. Insertion of Equation 1 in Equation 2 leads to the differential equation

$$\frac{dP}{dt} = k_1 R_{\text{tot}} e^{-k_2 t} \quad (\text{Eq. 3})$$

for peptide synthesis, which has the solution

$$P = R_{\text{tot}} \frac{k_1}{k_2} (1 - e^{-k_2 t}) \quad (\text{Eq. 4})$$

Using the *k*<sub>1</sub> value estimated from the experiment performed in the absence of josamycin, the parameter *k*<sub>2</sub> was varied to fit the Equation 4 model to experimental data with the help of the Marquardt algorithm (16) implemented in Origin 7 (OriginLab Corp.).

### Erythromycin and Peptide Dissociation Rates

The mixture for initiation of protein synthesis contained ribosomes (1.4 μM, ~70% active), [<sup>3</sup>H]Met-tRNA<sup>Met</sup> (1 μM), mRNA (2.5 μM), IF2 (0.5 μM), IF1 (1 μM), IF3 (1 μM), and when relevant [<sup>14</sup>C]erythromycin (2 μM). The protein elongation mixture contained EF-G (1.6 μM), EF-Tu (40 μM), EF-Ts (1 μM), and tRNA<sup>bulk</sup> (~0.18 mM), inorganic pyrophosphatase (5 μg/ml), myokinase (3 μg/ml), pyruvate kinase (50 μg/ml). Elongation was halted at the desired peptide lengths by exclusion of the amino acid and the aminoacyl-tRNA synthetase necessary to form the ternary complex that was reading next down-stream codon. The concentrations of the added aminoacyl-tRNA synthetase were (0.15 units/μl) (defined in Ehrenberg *et al.* (15)), and the added amino acids were (alanine 1.5 mM, leucine 300 μM, and 100 μM concentrations of each of the others). When stated, RF1 (3 μM) or RF2 (3 μM) was also added to the elongation mix, and unlabeled erythromycin (150 μM) was added to prevent rebinding of the [<sup>14</sup>C]erythromycin. Both initiation mix and elongation mix were preincubated for 10 min at 37 °C to allow for formation of initiation and ternary complexes, respectively.

*Nitrocellulose Filter Binding Assays*—Ribosomes stick to the nitrocellulose filters, whereas erythromycin, peptides, and peptidyl-tRNA do not. Hence, the nitrocellulose filter assay allows us to separate ribosome bound from other labeled molecules. After mixing 20 μl of the initiation

## Erythromycin Resistance Peptides

mix with 20  $\mu$ l of the elongation mix, reactions were quenched by the addition of 1 ml of ice-cold polymix and applied to nitrocellulose filters. The filters were washed twice with 1 ml of polymix, and both the  $^3\text{H}$  and  $^{14}\text{C}$  activity were counted for both the flow-through and the filters.

**Formic Acid Precipitation Assay**—After mixing 20  $\mu$ l of the initiation mix with 20  $\mu$ l of the elongation mix, reactions were quenched by the addition of 150  $\mu$ l of 20% formic acid, and the precipitates were pelleted by centrifugation. The  $^3\text{H}$  activities in the supernatants, containing released peptides were counted directly, whereas 160  $\mu$ l of 0.5 mM KOH was added to the pellets. After 10 min of incubation at room temperature, 10  $\mu$ l of 100% formic acid was added, and the precipitates were pelleted again. The  $^3\text{H}$  activities in the supernatants at this second step correspond to the peptides that were still bound to tRNA at the time point when the reaction was quenched.

**Data Evaluation**—The dissociation rate constants for erythromycin leaving the ribosome were estimated by fitting the data to a single exponential model. The corresponding peptide- and peptidyl-tRNA dissociation rate constants were also estimated by fitting to a single exponential because the peptide synthesis was much faster than the dissociation (data not shown), and thus, the dissociation could be approximated with a single step reaction. The fitting was performed using the Marquardt algorithm (16) implemented in Origin 7 (OriginLab Corp.).

### Docking of the Peptides to the Ribosome

Computational modeling was done to investigate the possible modes of interaction between peptides and erythromycin in different stages of peptide elongation. We used docking of the resistance peptide, fMet-Arg-Leu-Phe-Val-Stop (fMRLFV), to find a specific pattern of interaction with erythromycin. Furthermore, we used the peptide fMet-Asn-Ala-Ile-Lys-Stop (fMNAIK) as the negative control, in line with the experimental work (9). For this purpose we used GOLD 3.0 (CCDC, Cambridge, UK) in combination with the crystal structure 1Y12 (1), which contains the ribosome in complex with erythromycin. The docked peptide was covalently constrained to tRNA in either the A (acceptor) or the P (peptidyl) site. The position of the tRNA was taken from the crystal structure 1QVG (17). The docking study was carried out using 2,000,000 operations per docking. Atom c21 in erythromycin was defined as the floodfill center, and a radius of 10 Å was used in the floodfill. Thus an "active site" was defined around the erythromycin facing the A and P sites. The two peptides were docked as tri-, tetra-, penta- and hexapeptides (extended with Ala). Each peptide was docked 20 times, and the 15 best solutions were saved. We used the Chemscore option in GOLD for scoring the generated binding poses (18).

### Simulations of Peptide-mediated Resistance in the Living Cell

Based on our model for erythromycin ejection from the ribosome and biochemical data, we set up a system of differential equations of ribosomes in different states (see Fig. 3A). The model accounts for changes in the total concentration of intracellular erythromycin by the inflow and outflow of the macrolide over the membrane and the change of resistance peptide mRNA and protein mRNA through synthesis and degradation. All components are also diluted by cell growth. The system was solved numerically by Euler's method (26), after the introduction of a certain macrolide concentration in the medium. Cell growth was registered as volume expansion during the first 8 h after induction. Before macrolide exposure, the system resided at steady state for a certain synthesis rate of resistance peptide mRNA (rpmRNA). The used program software was MATLAB 6.5 (The MathWorks, Inc., Natick, MA). A detailed description of the model and the parameters used is presented in the supplemental material.

### Measurements on Cell Cultures

**Strains**—*E. coli* DH5 $\alpha$  strain (F'  $\phi$ 80dlacZ  $\Delta$ (lacZYA-argF)U169 deoR recA1 endA1 hsdR17 (rk $^-$ , mk $^+$ ) phoA supE44  $\lambda$ -thi-1 gyrA96 relA1/F' proAB+ lacIq $\Delta$ M15 Tn10(*tet*r)) was used in all experiments.

**Effects of Mini-gene Expression on Macrolide Resistance**—Overnight cultures of cells expressing resistance peptide (9) were grown at 37 °C in LB medium containing 100  $\mu$ g/ml ampicillin. Cultures were diluted into 96-well plates with fresh LB medium containing erythromycin and IPTG at different concentrations to final densities of  $A_{600} = 0.01$ . The cell cultures were grown in the shaker at 37 °C for 8 h, and the optical densities at  $A_{600}$  were recorded using the TECAN SUNRISE instrument.

**RNA Copy Number**—Cells expressing the resistance peptide were grown overnight in LB medium containing 100  $\mu$ g/ml ampicillin at 37 °C. Cultures were diluted with fresh LB medium containing IPTG and erythromycin at the concentrations as indicated. The cultures were grown for 2 h before 1-ml cultures were taken for total RNA isolation. Total RNA was purified with NucleoSpin RNA II kit (Macherey-Nagel). Concentrations of the resistance peptide and EF-Tu mRNAs were measured by reverse transcription real-time PCR using the TaqMan Gold reverse transcription PCR kit (Applied Biosystems). The reverse transcription real-time PCR program was as follows; 1) annealing of the forward primer to mRNA (75 °C for 2 min, 65 °C for 5 min, and 53 °C for 5 min); 2) reverse transcription reaction, started by adding TaqMan reverse transcription buffer, dNTPs, RNase inhibitor, and reverse transcriptase followed by incubation at 45 °C for 10 min, 48 °C for 30 min, and 95 °C for 30 min; 3) real-time PCR, started by the addition of PCR buffer, dNTP, AmpliTaq Gold DNA polymerase, and the respective reverse primers and Taqman probes followed by PCR steps (prePCR (50 °C for 2 min and 95 °C for 10 min) and 40 PCR cycles (95 °C for 15 s, 50 °C for 30 s, and 60 °C for 15 s). The final reaction volume was 25  $\mu$ l. The concentrations of forward and reverse primers were 900 nM each, and the probe concentration was 100 nM. Annealing and reverse transcription steps were done in GeneAmp PCR System 2700 (Applied Biosystems). Real-time PCR was run and monitored in Rotor-Gene 5.0.47.

**Primers**—Specific primers for resistance peptide encoding mRNA were: forward, d(AAAAGCCCGCTCATTAGG), reverse, d(TGCTAGTCTTAAGGAGGTCACAT), and Taqman probe, d(CTAGAGAATTCA-GCTAGTAAACAAACAAACCA). Specific primers for EF-Tu mRNA were: forward, d(GAGATGGAGAAATACGTCTTCGA), reverse, d(AC-CAGAGCGTGGATTG), and Taqman probe, d(CGGCAGCAG-GAACGGCTT). Taqman probes had the 5' end modified with a FAM fluorophore and the 3' end modified with a TAMRA fluorophore.

## RESULTS

**Stoichiometric Removal of Erythromycin by Resistance Peptide Synthesis**—To study the effects of resistance peptide synthesis on the rate of dissociation of erythromycin from the 50 S subunit, we took advantage of a cell-free translation system with purified components from *E. coli* (11). The resistance pentapeptide fMRLFV and a control pentapeptide, fMNAIK, were synthesized (9) on ribosomes in recycling mode (19). Erythromycin insignificantly affected the rate of synthesis of resistance and control peptide, whereas their synthesis was shut down by the presence of josamycin (Fig. 1). We took advantage of this by chasing the erythromycin, originally on the recycling ribosomes, with josamycin (Fig. 1). Because the two drugs have overlapping ribosomal binding sites (1, 20, 21), josamycin cannot bind and shut down peptide synthesis until after dissociation of erythromycin from the 50 S subunit. The josamycin concentration used in the chase (83  $\mu$ M) leads to an association rate of 2.7 s $^{-1}$  (21). Thus, the rate-limiting step in the josa-

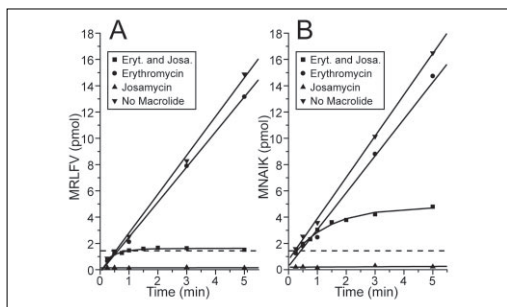


**FIGURE 1. Erythromycin chased with josamycin in a recycling experiment.** The amounts of resistance peptide (MRLFV, *panel A*) and control peptide (MNAIK, *panel B*) are plotted against time. Erythromycin (Eryt., ●) allows formation of both pentapeptides almost as well as without any antibiotic (▼), whereas josamycin (Josa., ▲) does not allow any pentapeptide formation. When erythromycin dissociates in the chase experiment (■) it is replaced by josamycin, and further pentapeptide formation is inhibited. The dashed lines correspond to the amount of active ribosomes in the experiments (1.7 pmol). Translation of the resistance peptide (MRLFV, *panel A*) is inhibited already after a single round of translation, which means that all erythromycin has dissociated and been replaced by josamycin before the next round of translation initiates. This is in contrast to the several rounds of recycling that is allowed when expressing the control peptide (MNAIK, *panel B*). The pentapeptide synthesis rate per ribosome in the absence of josamycin ( $k_2$ ) is  $0.03 \text{ s}^{-1}$  ( $3 \text{ pmol min}^{-1}/1.7 \text{ pmol of ribosomes} = 1.8 \text{ min}^{-1} = 0.03 \text{ s}^{-1}$ ). The erythromycin dissociation rate ( $k_1$ ) can be estimated from the value of  $k_2$  and the plateau level in the josamycin chase experiments (see "Experimental Procedures").

mycin-induced inhibition of peptide formation is the erythromycin dissociation. The value of the rate constant for dissociation of erythromycin from ribosomes synthesizing the control peptide was estimated as  $0.01 \text{ s}^{-1}$  (Fig. 1B), which corresponds to the rate constant for spontaneous dissociation of erythromycin from empty ribosomes (21). In contrast, the value of the rate constant for dissociation of erythromycin from ribosomes synthesizing the resistance peptide was estimated as  $0.03 \text{ s}^{-1}$ , a value coinciding with the rate ( $\text{s}^{-1}$ ) of pentapeptide synthesis per ribosome in the absence of josamycin (Fig. 1A). From these results follows that erythromycin was removed with high probability from the ribosome during each cycle of resistance, but not control peptide synthesis. Identification of the step at which drug dissociation was induced by the *cis*-acting peptide required further experiments, to be described in the next paragraph.

**Dissociation of Erythromycin during Different Stages of Resistance Peptide Synthesis**—To estimate the rate constants for dissociation of erythromycin at different stages of resistance peptide synthesis, we used nitrocellulose filtration techniques.

Ribosomes were initiated for synthesis of resistance (fMRLFV) or control (fMNAIK) peptides. By selective exclusion of amino acids and aminoacyl-tRNA synthetases in the peptide elongation assays, ribosomes carrying fMR, fMRL, fMRLF, or fMRLFV as well as fMN, fMNA, fMNAI, or fMNAIK peptides ester-bonded to the P-site tRNA were produced. Subsequently, [ $^{14}\text{C}$ ]erythromycin was chased from each one of these ribosome complexes by the addition of unlabeled erythromycin in excess, and the fraction of [ $^{14}\text{C}$ ]erythromycin-containing ribosomes was monitored by nitrocellulose filtration at different incubation times. From these data, rate constants for the dissociation of erythromycin were estimated, and the results are summarized in Table 1. The rate constant for dissociation of erythromycin increased from its smallest value ( $0.011 \text{ s}^{-1}$ ) in the initiation complex with every amino acid that was added, in accordance with the resistance peptide sequence to its largest value of  $0.068 \text{ s}^{-1}$  when the pentapeptide was completed (Fig. 2A and Table 1). There was at the same time little effect on the rate of

**TABLE 1**  
Erythromycin dissociation rate constants

Translated peptide	Erythromycin dissociation rate constant
Initial complex	$0.011 \pm 0.001$
MR	$0.017 \pm 0.005$
MRL	$0.025 \pm 0.004$
MRLF	$0.051 \pm 0.004$
MRLFV	$0.068 \pm 0.006$
MRLFVA	$0.014 \pm 0.001$
MRLFVAN	$0.014 \pm 0.001$
MN	$0.011 \pm 0.001$
MNA	$0.015 \pm 0.001$
MNAI	$0.016 \pm 0.001$
MNAIK	$0.017 \pm 0.001$

erythromycin dissociation by amino acid addition, in accordance with the control peptide sequence (Fig. 2B and Table 1).

It has been shown that active resistance peptides must have lengths between four and six amino acids (7). To clarify why this is so, we prepared mRNAs encoding the hexapeptide fMet-Arg-Leu-Phe-Val-Ala-Stop, which is the resistance peptide with a C-terminal addition of Ala, and the heptapeptide fMet-Arg-Leu-Phe-Val-Ala-Asn-Stop, which is the resistance peptide with a C-terminal addition of Ala-Asn. Both these C-terminal additions reduced the rate constant for erythromycin dissociation from  $0.068 \text{ s}^{-1}$  (in the presence of the authentic resistance peptide) to  $0.014 \text{ s}^{-1}$  (in the presence of the C-terminal extension) (Table 1).

These results show that when the resistance peptide grew from two to five amino acids, this led to successively faster dissociation of erythromycin. Because, however, synthesis of the resistance peptide was considerably faster than the largest rate of erythromycin dissociation, these data cannot explain why every round of resistance peptide synthesis resulted in near-stoichiometric removal of the 50 S-bound erythromycin (Fig. 1). This pointed at class 1 release factor-induced peptide release from the ribosome as the critical step for resistance peptide action. Experiments addressing this question follow.

**Termination of Resistance Peptide Synthesis Drives Dissociation of Erythromycin**—The largest rate constant for erythromycin dissociation ( $0.14 \text{ s}^{-1}$ ) was obtained when either one of the class 1 release factors was also present to terminate the synthesis of the resistance peptide at the UAA codon of its mRNA (Fig. 2C, Table 2). At the same time, there was no effect on the rate of erythromycin dissociation by release factor addition in the case of the control peptide (Fig. 2C, Table 2). To further investigate class 1 release factor action, we used nitrocellulose binding to monitor the release of different peptides from the ribosome and formic acid precipitation followed by peptide identification by HPLC to directly monitor hydrolysis of the ester bond connecting peptide and P-site tRNA. The rate of dissociation from the ribosome and the rate of ester bond hydrolysis were similar in the cases described below in this section of text, suggesting fast dissociation of peptides from the ribosome after the rate-limiting ester bond hydrolysis.

The rate of resistance peptide release from the ribosome, as induced by either one of the class 1 release factors ( $0.073 \text{ s}^{-1}$ ) as monitored by the ribosome-bound  $^3\text{H}$ -labeled fMet, was significantly smaller than the rate constant for dissociation of erythromycin ( $0.14 \text{ s}^{-1}$ ). At the same time, the rate of control peptide release as induced by RF2 ( $0.22 \text{ s}^{-1}$ ) was almost 30 times larger than the rate constant for erythromycin dissociation (Fig. 2E). These results in conjunction with the observation (Fig. 1) that every cycle of resistance peptide synthesis removed the ribosome-bound erythromycin with high probability suggest, first, that binding of a class 1 release factor to an erythromycin-containing ribosome carrying a resistance pentapeptide further destabilized the binding of the

## Erythromycin Resistance Peptides

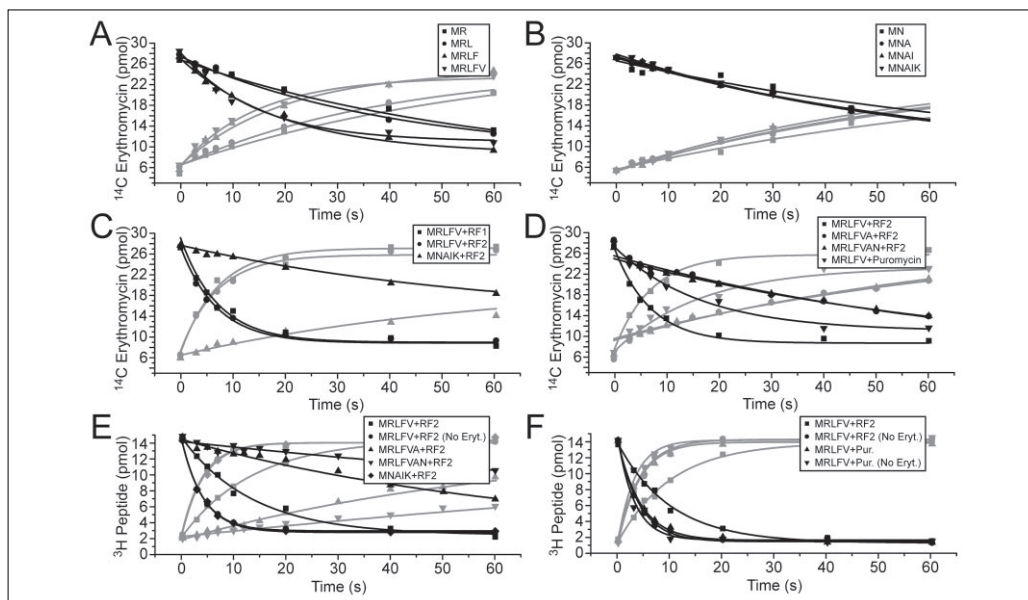


**FIGURE 2. Erythromycin and peptide dissociation rates.** Panels A–D show the amount of ribosome bound (or released) [ $^{14}\text{C}$ ]erythromycin as a function of time. Essentially all ribosomes contain [ $^{14}\text{C}$ ]erythromycin at time 0, and a 75-fold excess of cold erythromycin was added to the pre-initiated ribosome complexes together with the elongation mix to prevent re-binding of [ $^{14}\text{C}$ ]erythromycin. Panel E shows dissociation of the peptide labeled with [ $^3\text{H}$ ]Met as a function of time. The black symbols in panels A–E show the amount that is bound to ribosomes and thereby stick to the nitrocellulose filters, whereas the gray symbols show the amount that have gone through the filters. Panel F shows the release factor-mediated hydrolysis of the peptidyl-tRNA and the puromycin reaction as a function of time. The black symbols show the peptides that are still bound to tRNA and thereby precipitable with formic acid, whereas the gray symbols show the peptides in the supernatant. All lines are obtained by simultaneously fitting the data shown by black and gray symbols to single exponentials using least square fits. The estimated rate constants are collected in Tables 1 and 2.

**TABLE 2**  
Erythromycin and peptide dissociation rate constants

Translated peptide	Releasing agent	Erythromycin dissociation rate constant <sup>a</sup>	Peptide dissociation rate constant <sup>a</sup>	Peptidyl-tRNA hydrolysis rate constant <sup>b</sup>
		$s^{-1}$	$s^{-1}$	$s^{-1}$
MRLFV	RF1	$0.14 \pm 0.02$	$0.073 \pm 0.007$	
MRLFV	RF1	No erythromycin	$0.22 \pm 0.02$	
MRLFV	RF2	$0.13 \pm 0.01$	$0.074 \pm 0.01$	$0.10 \pm 0.01$
MRLFV	RF2	No erythromycin	$0.25 \pm 0.01$	$0.26 \pm 0.03$
MRLFV	Puromycin	$0.067 \pm 0.009$	Not determined <sup>c</sup>	$0.23 \pm 0.02$
MRLFV	Puromycin	No erythromycin	Not determined <sup>c</sup>	$0.31 \pm 0.03$
MRLFVA	RF2	$0.014 \pm 0.001$	$0.015 \pm 0.002$	$0.015 \pm 0.001$
MRLFVA	RF2	No erythromycin	$0.29 \pm 0.03$	$0.32 \pm 0.03$
MRLFVAN	RF2	$0.014 \pm 0.001$	$0.006 \pm 0.0004$	$0.004 \pm 0.0004$
MRLFVAN	RF2	No erythromycin	$0.27 \pm 0.03$	$0.44 \pm 0.03$
MNAIK	RF2	$0.015 \pm 0.001$	$0.26 \pm 0.03$	$0.28 \pm 0.02$
MNAIK	RF2	No erythromycin	$0.25 \pm 0.02$	$0.27 \pm 0.02$

<sup>a</sup> Measured by nitrocellulose filter binding.

<sup>b</sup> Measured by formic acid precipitation.

<sup>c</sup> Could not be determined because fMRLFV-puromycin bind to NC-filters.

drug to the ribosome and, second, that termination was slow enough to allow dissociation of erythromycin from the ribosome with a probability close to one, in accordance with the results in Fig. 1. It cannot be excluded that dissociation of erythromycin was strictly required for termination to occur, in which case the probability for drug rejection would be exactly 100%. The reason for the ambiguity relates to the experimental design in which [ $^{14}\text{C}$ ]erythromycin was chased with unlabeled erythromycin at a high concentration ( $75 \mu\text{M}$ ), which could allow for rapid re-binding of an unlabeled erythromycin after dissociation of the labeled one (21), before significant termination could occur. In this latter scenario, which leads to the simplest interpretation of the peptide

release data, termination in our *in vitro* experiments occurred in the presence of erythromycin.

The addition of RF2 to ribosomes carrying the resistance peptide with a C-terminal addition of one amino acid (the hexapeptide) led to peptide release with a rate constant of  $0.015 \text{ s}^{-1}$ , virtually identical with the rate constant of  $0.014 \text{ s}^{-1}$  for dissociation of erythromycin (Figs. 2, D and E and Table 2). The addition of RF2 to the resistance peptide with a C-terminal addition of two amino acids (the heptapeptide) led to peptide release with a considerably smaller rate constant of  $0.006 \text{ s}^{-1}$  but to a similar rate constant of  $0.014 \text{ s}^{-1}$  for dissociation of erythromycin (Figs. 2, D and E, and Table 2). This rate constant for dissociation of erythro-

mycin is similar to the corresponding rate constant for the peptide-lacking initiation complex. These experiments show that release of the extended peptides did not accelerate dissociation of erythromycin, in line with the previous observation of a strong sequence length dependence of resistance activity (7).

Treatment of ribosomes carrying full-length resistance peptides with puromycin, an antibiotic mimicking the aminoacylated 3'-adenosine of an aminoacylated tRNA (17), did not alter the rate of dissociation of erythromycin (Fig. 2D and Table 2). It was not possible to monitor release of the resistance peptide-puromycin complex from the ribosome, since it remained filter-bound in free as well as ribosome-bound configuration. We could, however, monitor peptidyl transfer to puromycin using HPLC after formic acid precipitation. We found that the rate constant for transfer of the resistance peptide to puromycin ( $0.23 \text{ s}^{-1}$ ) was much larger than the rate constant for dissociation of erythromycin ( $0.067 \text{ s}^{-1}$ ) (Figs. 2, D and F). This means that transfer of the resistance peptide to puromycin was unhindered by the presence of erythromycin, in contrast to the hydrolytic reaction induced by a class 1 release factor (Fig. 2C and Table 2). It is normally assumed that when a small peptide is transferred to puromycin, it rapidly leaves the ribosome. However, if this were the case, one would expect that the rate constant for erythromycin release would be reduced from its value of  $0.068 \text{ s}^{-1}$  in the absence of puromycin to its value of  $0.011 \text{ s}^{-1}$  in the absence of peptide. The experiments show, in contrast, that in response to puromycin treatment dissociation of erythromycin remained unaltered at  $0.067 \text{ s}^{-1}$ . This suggests that the resistance peptide-puromycin complex remained ribosome-bound long enough to allow for dissociation of the radio-labeled erythromycin.

**Docking of the Resistance Peptide to the Ribosome**—Previous genetic studies (7) and the biochemical data in this work suggest the existence of specific interactions between the resistance peptide and ribosome-bound erythromycin. To test this, we performed docking simulations with a resistance or a control peptide anchored to an A-site- or a P-site-bound tRNA of a ribosome in complex with erythromycin. In 8 of the top 15 simulations for the resistance pentapeptide anchored to the P-site tRNA, the leucine in fMRLFV was bound to a small hydrophobic cavity on the surface of erythromycin, between the cladinose and desosamine residues (see Fig. 4, E and F), and a similar result was obtained for the tetrapeptide fMRLF. Similar, but less pronounced leucine binding patterns were observed also for fMRLFV and fMRLF anchored to the A-site tRNA. At the same time, no distinct binding patterns were observed for amino acids other than leucine in the resistance peptide or for any of the amino acids in the control peptide fMNAIK. In the case of the resistance tripeptide, the leucine did not reach into the erythromycin cavity, and in the case of the resistance hexapeptide, the leucine binding pattern was gone, possibly due to steric hindrance.

**Validation of the Model for Resistance Peptide Action by Cell Population Experiments**—From the biochemical experiments described above, kinetic constants for resistance peptide action were obtained (Table 2). We constructed a model for erythromycin resistance in bacterial populations (Fig. 3A) based on these and other parameters (listed in the supplemental material) for protein synthesis obtained from our cell-free mRNA translation system (21). The model (detailed description in the supplemental material) contains seven different states of the large ribosomal subunit (50 S) (Fig. 3A); it accounts for dilution of all compounds due to cell volume growth and for a finite rate of diffusion across the cell membrane, which reduces the intracellular concentration in relation to the outer concentration of erythromycin. Furthermore, the model takes into account the efflux pumps used by *E. coli* to actively transport eryth-

romycin and other antibiotic drugs from the membrane and cytoplasm to the growth medium (22).

To validate the model, we varied the expression of rpmRNA under *tac* promoter control from a multicopy plasmid by varying the concentration of IPTG in an erythromycin-containing growth medium (6, 9). Cell growth at different IPTG and erythromycin concentrations was monitored along with reverse transcription real-time PCR analysis of the intracellular concentration of rpmRNA relative to the concentration of EF-Tu mRNA (Fig. 3C, inset). The *tac* promoter was leaky, and the response in rpmRNA synthesis to the external IPTG level was linear. At the highest IPTG concentration ( $600 \mu\text{M}$ ) in the medium, the mRNA level was 3-fold higher than in the absence of IPTG (Fig. 3C, inset). Increasing IPTG concentrations led to increasing erythromycin resistance until a plateau, specific for each concentration of erythromycin, was reached (Fig. 3C). The increase in bacterial mass (optical density) during 8 h of growth at varying concentrations of erythromycin and IPTG in the medium were monitored, and there was excellent agreement between the experimentally observed and model-simulated growth behavior in which the measured, relative rpmRNA levels had been taken into account (Fig. 3B).

## DISCUSSION

Erythromycin binds in the nascent peptide exit tunnel close to the peptidyl transferase center (1, 23) (Fig. 4A) and prevents synthesis of peptides longer than eight amino acids (2). Expression of a mini-gene buried in the 23 S rRNA causes low level resistance to erythromycin (6), and it has been suggested that synthesis of this resistance peptide on an erythromycin-containing ribosome can clean it from the drug, thereby making an erythromycin-free 50 S subunit available for a new round of initiation of protein synthesis with another mRNA (8). When the nascent peptide is longer than six to eight amino acids, it covers the erythromycin binding site, which makes the ribosome refractory to further inhibition by erythromycin, allowing for synthesis of full-length proteins (3, 21).

The present experiments directly demonstrate that synthesis of a resistance peptide can, indeed, remove erythromycin from the 50 S subunit. During every cycle of resistance peptide synthesis erythromycin dissociates with close to 100% probability, whereas the synthesis of a control peptide does not induce dissociation of the drug (Fig. 1). As the resistance peptide grows by successive amino acid additions, the rate constant for dissociation of erythromycin increases in a stepwise manner (Table 1). It is, however, not until class 1 release factor induced termination of the full-length resistance pentapeptide, that erythromycin is removed from the ribosome with high probability. Termination is, in other words, the crucial kinetic step for erythromycin dissociation and, therefore, the point at which resistance is conferred.

To validate the mechanism for resistance peptide action, we modeled it in the context of the cytoplasm of a living cell (Fig. 3A and supplemental material) using kinetic data from the present (Table 2) and earlier (21) work. We describe in particular the degree to which inhibition of the growth rate of a bacterial population due to the presence of varying concentrations of erythromycin in the cytoplasm is expected to be relieved by the expression of the resistance peptide at varying levels (Fig. 3B).

These simulations were compared with experimental observations from a bacterial population containing the resistance peptide gene under *tac* promoter control on a multicopy plasmid. The cells were grown in media containing varying concentrations of erythromycin as well as IPTG to control the level of resistance peptide expression. The increase in bacterial mass during 8 h of growth was monitored by optical

## Erythromycin Resistance Peptides

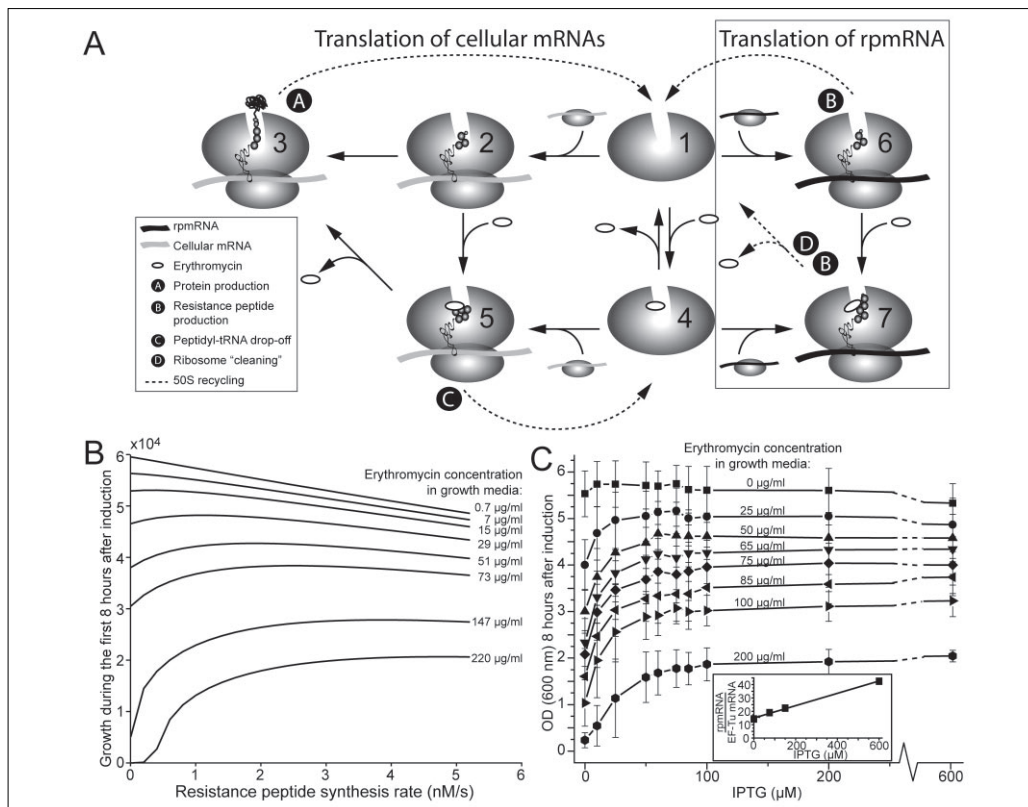


**FIGURE 3. The model, simulation data, and data from cell culture experiments.** Panel A shows a schematic of the model we have developed for simulating translation in the presence of erythromycin and the effect of translating a resistance peptide in the context of a growing *E. coli* cell. The 50 S subunits are in seven different states in the model. Free 50 S subunit (state 1) is susceptible to erythromycin binding and likewise is the newly initiated ribosomes (state 2 and state 6), whereas elongating ribosomes with a longer protein become refractory to macrolide binding (state 3) and, thus, this state always results in full-length product. If erythromycin is bound to the 50 S subunit (state 4) it can still initiate and translate the first codons before protein synthesis is inhibited (state 5). The ribosome is stuck in state 5 until either the peptidyl-tRNA drops off and the ribosome is recycled to state 4, or erythromycin dissociates and protein synthesis is resumed in state 3 and thus refractory to rebinding of erythromycin. If a ribosome with erythromycin (state 4) initiates on a resistance peptide mRNA (rpmRNA) (state 7) it will be "cleaned" and recycled as an erythromycin free 50 S (state 1). The model also contains the cell membrane and erythromycin efflux pumps present in *E. coli* that change the intracellular concentration in comparison to erythromycin concentration in the growth media. For further details about the model, see the supplemental material. Panel B, simulated growth (defined as how many times the cell volume has increased) during the first 8 h after the addition of erythromycin plotted against the rate of rpmRNA synthesis for different concentrations of erythromycin. Panel C, optical density (600 nm) measured 8 h after the addition of erythromycin plotted against the concentration of IPTG. Inset, level of expression of rpmRNA in relation to EF-Tu mRNA plotted against the IPTG concentration.

density (Fig. 3C) along with the level of resistance peptide mRNA normalized to the level of EF-Tu mRNA (Fig. 3C, inset), as measured by reverse transcription real-time PCR. The simulated growth rates in Fig. 3B, where the experimentally measured resistance peptide mRNAs are taken into account, are in excellent agreement with the measured growth rates in Fig. 3C. This shows that the mechanism we propose for peptide-mediated low level resistance against erythromycin (Fig. 3A) and the rate constants obtained from our cell-free *in vitro* translation system (Table 2 and Ref. 21) are sufficient to fully account for the *in vivo* induced resistance in a large interval of erythromycin concentrations and peptide expression levels (Figs. 3, B and C (and inset)).

The structural basis of resistance peptide action is of considerable interest, not the least because it is one special case of the general and poorly understood phenomenon of peptide-specific interactions with the ribosomal peptide exit tunnel (4, 24). Our data show that when the

control peptide grows from a di- to a pentapeptide, there is little change in the rate constant for erythromycin dissociation. When, furthermore, RF2 is added to terminate peptide synthesis, hydrolysis of the ester bond in the peptidyl-tRNA proceeds with the same rate as in the absence of erythromycin (Tables 1 and 2). For the resistance peptide, in contrast, our data show that the rate constant for erythromycin dissociation increases gradually by a factor of six as the peptide grows from just the fMet to di- and then to pentapeptide. In addition, when RF2 is added, the rate constant for erythromycin release is further enhanced by a factor of two, and the rate of ester bond hydrolysis is much smaller than in the absence of erythromycin (Tables 1 and 2). We know from data obtained from open reading frame libraries that the consensus sequence for peptide-mediated erythromycin resistance has two outstanding features; there is a leucine or isoleucine in the third position and a valine in the fifth, C-terminal position (7, 9). Resistance peptides for different

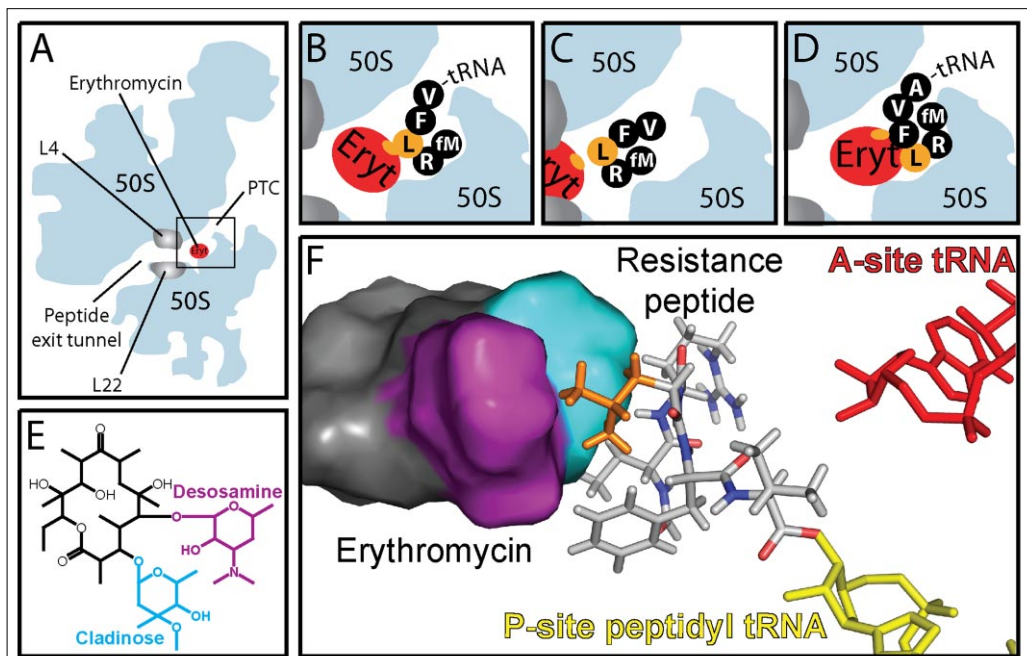


FIGURE 4. **A structural model for the mechanism of resistance peptide action.** Panel A shows a schematic of the large ribosomal subunit cut along the nascent peptide exit tunnel with an erythromycin molecule bound (red). The peptidyl transferase center (PTC) and the two ribosomal proteins (L4 and L22) constituting the constriction in the tunnel are indicated. The black rectangle indicates the section shown in panels B–D where our hypothesis about the mechanism of the resistance peptide action is shown. Panel B shows the pentapeptidyl-tRNA that interacts with erythromycin (Eryt). Panel C shows the resistance peptide that during termination of protein synthesis has removed erythromycin. Panel D shows the hexapeptidyl-tRNA which has lost its contact with erythromycin and is trapped in a dead end that eventually leads to peptidyl-tRNA drop-off. Panel E shows the chemical structure of erythromycin. Panel F presents the interaction between the conserved leucine residue (orange) in the resistance peptide and erythromycin as indicated by the docking studies.

types of macrolides have different consensus sequences, suggesting specific and perhaps direct interactions between the conserved residues and each type of ribosome bound macrolide (9, 10). From the present kinetic data (Tables 1 and 2) and docking simulations (Fig. 4F) along with previous open reading frame library data (7), we propose a structural model for peptide-mediated erythromycin resistance (Figs. 4, A–D).

Our docking studies based on the crystal structure of a *Haloarcula marismortui* 50 S subunit in complex with erythromycin (1) suggest that the side chain of leucine in the resistance peptide binds to the hydrophobic cleft between the two sugar moieties of erythromycin (Figs. 4, E and F). To date, there is no crystal structure of an *E. coli* 50 S subunit in complex with erythromycin, but the similarity of the 50 S subunits from the two organisms near the erythromycin binding site (1, 25) suggests that our docking data are relevant also for the erythromycin-bound *E. coli* ribosome. Leucine binding to erythromycin is observed both for resistance tetra- and pentapeptides, and the binding pattern is more distinct for resistance peptides anchored to the P-site than to the A-site tRNA. By hypothesis, the observed interaction between the resistance tetrapeptide and the drug weakens the affinity of erythromycin for the ribosome, which accounts for the fact that a leucine (or an isoleucine) is critical for resistance peptide action. Completion of the resistance pentapeptide by the addition of valine further increases the erythromycin dissociation rate constant, probably because the force by which the resistance

peptide pushes erythromycin out from its binding site increases (Fig. 4B). When a class 1 release factor binds to the pre-termination ribosome containing a resistance pentapeptide ester-bonded to the P-site tRNA, the rate constant for erythromycin dissociation increases by another factor of two. At the same time, the rate constant for ester bond hydrolysis of the peptidyl-tRNA decreases very significantly (Table 2), which partially accounts for the fact that every cycle of peptide synthesis led to erythromycin dissociation with near 100% probability (Fig. 1). It is, furthermore, possible that the resistance peptide forms a specific hydrophobic structure that prevents it from leaving the ribosome through the peptidyl transferase center after its release from the P-site tRNA. The peptide is then forced to leave the ribosome through the peptide exit tunnel, where its hydrophobic C terminus could interfere with the hydrophobic interactions between erythromycin and the exit tunnel wall and chase the drug out through the L4/L22 constriction in the tunnel (Fig. 4C). This would lead to 100% probability of drug ejection per cycle of resistance peptide synthesis. When instead of termination, an additional amino acid is added to the resistance pentapeptide, our simulations suggest that the leucine interaction with erythromycin becomes lost and that, accordingly, the hexa-peptide is expected to behave like any other peptide. It will fill up the space available between drug and peptidyl transfer center until further protein synthesis is inhibited by crowding (Fig. 4D).

## Erythromycin Resistance Peptides

### REFERENCES

1. Tu, D., Blaha, G., Moore, P. B., and Steitz, T. A. (2005) *Cell* **121**, 257–270
2. Tenson, T., Lovmar, M., and Ehrenberg, M. (2003) *J. Mol. Biol.* **330**, 1005–1014
3. Andersson, S., and Kurland, C. G. (1987) *Biochimie (Paris)* **69**, 901–904
4. Tenson, T., and Ehrenberg, M. (2002) *Cell* **108**, 591–594
5. Mayford, M., and Weisblum, B. (1990) *J. Bacteriol.* **172**, 3772–3779
6. Tenson, T., DeBlasio, A., and Mankin, A. (1996) *Proc. Natl. Acad. Sci. U. S. A.* **93**, 5641–5646
7. Tenson, T., Xiong, L., Kloss, P., and Mankin, A. S. (1997) *J. Biol. Chem.* **272**, 17425–17430
8. Tripathi, S., Kloss, P. S., and Mankin, A. S. (1998) *J. Biol. Chem.* **273**, 20073–20077
9. Vimberg, V., Xiong, L., Bailey, M., Tenson, T., and Mankin, A. (2004) *Mol. Microbiol.* **54**, 376–385
10. Tenson, T., and Mankin, A. S. (2001) *Peptides* **22**, 1661–1668
11. Freistroffer, D. V., Pavlov, M. Y., MacDougall, J., Buckingham, R. H., and Ehrenberg, M. (1997) *EMBO J.* **16**, 4126–4133
12. Jelenc, P. C., and Kurland, C. G. (1979) *Proc. Natl. Acad. Sci. U. S. A.* **76**, 3174–3178
13. Pavlov, M. Y., and Ehrenberg, M. (1996) *Arch. Biochem. Biophys.* **328**, 9–16
14. MacDougall, J., Holst-Hansen, P., Mortensen, K. K., Freistroffer, D. V., Pavlov, M. Y., Ehrenberg, M., and Buckingham, R. H. (1997) *Biochimie (Paris)* **79**, 243–246
15. Ehrenberg, M., Bilgin, N., and Kurland, C. G. (1990) *Design and Use of a Fast and Accurate in Vitro Translation System*, pp. 101–129, IRL Press at Oxford University Press, Oxford
16. Marquardt, D. W. (1963) *J. Soc. Ind. Appl. Math.* **11**, 431–441
17. Schmeing, T. M., Moore, P. B., and Steitz, T. A. (2003) *RNA* **9**, 1345–1352
18. Verdonk, M. L., Cole, J. C., Hartshorn, M. J., Murray, C. W., and Taylor, R. D. (2003) *Proteins* **52**, 609–623
19. Pavlov, M. Y., Freistroffer, D. V., MacDougall, J., Buckingham, R. H., and Ehrenberg, M. (1997) *EMBO J.* **16**, 4134–4141
20. Hansen, J. L., Ippolito, J. A., Ban, N., Nissen, P., Moore, P. B., and Steitz, T. A. (2002) *Mol. Cell* **10**, 117–128
21. Lovmar, M., Tenson, T., and Ehrenberg, M. (2004) *J. Biol. Chem.* **279**, 53506–53515
22. Zgurskaya, H. I., and Nikaido, H. (1999) *Proc. Natl. Acad. Sci. U. S. A.* **96**, 7190–7195
23. Schlunzen, F., Zarivach, R., Harms, J., Bashan, A., Tocilj, A., Albrecht, R., Yonath, A., and Franceschi, F. (2001) *Nature* **413**, 814–821
24. Cruz-Vera, L. R., Rajagopal, S., Squires, C., and Yanofsky, C. (2005) *Mol. Cell* **19**, 333–343
25. Schuwirth, B. S., Borovinskaya, M. A., Hau, C. W., Zhang, W., Vila-Sanjurjo, A., Holton, J. M., and Cate, J. H. (2005) *Science* **310**, 827–834
26. Heath, M. T. (1997) *Scientific Computing: An Introductory Survey*, pp. 274–275, The McGraw-Hill Inc., New York





Nilsson, K., Lovmar, M. , **Vimberg, V.**, Tenson, T.,  
Ehrenberg, M. 2006. Mechanisms and Requirements  
of Peptide Mediated Macrolide Resistance. Manuscript.

# Mechanisms and Requirements of Peptide-Mediated Macrolide Resistance

Karin Nilsson <sup>1,2\*</sup>, Martin Lovmar <sup>2\*</sup>, Vladimir Vimberg <sup>3</sup>, Tanel Tenson <sup>3</sup> and Måns Ehrenberg <sup>2</sup>

<sup>1</sup> Department of Biometry and Engineering, Swedish University of Agricultural Sciences, Uppsala S-75007, Sweden

<sup>2</sup> Department of Cell and Molecular Biology, Molecular Biology Program, Uppsala University, Uppsala S-75124, Sweden

<sup>3</sup> Institute of Technology, Tartu University, 51010 Tartu, Estonia

\* Equal contribution.

**Correspondence to:** Måns Ehrenberg  
Dept. of Cell and Molecular Biology,  
Molecular Biology Program,  
BMC, Box 596, Uppsala University,  
S-75124 Uppsala, Sweden  
E-mail: ehrenberg@xray.bmc.uu.se  
Tel: +46 18 471 42 13  
Fax: +46 18 471 42 62

## ABSTRACT

Macrolide antibiotics bind at the entrance of the nascent peptide exit tunnel of the large ribosomal subunit, inducing premature termination of translation by drop-off of peptidyl-tRNA. Expression of specific *cis*-acting peptides confers resistance to macrolides. Recently the molecular mechanism behind erythromycin resistance was revealed. The resistance peptide works like a “bottle-brush” and expels erythromycin from the ribosome upon termination of translation. Here, we have used a cell-free translation system to study the mechanism of peptide-mediated josamycin resistance. Distinct from erythromycin resistance peptides, expression of a josamycin resistance peptide did not lead to an increased dissociation of the drug. Instead, the rate of resistance di-peptidyl-tRNA drop-off is decreased by an order of magnitude compared to the control peptide. Further, the level of resistance is independent of the length of the josamycin resistance peptide mRNAs while erythromycin resistance peptides show strict length dependence. We propose therefore that josamycin resistance peptides work by “quarantining” the josamycin bound ribosomes. A quantitative model of the josamycin resistance was constructed and it mimics the degree of resistance in *Escherichia coli* cells expressing a resistance peptide and subjected to varying concentrations of josamycin. Both this model and the previous model for erythromycin resistance predict that an active efflux pump system is required for the resistance peptide mechanism to function. This prediction was tested using an *E. coli* mutant lacking a functional AcrAB-TolC efflux pump system and, indeed, no peptide mediated resistance was detected in the mutant.

## INTRODUCTION

Since the 1950s macrolide antibiotics have been used in the treatment of infections (Weisblum, 1995). Macrolides consist of several neutral or amino sugars attached to a 14-, 15- or 16-membered lactone ring (Leclercq, 2002). The first generation contains naturally occurring 14-membered ring macrolides, and includes erythromycin, currently the best-known macrolide. Josamycin belongs to the second generation, with a 16-membered lactone ring (Weisblum, 1998). Macrolides bind to the large ribosomal subunit, in the vicinity of the peptidyl transferase centre (Hansen *et al.*, 2002; Schlunzen *et al.*, 2001) and most likely inhibit protein synthesis by blocking the entrance to the tunnel through which nascent peptides exit the ribosome (Lovmar *et al.*, 2004; Tenson *et al.*, 2003). Resistance mechanisms to macrolide antibiotics include modifications of the drug-binding site, inactivation of the drug by degradation or modification and cellular efflux by specialized transporter proteins (Weisblum, 1998). However, in the focus in this study is a unique resistance mechanism conferred by expression of specific *cis*-acting peptides (Tenson and Mankin, 2001).

Peptides mediating macrolide resistance was first encountered in experiments where *E. coli* cells expressed random rRNA fragments of the *rrnB* operon (Tenson *et al.*, 1996). Biochemical and genetic studies revealed the presence of a 34 nucleotides long mini-gene ranging between positions 1235 and 1268 in domain II of the 23S rRNA in all resistant clones. Additional *in vitro* experiments, where resistance peptides or resistance peptide mRNA (rpmRNA<sup>eryt</sup>) were supplied, showed the necessity of active translation of the rpmRNA<sup>eryt</sup> for protection against erythromycin. Using selection

from random libraries it became clear that the resistance peptides require both specific length and sequence (Tenson *et al.*, 1997). Tripathi *et al.* (1998) proposed a “bottlebrush” model based on these experiments and further library studies selecting resistance peptides against a ketolide. The “bottlebrush” model suggests that synthesis of a resistance peptide removes the drug molecule, by direct interaction between macrolide and resistance peptide, thus restoring the protein synthesis capability of the ribosome. The resistance peptide acts as a “bottlebrush” and “cleans” the ribosome. Recently, Lovmar *et al.* (2006) showed that synthesis of a *cis*-acting peptide indeed accelerates the rate of erythromycin dissociation by destabilizing the binding of the drug to the ribosome. In addition, it was shown that erythromycin was most probably always expelled from the ribosome during release factor mediated translation termination. The biochemical data was also used within the framework of a mathematical model to predict resistance and finally the predictions of the model could be validated by growth experiments *in vivo*.

It has been suggested that the “bottlebrush” mechanism is general and work for all classes of macrolides with modulated specific sequences (Tenson and Mankin, 2001; Tripathi *et al.*, 1998; Vimberg *et al.*, 2004). However, in the case of josamycin there are at least two major features suggesting a closer examination of the effects of  $\text{rpmRNA}^{\text{josa}}$  expression. First, peptidyl transfer is inhibited already after 2 or 3 amino acids in the presence of josamycin (Lovmar *et al.*, 2004; Tenson *et al.*, 2003), and the selected resistance peptides, containing 4 or 5 amino acids (Vimberg *et al.*, 2004), will therefore never reach the stop codon and thus never reach the termination step which seems to be crucial for the “bottlebrush” mechanism. Secondly, josamycin is bound to the ribosome 1.5 h on the average (Lovmar *et al.*, 2004). This means that a dissociation rate increase of josamycin by a factor of 10 as measured for  $\text{rpmRNA}^{\text{eryt}}$  will still not render resistance since the peptidyl-tRNA drop-off rate would still be much higher (Lovmar *et al.*, 2006).

We begin this study with a biochemical characterization of the peptide mediated josamycin resistance. In combination with an examination of how the activities of  $\text{rpmRNA}^{\text{josa}}$  and  $\text{rpmRNA}^{\text{eryt}}$  depend on the length of the encoded peptides it enables us to conclude that they work through different mechanisms. Using the rate constants from the biochemistry in a mathematical model, similar to the previously published one (Lovmar *et al.*, 2006), we propose that the effect of  $\text{rpmRNA}^{\text{josa}}$  is to “quarantine” a fraction of the josamycin containing ribosomes from the active pool of ribosomes. How expression of  $\text{rpmRNA}^{\text{josa}}$  can be connected to the growth and survival of cells at different concentrations of josamycin is examined in the model, and the result is compared to *in vivo* growth curves.

Previous modeling of peptide-mediated erythromycin resistance resulted in one clear predicted requirement for the resistance mechanism to function; the intracellular concentration of erythromycin has to rapidly equilibrate with the surrounding media (Lovmar *et al.*, 2006). However, all *in vivo* experiments were performed with gram-negative *Escherichia coli* cells where the outer membrane offers an efficient barrier of permeation (Lovmar *et al.*, 2006; Tenson and Mankin, 2001). It seemed therefore that either the prediction, and thus also the model, has to be wrong or there had to be more to the story than appreciated at first. In the previous paper we argued that broad-specific multi-drug pumps located in the inner membrane, especially the AcrAB-TolC system (Zgurskaya and Nikaido, 1999), may account for the rapid antibiotic

equilibration required to confer peptide-mediated resistance (Lovmar *et al.*, 2006). This prediction is tested in this study using a mutant without a working AcrAB-TolC system and both the resulting increase in sensitivity and the loss of peptide mediated resistance of the mutant corresponds well with the model predictions.

## EXPERIMENTAL PROCEDURES

### Chemicals and buffers

GTP, ATP and [<sup>3</sup>H]Met were from GE Biosciences (Uppsala, Sweden). Putrescine, spermidine, phosphoenolpyruvate (PEP), myokinase (MK), inorganic pyrophosphatase (PPiase), erythromycin and non-radioactive amino acids were from Sigma-Aldrich (St. Louis, MO, USA). Pyruvate kinase (PK) was from Boehringer-Mannheim (Mannheim, Germany). Josamycin was from Alexis Biochemicals (Lausen, Switzerland).

All experiments were performed in polymix buffer, at working strength containing 5 mM magnesium acetate, 5 mM ammonium chloride, 95 mM potassium chloride, 0.5 mM calcium chloride, 8 mM putrescine, 1 mM spermidine, 5 mM potassium phosphate and 1 mM dithioerythritol (DTE) (Jelenc and Kurland, 1979).

### In vitro transcribed mRNA for the cell-free translation system

The template DNAs for *in vitro* transcription were prepared by annealing the following oligonucleotides at the complementary sequences (underlined) and filling the gaps by PCR.

Forward oligo: CTCTCTGGTACCGAAATTAATACGACTCACTATAGGGAATT  
CGGGCCCTTGTTAACAATTAAGGAGG.

Reverse oligo for MFLV: TTTTTTTTTTTTTTTTTTTTTTTTATACTAGGAACATAG  
TATACCTCCTTAATTGTTAACAAGGGCCCG

Reverse oligo for MVSN: TTTTTTTTTTTTTTTTTTTTTTTAGTTAGAAACCATAG  
TATACCTCCTTAATTGTTAACAAGGGCCCG

*In vitro* transcription and purification of mRNAs containing a poly(A) tail were as described in (Pavlov and Ehrenberg, 1996).

### DNA oligos used to create plasmids expressing peptides of variable lengths

DNA sequences of different length, designed were amplified by annealing the following oligonucleotides and fill the gaps with PCR. The PCR products were subsequently cut with *Eco*RI and *Afl*III restriction enzymes and cloned into a pPOT1AE vector (Tenson *et al.*, 1996).

Forward oligo for rpmRNA<sup>josa</sup>: ATACAATTGCTAGTCTTAAGGAGGTCACAT  
ATGTTT

Reverse oligo for rpmRNA<sup>josa+LLA</sup>: CTAGAGAATTCAGCTAGTTACGCCAG  
AAGTACTAGGAACATATGTGACCTC

Reverse oligo for rpmRNA<sup>josa+LLASGS</sup>: CTAGAGAATTCAGCTAGTTAGCTGCC  
TGACGCCAGAAGTACTAGGAACATATGTGACCTC

Reverse oligo for rpmRNA<sup>josaMF</sup>: CTAGAGAATTCAGCTAGTTAGAACAT  
ATGTGACCTC

Forward oligo for rpmRNA<sup>eryt</sup>: ATACAATTGCTAGTCTTAAGGAGGTCACAT  
ATGGTT

Reverse oligo for rpmRNA<sup>eryt+LL</sup>: CTAGAGAATTCAGCTAGTTACAGAAGAAC  
AAACAAAACCATATGTGACCTC

Reverse oligo for rpmRNA<sup>eryt+LLASG</sup>: CTAGAGAATTCAGCTAGTTAGCCTGAC  
GCCAGAAGAACAAAACAAAACCATATGTGACCTC

Reverse oligo for rpmRNA<sup>erytMV</sup>: CTAGAGAATTCAGCTAGTTAAACCAT  
ATGTGACCTC

## Procedures

### The components of the purified translation system

Components of the translation system were purified as described in (Tenson *et al.*, 2003), except for RF1, RF2 and RF3 which were purified as described in (Freistoffer *et al.*, 1997), RRF as described in (MacDougall *et al.*, 1997) and peptidyl-tRNA hydrolase (PTH) as described in (Dincbas *et al.*, 1999). All experiments were performed at 37 °C in polymix buffer with addition of ATP (1 mM), GTP (1 mM) and PEP (10 mM).

### Recycling experiments

The initiation mixture contained ribosomes (0.2 μM, ~50% active), [<sup>3</sup>H]fMet-tRNA<sup>fMet</sup> (5 μM), mRNA (0.5 μM), IF2 (0.5 μM), IF1 (1 μM), IF3 (1 μM) and josamycin (2.5 μMn). The recycling mixture contained EF-G (2 μM), EF-Tu (30 μM), EF-Ts (1 μM), RF2 (2 μM), RF3 (2 μM), RRF (2μM), tRNA<sup>bulk</sup> (~0.18 mM), PPIase (5 μg/ml), MK (3 μg/ml), PK (50 μg/ml), the relevant aminoacyl-tRNA synthetases (aaRS) (0.15 Units/μl) (defined in (Ehrenberg *et al.*, 1990)) and amino acids (aa) (leucine 300 μM and 100 μM each of the others). Erythromycin (100 μM) was also added to the recycling mixture when relevant.

Both initiation mixture and recycling mixture were pre-incubated for 8 minutes at 37 °C to allow for formation of ribosomal initiation complexes and ternary complexes, respectively. At time zero, the initiation mixture (10 μl) and the recycling mixture (10 μl) were mixed and at the specified time points the reactions were quenched by adding 155 μl 20% formic acid, and peptide formation were analyzed using RP-HPLC as described in (Tenson *et al.*, 2003). Peptidyl-tRNA hydrolase (~250 Units (hydrolysed tRNA/s) was added to the reaction mixture 15 s prior to quenching to allow detection of the drop-off products on the HPLC in parallel to the full-length peptide.

### Measuring the length dependence for josamycin- and erythromycin resistance peptides

Overnight cultures of cells expressing peptides of different length were grown in medium containing 100 μg/ml ampicillin. Cultures were diluted with fresh medium containing 100 μg/ml ampicillin, 1 mM IPTG, 75 μg/ml erythromycin or 200 μg/ml josamycin and in parallel with medium containing 100 μg/ml ampicillin, 1 mM IPTG to the final density of A<sub>600</sub> = 0.01. Cells were grown until the optical densities of cultures grown in the absence of macrolide reached A<sub>600</sub> of c.1. At this point the absorbance of the corresponding macrolide containing culture was measured, which is equal to the relative resistance because the absorbance of the culture grown without macrolide is one.

### Measuring growth with varying josamycin concentration and rpmRNA<sup>josA</sup> expression levels

Overnight cultures of cells expressing rpmRNA<sup>josA</sup> (MFLV-peptide) were grown in medium containing 100 µg/ml ampicillin. Cultures were diluted to A<sub>600</sub> = 0.01 into 96-well plates with fresh medium containing josamycin and IPTG at different concentrations. IPTG concentrations for rpmRNA<sup>josA</sup> expressing cells were 0 µM; 50 µM; 75 µM; 100 µM; 125 µM; 150 µM; 175 µM; 200 µM; 500 µM; 1000 µM. Josamycin concentrations were 0 µg/ml; 100 µg/ml; 150 µg/ml; 200 µg/ml; 250 µg/ml; 300 µg/ml; 500 µg/ml; 1000 µg/ml. The cell cultures were grown 8 hours and the absorbance at 600 nm were measured using a TECAN Sunrise instrument.

### Measuring the effect of efflux pump mutants on josamycin sensitivity and resistance

MG1655 cells and MG1655 TolC mutant cells, expressing rpmRNA<sup>eryT</sup> (MVLV-peptide) or rpmRNA<sup>josA</sup> (MFLVLLA-peptide), or possessing empty vector pPOT1 (Tenson *et al.*, 1996) were grown overnight in 2\*YT medium in the presence of ampicillin (100 µg/ml) at 37 °C. Overnight cultures were diluted to A<sub>600</sub> = 0.01 with fresh 2\*YT medium containing 100 µg/ml ampicillin, 100 µM IPTG and different concentrations of erythromycin and josamycin respectively. Cultures were grown in the microtiter plate for 4 hours at 37 °C and A<sub>600</sub> was measured using a TECAN Sunrise instrument. Expression of rpmRNA<sup>josA</sup> encoding MFLVLLA-peptide was used instead of the classical MFLV-peptide, because MFVLLA expression does not inhibit bacterial growth.

## RESULTS

### **Biochemical characterization of expression of josamycin resistance peptide**

Using a cell-free translation system with purified components from *E. coli* (Pavlov and Ehrenberg, 1996) we translated the rpmRNA<sup>josA</sup> encoding fMet-Phe-Leu-Val (Vimberg *et al.*, 2004) and a control mRNA encoding fMet-Val-Ser-Asn. The ribosomes were pre-incubated with either josamycin or erythromycin and used in recycling mode (Pavlov *et al.*, 1997), *i.e.* each ribosome produced several copies of the encoded peptide. In order to probe the dissociation of josamycin we chased it with an excess of erythromycin, which competes with josamycin binding but allows formation of tetrapeptides (Lovmar *et al.*, 2006; Lovmar *et al.*, 2004). The amounts of resistance- and control tetrapeptides produced at different time points are shown in Figs. 1A and 1B, respectively. As expected from the previous studies, josamycin blocked formation of both tetrapeptides, while erythromycin allowed tetrapeptide formation. From the chase experiments it is clear that translation of the rpmRNA<sup>josA</sup> does not significantly increase the josamycin dissociation rate over translation of the control peptide. From these chase experiments the josamycin dissociation rate constant could be estimated to 0.01 min<sup>-1</sup> which is similar to the previously estimated spontaneous dissociation rate constant (Lovmar *et al.*, 2004).

In parallel to the measurements of tetrapeptide formation we also studied the drop-off products formed during translation of rpmRNA<sup>josA</sup> (Fig. 1C) or control mRNA (Fig. 1D). Interestingly, josamycin-containing ribosomes produced much less dipeptidyl-tRNA when translating the rpmRNA<sup>josA</sup> rather than the control peptide. The “production” of drop-off products occurs at 0.28 min<sup>-1</sup> when josamycin containing ribosomes are translating rpmRNA<sup>josA</sup>, compared to 2.1 min<sup>-1</sup> when translating the control mRNA. The reason for this difference is that josamycin inhibits the peptidyl transfer to the phenylalanine acceptor much more efficiently than to the valine

acceptor (Lovmar *et al.*, 2004). This causes the  $\text{rpmRNA}^{\text{josa}}$  to block josamycin containing ribosomes as stable initiation complexes, while peptidyl transfer and subsequent josamycin induced peptidyl-tRNA drop-off is much faster for the control mRNA.

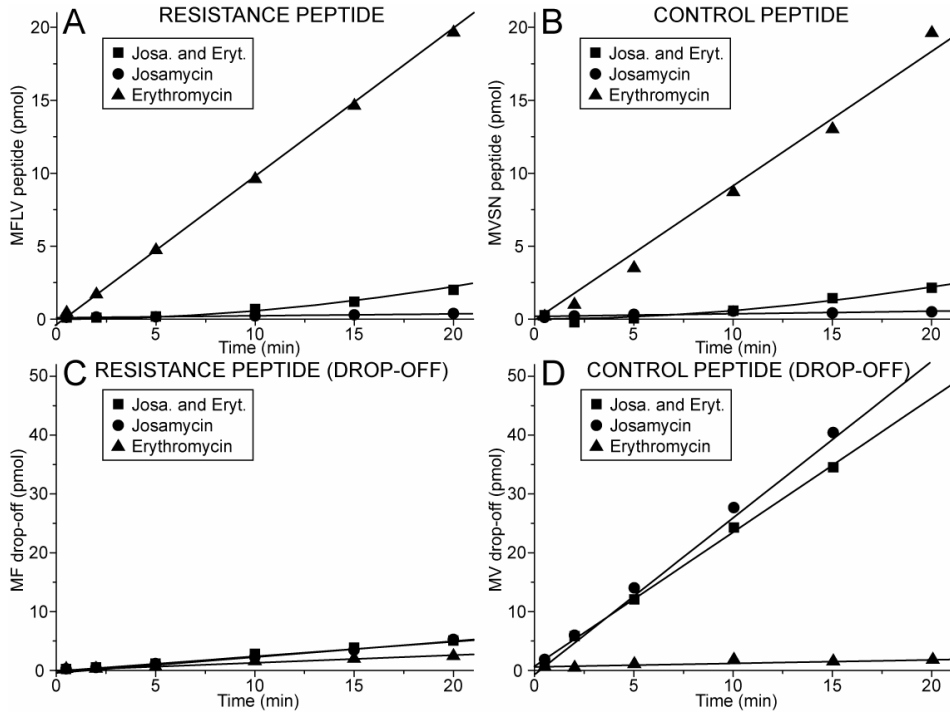


**FIGURE 1. Biochemical characterization of peptide mediated josamycin resistance.** The amounts of produced resistance peptide (MFLV, panel A) and control peptide (MVSN, panel B) are plotted against time. Erythromycin ( $\blacktriangle$ ) allows formation of both tetra-peptides, while josamycin ( $\bullet$ ) does not allow any tetra-peptide formation. When josamycin dissociates in the chase experiment ( $\blacksquare$ ) it is replaced by erythromycin which enables tetra-peptide formation. In panels C and D the accumulation of dipeptidyl-tRNA drop-off products are plotted against time. The symbols in panels C and D is the same as the corresponding experiment in panels A and B. All experiments contain 1 pmol of active ribosomes.

### Erythromycin resistance is strictly dependent on the length of the encoded peptide while josamycin resistance is not

The biochemical data propose that the mechanism of  $\text{rpmRNA}^{\text{josa}}$  is different to the previously described “bottle-brush” mechanism, and that it instead depends on the reduced rate of peptidyl tRNA-drop-off. The prediction is therefore that  $\text{rpmRNA}^{\text{josa}}$ , in contrast to  $\text{rpmRNA}^{\text{eryt}}$ , is insensitive to the length of the encoded peptide. This prediction was tested by measuring the resistance activity *in vivo* of both  $\text{rpmRNA}^{\text{josa}}$  and  $\text{rpmRNA}^{\text{eryt}}$  encoding peptides with varying lengths (Fig. 2).

The length of the open reading frames of both rpmRNAs were decreased to two codons and increased to seven or ten codons. Bacteria expressing the natural or the modified variants of rpmRNA<sup>eryt</sup> and rpmRNA<sup>josa</sup> were grown in the presence and in the absence of the corresponding macrolide. The ratios of the optical densities with or without the respective macrolide are plotted for these strains in figure 2. The length of rpmRNA<sup>eryt</sup> is crucial for resistance against erythromycin (Fig. 2A), while josamycin resistance by rpmRNA<sup>josa</sup> is solely dependent on the nature of the second codon and independent of the length in accordance with the prediction (Fig. 2B).

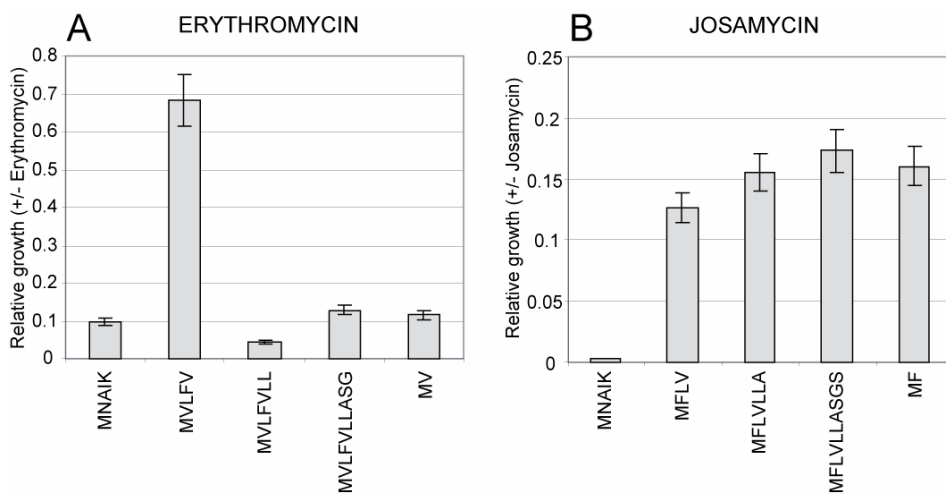


**FIGURE 2. The degree of erythromycin resistance is strictly dependent on resistance peptide length but not peptide-mediated josamycin resistance.** Resistance is given as the ratio of bacterial growth as measured by optical density of resistance peptide expressing cells in the presence of (A) erythromycin (75  $\mu\text{g/ml}$ ) or (B) josamycin (200  $\mu\text{g/ml}$ ), respectively, and bacterial growth in the absence of the macrolide for the indicated peptide sequences.

### Expression of rpmRNA<sup>josa</sup> “quarantines” ribosomes with josamycin and reduces peptidyl-tRNA drop-off

The biochemical experiments described above in combination with previous studies provide kinetic constants that allow modeling of the direct effects of expression of rpmRNA<sup>josa</sup> (Table 1 in Appendix). We adapted our previously developed model of peptide-mediated erythromycin resistance to josamycin as illustrated in Fig. 3A (see Appendix for details), but because expression of rpmRNA<sup>josa</sup> does not promote dissociation of josamycin it can not increase protein synthesis directly.

Instead, expression of rpmRNA<sup>josa</sup> “quarantines” josamycin containing ribosomes in form of initiation complexes encoded with rpmRNA<sup>josa</sup>. The direct effect of this “quarantine” is that the amount of peptidyl-tRNA drop-off is reduced (Fig. 3B), and thereby there is a reduced risk of peptidyl-tRNA hydrolase (Pth) saturation leading to depletion of tRNA pools. The selectivity of the “quarantine” mechanism allows a large fraction of the josamycin-free ribosomes to continue translating cellular mRNAs, despite the competition with high concentration of rpmRNA<sup>josa</sup>.

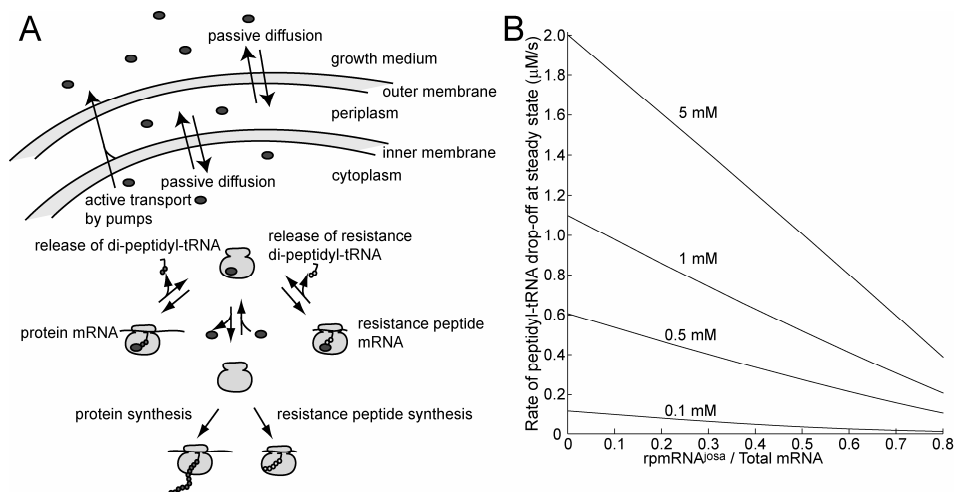


**FIGURE 3. Modeling the “quarantine” mechanism.** Panel A show a schematic of the model. A josamycin-carrying ribosome stalls on a  $\text{rpmRNA}^{\text{josa}}$  (right) or on a protein mRNA (left) which results in drop-off of di-peptidyl-tRNA while josamycin stays bound on the ribosome. A drug-free ribosome completes both protein and resistance peptides synthesis (bottom). The uppermost part illustrates influx and efflux of josamycin in the cell (gram-negative bacterium). Panel B shows how the amount of peptidyl-tRNA drop-off is decreased by expression of  $\text{rpmRNA}^{\text{josa}}$ .

### mRNA limitation might account for the observed resistance peptide action *in vivo*

In addition to the “quarantine” effects described above will expression of  $\text{rpmRNA}^{\text{josa}}$  lead to an increase in the total number of ribosome binding sites (RBS) because of the small size of  $\text{rpmRNA}^{\text{josa}}$  (assuming a fixed capacity of the RNA polymerases). This increase may be important because josamycin-containing ribosomes block RBS, eventually leading to mRNA depletion. Further, an increased concentration of RBS may lead to more rapid initiation and thus josamycin will have a smaller time window for binding the josamycin-free ribosomes. It is therefore possible that expression of  $\text{rpmRNA}^{\text{josa}}$  indirectly can decrease the fraction of ribosomes that contains josamycin.

We modeled the quantitative effects of  $\text{rpmRNA}^{\text{josa}}$  expression by focusing on mRNA supply. Especially, the degradation of a protein mRNA with a stalled josamycin-ribosome in the 5' end was modeled in detail. As previously, the model also described both synthesis and degradation of both mRNA and  $\text{rpmRNA}^{\text{josa}}$  as well as dynamics of the antibiotic exchange over the inner and outer cell membranes. In addition, the model accounts for the dilution of all compounds due to cell growth. Using this model we predicted the growth at 8 hours after expression of  $\text{rpmRNA}^{\text{josa}}$  at different levels in the presence of different concentrations of josamycin (Fig. 4A). It should be pointed out that modeled resistance by mRNA limitation crucially depends on a much slower drop-off rate of the resistance di-peptidyl-tRNA than of other dipeptidyl-tRNAs.

## Peptide-mediated josamycin resistance demonstrated by cell population growth

The expression of resistance peptide mRNA coding for peptide MFLV was under *tac* promoter control on a multi-copy plasmid and the expression level could therefore be varied by varying the concentration of IPTG. Cell growth at different IPTG and josamycin concentrations was detected by optical density at 600 nm after 8 hours following the addition of josamycin to the growth medium (Fig. 4B). The results correspond well with the predicted behavior from the mRNA depletion model (Fig. 4A).

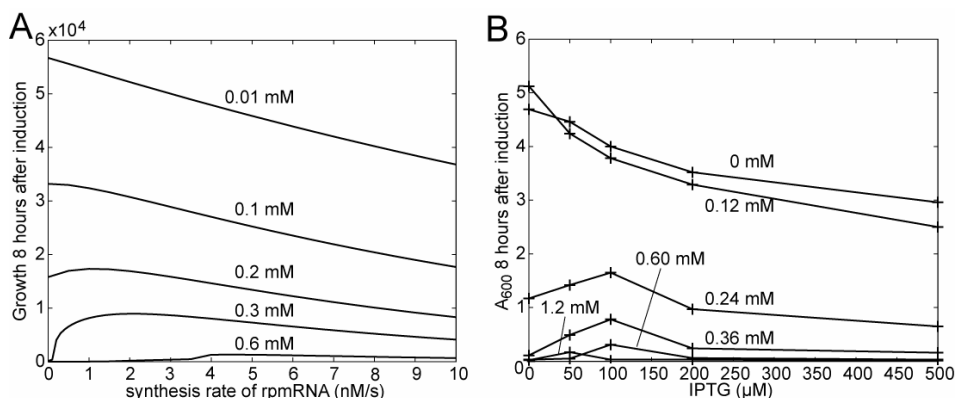


**FIGURE 4. Comparison between modeled and *in vivo* peptide-mediated josamycin resistance.** A. Simulated growth (defined as how many times the cell volume has increased during the first 8 hours after the addition of josamycin) plotted against the rate of resistance peptide mRNA synthesis for different concentrations of josamycin. B. Optical density (600 nm) measured 8 hours after the addition of josamycin plotted against the concentration of IPTG.

## Peptides mediate macrolide resistance in wild-type *E. coli* cells but not in a pump mutant

It has previously been predicted that the resistance peptide mechanism requires rapid equilibration between the intracellular macrolide concentration and the concentration in the surrounding media. It was further proposed that this could be accomplished by a naturally occurring drug-efflux system (Lovmar *et al.*, 2006). Therefore, the resistance models for josamycin and erythromycin were used with the more detailed description of the flows of the antibiotic over the cell membranes described here to study resistance with and without antibiotic efflux pumps (see Appendix). As expected, removal of the antibiotic efflux pump system makes the cells hypersensitive to both erythromycin and josamycin, but in addition the model predicts that the peptide mediated resistance disappears (Fig. 5).

To validate these results we studied growth in bacterial populations of both wild-type *E. coli* cells and *E. coli* cells (TolC) with a mutated efflux pump system, containing a multi-copy vector expressing rpmRNA or containing a control vector. Expression of rpmRNA was under the control of a *tac* promoter induced by 100  $\mu$ M of IPTG which corresponds to maximal resistance as observed in Fig. 4B for josamycin and as

previously reported for erythromycin (Fig. 3C in (Lovmar *et al.*, 2006)). Bacterial mass was monitored as absorbance at 600 nm 4 hours after addition of varying concentrations of erythromycin or josamycin to the growth medium. Both the increased sensitivity and the loss of resistance were observed in the TolC mutant (Fig. 6).

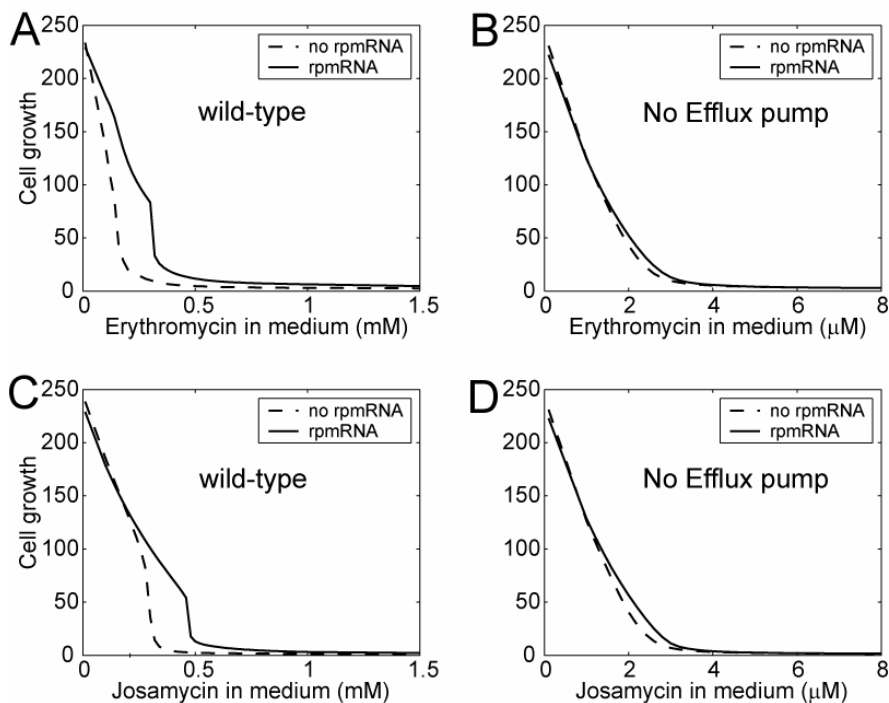


**FIGURE 5. Modeled peptide-mediated resistance with but not without pumps.** Cell growth is given as volume expansion (defined as how many times the cell volume has increased) 4 hours following the introduction of the indicated macrolide concentrations in the growth medium in the model, with resistance peptide mRNA (rpmRNA) expression (solid line), without rpmRNA expression (broken line). The wild-type (A and C) is modelled with pumps in the inner membrane but not the TolC mutant (B and D). The rate constant of rpmRNA synthesis was  $2 \text{ nMs}^{-1}$ .

## DISCUSSION

Although the clinical relevance of peptide mediated resistance is not clear, it is still an interesting phenomenon that reveals more information about the mechanisms by which macrolide antibiotics inhibit cell growth. It was previously shown that rpmRNA<sup>eryt</sup> works through a “bottle-brush” mechanism, *i.e.* expression of a resistance peptide “cleans” the nascent peptide exit tunnel from erythromycin (Lovmar *et al.*, 2006). Both the amino acid sequence and the length of the encoded peptide are essential parameters for the “bottle-brush” mechanism to work (Tenson *et al.*, 1997) and, at least in the erythromycin case, the drug seems to be stoichiometrically expelled at the termination step (Lovmar *et al.*, 2006). The “bottle-brush” mechanism has been proposed to be general for all classes of macrolides, albeit with modulated

sequence specificity (Vimberg *et al.*, 2004). The 16-membered macrolide josamycin has been shown to in most cases only allow a single peptidyl transfer reaction to occur before the peptidyl-tRNA dissociates (Tenson *et al.*, 2003) and it was therefore surprising that  $\text{rpmRNA}^{\text{josa}}$  expressing tetra- or pentameric peptides could be selected (Vimberg *et al.*, 2004). The present study clearly shows that the “bottle-brush” mechanism is not responsible for the peptide-mediated resistance against josamycin; instead we propose a “quarantine” mechanism to be responsible for the observed resistance.

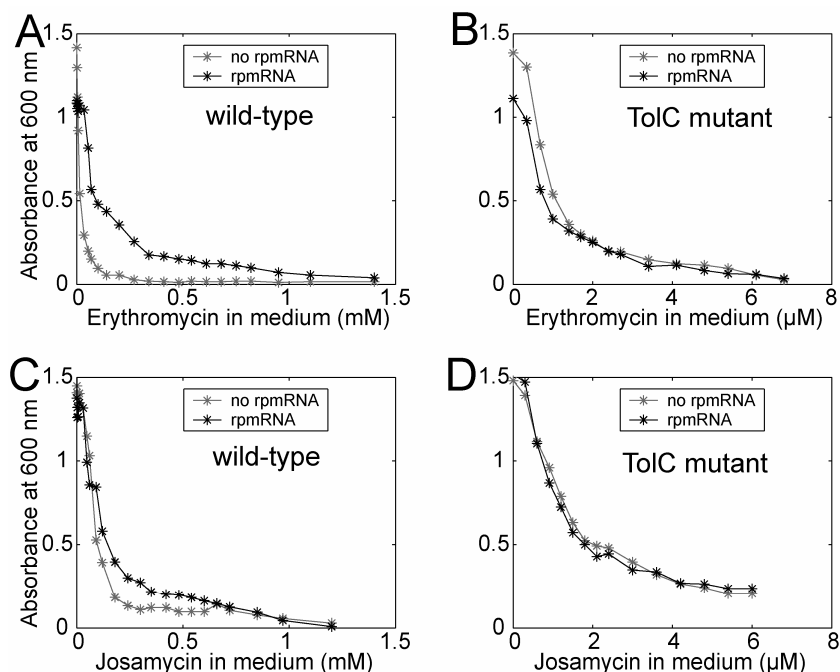


**FIGURE 6. Peptide-mediated resistance *in vivo* in the wild-type but not in a pump mutant.** Absorbance (600 nm) of wild-type (A and C) and ToIC (pump) mutant (B and D) *Escherichia coli* cells with a resistance peptide expressing vector ( $\text{rpmRNA}$ ) or a control vector (no  $\text{rpmRNA}$ ) after 4 hours of growth following addition of the indicated macrolide concentrations.

### Comparison between $\text{rpmRNA}^{\text{josa}}$ and $\text{rpmRNA}^{\text{eryt}}$

Expression of  $\text{rpmRNA}^{\text{eryt}}$  increase the erythromycin dissociation rate constant by an order of magnitude in concordance with the suggested “bottle-brush” mechanism (Lovmar *et al.*, 2006). In contrast, expression of  $\text{rpmRNA}^{\text{josa}}$  did not change the dissociation rate constant of josamycin (Figs. 1A and 1B), but instead it slowed down the rate of peptidyl-tRNA drop-off by an order of magnitude (Fig. 1C) compared to the control mRNA (Fig. 1D). Peptidyl-tRNA drop-off is not an issue during  $\text{rpmRNA}^{\text{eryt}}$  expression, because erythromycin leaves enough space in the tunnel to allow translation of the complete penta-peptide (Tenson *et al.*, 2003). The present results on  $\text{rpmRNA}^{\text{josa}}$  suggest that it is never completely translated and thus the resistance mechanism for josamycin should be independent of the length of the encoded peptide. This is in contrast to the results on erythromycin resistance where

the peptide length was shown to be crucial for erythromycin resistance both in living cells (Tenson *et al.*, 1997) and in a cell-free translation system (Lovmar *et al.*, 2006).

The prediction on the length dependence was tested by expressing peptides with lengths varying between 2 and 10 amino acids with sequences according to the consensus for rpmRNA<sup>eryt</sup> and rpmRNA<sup>josa</sup> respectively (Vimberg *et al.*, 2004). The resistance activity of rpmRNA<sup>eryt</sup> was shown to be strongly peptide length dependent in agreement with previous experiments (Fig. 2A). In contrast to rpmRNA<sup>eryt</sup>, but in agreement with the prediction, is the activity of rpmRNA<sup>josa</sup> not sensitive to the length of the expressed peptides (Fig. 2B). The reason that most of the selected rpmRNA<sup>josa</sup> encoded pentamers was simply that the mini-gene library encoded pentamers with randomized sequences (Vimberg *et al.*, 2004). In conclusion, it seems that the only important feature of rpmRNA<sup>josa</sup> appears to be that it encodes a phenylalanine or tyrosine in the second position (Vimberg *et al.*, 2004).

### Josamycin resistance through “quarantining” josamycin containing ribosomes

At first it might be hard to imagine how expression of an mRNA encoding phenylalanine or tyrosine in the second position can render resistance to josamycin. The key to understand the mechanism can be found in the slow peptidyl-tRNA drop-off rate when expressing rpmRNA<sup>josa</sup> compared to other mRNAs. Because rpmRNA<sup>josa</sup> can not expel josamycin from the ribosomes, it instead works by minimizing the negative effects of josamycin bound ribosomes through “quarantining” them on rpmRNA<sup>josa</sup>. The “quarantine” can be understood as follows; ribosomes containing josamycin will be stuck on the rpmRNA<sup>josa</sup> ten times longer than on other mRNAs, while ribosomes without josamycin recycles much faster on the short rpmRNA<sup>josa</sup> than on other mRNAs. These combined effects lead to an enrichment of josamycin containing ribosomes on rpmRNA<sup>josa</sup>, while the ribosomes without josamycin are enriched on protein mRNAs where they continue synthesizing proteins with less interference from ribosomes containing josamycin. A requirement for the “quarantine” to work is a very slow exchange of josamycin between different ribosomes, so that most of the ribosomes keep their identity as “josamycin-containing” or “josamycin-free” at least within the time range of ribosome recycling. The average recycling time for josamycin containing ribosomes on rpmRNA<sup>josa</sup> is 4 minutes, and josamycin stays bound to a ribosome for an average time of 1.5 hours (Lovmar *et al.*, 2004) which clearly fulfils this requirement. It should further be noted that only very few natural mRNAs encodes phenylalanine or tyrosine in the second position, thus over-expression of rpmRNA<sup>josa</sup> will have a strong impact on the fraction of mRNAs encoding these amino acids in the second position resulting in the “quarantine” effect.

The apparent explanation to why “quarantining” josamycin containing ribosomes on rpmRNA<sup>josa</sup> confer resistance is that it reduces the demand of a component necessary for translation or recycling of ribosomes, thus allowing the josamycin-free ribosomes to continue translation at a close to normal rate. For example, the josamycin induced peptidyl-tRNA drop-off may accumulate peptidyl-tRNA in the cells, thus the pools of free tRNA isoacceptors will be depleted when the capacity of peptidyl-tRNA hydrolase (Pth) is saturated (Heurgue-Hamard *et al.*, 2000; Heurgue-Hamard *et al.*, 1996; Tenson *et al.*, 1999). There are also some unpublished results indicating that depletion of tRNA pools contributes to the josamycin toxicity, *i.e.* suppression of Pth expression makes cells hyper-sensitive to josamycin, while a slight over-expression of

Pth leads to low-level resistance (Tenson T, unpublished results). However, a fraction of ribosomes containing josamycin might deplete other components of the translation machinery before the pools of tRNAs, and therefore the “quarantine” mechanism might render resistance also without saturated Pth.

### **Resistance can occur through avoiding depletion of mRNA pools by “quarantining” the josamycin containing ribosomes**

A bacterial population containing a plasmid-borne  $\text{rpmRNA}^{\text{josa}}$  under control of the *tac* promoter was grown in media with varying IPTG concentrations to regulate the level of resistance peptide expression combined with varying josamycin concentrations. The increase in bacterial mass after 8 hours of growth after induction was monitored by absorbance as a function of the IPTG concentration in the medium. To test whether it is possible to reproduce the *in vivo* effects of  $\text{rpmRNA}^{\text{josa}}$  expression without considering the tRNA pools we adapted the model previously developed for peptide-mediated erythromycin resistance (Lovmar *et al.*, 2006) to the parameter values for josamycin. The mathematical model was changed to account for josamycin resistance by modeling a delayed di-peptidyl-tRNA drop-off from a josamycin-carrying ribosome expressing the resistance peptide while the antibiotic stays bound to the ribosome. By assuming a low rate of degradation of mRNAs with a stalled ribosome in the 5' end (Joyce and Dreyfus, 1998), we obtained growth curves mimicking the *in vivo* observed growth curves (Fig. 4).

The importance of the modeled mRNA degradation can be understood as follows. The concentration of protein mRNAs in a cell is much lower than the concentration of ribosomes. Thus, only a small fraction of drug-inhibited ribosomes, stalled on mRNA can potentially severely slow down protein synthesis. When protein mRNAs with a stalled ribosome is slowly degraded, the free concentration of protein mRNAs on which a ribosome can initiate translation drastically declines (not shown). The delay at initiation increases the impact of josamycin since 50S subunits exist in a josamycin-susceptible state a longer period of time. The result is a larger fraction of non-translating and josamycin bound 50S subunits as well as a larger fraction of ribosomes stalled on mRNAs (not shown), which contributes to further lowering the concentration of free mRNAs. The feedback between the low concentration of free protein mRNAs and increased concentration of inactivated 50S subunits makes the growth rate severely reduced at a certain antibiotic concentration. When  $\text{rpmRNA}^{\text{josa}}$  is present in the cell, josamycin-infected ribosomes are “quarantined” on the  $\text{rpmRNA}^{\text{josa}}$ . The free concentration of protein mRNAs boosts and ribosomes can initiate translation at a higher rate and escapes josamycin to a larger extent. The concentration of josamycin-free translating ribosomes increases, thereby raising the cell growth rate.

### **Peptide-mediated macrolide resistance requires a fast outflow rate of the antibiotic over the cell membrane**

Previous modeling of peptide-mediated erythromycin resistance predicted the requirement of a fast outflow rate of the drug over the cell membrane to confer resistance against a macrolide with the binding kinetics of erythromycin. In gram-positive bacteria the cell wall does not offer much resistance to diffusion of small molecules and the rate of exchange of macrolides over the cell membrane is expected to be rapid, but previous *in vivo* experiments were done with gram-negative *E. coli*

cells (Lovmar *et al.*, 2006; Tenson and Mankin, 2001). In gram-negatives the outer membrane confers an efficient barrier of permeation and the entrance rate of antibiotics are expected to be slow. Gram-negative bacteria also harbor broad-specific multidrug pumps in their inner membrane, which together with the outer membrane may explain the “intrinsic” resistance that gram-negatives exhibit (Li and Nikaido, 2004). The AcrAB-TolC pump system is the major contributor of erythromycin resistance (Ma *et al.*, 1995). The efflux pump, AcrB, resides in the inner membrane and seems to form a complex with a periplasmic protein, AcrA, which links or fuses the inner and outer membrane. Then, the channel, TolC, most likely provides the exit path back to the medium for drugs, solvents, detergents etc. (Zgurskaya and Nikaido, 1999). Very little is known about the capacity of the AcrAB-TolC pump system in general and for erythromycin and josamycin in particular.

To validate the model prediction we grew wild-type and TolC mutant *E.coli* cells containing either a resistance peptide expressing plasmid or a control plasmid in the presence of varying concentrations of erythromycin in the growth medium. Corresponding experiments were done with varying concentrations of josamycin in the growth medium. Growth was recorded by absorbance after 4 hours following induction and was registered as a function of the macrolide concentration and at an IPTG concentration corresponding to maximal resistance in the wild-type as seen in previous *in vivo* growth experiments. The *in vivo* experiments confirmed the model prediction for erythromycin. No resistance was observed in the TolC mutant (Fig. 6B). The *in vivo* experiments also showed no josamycin resistance in the TolC mutant (Fig. 6D), which resistance mechanism clearly differs from that of erythromycin.

The TolC mutant is as sensitive to macrolides as the AcrB mutant, why we do not expect the pump to function in the TolC mutant. The TolC mutant was therefore modeled without pumps. The models reproduced the *in vivo* growth curves. Resistance was substantially reduced in the TolC mutant for both erythromycin and josamycin (Fig. 5B and D). In the case of erythromycin, where expression of a resistance peptide actively removes a bound drug molecule from the ribosome (Lovmar *et al.*, 2006) resistance is a consequence of an increased dissociation of erythromycin. Such a resistance mechanism is sensitive to the fate of the drug molecule after ejection. It can either leave the cell (by passive diffusion over the membrane or be actively transported by efflux pumps) or it re-associates to another ribosome. The value of the rate constant for leaving the cell in relation to the association rate constant of the antibiotic becomes very important. The requirement of a fast outflow rate for erythromycin resistance mechanism to work is then rather a requirement of a fast enough rate constant of leaving the cell once inside compared to the association rate constant to a ribosome of the antibiotic. We argue that the AcrAB-TolC efflux pump system provide the required high efflux rate. Thus, a macrolide with a lower association rate constant but with the same or lower dissociation rate constant of erythromycin is predicted by the model to confer resistance also in the TolC mutant, if resistance is mediated by active removal of the drug by the same rate as of erythromycin. For instance, a macrolide with an association rate constant of josamycin but with a dissociation rate constant of erythromycin confer resistance in the simulated TolC mutant (not shown), while a macrolide with an 100 times higher association rate constant than erythromycin gives almost no resistance in the wild-type (not shown).

In the case of josamycin, the absence of resistance in the modelled TolC mutant is also a consequence of a too high association rate constant compared to the rate constant of efflux of the drug. This creates a sharp boost of the intracellular concentration of josamycin within a very narrow interval of concentrations of the antibiotic in the medium accompanied by a dramatic reduction of the growth rate and leaves the resistance mechanism ineffective since it cannot remove josamycin once bound to the ribosomes. For example, if the association rate constant is increased 100 times, resistance is greatly reduced even in the wild-type.

## REFERENCES

- Bremer, H., and Dennis, P. P. (1996). Modulation of Chemical Composition and Other Parameters of the Cell by Growth Rate, In *Escherichia coli* and *Salmonella*: cellular and molecular biology, F. C. Neidhardt, ed. (Washington: ASM Press), pp. 1553-1569.
- Dincbas, V., Heurgue-Hamard, V., Buckingham, R. H., Karimi, R., and Ehrenberg, M. (1999). Shutdown in protein synthesis due to the expression of mini-genes in bacteria. *J Mol Biol* 291, 745-759.
- Ehrenberg, M., Bilgin, N., and Kurland, C. G. (1990). Design and use of a fast and accurate *in vitro* translation system., In *Ribosomes and protein synthesis: a practical approach*, G. Spedding, ed. (Oxford: IRL Press), pp. 101-128.
- Freistroffer, D. V., Pavlov, M. Y., MacDougall, J., Buckingham, R. H., and Ehrenberg, M. (1997). Release factor RF3 in *E.coli* accelerates the dissociation of release factors RF1 and RF2 from the ribosome in a GTP-dependent manner. *Embo J* 16, 4126-4133.
- Hansen, J. L., Ippolito, J. A., Ban, N., Nissen, P., Moore, P. B., and Steitz, T. A. (2002). The structures of four macrolide antibiotics bound to the large ribosomal subunit. *Mol Cell* 10, 117-128.
- Heath, M. T. (1997). *Scientific computing: an introductory survey* (New York: McGraw-Hill).
- Heurgue-Hamard, V., Dincbas, V., Buckingham, R. H., and Ehrenberg, M. (2000). Origins of minigene-dependent growth inhibition in bacterial cells. *Embo J* 19, 2701-2709.
- Heurgue-Hamard, V., Mora, L., Guarneros, G., and Buckingham, R. H. (1996). The growth defect in *Escherichia coli* deficient in peptidyl-tRNA hydrolase is due to starvation for Lys-tRNA(Lys). *Embo J* 15, 2826-2833.
- Jelenc, P. C., and Kurland, C. G. (1979). Nucleoside triphosphate regeneration decreases the frequency of translation errors. *Proc Natl Acad Sci U S A* 76, 3174-3178.

- Joyce, S. A., and Dreyfus, M. (1998). In the absence of translation, RNase E can bypass 5' mRNA stabilizers in *Escherichia coli*. *J Mol Biol* 282, 241-254.
- Leclercq, R. (2002). Mechanisms of resistance to macrolides and lincosamides: nature of the resistance elements and their clinical implications. *Clin Infect Dis* 34, 482-492.
- Li, X. Z., and Nikaido, H. (2004). Efflux-mediated drug resistance in bacteria. *Drugs* 64, 159-204.
- Lovmar, M., Nilsson, K., Vimberg, V., Tenson, T., Nervall, M., and Ehrenberg, M. (2006). The Molecular Mechanism of Peptide-mediated Erythromycin Resistance. *J Biol Chem* 281, 6742-6750.
- Lovmar, M., Tenson, T., and Ehrenberg, M. (2004). Kinetics of macrolide action: the josamycin and erythromycin cases. *J Biol Chem* 279, 53506-53515.
- Ma, D., Cook, D. N., Alberti, M., Pon, N. G., Nikaido, H., and Hearst, J. E. (1995). Genes *acrA* and *acrB* encode a stress-induced efflux system of *Escherichia coli*. *Mol Microbiol* 16, 45-55.
- MacDougall, J., Holst-Hansen, P., Mortensen, K. K., Freistroffer, D. V., Pavlov, M. Y., Ehrenberg, M., and Buckingham, R. H. (1997). Purification of active *Escherichia coli* ribosome recycling factor (RRF) from an osmo-regulated expression system. *Biochimie* 79, 243-246.
- Neidhardt, F. C., and Umberger, H. E. (1996). Chemical compositions of *Escherichia coli*, In *Escherichia coli and Salmonella: cellular and molecular biology*, F. C. Neidhardt, ed. (Washington: ASM Press), pp. 13-16.
- Pavlov, M. Y., and Ehrenberg, M. (1996). Rate of translation of natural mRNAs in an optimized in vitro system. *Arch Biochem Biophys* 328, 9-16.
- Pavlov, M. Y., Freistroffer, D. V., MacDougall, J., Buckingham, R. H., and Ehrenberg, M. (1997). Fast recycling of *Escherichia coli* ribosomes requires both ribosome recycling factor (RRF) and release factor RF3. *Embo J* 16, 4134-4141.
- Schlunzen, F., Zarivach, R., Harms, J., Bashan, A., Tocilj, A., Albrecht, R., Yonath, A., and Franceschi, F. (2001). Structural basis for the interaction of antibiotics with the peptidyl transferase centre in eubacteria. *Nature* 413, 814-821.
- Tenson, T., DeBlasio, A., and Mankin, A. (1996). A functional peptide encoded in the *Escherichia coli* 23S rRNA. *Proc Natl Acad Sci U S A* 93, 5641-5646.
- Tenson, T., Herrera, J. V., Kloss, P., Guarneros, G., and Mankin, A. S. (1999). Inhibition of translation and cell growth by minigene expression. *J Bacteriol* 181, 1617-1622.

Tenson, T., Lovmar, M., and Ehrenberg, M. (2003). The mechanism of action of macrolides, lincosamides and streptogramin B reveals the nascent Peptide exit path in the ribosome. *J Mol Biol* 330, 1005-1014.

Tenson, T., and Mankin, A. S. (2001). Short peptides conferring resistance to macrolide antibiotics. *Peptides* 22, 1661-1668.

Tenson, T., Xiong, L., Kloss, P., and Mankin, A. S. (1997). Erythromycin resistance peptides selected from random peptide libraries. *J Biol Chem* 272, 17425-17430.

Tripathi, S., Kloss, P. S., and Mankin, A. S. (1998). Ketolide resistance conferred by short peptides. *J Biol Chem* 273, 20073-20077.

Weisblum, B. (1995). Erythromycin resistance by ribosome modification. *Antimicrob Agents Chemother* 39, 577-585.

Weisblum, B. (1998). Macrolide resistance. *Drug Res Updates* 1, 29-41.

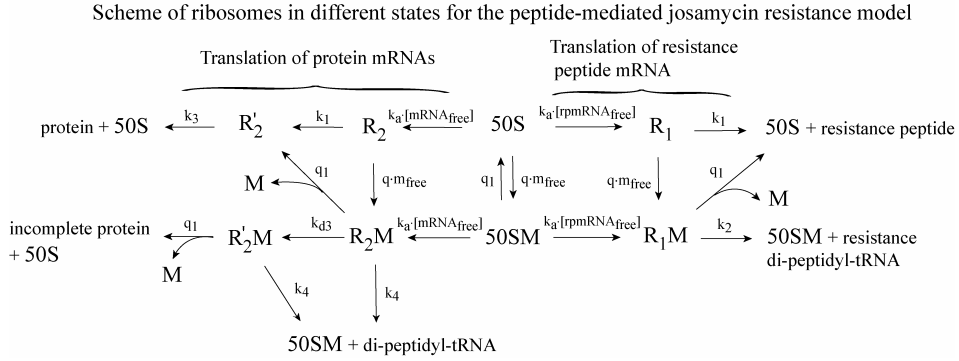
Vimberg, V., Xiong, L., Bailey, M., Tenson, T., and Mankin, A. (2004). Peptide-mediated macrolide resistance reveals possible specific interactions in the nascent peptide exit tunnel. *Mol Microbiol* 54, 376-385.

Zgurskaya, H. I., and Nikaido, H. (1999). Bypassing the periplasm: reconstitution of the AcrAB multidrug efflux pump of *Escherichia coli*. *Proc Natl Acad Sci U S A* 96, 7190-7195.

## APPENDIX

### Model of peptide-mediated resistance against josamycin

Below is a detailed description of the different states of ribosomes in the model.



The model is described by the following system of differential equations,

$$\begin{aligned}
 \frac{d[50SM]}{dt} &= q \cdot [m_{free}] \cdot [50S] + k_4 \cdot ([R_2M] + [R_2'M]) + k_2 \cdot [R_1M] - (k_a \cdot ([mRNA_{free}] + [rpmRNA_{free}]) + q_1 + \mu) \cdot [50SM], \\
 \frac{d[R_1]}{dt} &= k_a \cdot [rpmRNA_{free}] \cdot [50S] - (k_1 + q \cdot [m_{free}] + \mu) \cdot [R_1], \\
 \frac{d[R_1M]}{dt} &= k_a \cdot [rpmRNA_{free}] \cdot [50SM] + q \cdot [m_{free}] \cdot [R_1] - (k_2 + q_1 + \mu) \cdot [R_1M], \\
 \frac{d[R_2]}{dt} &= k_a \cdot [mRNA_{free}] \cdot [50S] - (k_1 + q \cdot [m_{free}] + \mu) \cdot [R_2], \\
 \frac{d[R_2M]}{dt} &= k_a \cdot [mRNA_{free}] \cdot [50SM] + q \cdot [m_{free}] \cdot [R_2] - (k_4 + q_1 + k_{d3} + \mu) \cdot [R_2M], \\
 \frac{d[R_2']}{dt} &= k_1 \cdot [R_2] + q_1 \cdot [R_2M] - (k_3 + \mu) \cdot [R_2'], \\
 \frac{d[R_2'M]}{dt} &= k_{d3} \cdot [R_2M] - (k_4 + q_1 + \mu) \cdot [R_2'M], \\
 \frac{d[rpmRNA_{tot}]}{dt} &= k_{s1} - k_{d1} \cdot [rpmRNA_{free}] - \mu \cdot [rpmRNA_{tot}], \\
 \frac{d[mRNA_{tot}]}{dt} &= k_{s2} - k_{d2} \cdot [mRNA_{free}] - (k_4 + q_1) \cdot [R_2'M] - \mu \cdot [mRNA_{tot}].
 \end{aligned} \tag{A1}$$

with pumps (wild-type)

$$\frac{d[m_{tot}]}{dt} = c_{II} \cdot \frac{(c_I \cdot [m_m] + c_{II} \cdot [m_{free}])}{c_I + c_{II} + c_{III} + \mu} - (c_{II} + c_{III}) \cdot [m_{free}] - \mu \cdot [m_{tot}],$$

or without pumps (TolC mutant)

$$\frac{d[m_{tot}]}{dt} = c_{II} \cdot \frac{(c_I \cdot [m_m] + c_{II} \cdot [m_{free}])}{c_I + c_{II} + \mu} - c_{II} \cdot [m_{free}] - \mu \cdot [m_{tot}].$$

A large ribosomal subunit can exist in eight different states. The 50S subunit may be free without ( $[50S]$ ) or with ( $[50SM]$ ) a bound macrolide. It may be a part of a ribosome ready to translate the first codons of a protein mRNA without ( $[R_2]$ ) or with ( $[R_2M]$ ) a bound macrolide or it may have translated the first codons and become temporarily immune to the drug ( $[R'_2]$ ). If the mRNA starts to degrade before dipeptidyl-tRNA drop-off or spontaneous dissociation of the macrolide it ends up in state ( $[R'_2M]$ ). State  $[R'_2M]$  provides a more detailed description of the fate of ribosomes with a degrading mRNA but was not included in the erythromycin model (Lovmar *et al.*, 2006), where  $q_1 \gg k_{d3}$ . However, the same approximations as in the erythromycin model are also valid in the josamycin model although they are less intuitive. The subunit may also be a part of a ribosome ready to translate a resistance peptide mRNA (rpmRNA) without ( $[R_1]$ ) or with ( $[R_1M]$ ) a bound antibiotic molecule. The rate constant of association and spontaneous dissociation of the antibiotic is  $q$  and  $q_1$ , respectively. Association of the ribosomal subunits occurs with rate constant  $k_a$  times the free concentration of protein mRNAs ( $[mRNA_{free}]$ ) and free rpmRNA ( $[rpmRNA_{free}]$ ). The first rounds of translation when the antibiotic can attack a ribosome (which is approximately the length of a resistance peptide) occur with rate  $k_1$ . The rate for completing synthesis of a protein beyond translation of the first codons is  $k_3$ , the drop-off rate of an antibiotic-carrying, stalled ribosome on a protein mRNA is  $k_4$  and the rate of drop-off of resistance dipeptidyl-tRNA is  $k_2$ . The system of equations also contains differential equations describing the change of the total concentration of the macrolide in the cell ( $[m_{tot}]$ ) and of the total concentration of protein mRNAs ( $[mRNA_{tot}]$ ) and rpmRNA ( $[rpmRNA_{tot}]$ ), respectively. The macrolide passively diffuses over the outer membrane with rate constant  $c_I$  and over the inner membrane with rate constant  $c_{II}$ . The antibiotic is actively transported out of the cell by pumps (either from the cytoplasm or the periplasm) with rate constant  $c_{III}$ . The free intracellular (cytoplasmic) concentration of the macrolide is defined by  $[m_{free}] = [m_{tot}] - [50SM] - [R_1M] - [R_2M] - [R'_2M]$ . The macrolide concentration in the periplasm is assumed to be quickly equilibrated. The synthesis rate of rpmRNA is  $k_{s1}$  and active degradation of free rpmRNA occurs with rate constant  $k_{d1}$ . The corresponding rates of synthesis and degradation of protein mRNAs are denoted  $k_{s2}$  and  $k_{d2}$ , respectively. It is also assumed that a stalled, macrolide-carrying ribosome on the 5' end of an mRNA does not fully protect the mRNA from degradation, but it is degraded by a low rate constant,  $k_{d3}$ . The free concentration of rpmRNA and protein mRNAs is defined by  $[rpmRNA_{free}] = [rpmRNA_{tot}] - [R_1] - [R_1M]$  and  $[mRNA_{free}] = [mRNA_{tot}] - [R_2] - [R_2M] - [R'_2M]$ , respectively. The system expands by exponential growth with cell growth rate  $\mu$ , defined by

$$\mu = \frac{v_e \cdot [R'_2]}{\rho_0}, \quad [A2]$$

where  $v_e$  is the average elongation rate of an uninhibited ribosome and  $\rho_0$  is the concentration of amino acids incorporated in proteins. The total concentration of 50S subunits ( $[50S_{tot}]$ ) is kept constant and new 50S subunits are thus synthesised by rate  $\mu \cdot [50S_{tot}]$  and the free concentration of 50S subunits varies according to  $[50S] = [50S_{tot}] - [50SM] - [R_1] - [R_1M] - [R_2] - [R'_2] - [R_2M] - [R'_2M]$ .

The system was solved numerically by Euler's method (Heath, 1997). Cell growth was calculated for the first 4 (Fig. 5) or 8 (Fig. 3A) hours after introduction of a certain macrolide concentration in the growth medium,  $[m_m]$  by

$$V_t = V_{t-dt} \cdot e^{\mu \cdot dt}, \quad [A3]$$

where  $dt$  is a small time-step and  $V_{t-dt}$  and  $V_t$  is the volume prior and after time-step  $dt$ , respectively. Prior to macrolide exposure, the system resided at steady state for a certain synthesis rate of resistance peptide mRNA. The used program software was MATLAB 6.5 (The MathWorks, Inc., Natick, Massachusetts, U.S.A.).

### **Peptide-mediated resistance against erythromycin**

The previously developed model for peptide-mediated erythromycin resistance was used for Fig. 5 (A and B) (see Supplementary material online of (Lovmar *et al.*, 2006)) but with the more detailed description of the flows over the inner membrane described in the differential equation for  $m_{tot}$  in eq. [A1]. The extension of the model account for the difference in macrolide concentrations where cell growth are affected in the wild-type and in the TolC mutant.

**Appendix table 1. Definitions and values of used parameters.**

	<b>Description</b>	<b>Value</b>	<b>Reference</b>
$k_a$	association rate constant of ribosomal subunits at initiation of translation	$2 \cdot 10^6 \text{ M}^{-1} \text{ s}^{-1}$	(1)
$k_1$	rate constant for translation of the first codons when the ribosome is susceptible for the antibiotic or for translation of a resistance peptide by a drug-free ribosome	$1 \text{ s}^{-1}$	(2)
$k_2$	rate constant for translation of a resistance peptide by an erythromycin-infected ribosome	$0.008 \text{ s}^{-1}$ (josa) $0.1 \text{ s}^{-1}$ (eryt)	Present study and (3)
$k_3$	rate constant for translation beyond the first codons of a protein mRNA and translation termination	$0.03 \text{ s}^{-1}$	(2)
$k_4$	drop-off rate constant of peptidyl-tRNA from a stalled ribosome on a protein mRNA	$0.06 \text{ s}^{-1}$	Lovmar, unpublished results
$q$	association rate constant of erythromycin	$3.3 \cdot 10^4 \text{ M}^{-1} \text{ s}^{-1}$ (josa) $10^6 \text{ M}^{-1} \text{ s}^{-1}$ (eryt)	(4)
$q_1$	dissociation rate constant of erythromycin	$1.8 \cdot 10^{-4} \text{ s}^{-1}$ (josa) $0.01 \text{ s}^{-1}$ (eryt)	(4)
$k_{s1}$	synthesis rate of resistance peptide mRNA (rpmRNA)	0 - 10 nMs <sup>-1</sup> in Fig. 3A 2 nMs <sup>-1</sup> in Figs. 5-6	
$k_{d1}$	degradation rate constant of free rpmRNA	$8.3 \cdot 10^{-3} \text{ s}^{-1}$	
$k_{s2max}$	maximal synthesis rate of protein mRNAs (in the absence of rpmRNA)	$8.3 \cdot 10^{-9} \text{ Ms}^{-1}$	(5)
$k_{s2}$	synthesis rate of protein mRNAs	$k_{s2max} - 0.05 \cdot k_{s1} \text{ Ms}^{-1}$	
$k_{d2}$	degradation rate constant of free protein mRNAs	$8.3 \cdot 10^{-3} \text{ s}^{-1}$	(6)
$k_{d3}$	degradation rate constant of protein mRNAs with a drug-inhibited, stalled ribosome	$4.2 \cdot 10^{-4} \text{ s}^{-1}$	
$c_I$	rate constant of passive diffusion over outer cell membrane	$2 \cdot 10^{-3} \text{ s}^{-1}$	
$c_{II}$	rate constant of passive diffusion over inner cell membrane	$0.1 \text{ s}^{-1}$	(7)
$c_{III}$	rate constant of active transport by pump	$0.9 \text{ s}^{-1}$	
$v_e$	elongation rate of an uninhibited ribosome	$20 \text{ s}^{-1}$	(2)
$\rho_0$	concentration of amino acids in proteins	2 M	(2)
[50S <sub>tot</sub> ]	total concentration of 50S ribosomal subunits	$4 \cdot 10^{-5} \text{ M}$	(2)
[m <sub>m</sub> ]	concentration of macrolide in the growth medium	$10^{-7} - 1.5 \cdot 10^{-3} \text{ M}$ (see figures)	

1. Antoun, A., Pavlov, M., Andersson, A., Tenson, T. & Ehrenberg M. (2003) *EMBO J.* **22**, 5593-5601.
2. Bremer, H. & Dennis, P. (1996) in *Escherichia coli and Salmonella typhimurium Cellular and Molecular Biology*, ed. Neidhardt, F. C. (ASM Press, Washington, DC.), pp. 1553-1569.
3. Lovmar, M., Nilsson, K., Vimberg, V., Tenson T., Nervall, M., & Ehrenberg, M. (2006) *J. Biol. Chem.* **281**, 6742-6750.
4. Lovmar, M., Tenson T. & Ehrenberg, M. (2004) *J. Biol. Chem.* **279**, 53506-53515.
5. Neidhardt, F. C. & Umbarger, H. E. (1996) in *Escherichia coli and Salmonella typhimurium Cellular and Molecular Biology*, ed. Neidhardt, F. C. (ASM Press, Washington, DC.), pp. 13-16.
6. Kushner, S. R. (1996) in *Escherichia coli and Salmonella typhimurium Cellular and Molecular Biology*, ed. Neidhardt, F. C. (ASM Press, Washington, DC.), pp. 849-860.
7. Zgurskaya, H. I. & Nikaido, H. (1999) *PNAS* **96**, 7190-7195



Lovmar, M., Nilsson, K., Lukk, E., **Vimberg, V.**, Tenson, T., Ehrenberg, M. 2008. Kinetic Coupling Between Target Binding and Efflux Pump Efficiency – the Case of Erythromycin Resistance. Manuscript.

Editorial Manager(tm) for Cell  
Manuscript Draft

Manuscript Number:

Title: KINETIC COUPLING BETWEEN TARGET BINDING AND EFFLUX PUMP EFFICIENCY - THE CASE OF ERYTHROMYCIN RESISTANCE

Article Type: Research Article

Section/Category:

Keywords: erythromycin; efflux pump; ribosome; ribosomal proteins; L4; L22; macrolide; antibiotic; resistance; molecular crowding; peptide exit tunnel; resistance development

Corresponding Author: Prof. Måns Ehrenberg,

Corresponding Author's Institution: Uppsala University

First Author: Martin Lovmar

Order of Authors: Martin Lovmar; Karin Nilsson; Eliisa Lukk; Vladimir Vimberg; Tanel Tenson; Måns Ehrenberg

Abstract: We demonstrated with mathematical modelling that decreasing drug efflux pump efficiency eliminates differential effects of resistance mutations in strong drug targets. The predictions were tested with erythromycin, a clinically important macrolide antibiotic targeting the ribosome. We constructed the erythromycin resistant mutations L4(Lys63Glu), L4( $\Delta$ 63-64) and L22( $\Delta$ 82-84) in ribosomal proteins L4 and L22. In biochemical experiments we showed that all mutations decreased the erythromycin association rate constant 100-fold. We found in bacterial growth experiments that all target mutations similarly increased erythromycin resistance for *E. coli* cells growing in a tolC efflux pump proficient, but not in a tolC deficient background, which confirmed the theoretical predictions. Our findings suggest likely evolutionary pathways for the emergence of drug resistance and are therefore relevant to the choice of clinical strategies to slow down drug resistance evolution. The coupling between drug efflux and target binding is general, and cases other than antibiotic resistance are discussed.

Suggested Reviewers: Michael Surette  
surette@ucalgary.ca  
Systems biology expert

Richard Losick  
losick@mcb.harvard.edu  
microbiology expert

Venki Ramakrishnan  
ramak@mrc-lmb.cam.ac.uk  
Ribosome expert

Peter Moore  
peter.moore@yale.edu  
Ribosome and macrolide expert

Christopher Walsh  
christopher\_walsh@hms.harvard.edu  
Antibiotic and enzyme kinetics expert

Olga Lomovskaya  
olomovskaya@mpexpharma.com  
Efflux pump and drug development expert

Opposed Reviewers:

## [A] Abstract

### SUMMARY

We demonstrated with mathematical modelling that decreasing drug efflux pump efficiency eliminates *differential* effects of resistance mutations in strong drug targets. The predictions were tested with erythromycin, a clinically important macrolide antibiotic targeting the ribosome. We constructed the erythromycin resistant mutations L4(Lys63Glu), L4( $\Delta$ 63-64) and L22( $\Delta$ 82-84) in ribosomal proteins L4 and L22. In biochemical experiments we showed that all mutations decreased the erythromycin association rate constant 100-fold. We found in bacterial growth experiments that all target mutations similarly increased erythromycin resistance for *E. coli* cells growing in a *tolC* efflux pump proficient, but not in a *tolC* deficient background, which confirmed the theoretical predictions. Our findings suggest likely evolutionary pathways for the emergence of drug resistance and are therefore relevant to the choice of clinical strategies to slow down drug resistance evolution. The coupling between drug efflux and target binding is general, and cases other than antibiotic resistance are discussed.

\* [B] Cover Letter

To the Editorial Board of Cell  
Cell Press  
600 Technology Square, 5th Floor  
Cambridge, MA 02139

Dec 20, 2007

We wish to submit the manuscript “Kinetic coupling between target binding and efflux pump efficiency-the case of erythromycin resistance” by Lovmar *et al.* for publication in Cell. The manuscript has three parts: (i) mathematical modeling of the interplay between antibiotic drug efflux pumps and target mutations, (ii) biochemical experiments on the binding of the macrolide antibiotic to wild type ribosomes and three ribosomal mutants giving macrolide resistance, and (iii) growth rate experiments on *E. coli* populations with combinations of drug efflux and ribosomal mutations.

The main conclusion of the work is that resistance caused by drug target mutations may be completely masked at low drug efflux efficiency and are maximally expressed at enhanced drug efflux efficiency. This conclusion, based on *in vivo* experiments and confirmed by theory, is important for our understanding the evolution of drug resistance. Our work also clarifies the nature of classical ribosome mutants conferring erythromycin resistance and the role of the peptide exit tunnel for drug traffic to and from the peptidyl-transferase centre.

Sincerely,

Måns Ehrenberg  
Prof. (Chair) of Molecular Biology  
ICM, BMC. Box 596  
Uppsala university  
S-751 24 Uppsala  
Sweden  
Email: [ehrenberg@xray.bmc.uu.se](mailto:ehrenberg@xray.bmc.uu.se)  
Telephone: +46 18 4714213

\* [D] Manuscript

## **KINETIC COUPLING BETWEEN TARGET BINDING AND EFFLUX PUMP EFFICIENCY - THE CASE OF ERYTHROMYCIN RESISTANCE**

**Martin Lovmar<sup>1\*</sup>, Karin Nilsson<sup>1</sup>, Eliisa Lukk<sup>2</sup>, Vladimir Vimberg<sup>2</sup>,  
Tanel Tenson<sup>2</sup> and Måns Ehrenberg<sup>1</sup>**

<sup>1</sup> Department of Cell and Molecular Biology, Molecular Biology Program, Uppsala University, Uppsala S-75124, Sweden

<sup>2</sup> Institute of Technology, University of Tartu, 50411 Tartu, Estonia

\* Present address: CMB/Microbiology, Göteborg University, S-40530 Göteborg, Sweden

**Running title: Drug target binding and efflux pump efficiency**

**Correspondence to:** Måns Ehrenberg  
Dept. of Cell and Molecular Biology,  
Molecular Biology Program,  
BMC, Box 596, Uppsala University,  
S-75124 Uppsala, Sweden

E-mail: ehrenberg@xray.bmc.uu.se

Tel: +46 18 471 42 13

Fax: +49 18 471 42 62

## SUMMARY

We demonstrated with mathematical modelling that decreasing drug efflux pump efficiency eliminates *differential* effects of resistance mutations in strong drug targets. The predictions were tested with erythromycin, a clinically important macrolide antibiotic targeting the ribosome. We constructed the erythromycin resistant mutations L4(Lys63Glu), L4( $\Delta$ 63-64) and L22( $\Delta$ 82-84) in ribosomal proteins L4 and L22. In biochemical experiments we showed that all mutations decreased the erythromycin association rate constant 100-fold. We found in bacterial growth experiments that all target mutations similarly increased erythromycin resistance for *E. coli* cells growing in a *tolC* efflux pump proficient, but not in a *tolC* deficient background, which confirmed the theoretical predictions. Our findings suggest likely evolutionary pathways for the emergence of drug resistance and are therefore relevant to the choice of clinical strategies to slow down drug resistance evolution. The coupling between drug efflux and target binding is general, and cases other than antibiotic resistance are discussed.

## INTRODUCTION

The increasing antibiotic resistance among pathogens creates ever increasing problems in the clinical treatments of bacterial disease. Drug resistance may arise due to various combinations of three principally different mechanisms: modifications of drug target sites, chemical modifications of drugs and increased drug efflux from the bacterial cells. To study the combined effects of drug efflux efficiency and target mutations we first modeled in a general fashion their kinetic coupling in growing bacteria, and found that *pump efflux deficiency may completely mask the differential effects of target resistance mutations*. For experimental testing of these predictions, we used *Escherichia coli* and focused on combinations of macrolide resistance due to ribosomal protein mutations and alterations in the AcrAB-TolC drug efflux pump system (Lomovskaya et al., 2007).

Macrolides constitute a growing set of clinically useful antibiotics (Omura, 2002), with the first generation member erythromycin in extensive clinical use for more than fifty years. The structural mode of erythromycin binding to the entrance of the peptide exit tunnel of the large (50S) ribosomal subunit (Fig. 1A) has been characterized at atomic resolution with X-ray crystallography (Schlunzen et al., 2001; Tu et al., 2005). Although erythromycin and other macrolides bind in the vicinity of the peptidyl-transferase center, they do not inhibit peptide bond formation *per se*, but block entrance of the nascent chain to the peptide exit tunnel. This allows for the synthesis of short nascent peptides with a maximal length regulated by the space available for peptide growth between the macrolide and the peptidyl-transferase center (Tenson et al., 2003). In the case of erythromycin, ribosome stalling occurs for nascent peptide lengths between six and eight amino acids (Tenson et al., 2003), and

the stalled ribosome complex may eventually be resolved by peptidyl-tRNA drop-off and recycling of the ribosome to a new round of initiation (Karimi et al., 1999). When, in contrast, erythromycin dissociation precedes drop-off, protein synthesis is rapidly resumed, now with the ribosome refractory to drug re-binding until termination and release of the full length protein (Lovmar et al., 2004; Tenson et al., 2003), in correspondence with earlier *E. coli* cell growth data showing that erythromycin can only inhibit peptide elongation at or just after initiation of protein synthesis (Andersson and Kurland, 1987). These idiosyncratic features of erythromycin action require detailed modeling for prediction of the drug effects on bacterial growth. The present modeling work is based on previous results, where we successfully predicted the effects of cis-acting resistance peptides on bacterial growth in the presence of erythromycin (Lovmar et al., 2006).

Mutations in ribosomal RNA and ribosomal proteins conferring reduced macrolide susceptibility (Weisblum, 1995; Vester and Douthwaite, 2001) were first identified for proteins L4 and L22 in the 50S subunit of the *E. coli* ribosome (Apirion, 1967; Wittmann et al., 1973). These mutations, eventually recognized as a lysine to glutamic acid substitution at position 63 of L4 and a deletion of methionine, lysine and arginine at positions 82-84 of L22 (Fig. 1B) (Chittum and Champney, 1994), will here be referred to as L4(Lys63Glu) and L22( $\Delta$ 82-84), respectively. While the equilibrium binding affinity of erythromycin to the L4 protein seemed greatly reduced by the mutation, the erythromycin affinity to the L22 mutant appeared unaltered by the three amino acids deletion (Wittmann et al., 1973). These observations suggested that the drug resistance conferred by the L4 mutation is due to strongly reduced binding affinity, but left unexplained the resistance conferred by the L22 mutation. Since, however, these previous observations were qualitative, we have now quantified

the kinetic effects of the classical mutations L4 and L22 mutations with the help of our cell free system for protein synthesis with *in vivo* like properties (Lovmar et al., 2004; Pavlov and Ehrenberg, 1996), and used these observations as input data for detailed growth modeling.

The theoretical predictions were subsequently tested in experiments with growing *E. coli* cells containing combinations of ribosome and *acrAB-tolC* mutations. The message from the experiments was strikingly clear: the L4 and L22 mutations conferred reduced erythromycin susceptibility only in combination with *acrAB-tolC* proficiency and not in combination with *acrAB-tolC* deficiency, perfectly in line with our hypothesis. In order to get quantitative correspondence between modeling and experiments not only for the L22, but also for the L4, mutated ribosomes, we uniformly decreased the rate constants for erythromycin dissociation from *all* ribosomal phenotypes.

The novel finding here that reduced affinity of antibiotic drugs to strong intracellular targets leads to decreased drug sensitivity only in the presence of efficient drug efflux pumps is important. It suggests that evolution of drug resistance by target mutations will be greatly slowed down when combined with pump efflux inhibition and greatly accelerated when combined with pump efflux activation. It therefore provides a new angle to the evolution of drug resistance and further emphasizes the paramount importance of combining inhibition of intracellular target function with inhibition of drug efflux efficiency (Lomovskaya et al., 2007).

## RESULTS

### Mathematical modeling of the interplay between drug efflux pumps and target resistance mutations

To clarify the kinetic interactions between drug efflux pumps and target resistance mutations in pathogens, we formulated a general mathematical model for cases in which there is a well defined relation between bacterial growth-inhibition and the fraction of drug-bound targets, with the ribosome as a typical example (Supplementary on line material). According to this model the relative extent  $-\Delta\mu/\mu_0$  of growth reduction by the drug at the onset of growth inhibition can be written as (Supplementary on line material):

$$-\Delta \frac{\mu}{\mu_0} \approx \frac{[A_{ext}] \cdot k_{in}}{\frac{(\mu_0 + k_{out}) \cdot (\mu_0 + k_d)}{k_a} + [T_0] \cdot \mu_0} \quad (1)$$

Membrane transport in to and out from the cytoplasm can be approximated by first order rate constants  $k_{in}$  and  $k_{out}$ , respectively. The parameters  $\mu$  and  $\mu_0$  are the growth rates in the presence and absence of the drug, respectively and the total intracellular target concentration is  $[T_0]$ . The external drug concentration is  $[A_{ext}]$ , and the intracellular rate constants for drug dissociation from and drug association to the target are  $k_d$  and  $k_a$ , respectively. Two special cases may serve to illustrate the meaning of Eq. 1. When the left term in the denominator is much larger than the right term, Eq. 1 is approximated by

$$-\Delta \frac{\mu}{\mu_0} \approx \frac{[A_{ext}] \cdot k_{in}}{(\mu_0 + k_{out})} \cdot \frac{k_a}{(\mu_0 + k_d)} = [A_f] \cdot \frac{k_a}{(\mu_0 + k_d)} \quad (2)$$

In this limit, the free concentration,  $[A_f]=[A_{ext}] \cdot k_{in}/(\mu_0+k_{out})$ , of drug inside the cell depends neither on target binding parameters ( $k_a, k_d$ ) nor on target concentration  $[T_0]$ . This limit is reached when the target is weak, *i.e.* with low affinity to the drug or present at a very low concentration. It is also reached for strong targets, provided that the drug efflux efficiency,  $k_{out}/k_{in}$ , is sufficiently large. In this limit, changes in the binding kinetics by target resistance mutations have maximal impact on growth inhibition by the drug (Fig. 2). From Eq. 2 it also follows that if  $k_d \ll \mu_0$  it is only changes in the association rate constant  $k_a$  that modifies growth rate (Fig. 2A), while if  $k_d \gg \mu_0$  it is changes in the equilibrium dissociation constant  $K_d (=k_d/k_a)$  that alter the growth rate (Fig. 2B).

When, instead, the right term in the denominator of Eq. 1 is much larger than the left term, Eq. 1 is approximated by

$$-\Delta \frac{\mu}{\mu_0} \approx \frac{[A_{ext}] \cdot k_{in}}{[T_0] \cdot \mu_0}. \quad (3)$$

In this remarkable limit, changes in the kinetic parameters  $k_a$  and  $k_d$  due to target mutations have no impact on growth inhibition by the drug. This limit is reached for strong targets, *i.e.* those with high affinity to the drug and high concentration, provided that the drug efflux efficiency,  $k_{out}/k_{in}$ , is not too high (Fig. 2). Here, virtually every drug molecule that enters the cell becomes target bound.

From this analysis follows that a drug efflux deficient pathogen with a strong antibiotic target will be subjected to growth inhibition according to the limit in Eq. 3, and thus be insensitive to target mutations. However, when the same pathogen is drug efflux proficient, it will be subjected to growth inhibition according to the limit in Eq. 2, and thus be maximally sensitive to target mutations. This means, apart from the

well known fact that efflux pump deficiency increases the drug sensitivity of pathogens, that *low drug efflux efficiency may completely mask the effects of a large set of target resistance mutations that would give a clear fitness advantage at high drug efflux efficiency*. This prediction by theory is relevant to the evolution of drug resistance among pathogens and may be important also in other contexts of interaction between efflux pumps and intracellular drug binding sites (see Discussion). To test this prediction, we studied the effects of drug efflux pump efficiency and target mutations on the growth inhibitory effect of erythromycin, a macrolide antibiotic with the ribosome as its strong target and previously characterized resistance mutations in ribosomal proteins.

### **Kinetics of erythromycin binding to wild type and mutant ribosomes**

To study the mechanisms of erythromycin resistance conferred by the ribosomal protein mutations L22( $\Delta$ 82-84) and L4(Lys63Glu) (Apirion, 1967; Chittum and Champney, 1994; Wittmann et al., 1973), these alterations were engineered into the *E. coli* MG1655 strain. By sequencing, we also identified L4( $\Delta$ 63-64) as a previously unknown erythromycin resistant mutant. In the absence of erythromycin, in a rich LB medium at 37 °C, the L22( $\Delta$ 82-84), L4(Lys63Glu) and L4( $\Delta$ 63-64) strains had doubling times between 42 and 50 min, while the isogenic wild type MG1655 strain had a doubling time of 29 min. We prepared ribosomes at high activity and purity from these four strains to study the kinetics of their binding to  $^{14}\text{C}$ -labelled erythromycin with nitrocellulose filtration; all results are summarized in Table 1.

### Rate constants for erythromycin dissociation from wild-type and mutant ribosomes

Dissociation rate constants for erythromycin in complex with wild-type and mutant ribosomes were obtained from chase experiments. Here, the different ribosome types were initially equilibrated with  $^{14}\text{C}$ -labelled erythromycin, which was subsequently

chased with an excess of unlabeled erythromycin. The remaining fractions of ribosome bound  $^{14}\text{C}$ -labelled erythromycin were estimated by nitrocellulose filtration at varying incubation times, and the results are shown in Fig. 3. In the wild type case, the dissociation rate constant ( $k_d$ ) was estimated as  $0.013\text{ s}^{-1}$ , in line with a previous estimate obtained with a different method (Lovmar et al., 2004). In the L22 case, the dissociation rate constant was estimated as  $0.0011\text{ s}^{-1}$ , a value much smaller than the  $k_d$ -value in the wild type case. In the L4 cases, the dissociation rate constants were slightly larger than in the wild type case, *i.e.*  $0.018\text{ s}^{-1}$  for the L4(Lys63Glu) and  $0.029\text{ s}^{-1}$  for the L4( $\Delta$ 63-64) mutant.

#### Rate constants for erythromycin association to wild-type and L22( $\Delta$ 82-84) ribosomes

The association rate constants for complex formation between erythromycin and wild type or L22( $\Delta$ 82-84) ribosomes were estimated as  $1.0\text{ }\mu\text{M}^{-1}\text{s}^{-1}$  (Fig. 4A) or  $0.019\text{ }\mu\text{M}^{-1}\text{s}^{-1}$  (Fig. 4B), respectively. In these experiments the ribosomes were mixed with  $^{14}\text{C}$ -labelled erythromycin at time zero of the incubation and the fractions of erythromycin bound ribosomes were monitored by nitrocellulose filtering at varying incubation times (Figs. 4A and 4B). The estimate of the wild type association rate constant is similar to that obtained with a different method (Lovmar et al., 2004).

It has been suggested that erythromycin binding to the ribosome occurs via a pre-equilibrium step (Dinos and Kalpaxis, 2000), but we demonstrated in previous work that such a putative pre-equilibrium must have an (equilibrium) dissociation constant ( $K_D$ ) larger than  $\sim 1\text{ }\mu\text{M}$  (Lovmar et al., 2004). Here, we show that such a putative pre-equilibrium for the L22( $\Delta$ 82-84) ribosome must have a  $K_D$ -value larger than  $\sim 10\text{ }\mu\text{M}$  (Fig. 4B, insert).

Equilibrium dissociation constants for complexes between erythromycin and L4(Lys63Glu) or L4( $\Delta$ 63-64) ribosomes

The low affinity of erythromycin binding to the L4 mutants made it technically difficult to directly measure the association rate constants as in the previous section, but it was possible to estimate the dissociation (equilibrium) constants ( $K_D$ ).

Accordingly,  $K_D$ -values for the L4(Lys63Glu) and L4( $\Delta$ 63-64) mutants were estimated as 4.6  $\mu$ M and 3  $\mu$ M, respectively, from experiments in which the fractions of erythromycin bound ribosomes were monitored by nitrocellulose filtration at varying erythromycin concentrations (Fig. 4C).

**Erythromycin-dependent growth inhibition of wild-type and mutant *E. coli* populations**

We studied the effects of erythromycin on the growth rate of the wild type, L4(Lys63Glu), L4( $\Delta$ 63-64) and L22( $\Delta$ 82-84) mutated variants of the MG1655 *E. coli* strain in a wild type genetic background or in combination with  $\Delta$ *tolC* or  $\Delta$ *acrB* drug efflux pump deficient strains (Okusu et al., 1996). The growth rates were estimated as OD-values after four hours of growth, and the results are shown in Figs. 5A and 5B. In the pump proficient genetic background, the ribosomal wild type was most growth sensitive to erythromycin, and the level of resistance was similar for the three ribosomal mutants (Fig. 5A). The erythromycin sensitivity for the ribosomal wild type was greatly increased by the  $\Delta$ *acrB* deletion, but the largest sensitivity was conferred by the  $\Delta$ *tolC* deletion (Fig. 5A). We interpret this to mean that the erythromycin efflux pump activity was insignificant for the  $\Delta$ *tolC* strain, and that the  $\Delta$ *acrB* strain retained a small but significant efflux pump activity. The erythromycin sensitivity of the L4 and L22 ribosome mutants was similar to that of the wild type ribosome in the  $\Delta$ *tolC* but smaller in the  $\Delta$ *acrB* genetic background (Fig. 5B). This implies that

elimination of the drug efflux activity by the  $\Delta tolC$  alteration also eliminated the growth advantage of the L4 and L22 mutants in relation to the ribosomal wild type population. To investigate whether our kinetic data could quantitatively account for the growth inhibition by erythromycin (Figs. 5A and 5B), we used detailed mathematical modeling based on these and previous (Lovmar et al., 2004) data on ribosome function to predict the growth rate inhibition curves for different *E. coli* strains as displayed in Figs. 5C and 5D.

### **Detailed mathematical modeling of erythromycin-dependent growth inhibition for wild type and mutated *E. coli* strains**

The erythromycin growth inhibition curves described in the previous section (Figs. 5A and 5B) suggested that the drug resistance conferred by the L4 and L22 mutations in relation to wild type was conditional on a fully active AcrAB-TolC efflux pump system. An essential part of the detailed mathematical model for growth inhibition by erythromycin (see Supplementary on-line material) is therefore drug transport over the two cell membranes of *E. coli* (Fig. 6A). *E. coli* is a gram-negative bacterium, and we assumed passive diffusion over the outer and inner cell membranes with rate coefficients  $C_I$  and  $C_{II}$ , respectively, with  $C_I \ll C_{II}$  (Elf et al., 2006). We assumed, in addition, active transport with a rate coefficient  $C_{III}$  from the periplasm to the medium. We set  $C_{III}$  to zero for  $\Delta tolC$ , to an intermediate value for  $\Delta acrB$  and to a large value for wild-type cells. When  $C_{III}$  is smaller than  $C_{II}$ , variation in  $C_{III}$  mainly affects the effective rate constant,  $k_{out}$ , for drug efflux from the cytoplasm and when  $C_{III}$  is larger than  $C_{II}$ , variation in  $C_{III}$  mainly affects the effective rate constant,  $k_{in}$ , for drug influx to the cytoplasm. In the former case, variation of  $C_{III}$  has profound effects on the propensity for bi-stable growth response to drug exposure (Elf et al., 2006) and, as demonstrated here, on the relative growth advantage conferred by ribosomal

drug resistance mutations. In the latter case, variation of  $C_{III}$  can trivially be mimicked by an inverse variation of the external drug concentration.

The protein synthesis part of the model (Fig. 6B) is a modified version of a previous model (Lovmar et al., 2006), successfully used to account for erythromycin resistance conferred by *cis*-acting peptides (Lovmar et al., 2006; Tenson et al., 1996; Vimberg et al., 2004). Kinetic data from the present (Table 1) and previous (Antoun et al., 2006; Bremer and Dennis, 1996) work have been integrated in the model, and the magnitude of the permeability parameters  $C_I$ ,  $C_{II}$  and  $C_{III}$  have been adjusted to fit the *in vivo* data (Figs. 5A and 5B). All parameters used in the model are given in Table S1 of the Supplementary on-line material. This detailed model, in which the idiosyncrasies of erythromycin dependent inhibition of bacterial protein synthesis are explicitly taken into account, agrees well with the general scheme leading to Eqs 1-3 above. Our numerical comparisons show, in particular, that the relations between drug efflux efficiency and target mutation sensitivity are model independent.

The model faithfully reproduces the erythromycin dependent growth inhibition for wild type and L22 mutated ribosomes in wild type as well as in  $\DeltaacrB$  or  $\DeltatolC$  genetic backgrounds, as can be seen by comparing Fig. 5C with Fig. 5A and Fig. 5D with Fig. 5B. Accordingly, the model accounts for the observation that the resistance conferred by the L22 alteration in relation to the wild type ribosome was largest in the presence of the wild type AcrAB-TolC system, smaller in the  $\DeltaacrB$  and insignificant in the  $\DeltatolC$  background. It also accounts for the observation that the residual efflux pump activity in the  $\DeltaacrB$  strain led to larger erythromycin resistance than in the  $\DeltatolC$  strain when the ribosome was L22 mutated, but not when the ribosome was of wild type. These results confirm the prediction of a previously unknown link between

the drug efflux system and the relative resistance increase by mutations in the ribosome and, by inference, in other drug targets in the cytoplasm. Although we successfully accounted for how the relative drug resistance conferred by the L22 alteration depended on the efflux pump efficiency, there was a quantitative deviation between model and experiments concerning the two L4 mutants. Experimentally, we observed similar drug resistance for all three ribosomal mutants in all three efflux pump backgrounds (Figs. 5A and 5B), but the model predicted greater drug resistance for the two L4 mutants than for the L22 mutant (Figs. 5C and 5D). The deviation may be caused by a profound effect of molecular crowding (Berg, 1990; Ellis, 2001; Minton, 1981; Zimmerman and Trach, 1991) on intracellular rate constants, since a uniform re-scaling of all dissociation constants by a factor of a hundred resulted in a good fit between model and experimental growth inhibition curves for all combinations of ribosomal and pump-efflux mutants. (Compare Fig. 5A with Fig. 5E and Fig. 5B with Fig. 5F). After re-scaling, the  $k_d$  values were smaller than the growth rate  $\mu_0$ , so that the resistance conferred by all three ribosomal mutations in the efflux proficient background was due to their similarly reduced association rate constant,  $k_a$ . The remaining deviations between model and experiments are, we suggest, due to relatively large errors in our *indirect* estimates of the rate constants for drug association to the L4 ribosome mutants (Figs. 3 and 4).

## DISCUSSION

### **Increased drug resistance by intracellular target mutations conditional on efficient drug efflux pumping**

Our *in vivo* observations demonstrate that the selective growth advantage in the presence of erythromycin, conferred by the L22 and L4 mutations in relation to the wild type, disappears in the  $\Delta tolC$  genetic background (Fig. 5B). This appears to be a

general phenomenon for high affinity drug targets and its origin can be traced to the efficiency by which drug efflux competes with drug-target binding, as illustrated by Eq. 1 and Fig. 2 above. In the drug efflux deficient case, described by Eq. 3, growth inhibition by the drug is virtually insensitive to mutation driven variations in the association ( $k_a$ ) and dissociation ( $k_d$ ) rate constants for the ribosome-erythromycin interaction. This means that as long as Eq. 3 approximates Eq. 1, all drug molecules that enter the cell become ribosome bound in spite of variations in target affinity to the drug. In the drug efflux proficient case, described by Eq. 2, growth inhibition by the drug is maximally sensitive to variations in target affinity to the drug. Here, the pump efficiency is sufficiently high to establish a target-independent steady state relation between the external drug concentration in the medium and the free drug concentration in the cytoplasm.

Our detailed model for *E. coli* growth with our biochemical data as input accounts for the erythromycin dependent growth inhibition for wild type and L22 mutated cell populations in wild type,  $\Delta tolC$  and  $\Delta acrB$  genetic backgrounds (Fig. 5). There is a quantitative deviation between model predictions and the growth data from the L4 mutated strains (Compare Fig. 5A with 5C and Fig. 5B with 5D), primarily due to the large  $K_D$ -values that characterize the binding of their ribosomes to erythromycin (Table 1). However, a uniform decrease of the rate constants for erythromycin dissociation from all ribosome types gives a good correspondence between model predictions and growth data for all combinations of ribosome and pump efflux mutants (Compare Fig. 5A with 5E and Fig. 5B with 5F). This suggests that re-scaling of kinetic *in vitro* data may in some cases be necessary to obtain the corresponding *in vivo* data. One reason for the need to rescale, could be that, in contrast to the situation in the test-tube, the interior of the bacterium is densely packed with RNA, protein,

DNA and other molecules (Cayley et al., 1991). According to theory (Berg, 1990; Ellis, 2001; Minton, 1981; Zimmerman and Trach, 1991), this “molecular crowding” may have profound effects on the affinity of ligand binding to targets in the cell, but other explanations for the need of parameter re-scaling are conceivable. Direct measurements of specific dissociation rate constants in the living cell are hard to come by, but may soon be amenable to precise experimentation through novel techniques for single cell spectroscopy (Elf et al., 2007; Zlatanova and van Holde, 2006).

### **The rate of emergence of target resistance mutations and drug efflux efficiency**

**The present theory (Eq. 1, supplementary on line material) and experimental results (Figs 5A and 5B) demonstrate how the “space” of target resistance mutations contracts with reduced and expands with enhanced drug efflux efficiency.** That is, in a drug efflux proficient background there will be a multitude of target mutations that lead to increased fitness in the presence of an antibiotic drug, which are masked in an efflux deficient background. Since the size of the space of possible resistance mutations will determine the rate of fixation of resistance mutations among pathogens, we infer that the evolution of target-conferred drug resistance will be much faster among pathogens with highly than among those with lowly efficient drug efflux systems. This is, in particular, the case for intracellular targets at high concentration and with high-affinity drug binding, as here exemplified experimentally by the strong erythromycin binding to the abundant *E. coli* ribosome. When, accordingly, antibiotics with intracellular targets are delivered together with drug efflux inhibiting molecules (Lomovskaya et al., 2007), our theory predicts that this will drastically slow down the rate of emergence of target resistance mutations.

### **How does erythromycin interact with the ribosome?**

Our biochemical data show that L4(Lys63Glu) and L22( $\Delta$ 82-84) ribosomes have equilibrium dissociation constants for erythromycin binding about three hundred times and five times larger than wild type ribosomes, respectively (Figures 3 and 4 and Table 1). The association rate constants for all ribosomal mutants are about a factor of hundred smaller than for wild type ribosomes. While the dissociation rate constant for the L4(Lys63Glu) ribosome is much larger than for wild type, the dissociation rate constant for the L22( $\Delta$ 82-84) ribosome is much smaller than for wild type. Accordingly, previous conclusions based on qualitative data that erythromycin has zero binding affinity to L4(Lys63Glu) ribosomes and wild type binding affinity to L22( $\Delta$ 82-84) ribosomes (Wittmann et al., 1973) must be revised in light of the present results along with more recent conclusions based on these previous data in conjunction with structural data from cryo-EM (Gabashvili et al., 2001) and x-ray crystallography (Tu et al., 2005).

Using rolling sphere simulations on crystallographic atom coordinates, Moore and colleagues showed that the tunnel wall is impermeable to molecules with the size of erythromycin (Voss et al., 2006). Therefore, erythromycin either has to bind from the subunit interface through the peptidyl transferase center (PTC) or from the ribosome surface through the L4/L22 constriction in the peptide exit tunnel (Fig. 1A). The similar kinetics of erythromycin binding to initiation complexes (Lovmar et al., 2004), empty ribosomes (Table 1) and 50S subunits (data not shown) makes binding *via* the interface less likely. In addition, it is reasonable to assume that the peptide exit tunnel of the wild type ribosome has been optimized for passage of the nascent peptide chain (Nissen et al., 2000), and that such an optimization may facilitate the passive transport of other ligands, like macrolides, through the tunnel. Accordingly,

mutations in the L4 and L22 tunnel proteins are expected to move the tunnel away from its optimal design and thus to reduced rate of passive transport, as observed in our biochemical experiments.

We suggest, therefore, that the second order (microscopic) rate constant (Berg, 1985),  $k_{pt}$ , for passage through the peptide exit tunnel constriction, as defined by the L4 and L22 ribosomal proteins (Nissen et al., 2000), is maximal for wild type and greatly reduced for the L22 mutant and the two L4 mutants. Our data demonstrate, furthermore, that the dissociation constant,  $K_D$ , for erythromycin binding to its specific site (Schlunzen et al., 2001; Tu et al., 2005) is increased about five fold for the L22 and about three hundred fold for the L4 mutations. Putting these two features together, suggests that the association rate constant ( $k_a$ ) is given by  $k_a=k_{pt}$  and the dissociation rate constant  $k_d$  by  $k_d=k_{pt}\cdot K_D$ . Although our data do not prove erythromycin binding *via* the peptide exit tunnel, they are consistent with this scenario, which furthermore offers a simple explanation to the decreased rate constants for erythromycin binding as caused by reduced rate of passage through the L4/L22 constriction due to a mutation in either one of L4 or L22.

#### **Outlook: target binding affinities and compound efflux efficiencies in other contexts**

Other examples of the general coupling between drug efflux efficiency and evolution of resistance discovered in the present work are provided by members of the fluoroquinolone family (inhibitors of DNA topoisomerases), where resistance often occurs as combinations of drug efflux and target site mutations (Ho *et al.*, 2001; Kriengkauykiat *et al.*, 2005).

Similarly, during chemotherapy against eukaryotic parasites, target site resistance mutations are often combined with drug efflux pump activation

(Nascimento et al., 2003; Wintermeyer and Zachau, 1979). In these cases it is not known whether the efflux activation or the target site mutation occurs first. Since, however, we predict the space of possible target site mutations to greatly increase with increased drug efflux pump efficiency, we propose that pump activation precedes target site mutation.

Our theoretical results may also be relevant to the evolution of drug resistance among cancer cells. During cancer chemotherapy, resistance from target site mutations (Leontiou *et al.*, 2004) and membrane efflux pump activation (Chen et al., 1986; Cole et al., 1992; Gottesman and Ling, 2006) is often observed. The present findings suggest that there will be a large class of target site mutations that confer drug resistance only when combined with highly efficient membrane pumps. Since current mathematical models of P-glycoprotein efflux pump action (Michelson and Slate, 1992; Michelson and Slate, 1994; Zhou and Jin, 1998) do not consider target site binding parameters, they must be expanded to account for the expected coupling between drug efflux efficiency and target resistance mutations.

Finally, the present conclusions may be relevant to the increasing number of studies, where the effects of genetic polymorphisms on drug and biomolecule binding sites are estimated. For example, the glucocorticoids have to reach their receptors inside the cell but are also substrates of the P-glycoprotein efflux pump (Mark and Waddell, 2006). Receptor polymorphisms that change hormone binding parameters have been described (Heeley *et al.*, 2002), and we suggest that the effects of these polymorphisms may well be strongly dependent on the efflux parameters of the cells. Therefore, different choices of model cell lines or tissues (Rockett *et al.*, 2004) may

lead to apparently contradicting conclusions, if the interplay between drug efflux efficiency and receptor binding is neglected in the interpretation of experimental data.

## **EXPERIMENTAL PROCEDURES**

### **Chemicals and buffers**

GTP and ATP were from GE Healthcare. Putrescine, spermidine, phosphoenolpyruvate (PEP) and erythromycin were from Sigma-Aldrich. [<sup>14</sup>C]erythromycin was from Perkin-Elmer. Pyruvate kinase (PK) was from Boehringer-Mannheim. Nitrocellulose filters Protran BA85 were from VWR.

All cell-free experiments were performed at 37 °C in polymix buffer (Antoun et al., 2004; Jelenc and Kurland, 1979) supplemented with 1 mM GTP, 1 mM ATP and 10 mM PEP.

### **Procedures**

#### Construction of mutations in ribosomal protein L4 and L22 in an isogenic background

*E. coli* MG1655 cells (Blattner et al., 1997), transformed with plasmid pKD46 (Datsenko and Wanner, 2000) were grown in SOB medium containing ampicillin (100 µg/ml). 20ml of the culture was grown at 30 °C until OD(A600 nm) 0.6. The cells were collected by centrifugation (8 min, 5500g, 4 °C) and resuspended in ice cold sterile water. The washing procedure was repeated two more times and the cells were finally resuspended in 100 µl of water. 50 µl of the cells were electroporated with 10 ng (3 µl) of DNA oligonucleotide using Bio-Rad Gene Pulser at 1.8 kV, 25 µF (2 mm cuvettes). The electroporated cells were diluted with 1 ml of LB medium, incubated for 2 h at 37 °C and plated on LB-agar containing erythromycin (300 µg/ml). The recombinase coding plasmid pKD46 was removed as described

previously (Datsenko and Wanner, 2000). The mutations were confirmed by sequencing.

Oligonucleotides used:

L4:

TAACTGGTTCCGGTAAAAAACCG\_TGGCGCCAGGAAGGCACCGGC\_CGTG  
CGCGTTCTGGTTCTATCAAGAG

L22:

AAGTTACGAAAATTTTCGTAGACGAAGGC\_CCGAGCATTATG\_CCGCGTGC  
AAAAGGTCGTGCAGATCGCAT

#### Construction of the double mutants

The *acrB* and *tolC* knockouts were made in both the wild-type and the erythromycin resistant strains (described above) by using the method of Datsenko and Wanner (Datsenko and Wanner, 2000). The PCR products for transforming the strains were made from plasmid pKD13 with following oligonucleotides:

TolC1(/forward):AATTTTACAGTTTGATCGCGCTAAATACTGCTTCACAAGG  
AATGCAAGTGTAGGCTGGAGCTGCTTC

TolC2(/reverse):TTTACGTTGCCTTACGTTTCAGACGGGGCCGAAGCCCCGTC  
GTCATCAATTCCGGGGATCCGTCGACC

AcrB1(/forward):TGCTCAGCCTGAACAGTCCAAGTCTTAACTTAAACAGGA  
GCCGTTAAGACGTGTAGGCTGGAGCTGCTTC

AcrB2(/reverse):ATGCATAAAAAAGGCCGCTTACGCGGCCTTAGTGATTACA  
CGTTGTATCAATTCCGGGGATCCGTCGACC

### Inhibition curves

Overnight cultures were diluted into 10 ml of LB medium to OD (600 nm) 0.1. The cultures were grown at 37 °C until OD 0.4-0.6 and again diluted to OD 0.1. 2 ml of the culture was used for one experimental point; erythromycin was added at concentrations indicated. OD was measured after 4 h of growth at 37 °C.

### Ribosome purification

Mutant and wild-type ribosomes were purified by ultra-centrifugation as previously described (Tenson et al., 2003). Bacterial DNA from aliquots of the cultures used for purification was used for sequencing of the L4 and L22 coding genes to ensure the absence of revertants among the purified ribosomes.

### Nitro cellulose filter assays

Ribosomes stick to nitrocellulose (NC) filters while erythromycin does not. Hence, the NC filter assay allows us to separate ribosome-bound [<sup>14</sup>C]erythromycin from the free [<sup>14</sup>C]erythromycin. The filters were pre-soaked in cold polymix buffer containing 10 μM erythromycin. After each sample was applied, the filter was rapidly washed twice with 1 ml ice-cold polymix buffer before the radioactivity on the filter was measured in a scintillation counter.

### Chase experiment

The ribosome mixture contained ~2 μM ribosomes (wild-type or mutant) and [<sup>14</sup>C]erythromycin (10 μM), and the chase mixture contained 225 μM erythromycin. After mixing 20 μl of the ribosome mixture with 20 μl of the chase mixture, reactions were quenched at different times by addition of 1 ml ice cold polymix and then rapidly applied to the nitrocellulose filter.

Least square fitting of these data points (*i.e.* bound fraction *vs.* time) to a single exponential function gives the erythromycin dissociation rate constants from wild-type and mutant ribosomes as presented in Table 1.

#### Association rate experiment

The ribosome mixture contained  $\sim 0.32 \mu\text{M}$  wild-type ribosomes or  $\sim 0.2 \mu\text{M}$  L22-mutant ribosomes, and the erythromycin mixture contained [ $^{14}\text{C}$ ]erythromycin (at different concentrations). After mixing 40  $\mu\text{l}$  of the ribosome mixture with 40  $\mu\text{l}$  of the erythromycin mixture, reactions were quenched at different times by addition of 1 ml ice cold polymix containing 40  $\mu\text{M}$  erythromycin and then rapidly applied to the nitrocellulose filter.

Least square fitting of the data points (*i.e.* bound fraction *vs.* time) to a hyperbolic function gives the erythromycin association rate constant to the wild-type ribosomes (Table 1) because the concentration of erythromycin is similar to the concentration of ribosomes in the experiment. In contrast, the data points for the L22-mutant were fitted to single exponential functions because the concentration of erythromycin in this setup was much higher than the ribosome concentration. Thus, the free erythromycin concentration can be regarded as a constant throughout the experiment. The linear relation between the estimated rates and the erythromycin concentration was used to estimate the erythromycin association rate constant for the L22-mutant ribosome presented in Table 1.

#### Equilibrium binding experiment

The ribosome mixture contained  $\sim 0.7 \mu\text{M}$  L4-mutant ribosomes, and the erythromycin mixture contained [ $^{14}\text{C}$ ]erythromycin (at different concentrations). After mixing 40  $\mu\text{l}$  of the ribosome mixture with 40  $\mu\text{l}$  of the erythromycin mixture,

reactions were incubated for ~15 minutes before quenched with 1 ml ice cold polymix buffer and then rapidly applied to the nitrocellulose filter.

Least square fitting of these data points (*i.e.* bound fraction *vs.* erythromycin concentration) to a hyperbolic function gives the erythromycin equilibrium binding constants for both L4 mutants as presented in Table 1.

#### Cell growth simulations

Based on our previously published model for peptide-mediated erythromycin resistance (Lovmar et al., 2006), we set up a system of differential equations of the large ribosomal subunit in different states in a growing system, *i.e.* each equation contains a term for dilution. The model accounts for changes in the total concentration of intracellular erythromycin by the passive inflow and outflow of the macrolide over the cell membranes and the active transport out from the cell by the AcrAB-TolC pump system. The system of equations was solved numerically by Euler's method, after the introduction of a certain macrolide concentration in the growth medium. Cell growth was registered as volume expansion during the first 4 h after induction. Before macrolide exposure, the system resided at steady state. The used program software was MATLAB 6.5 (The MathWorks Inc., Natick, MA). A detailed description of the model and the parameter values used are presented in the on-line supplemental material.

## **REFERENCES**

- Andersson, S., and Kurland, C. G. (1987). Elongating ribosomes in vivo are refractory to erythromycin. *Biochimie* 69, 901-904.
- Antoun, A., Pavlov, M. Y., Lovmar, M., and Ehrenberg, M. (2006). How initiation factors tune the rate of initiation of protein synthesis in bacteria. *Embo J* 25, 2539-2550.

- Antoun, A., Pavlov, M. Y., Tenson, T., and Ehrenberg, M. M. (2004). Ribosome formation from subunits studied by stopped-flow and Rayleigh light scattering. *Biol Proced Online* 6, 35-54.
- Apirion, D. (1967). Three genes that affect *Escherichia coli* ribosomes. *J Mol Biol* 30, 255-275.
- Berg, O. G. (1985). Orientation constraints in diffusion-limited macromolecular association. The role of surface diffusion as a rate-enhancing mechanism. *Biophys J* 47, 1-14.
- Berg, O. G. (1990). The influence of macromolecular crowding on thermodynamic activity: solubility and dimerization constants for spherical and dumbbell-shaped molecules in a hard-sphere mixture. *Biopolymers* 30, 1027-1037.
- Berk, V., Zhang, W., Pai, R. D., and Cate, J. H. (2006). Structural basis for mRNA and tRNA positioning on the ribosome. *Proc Natl Acad Sci U S A* 103, 15830-15834.
- Blattner, F. R., Plunkett, G., 3rd, Bloch, C. A., Perna, N. T., Burland, V., Riley, M., Collado-Vides, J., Glasner, J. D., Rode, C. K., Mayhew, G. F., *et al.* (1997). The complete genome sequence of *Escherichia coli* K-12. *Science* 277, 1453-1474.
- Bremer, H., and Dennis, P. P. (1996). Modulation of Chemical Composition and Other Parameters of the Cell by Growth Rate, In *Escherichia coli* and *Salmonella* : cellular and molecular biology, F. C. Neidhardt, ed. (Washington: ASM Press), pp. 1553-1569.
- Cayley, S., Lewis, B. A., Guttman, H. J., and Record, M. T., Jr. (1991). Characterization of the cytoplasm of *Escherichia coli* K-12 as a function of external osmolarity. Implications for protein-DNA interactions in vivo. *J Mol Biol* 222, 281-300.
- Chen, C. J., Chin, J. E., Ueda, K., Clark, D. P., Pastan, I., Gottesman, M. M., and Roninson, I. B. (1986). Internal duplication and homology with bacterial transport proteins in the *mdr1* (P-glycoprotein) gene from multidrug-resistant human cells. *Cell* 47, 381-389.
- Chittum, H. S., and Champney, W. S. (1994). Ribosomal protein gene sequence changes in erythromycin-resistant mutants of *Escherichia coli*. *J Bacteriol* 176, 6192-6198.
- Cole, S. P., Bhardwaj, G., Gerlach, J. H., Mackie, J. E., Grant, C. E., Almquist, K. C., Stewart, A. J., Kurz, E. U., Duncan, A. M., and Deeley, R. G. (1992). Overexpression of a transporter gene in a multidrug-resistant human lung cancer cell line. *Science* 258, 1650-1654.
- Datsenko, K. A., and Wanner, B. L. (2000). One-step inactivation of chromosomal genes in *Escherichia coli* K-12 using PCR products. *Proc Natl Acad Sci U S A* 97, 6640-6645.

- Dinos, G. P., and Kalpaxis, D. L. (2000). Kinetic studies on the interaction between a ribosomal complex active in peptide bond formation and the macrolide antibiotics tylosin and erythromycin. *Biochemistry* 39, 11621-11628.
- Elf, J., Li, G. W., and Xie, X. S. (2007). Probing transcription factor dynamics at the single-molecule level in a living cell. *Science* 316, 1191-1194.
- Elf, J., Nilsson, K., Tenson, T., and Ehrenberg, M. (2006). Bistable bacterial growth rate in response to antibiotics with low membrane permeability. *Phys Rev Lett* 97, 258104.
- Ellis, R. J. (2001). Macromolecular crowding: obvious but underappreciated. *Trends Biochem Sci* 26, 597-604.
- Gabashvili, I. S., Gregory, S. T., Valle, M., Grassucci, R., Worbs, M., Wahl, M. C., Dahlberg, A. E., and Frank, J. (2001). The polypeptide tunnel system in the ribosome and its gating in erythromycin resistance mutants of L4 and L22. *Mol Cell* 8, 181-188.
- Gottesman, M. M., and Ling, V. (2006). The molecular basis of multidrug resistance in cancer: the early years of P-glycoprotein research. *FEBS Lett* 580, 998-1009.
- Heeley, R. P., Rusconi, S. G., Sutcliffe, R. G., and Kenyon, C. J. (2002). Mutations flanking the polyglutamine repeat in the modulatory domain of rat glucocorticoid receptor lead to an increase in affinity for hormone. *Endocr Res* 28, 217-229.
- Ho, P. L., Yam, W. C., Que, T. L., Tsang, D. N., Seto, W. H., Ng, T. K., and Ng, W. S. (2001). Target site modifications and efflux phenotype in clinical isolates of *Streptococcus pneumoniae* from Hong Kong with reduced susceptibility to fluoroquinolones. *J Antimicrob Chemother* 47, 655-658.
- Jelenc, P. C., and Kurland, C. G. (1979). Nucleoside triphosphate regeneration decreases the frequency of translation errors. *Proc Natl Acad Sci U S A* 76, 3174-3178.
- Karimi, R., Pavlov, M. Y., Buckingham, R. H., and Ehrenberg, M. (1999). Novel roles for classical factors at the interface between translation termination and initiation. *Mol Cell* 3, 601-609.
- Kriengkauykiat, J., Porter, E., Lomovskaya, O., and Wong-Beringer, A. (2005). Use of an efflux pump inhibitor to determine the prevalence of efflux pump-mediated fluoroquinolone resistance and multidrug resistance in *Pseudomonas aeruginosa*. *Antimicrob Agents Chemother* 49, 565-570.
- Leontiou, C., Lakey, J. H., and Austin, C. A. (2004). Mutation E522K in human DNA topoisomerase IIbeta confers resistance to methyl N-(4'-(9-acridinylamino)-phenyl)carbamate hydrochloride and methyl N-(4'-(9-acridinylamino)-3-methoxy-phenyl) methane sulfonamide but hypersensitivity to etoposide. *Mol Pharmacol* 66, 430-439.

- Lomovskaya, O., Zgurskaya, H. I., Totrov, M., and Watkins, W. J. (2007). Waltzing transporters and 'the dance macabre' between humans and bacteria. *Nat Rev Drug Discov* 6, 56-65.
- Lovmar, M., Nilsson, K., Vimberg, V., Tenson, T., Nervall, M., and Ehrenberg, M. (2006). The Molecular Mechanism of Peptide-mediated Erythromycin Resistance. *J Biol Chem* 281, 6742-6750.
- Lovmar, M., Tenson, T., and Ehrenberg, M. (2004). Kinetics of macrolide action: the josamycin and erythromycin cases. *J Biol Chem* 279, 53506-53515.
- Mark, P. J., and Waddell, B. J. (2006). P-glycoprotein restricts access of cortisol and dexamethasone to the glucocorticoid receptor in placental BeWo cells. *Endocrinology* 147, 5147-5152.
- Michelson, S., and Slate, D. (1992). A mathematical model of the P-glycoprotein pump as a mediator of multidrug resistance. *Bull Math Biol* 54, 1023-1038.
- Michelson, S., and Slate, D. (1994). A mathematical model for the inhibition of the multidrug resistance-associated P-glycoprotein pump. *Bull Math Biol* 56, 207-223.
- Minton, A. P. (1981). Excluded volume as a determinant of macromolecular structure and reactivity. *Biopolymers* 20, 2093-2120.
- Nascimento, A. M., Goldman, G. H., Park, S., Marras, S. A., Delmas, G., Oza, U., Lolans, K., Dudley, M. N., Mann, P. A., and Perlin, D. S. (2003). Multiple resistance mechanisms among *Aspergillus fumigatus* mutants with high-level resistance to itraconazole. *Antimicrob Agents Chemother* 47, 1719-1726.
- Nissen, P., Hansen, J., Ban, N., Moore, P. B., and Steitz, T. A. (2000). The structural basis of ribosome activity in peptide bond synthesis. *Science* 289, 920-930.
- Okusu, H., Ma, D., and Nikaido, H. (1996). AcrAB efflux pump plays a major role in the antibiotic resistance phenotype of *Escherichia coli* multiple-antibiotic-resistance (Mar) mutants. *J Bacteriol* 178, 306-308.
- Omura, S. (2002). *Macrolide Antibiotics : Chemistry, Biology, and Practice*, 2nd edn (Orlando: Academic Press).
- Pavlov, M. Y., and Ehrenberg, M. (1996). Rate of translation of natural mRNAs in an optimized in vitro system. *Arch Biochem Biophys* 328, 9-16.
- Rockett, J. C., Burczynski, M. E., Fornace, A. J., Herrmann, P. C., Krawetz, S. A., and Dix, D. J. (2004). Surrogate tissue analysis: monitoring toxicant exposure and health status of inaccessible tissues through the analysis of accessible tissues and cells. *Toxicol Appl Pharmacol* 194, 189-199.
- Schlunzen, F., Zarivach, R., Harms, J., Bashan, A., Tocilj, A., Albrecht, R., Yonath, A., and Franceschi, F. (2001). Structural basis for the interaction of antibiotics with the peptidyl transferase centre in eubacteria. *Nature* 413, 814-821.

- Tenson, T., DeBlasio, A., and Mankin, A. (1996). A functional peptide encoded in the *Escherichia coli* 23S rRNA. *Proc Natl Acad Sci U S A* *93*, 5641-5646.
- Tenson, T., Lovmar, M., and Ehrenberg, M. (2003). The mechanism of action of macrolides, lincosamides and streptogramin B reveals the nascent Peptide exit path in the ribosome. *J Mol Biol* *330*, 1005-1014.
- Tu, D., Blaha, G., Moore, P. B., and Steitz, T. A. (2005). Structures of MLS(B)K Antibiotics Bound to Mutated Large Ribosomal Subunits Provide a Structural Explanation for Resistance. *Cell* *121*, 257-270.
- Weisblum, B. (1995). Erythromycin resistance by ribosome modification. *Antimicrob Agents Chemother* *39*, 577-585.
- Vester, B., and Douthwaite, S. (2001). Macrolide resistance conferred by base substitutions in 23S rRNA. *Antimicrob Agents Chemother* *45*, 1-12.
- Vimberg, V., Xiong, L., Bailey, M., Tenson, T., and Mankin, A. (2004). Peptide-mediated macrolide resistance reveals possible specific interactions in the nascent peptide exit tunnel. *Mol Microbiol* *54*, 376-385.
- Wintermeyer, W., and Zachau, H. G. (1979). Fluorescent derivatives of yeast tRNAPhe. *Eur J Biochem* *98*, 465-475.
- Wittmann, H. G., Stoffler, G., Apirion, D., Rosen, L., Tanaka, K., Tamaki, M., Takata, R., Dekio, S., and Otaka, E. (1973). Biochemical and genetic studies on two different types of erythromycin resistant mutants of *Escherichia coli* with altered ribosomal proteins. *Mol Gen Genet* *127*, 175-189.
- Voss, N. R., Gerstein, M., Steitz, T. A., and Moore, P. B. (2006). The geometry of the ribosomal polypeptide exit tunnel. *J Mol Biol* *360*, 893-906.
- Zhou, Y. N., and Jin, D. J. (1998). The *rpoB* mutants destabilizing initiation complexes at stringently controlled promoters behave like "stringent" RNA polymerases in *Escherichia coli*. *Proc Natl Acad Sci U S A* *95*, 2908-2913.
- Zimmerman, S. B., and Trach, S. O. (1991). Estimation of macromolecule concentrations and excluded volume effects for the cytoplasm of *Escherichia coli*. *J Mol Biol* *222*, 599-620.
- Zlatanova, J., and van Holde, K. (2006). Single-molecule biology: what is it and how does it work? *Mol Cell* *24*, 317-329.

## ACKNOWLEDGEMENTS

We thank Drs Richard Buckingham and Carl-Henrik Heldin, for valuable discussions. This work was supported by grants from the Swedish Research Council (ML and ME), NIH (GM70768)(ME), the Wellcome Trust International Senior Fellowship (070210/Z/03/Z)(TT) and the Estonian Science Foundation grant no. 6768 (TT).

## FIGURE LEGENDS

**FIGURE 1. Localization of the erythromycin resistance mutations.** Panel A is a cartoon showing a cross-section of the large ribosomal subunit along the nascent peptide exit tunnel, with the subunit interface to the right. The position of the ribosomal proteins L4 and L22 are shown in light brown and green respectively and the erythromycin binding site is indicated in blue. Panel B shows the positions of the mutated amino acids in L4 and L22 that leads to erythromycin resistance in relation to the erythromycin binding site. A dashed arrow indicates the flexibility of the  $\beta$  hairpin in the L22( $\Delta$ 82-84) mutant (Tu et al., 2005). The figure is constructed using the ribosomal proteins from the crystal structure of 70S from *E. coli* (pdb: 2I2V) (Berk et al., 2006) combined with erythromycin from (pdb: 1YI2) (Tu et al., 2005) by aligning the nucleotide A2058 (*E. coli* numbering) from both structures.

**FIGURE 2. Drug sensitivity at different pump capacities as predicted by Eq 1.** Three important features of Eq 1 are illustrated in these plots: (i) the elementary feature that drug sensitivity decreases with increasing efflux pump capacity; (ii) no or low efflux pump activities prevent differences in target site binding properties to be manifested in modified drug sensitivity; and (iii) if  $k_d$  is much smaller than the growth rate the drug sensitivity only depends on  $k_a$  (panel A), while the drug sensitivity depends on the equilibrium constant  $K_d (=k_d/k_a)$  if  $k_d$  is larger than the growth rate (panel B). These plots are made with the following parameter values:  $[A_{ext}]=10^{-5}$  M,  $k_{in}=5 \cdot 10^{-4}$  s $^{-1}$ ,  $[T_0]=4 \cdot 10^{-5}$  M and  $\mu_0=10^{-4}$  s $^{-1}$ .

**FIGURE 3. Determination of rate constants for dissociation of erythromycin from wild-type and mutant ribosomes.**  $^{14}$ C-labeled erythromycin was pre-bound to wild-type and mutant ribosomes and a chase with a large excess of non-labeled erythromycin started at time zero. At the specified time points the reactions were quenched with ice-cold buffer and filtered through nitrocellulose filters. The amount of  $^{14}$ C-labeled erythromycin on the filters corresponds to the amount that remained bound to the ribosomes. The lines are least square fits to single exponentials and were used to estimate the dissociation rate constants presented in Table 1. *Insert.* The same experimental points limited to a short time range between zero and 300 s.

**FIGURE 4. Determination of erythromycin association rate constants for wild-type and L22 mutant ribosomes and equilibrium dissociation constants for both L4 mutants.** In panels A and B, the ribosomes were mixed with  $^{14}$ C-labeled erythromycin at time zero and at the specified time points

quenched with ice-cold buffer containing a large excess of non-labeled erythromycin. The quenched reactions were rapidly filtered through nitrocellulose. The amount of filter-bound  $^{14}\text{C}$ -labeled erythromycin reflects the fraction of ribosomes at which the exchange of labeled versus unlabeled drug has not taken place. The line in panel A are a least square fit to a hyperbolic function and the lines in panel B are least square fits to single exponentials. These fits were used to estimate the association rate constants presented in Table 1. The insert in panel B show the rates of erythromycin association to the L22-mutant ribosomes as a function of erythromycin concentration. In panel C, the ribosomes were mixed with different concentrations of  $^{14}\text{C}$ -labeled erythromycin and incubated for 15 minutes before quenched with cold buffer and rapidly filtered through nitro-cellulose filters. The lines are least square fits to a hyperbolic function and were used to estimate the equilibrium dissociation constants presented in Table 1.

**FIGURE 5. Erythromycin sensitivity measurements.** The relative ODs after 4 hours are plotted as a function of the erythromycin concentration. The values are normalized to the ODs reached after 4 hours in the absence of erythromycin. Panel A shows the results of an erythromycin titration in the concentration range required for inhibiting growth in *E. coli* with intact AcrAB-TolC efflux pumps. The level of resistance caused by the ribosomal protein mutants is best shown in this range. Panel B shows the results of an erythromycin titration in the lower concentration range required to study the efflux pump mutants. Panels C and D shows the corresponding simulation using the estimated binding constants, while Panels E and F shows the same simulation but with rescaled erythromycin dissociation rate constant  $k_d$ .

**FIGURE 6. Cartoon illustrating the model used for the mathematical simulations.** Panel A shows how the erythromycin entry into the cells is modeled. Erythromycin diffuses over the outer membrane with a permeability constant  $C_I$  and over the inner membrane with a permeability constant  $C_{II}$ . In addition, erythromycin is actively pumped out over the outer membrane with a rate constant  $C_{III}$  by the AcrAB-TolC efflux pump system. Panel B shows the states used to model the inhibition of protein synthesis caused by erythromycin. A 50S subunit with (5) or without (1) erythromycin bound initiate with the rate  $k$  to form initiated 70S complexes (6) or (2) respectively. Elongation of the first few amino acids is made with rate  $k_I$  independently of erythromycin. However, if no erythromycin is bound (3) the ribosome continue elongation and becomes refractory to the drug (4) with the rate  $k_2$ , and finally a new protein is produced and the 50S is recycled (1) with a rate  $k_3$ . In contrast, if the elongating

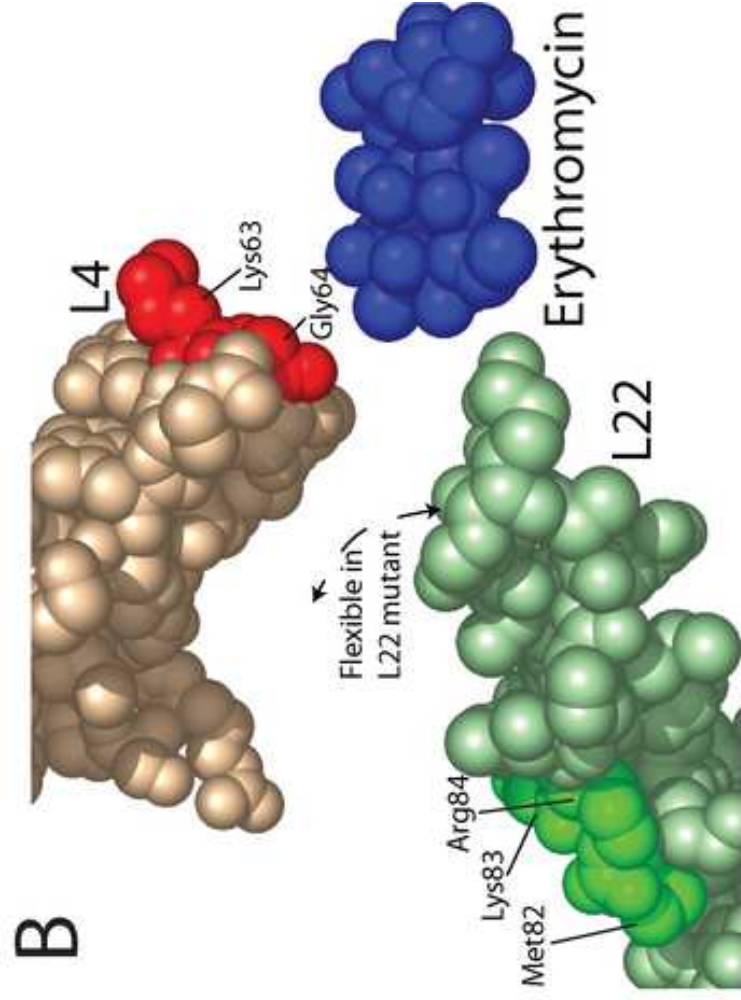
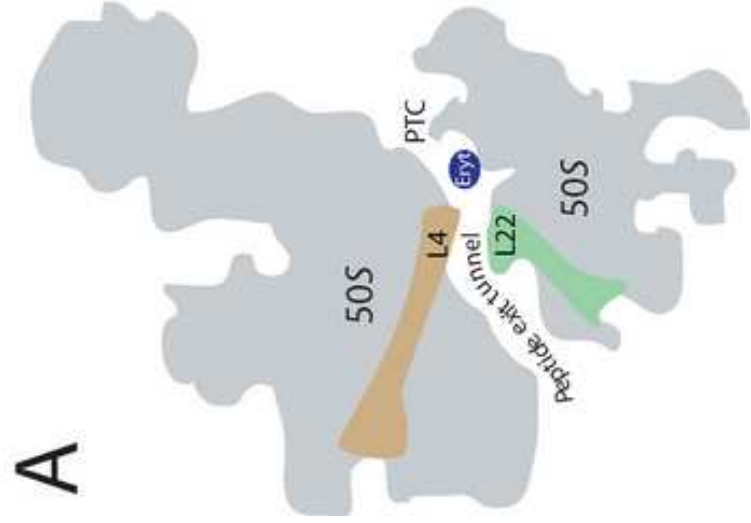
ribosome contains erythromycin (7) it is stalled until either erythromycin dissociates with a rate  $k_d$  or peptidyl-tRNA drops off and the erythromycin containing 50S is recycled with a rate  $k_r$ . Erythromycin binds to state 1, 2 and 3 with a second order rate constant  $k_a$  and dissociates from states 5, 6 and 7 with the rate constant  $k_d$ .

**Table 1. Erythromycin binding properties to wild-type and mutant ribosomes**

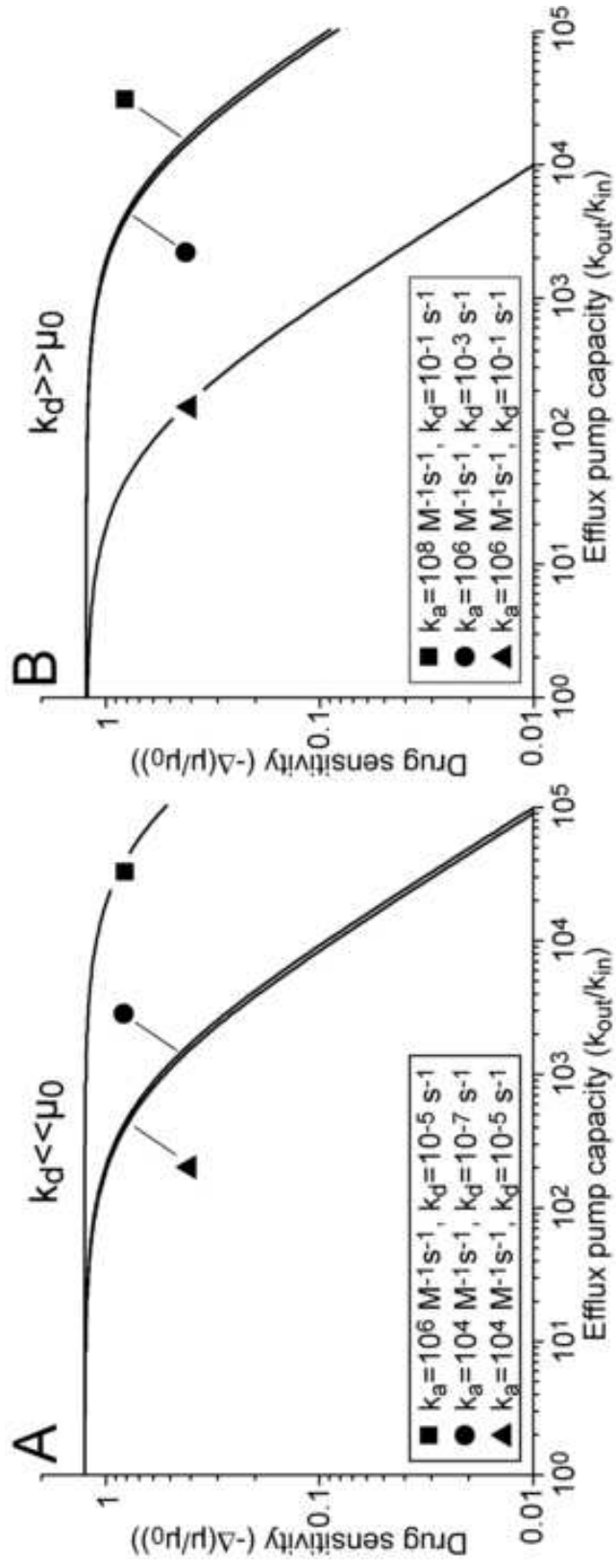
Strain	$k_a$ ( $\mu\text{M}^{-1}\text{s}^{-1}$ )	$k_d$ ( $\text{s}^{-1}$ )	$K_D$ ( $\mu\text{M}$ )
wt	$1.0 \pm 0.1$	$0.013 \pm 0.0006$	<i><math>0.012 \pm 0.001</math></i>
L22 ( $\Delta 82-84$ )	$0.019 \pm 0.0006$	$0.0011 \pm 0.00004$	<i><math>0.059 \pm 0.003</math></i>
L4 (Lys63Glu)	<i><math>0.0040 \pm 0.0006</math></i>	$0.018 \pm 0.001$	$4.6 \pm 0.7$
L4 ( $\Delta 63-64$ )	<i><math>0.0096 \pm 0.001</math></i>	$0.029 \pm 0.002$	$3.0 \pm 0.4$

Numbers in *Italic* are calculated from the other two parameter values.

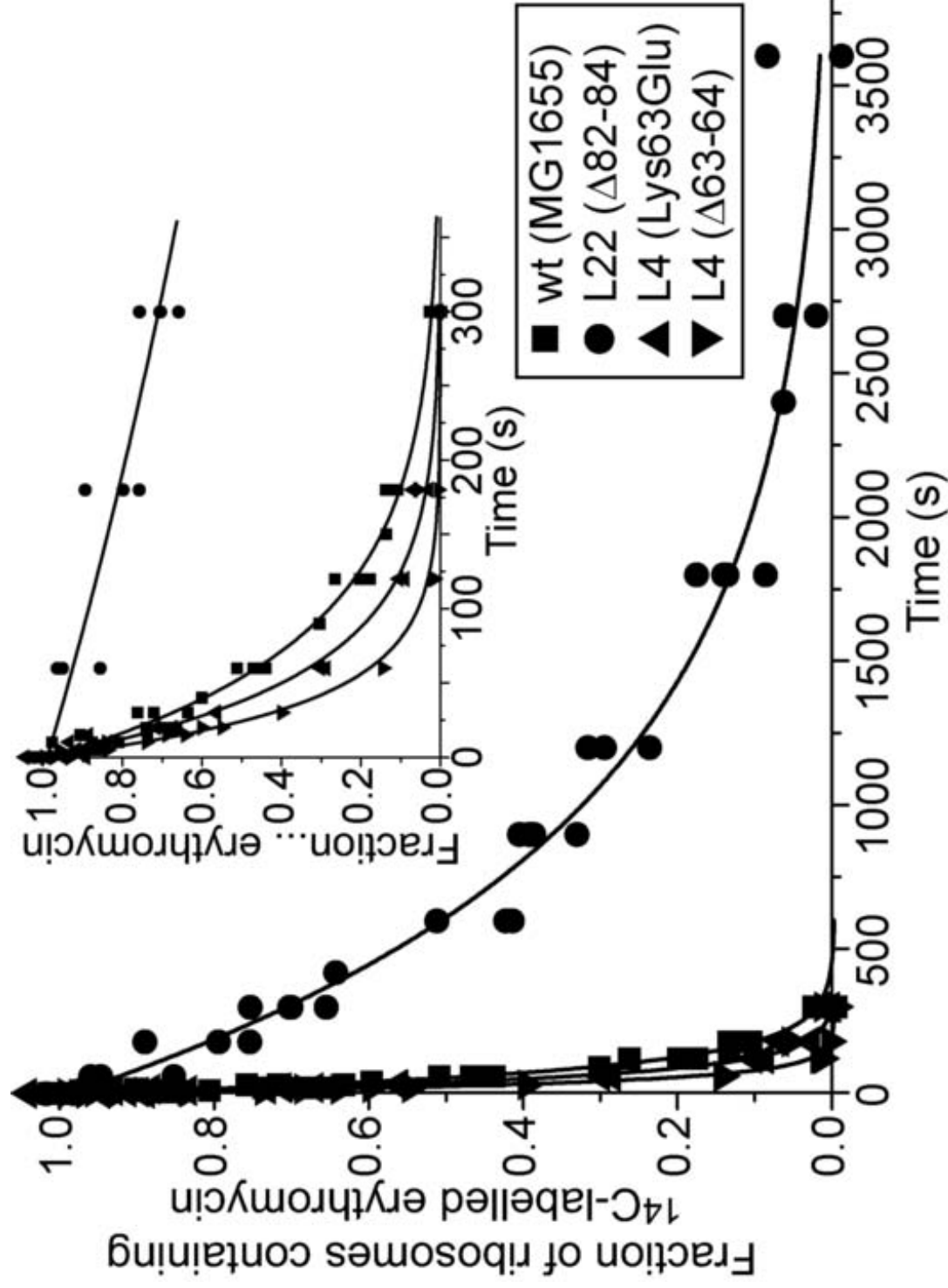
[F] Figure 1  
Click here to download high resolution image



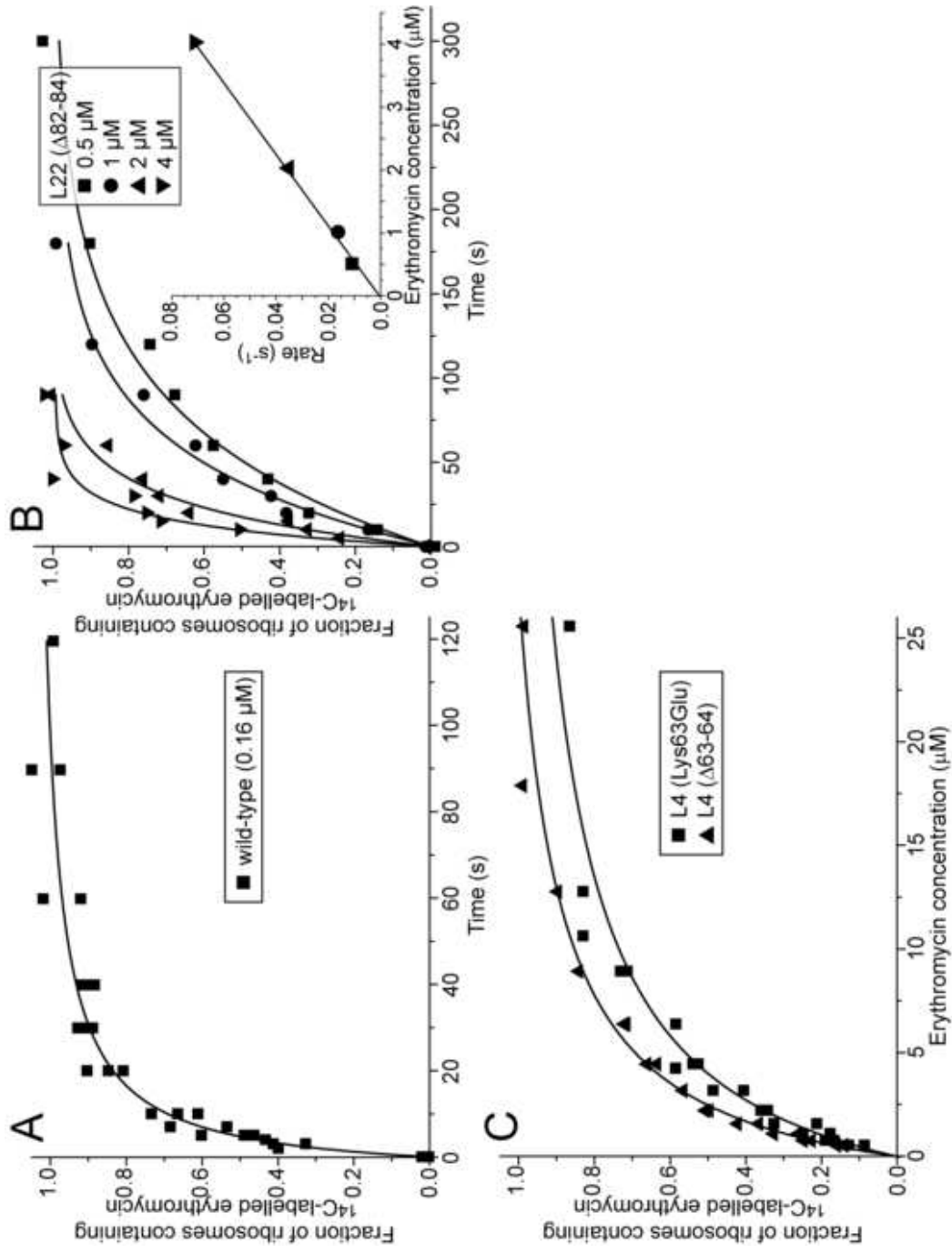
[F] Figure 2  
Click here to download high resolution image



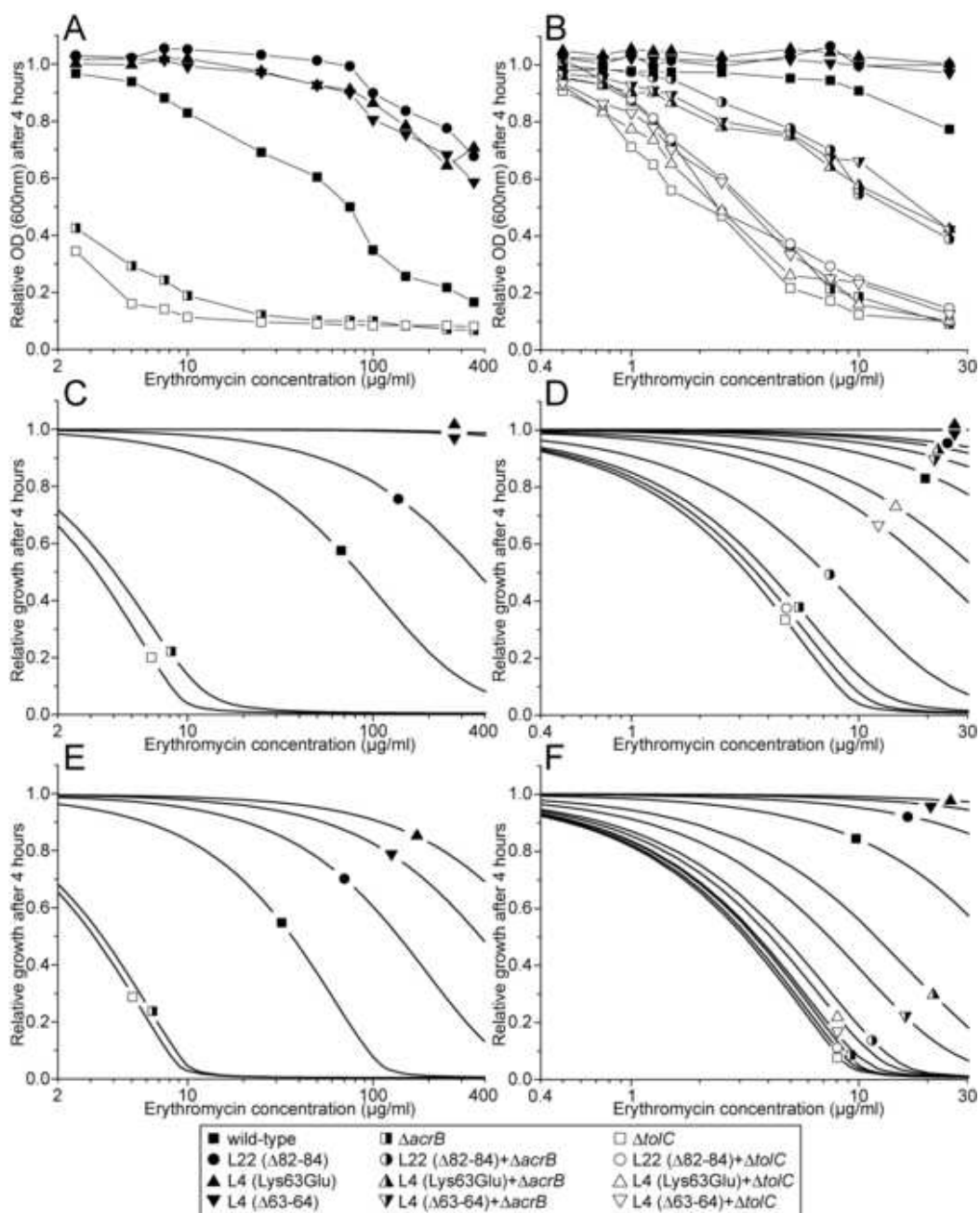
[F] Figure 3  
[Click here to download high resolution image](#)



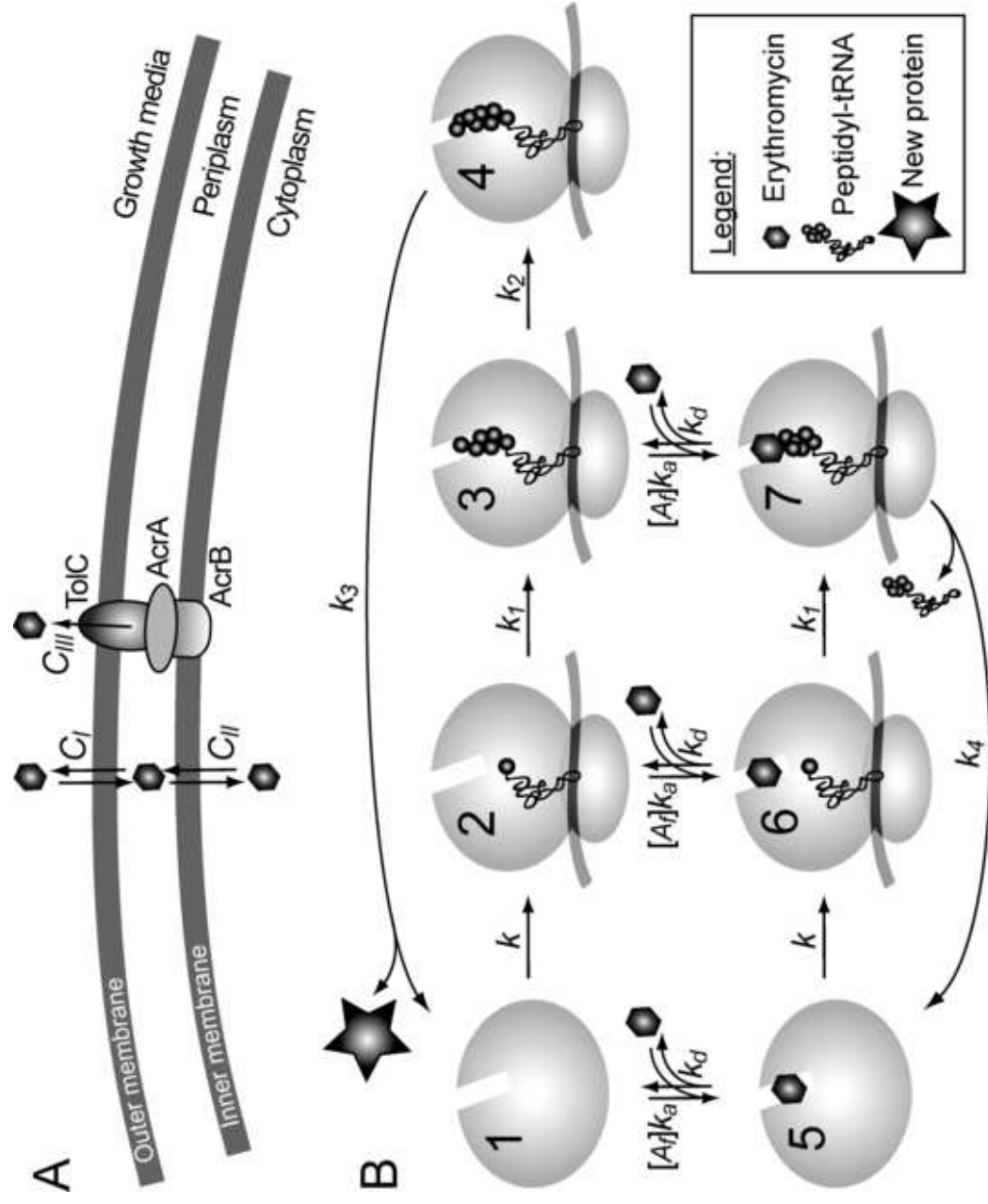
[F] Figure 4  
Click here to download high resolution image



[F] Figure 5  
[Click here to download high resolution image](#)



[F] Figure 6  
 Click here to download high resolution image



## SUPPLEMENTARY MATERIAL

### 1. Target inhibition in growing cells

Here we will discuss target binding of growth inhibitors that enter and exit growing cells in all cases where there is a well defined relation between the fraction  $\alpha$ , of inhibitor bound targets and the normalized growth rate,  $\mu$ , of the cells

$$\alpha = \frac{[T_b]}{[T_0]}, \quad \text{where } 0 \leq \alpha \leq 1; \quad [S1]$$

$$\frac{\mu}{\mu_0} = 1 - f(\alpha), \quad \text{where } 0 \leq f(\alpha) \leq 1$$

Here, the total, inhibitor bound and free intracellular target concentrations are  $[T_0]$ ,  $[T_b]$  and  $[T_f]$ , respectively. The growth rate  $\mu$  decreases monotonically from its highest value  $\mu_0$  in the absence of inhibitor ( $\alpha=0$ ) to zero when all targets are inhibitor bound ( $\alpha=1$ ).

When the intracellular inhibitor concentration is spatially uniform, changes in the concentration,  $[T_f]$ , of free targets are determined by the differential equations

$$\frac{d[T_f]}{dt} = \mu \cdot [T_0] + k_d \cdot [T_b] - k_a \cdot [A_f] \cdot [T_f] - \mu \cdot [T_f], \quad [S2]$$

$$\frac{d[A_0]}{dt} = k_{in} \cdot [A_{ext}] - k_{out} \cdot [A_f] - \mu \cdot [A_0], \quad [S3]$$

supplemented by the conservation conditions

$$\begin{aligned} [T_0] &= [T_f] + [T_b], \\ [A_0] &= [A_f] + [A_b] = [A_f] + [T_b] \end{aligned} \quad [S4]$$

Here,  $[A_0]$ ,  $[A_b]$  and  $[A_f]$  are the total, target bound and free intracellular concentrations of inhibitor, respectively, while  $[A_{ext}]$  is the extracellular concentration of inhibitor in the medium. The rate constants for inhibitor binding to and dissociation from a target are given by  $k_a$  and  $k_d$ , respectively. The parameters  $k_{in}$  and  $k_{out}$  are the effective rate constants by which the inhibitor enters or exits the cell, respectively. The case when  $k_{in}=k_{out}$ , corresponds to passive diffusion through the cell wall. The case when  $k_{in}<k_{out}$ , corresponds to active pumping of inhibitors out from the cell. When there is a single cell membrane, like for gram-positive bacteria, these effective first order rate constants relate to membrane permeability through

$$\begin{aligned} k_{in} &= C_I \cdot A/V, \\ k_{out} &= (C_I + C_{III}) \cdot A/V \end{aligned} \quad [S5]$$

$A$  is the surface area of the cell,  $V$  is the cell volume,  $C_I$  is the permeability due to passive inhibitor diffusion, while  $C_{III}$  accounts for active pumping of inhibitor out from the cell. In the case of gram-negative bacteria with two membranes and a periplasmic space, the same rate constant formalism with effective rate constants  $k_{in}$  and  $k_{out}$  approximates the in and out flux of inhibitors, provided that the periplasmic volume is much smaller than the internal cell volume  $V$  (see below).

## 2. Steady state relations for growth inhibition at low inhibitor concentration

The steady state condition with all concentrations constant in time is described by equations [S2] and [S3] with their right side time derivatives set to zero. The resulting algebraic equations that relate the growth  $\mu$  to the external inhibitor concentration,  $[A_{ext}]$ , are strongly non-linear with interesting properties. These have been described in the special case that drug binding to the target is equilibrated and on the assumption that  $f(\alpha)=\alpha$  in Eq. S1 (Elf et al., 2006). Here, we relax the equilibrium constraint and illustrate in what we hope is an intuitively accessible way the kinetic interplay between drug efflux pump efficiency and the antibiotic resistance conferred by target mutations affecting the rate constants  $k_a$  and  $k_d$  in Eq. S2. For this, we will inspect the first order approximation to the steady state version of Eqs. S2 and S3, when  $\alpha$ , defined in Eq. S1, is much smaller than one. It follows from the definition of  $\alpha$  in conjunction with Eqs S2 and S4, that in the steady state

$$\frac{[T_f]}{[T_0]} = 1 - \alpha = \frac{k_d + \mu}{k_a \cdot [A_f] + k_d + \mu} \quad [S6]$$

Furthermore, from Eqs S3 and S6 it follows that

$$\alpha \cdot \left[ \frac{(k_d + \mu) \cdot (k_{out} + \mu)}{(1 - \alpha) \cdot k_a} + \mu \cdot [T_0] \right] = k_{in} \cdot [A_{ext}], \quad [S7]$$

where the growth rate  $\mu$  is given by Eq. S1. Eq. S7 is an exact expression, but for small values of  $\alpha$ , the relative growth rate  $\mu$  is to first order in  $\alpha$  approximated by

$$\frac{\mu}{\mu_0} - 1 = \Delta \frac{\mu}{\mu_0} = -C \cdot \alpha = -\frac{C \cdot k_{in} \cdot [A_{ext}]}{\frac{(k_d + \mu_0) \cdot (k_{out} + \mu_0)}{k_a} + \mu_0 \cdot [T_0]}, \quad [S8]$$

where

$$C = \left( \frac{df(\alpha)}{d\alpha} \right)_{\alpha=0}. \quad [S9]$$

Eq. 1 in the main text is derived on the assumption that  $f(\alpha)=\alpha$  and, hence, that  $C=1$ .

## 3. Drug flows into and out from gram negative bacteria with two cell membranes

The concentration,  $[A_p]$ , of the drug in the periplasm is governed by the equation (Fig. S1):

$$\frac{d[A_p]}{dt} = \frac{A}{V_p} \cdot (C_I \cdot [A_{ext}] + C_{II} \cdot [A_f]) - (C_I + C_{II} + C_{III} + \mu \cdot V_p / A) \cdot [A_p] \quad [S10]$$

$V_p$  is the volume of the periplasm and  $A$  is the area of each of the two cell walls that define the periplasm, which for simplicity are assumed to be the same.  $C_I$  and  $C_{II}$  are the drug permeability for the outer and inner membrane, respectively, while  $C_{III}$  is the active permeability due to pumping of the drug from the periplasm into the growth medium.

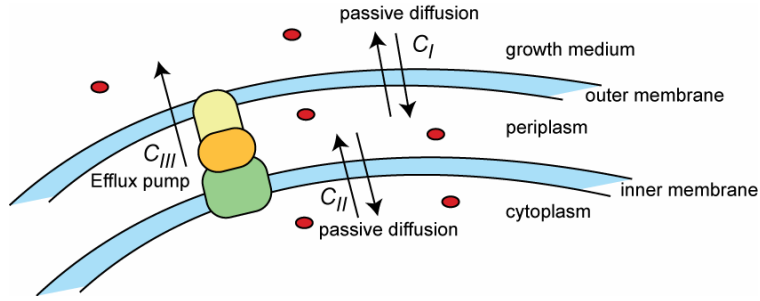


**Figure S1.** A schematic of the flow of inhibitor over the cell membranes in a Gram-negative cell.

The total concentration,  $[A_0]$ , of the drug in the cytoplasm is governed by the equation:

$$\frac{d[A_0]}{dt} = \frac{C_{II} \cdot A}{V} \cdot ([A_p] - [A_f]) - \mu \cdot [A_0], \quad [S11]$$

where  $[A_f]$  is the free drug concentration in the cytoplasm as before. Assuming that the concentration of drug in the cytoplasm is in the steady state with the external and the cytoplasmic drug concentration due to the small periplasmic volume and neglecting the term  $\mu \cdot V_p/A$  in Eq. S10 give

$$[A_p] = \frac{C_I \cdot [A_{ext}] + C_{II} \cdot [A_f]}{C_I + C_{II} + C_{III}} \quad [S12]$$

Introducing this expression into Eq. S11 leads to an expression equal for the total drug concentration,  $[A_0]$ , in the cell identical to that in Eq. S3, with the rate constants  $k_{in}$  and  $k_{out}$  defined as

$$\begin{aligned} k_{in} &= C_I \cdot \frac{A}{V} \cdot \frac{C_{II}}{C_I + C_{II} + C_{III}}, \\ k_{out} &= C_{II} \cdot \frac{A}{V} \cdot \frac{C_I + C_{III}}{C_I + C_{II} + C_{III}}. \end{aligned} \quad [S13]$$

#### 4. Detailed model of inhibition of protein synthesis by erythromycin

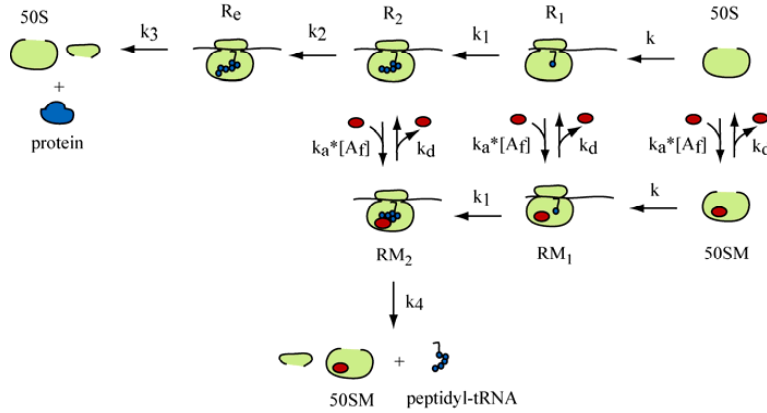


**Figure S2.** A schematic of the model for binding and translation inhibition by erythromycin.

The model includes seven different states of the large ribosomal subunit (Figure S2), which are defined by the following system of differential equations

$$\begin{aligned}
 \frac{d[50SM]}{dt} &= k_a \cdot [A_f] \cdot [50S] + k_4 \cdot [RM_2] - (k + k_d + \mu) \cdot [50SM], \\
 \frac{d[R_1]}{dt} &= k \cdot [50S] + k_d \cdot [RM_1] - (k_1 + k_a [A_f] + \mu) \cdot [R_1], \\
 \frac{d[R_2]}{dt} &= k_1 \cdot [R_1] + k_d \cdot [RM_2] - (k_2 + k_a [A_f] + \mu) \cdot [R_2], \\
 \frac{d[R_e]}{dt} &= k_2 \cdot [R_2] - (k_3 + \mu) \cdot [R_e], \\
 \frac{d[RM_1]}{dt} &= k \cdot [50SM] + k_a \cdot [A_f] \cdot [R_1] - (k_1 + k_d + \mu) \cdot [RM_1], \\
 \frac{d[RM_2]}{dt} &= k_1 \cdot [RM_1] + k_a \cdot [A_f] \cdot [R_2] - (k_4 + k_d + \mu) \cdot [RM_2],
 \end{aligned}
 \tag{S14}$$

A 50S ribosomal subunit may be either bound [50SM] or not bound [50S] to erythromycin. It may also be in complex with a 30S subunit thus forming a ribosome ready to initiate translation, either bound [RM<sub>1</sub>] or not bound [R<sub>1</sub>] to erythromycin. The ribosome may be translating the first few codons either bound [RM<sub>2</sub>], or not bound, but still susceptible, to erythromycin, [R<sub>2</sub>]. Without erythromycin, the ribosome continues in elongation and become temporarily immune to erythromycin [R<sub>e</sub>].

The rate constant of association and spontaneous dissociation of the antibiotic is  $k_a$  and  $k_d$ , respectively. Association of the ribosomal subunits occurs with rate constant  $k$  and translation of the first few codons occurs with rate constant  $k_1$ . The rate constant for translating the codon that makes the ribosome temporarily immune for erythromycin binding is  $k_2$ . The rate constant for completing synthesis of the protein

and recycling the ribosomal subunits is  $k_3$ , and the rate constant of peptidyl-tRNA drop-off from erythromycin bound, stalled ribosome is  $k_4$ . In addition, all concentrations are diluted by the cell growth rate  $\mu$ . The total concentration of 50S subunits  $[50S_{tot}]$  is kept constant and new 50S subunits are thus synthesized by rate  $\mu \cdot [50S_{tot}]$  and the free concentration of 50S subunits varies according to  $[50S] = [50S_{tot}] - [50SM] - [R_1] - [R_2] - [RM_1] - [RM_2] - [R_e]$ .

The system expands by exponential growth with cell growth rate  $\mu$ , defined by (Ehrenberg and Kurland, 1984)

$$\mu = \frac{v_e \cdot [R_e]}{\rho_0}, \quad [S15]$$

where  $v_e$  is the average elongation rate of an uninhibited ribosome and  $\rho_0$  is the concentration of amino acids incorporated in proteins. The system was solved numerically by Euler's method (Heath, 1997). Cell growth was calculated for the first 4 hours after introduction of a certain erythromycin concentration in the growth medium,  $[A_{ext}]$  by

$$V_t = V_{t-dt} \cdot e^{\mu \cdot dt}, \quad [S16]$$

where  $dt$  is a small time-step and  $V_{t-dt}$  and  $V_t$  is the volume prior and after time-step  $dt$ , respectively. Prior to erythromycin exposure, the system resided at steady state. The used program software was MATLAB 6.5 (The MathWorks, Inc., Natick, Massachusetts, U.S.A.).

## References

Antoun, A., Pavlov, M. Y., Lovmar, M., and Ehrenberg, M. (2006). How initiation factors tune the rate of initiation of protein synthesis in bacteria. *Embo J* 25, 2539-2550.

Bremer, H., and Dennis, P. P. (1996). Modulation of Chemical Composition and Other Parameters of the Cell by Growth Rate, In *Escherichia coli and Salmonella : cellular and molecular biology*, F. C. Neidhardt, ed. (Washington: ASM Press), pp. 1553-1569.

Ehrenberg, M., and Kurland, C. G. (1984). Costs of accuracy determined by a maximal growth rate constraint. *Q Rev Biophys* 17, 45-82.

Elf, J., Nilsson, K., Tenson, T., and Ehrenberg, M. (2006). Bistable bacterial growth rate in response to antibiotics with low membrane permeability. *Phys Rev Lett* 97, 258104.

Heath, M. T. (1997). *Scientific computing : an introductory survey* (New York: McGraw-Hill).

**Table S1. Definitions and values of used parameters in the macrolide model.**

Model parameter	Value	Reference
$k$ = association rate of ribosomal subunits at initiation of translation	$1 \text{ s}^{-1}$	(Antoun et al., 2006)
$k_1$ = rate constant for translation of the first codons when the ribosome is susceptible for the antibiotic	$5 \text{ s}^{-1}$	(Bremer and Dennis, 1996)
$k_2$ = rate constant for translation of the codon rendering the ribosome temporarily immune to erythromycin	$20 \text{ s}^{-1}$	(Bremer and Dennis, 1996)
$k_3$ = rate constant for translation beyond the first codons and translation termination	$0.03 \text{ s}^{-1}$	(Bremer and Dennis, 1996)
$k_4$ = drop-off rate constant of peptidyl-tRNA from a stalled ribosome	$0.1 \text{ s}^{-1}$	(Lovmar, unpublished results)
$k_a$ = association rate constant of erythromycin	Table 1	This paper
$k_d$ = dissociation rate constant of erythromycin	Table 1*	This paper
$C_I A/V$ = membrane permeability over the outer membrane	$5 \cdot 10^{-4} \text{ s}^{-1}$	
$C_{II} A/V$ = membrane permeability over the inner membrane	$0.1 \text{ s}^{-1}$	
$C_{III} A/V$ = rate constant of erythromycin efflux over cell membrane by pumps (pump efficiency)	$0 \text{ s}^{-1}$ ( <i>tolC</i> ), $0.01 \text{ s}^{-1}$ ( <i>acrB</i> ) $1 \text{ s}^{-1}$ (wt pumps)	
$V_p / V_C$ = the volume of the periplasm divided by the volume of the cytoplasm (approximated to be constant)	0.1	
$v_e$ = ribosome elongation rate	$20 \text{ s}^{-1}$	(Bremer and Dennis, 1996)
$\rho_0$ = concentration of amino acids in proteins	2 M	(Bremer and Dennis, 1996)
$[50S_{tot}]$ = total concentration of 50S	$4 \cdot 10^{-5} \text{ M}$	(Bremer and Dennis, 1996)
$[A_{ext}]$ = concentration of erythromycin in the growth medium	0.4 – 400 $\mu\text{g/ml}$ (Fig. 5)	

\*  $k_d$  is decreased by a factor 100 in Fig. 5 E-F.



# **CURRICULUM VITAE**

## **Vladimir Vimberg**

Date of birth: 24.06.1981  
Marital status: Married, two children  
Address: Institute of Technology, Nooruse 1, 50411, Tartu, Estonia  
E-mail: riboloom@hotmail.ee

### **Education**

1987–1999 Narva School of Humanities  
1999–2003 BSc in Gene Technology, Faculty of Biology and Geography, University of Tartu. Title of the thesis: “Mutations in 16S Ribosomal RNA Effect the Competitive Translation Initiation on mRNAs with Different Translation Initiation Regions”.  
2003–2005 MSc in Gene Technology, Faculty of Biology and Geography, University of Tartu. Title of the thesis: “Peptide Mediated Macrolide Resistance”.  
2005–... Graduate studies in Molecular Biology, Faculty of Science and Technology, University of Tartu.

### **Professional employment**

2007–... Extraordinary Researcher at the University of Tartu, Faculty of Science and Technology, Institute of Technology, University of Tartu;

### **Scientific work**

I have been studying different aspects of macrolide antibiotic resistance and regulation of translation initiation.

# CURRICULUM VITAE

## Vladimir Vimberg

Sünniaeg ja koht: 24.06.1981. a., Narva  
Perekonnaseis: abielus, kaks last  
Aadress: Tehnoloogiainstituut, Nooruse 1, 50411, Tartu, Eesti  
E-mail: riboloom@hotmail.ee

## Haridus

1987–1999 Narva Humanitaargümnaasium  
1999–2003 BSc (*cum laude*) geenitehnoloogia erialal, Bioloogia-geograafia teaduskond, Tartu Ülikool, Töö pealkiri: “Mutations in 16S Ribosomal RNA Effect the Competitive Translation Initiation on mRNAs with Different Translation Initiation Regions”.  
2003–2005 MSc geenitehnoloogia erialal, Bioloogia-geograafia teaduskond, Tartu Ülikool, Töö pealkiri: “Peptide Mediated Macrolide Resistance”.  
2005–... TÜ MRI doktorant, Tartu Ülikool Loodus- ja tehnoloogia-teaduskond

## Erialane teenistuskäik

2007–... Erakorraline teadur, Tehnoloogiainstituut, Loodus- ja tehnoloogiateaduskond, Tartu Ülikool

## Teadustegevus

Mina olen uurinud antibiootikumresistentsuse mehhanisme ja translatsiooni initsiatsiooni.

## DISSERTATIONES BIOLOGICAE UNIVERSITATIS TARTUENSIS

1. **Toivo Maimets.** Studies of human oncoprotein p53. Tartu, 1991, 96 p.
2. **Enn K. Seppet.** Thyroid state control over energy metabolism, ion transport and contractile functions in rat heart. Tartu, 1991, 135 p.
3. **Kristjan Zobel.** Epifüütsete makrosamblike väärtus õhu saastuse indikaatoritena Hamar-Dobani boreaalsetes mägimetsades. Tartu, 1992, 131 lk.
4. **Andres Mäe.** Conjugal mobilization of catabolic plasmids by transposable elements in helper plasmids. Tartu, 1992, 91 p.
5. **Maia Kivisaar.** Studies on phenol degradation genes of *Pseudomonas* sp. strain EST 1001. Tartu, 1992, 61 p.
6. **Allan Nurk.** Nucleotide sequences of phenol degradative genes from *Pseudomonas* sp. strain EST 1001 and their transcriptional activation in *Pseudomonas putida*. Tartu, 1992, 72 p.
7. **Ülo Tamm.** The genus *Populus* L. in Estonia: variation of the species biology and introduction. Tartu, 1993, 91 p.
8. **Jaanus Remme.** Studies on the peptidyltransferase centre of the *E.coli* ribosome. Tartu, 1993, 68 p.
9. **Ülo Langel.** Galanin and galanin antagonists. Tartu, 1993, 97 p.
10. **Arvo Käär.** The development of an automatic online dynamic fluorescence-based pH-dependent fiber optic penicillin flowthrough biosensor for the control of the benzylpenicillin hydrolysis. Tartu, 1993, 117 p.
11. **Lilian Järvekülg.** Antigenic analysis and development of sensitive immunoassay for potato viruses. Tartu, 1993, 147 p.
12. **Jaak Palumets.** Analysis of phytomass partition in Norway spruce. Tartu, 1993, 47 p.
13. **Arne Sellin.** Variation in hydraulic architecture of *Picea abies* (L.) Karst. trees grown under different environmental conditions. Tartu, 1994, 119 p.
13. **Mati Reeben.** Regulation of light neurofilament gene expression. Tartu, 1994, 108 p.
14. **Urmas Tartes.** Respiration rhythms in insects. Tartu, 1995, 109 p.
15. **Ülo Puurand.** The complete nucleotide sequence and infections *in vitro* transcripts from cloned cDNA of a potato A potyvirus. Tartu, 1995, 96 p.
16. **Peeter Hõrak.** Pathways of selection in avian reproduction: a functional framework and its application in the population study of the great tit (*Parus major*). Tartu, 1995, 118 p.
17. **Erkki Truve.** Studies on specific and broad spectrum virus resistance in transgenic plants. Tartu, 1996, 158 p.
18. **Illar Pata.** Cloning and characterization of human and mouse ribosomal protein S6-encoding genes. Tartu, 1996, 60 p.
19. **Ülo Niinemets.** Importance of structural features of leaves and canopy in determining species shade-tolerance in temperature deciduous woody taxa. Tartu, 1996, 150 p.

20. **Ants Kurg.** Bovine leukemia virus: molecular studies on the packaging region and DNA diagnostics in cattle. Tartu, 1996, 104 p.
21. **Ene Ustav.** E2 as the modulator of the BPV1 DNA replication. Tartu, 1996, 100 p.
22. **Aksel Soosaar.** Role of helix-loop-helix and nuclear hormone receptor transcription factors in neurogenesis. Tartu, 1996, 109 p.
23. **Maido Remm.** Human papillomavirus type 18: replication, transformation and gene expression. Tartu, 1997, 117 p.
24. **Tiiu Kull.** Population dynamics in *Cypripedium calceolus* L. Tartu, 1997, 124 p.
25. **Kalle Olli.** Evolutionary life-strategies of autotrophic planktonic microorganisms in the Baltic Sea. Tartu, 1997, 180 p.
26. **Meelis Pärtel.** Species diversity and community dynamics in calcareous grassland communities in Western Estonia. Tartu, 1997, 124 p.
27. **Malle Leht.** The Genus *Potentilla* L. in Estonia, Latvia and Lithuania: distribution, morphology and taxonomy. Tartu, 1997, 186 p.
28. **Tanel Tenson.** Ribosomes, peptides and antibiotic resistance. Tartu, 1997, 80 p.
29. **Arvo Tuvikene.** Assessment of inland water pollution using biomarker responses in fish *in vivo* and *in vitro*. Tartu, 1997, 160 p.
30. **Urmas Saarma.** Tuning ribosomal elongation cycle by mutagenesis of 23S rRNA. Tartu, 1997, 134 p.
31. **Henn Ojaveer.** Composition and dynamics of fish stocks in the gulf of Riga ecosystem. Tartu, 1997, 138 p.
32. **Lembi Lõugas.** Post-glacial development of vertebrate fauna in Estonian water bodies. Tartu, 1997, 138 p.
33. **Margus Pooga.** Cell penetrating peptide, transportan, and its predecessors, galanin-based chimeric peptides. Tartu, 1998, 110 p.
34. **Andres Saag.** Evolutionary relationships in some cetrarioid genera (Lichenized Ascomycota). Tartu, 1998, 196 p.
35. **Aivar Liiv.** Ribosomal large subunit assembly *in vivo*. Tartu, 1998, 158 p.
36. **Tatjana Oja.** Isoenzyme diversity and phylogenetic affinities among the eurasian annual bromes (*Bromus* L., Poaceae). Tartu, 1998, 92 p.
37. **Mari Moora.** The influence of arbuscular mycorrhizal (AM) symbiosis on the competition and coexistence of calcareous crassland plant species. Tartu, 1998, 78 p.
38. **Olavi Kurina.** Fungus gnats in Estonia (*Diptera: Bolitophilidae, Kero-platidae, Macroceridae, Ditomyiidae, Diadocidiidae, Mycetophilidae*). Tartu, 1998, 200 p.
39. **Andrus Tasa.** Biological leaching of shales: black shale and oil shale. Tartu, 1998, 98 p.
40. **Arnold Kristjuhan.** Studies on transcriptional activator properties of tumor suppressor protein p53. Tartu, 1998, 86 p.

41. **Sulev Ingerpuu.** Characterization of some human myeloid cell surface and nuclear differentiation antigens. Tartu, 1998, 163 p.
42. **Veljo Kisand.** Responses of planktonic bacteria to the abiotic and biotic factors in the shallow lake Võrtsjärv. Tartu, 1998, 118 p.
43. **Kadri Põldmaa.** Studies in the systematics of hypomyces and allied genera (Hypocreales, Ascomycota). Tartu, 1998, 178 p.
44. **Markus Vetemaa.** Reproduction parameters of fish as indicators in environmental monitoring. Tartu, 1998, 117 p.
45. **Heli Talvik.** Prepatent periods and species composition of different *Oesophagostomum* spp. populations in Estonia and Denmark. Tartu, 1998, 104 p.
46. **Katrin Heinsoo.** Cuticular and stomatal antechamber conductance to water vapour diffusion in *Picea abies* (L.) karst. Tartu, 1999, 133 p.
47. **Tarmo Annilo.** Studies on mammalian ribosomal protein S7. Tartu, 1998, 77 p.
48. **Indrek Ots.** Health state indicies of reproducing great tits (*Parus major*): sources of variation and connections with life-history traits. Tartu, 1999, 117 p.
49. **Juan Jose Cantero.** Plant community diversity and habitat relationships in central Argentina grasslands. Tartu, 1999, 161 p.
50. **Rein Kalamees.** Seed bank, seed rain and community regeneration in Estonian calcareous grasslands. Tartu, 1999, 107 p.
51. **Sulev Kõks.** Cholecystokinin (CCK) — induced anxiety in rats: influence of environmental stimuli and involvement of endopioid mechanisms and erotonin. Tartu, 1999, 123 p.
52. **Ebe Sild.** Impact of increasing concentrations of O<sub>3</sub> and CO<sub>2</sub> on wheat, clover and pasture. Tartu, 1999, 123 p.
53. **Ljudmilla Timofejeva.** Electron microscopical analysis of the synaptone-mal complex formation in cereals. Tartu, 1999, 99 p.
54. **Andres Valkna.** Interactions of galanin receptor with ligands and G-proteins: studies with synthetic peptides. Tartu, 1999, 103 p.
55. **Taavi Virro.** Life cycles of planktonic rotifers in lake Peipsi. Tartu, 1999, 101 p.
56. **Ana Rebane.** Mammalian ribosomal protein S3a genes and intron-encoded small nucleolar RNAs U73 and U82. Tartu, 1999, 85 p.
57. **Tiina Tamm.** Cocksfoot mottle virus: the genome organisation and translational strategies. Tartu, 2000, 101 p.
58. **Reet Kurg.** Structure-function relationship of the bovine papilloma virus E2 protein. Tartu, 2000, 89 p.
59. **Toomas Kivisild.** The origins of Southern and Western Eurasian popula-tions: an mtDNA study. Tartu, 2000, 121 p.
60. **Niilo Kaldalu.** Studies of the TOL plasmid transcription factor XylS. Tartu 2000. 88 p.

61. **Dina Lepik.** Modulation of viral DNA replication by tumor suppressor protein p53. Tartu 2000. 106 p.
62. **Kai Vellak.** Influence of different factors on the diversity of the bryophyte vegetation in forest and wooded meadow communities. Tartu 2000. 122 p.
63. **Jonne Kotta.** Impact of eutrophication and biological invasions on the structure and functions of benthic macrofauna. Tartu 2000. 160 p.
64. **Georg Martin.** Phytobenthic communities of the Gulf of Riga and the inner sea the West-Estonian archipelago. Tartu, 2000. 139 p.
65. **Silvia Sepp.** Morphological and genetical variation of *Alchemilla L.* in Estonia. Tartu, 2000. 124 p.
66. **Jaan Liira.** On the determinants of structure and diversity in herbaceous plant communities. Tartu, 2000. 96 p.
67. **Priit Zingel.** The role of planktonic ciliates in lake ecosystems. Tartu 2001. 111 p.
68. **Tiit Teder.** Direct and indirect effects in Host-parasitoid interactions: ecological and evolutionary consequences. Tartu 2001. 122 p.
69. **Hannes Kollist.** Leaf apoplastic ascorbate as ozone scavenger and its transport across the plasma membrane. Tartu 2001. 80 p.
70. **Reet Marits.** Role of two-component regulator system PehR-PehS and extracellular protease PrtW in virulence of *Erwinia Carotovora* subsp. *Carotovora*. Tartu 2001. 112 p.
71. **Vallo Tilgar.** Effect of calcium supplementation on reproductive performance of the pied flycatcher *Ficedula hypoleuca* and the great tit *Parus major*, breeding in Northern temperate forests. Tartu, 2002. 126 p.
72. **Rita Hõrak.** Regulation of transposition of transposon Tn4652 in *Pseudomonas putida*. Tartu, 2002. 108 p.
73. **Liina Eek-Piirsoo.** The effect of fertilization, mowing and additional illumination on the structure of a species-rich grassland community. Tartu, 2002. 74 p.
74. **Krõõt Aasamaa.** Shoot hydraulic conductance and stomatal conductance of six temperate deciduous tree species. Tartu, 2002. 110 p.
75. **Nele Ingerpuu.** Bryophyte diversity and vascular plants. Tartu, 2002. 112 p.
76. **Neeme Tõnisson.** Mutation detection by primer extension on oligonucleotide microarrays. Tartu, 2002. 124 p.
77. **Margus Pensa.** Variation in needle retention of Scots pine in relation to leaf morphology, nitrogen conservation and tree age. Tartu, 2003. 110 p.
78. **Asko Lõhmus.** Habitat preferences and quality for birds of prey: from principles to applications. Tartu, 2003. 168 p.
79. **Viljar Jaks.** p53 — a switch in cellular circuit. Tartu, 2003. 160 p.
80. **Jaana Männik.** Characterization and genetic studies of four ATP-binding cassette (ABC) transporters. Tartu, 2003. 140 p.
81. **Marek Sammul.** Competition and coexistence of clonal plants in relation to productivity. Tartu, 2003. 159 p.

82. **Ivar Ilves.** Virus-cell interactions in the replication cycle of bovine papillomavirus type 1. Tartu, 2003. 89 p.
83. **Andres Männik.** Design and characterization of a novel vector system based on the stable replicator of bovine papillomavirus type 1. Tartu, 2003. 109 p.
84. **Ivika Ostonen.** Fine root structure, dynamics and proportion in net primary production of Norway spruce forest ecosystem in relation to site conditions. Tartu, 2003. 158 p.
85. **Gudrun Veldre.** Somatic status of 12–15-year-old Tartu schoolchildren. Tartu, 2003. 199 p.
86. **Ülo Väli.** The greater spotted eagle *Aquila clanga* and the lesser spotted eagle *A. pomarina*: taxonomy, phylogeography and ecology. Tartu, 2004. 159 p.
87. **Aare Abroi.** The determinants for the native activities of the bovine papillomavirus type 1 E2 protein are separable. Tartu, 2004. 135 p.
88. **Tiina Kahre.** Cystic fibrosis in Estonia. Tartu, 2004. 116 p.
89. **Helen Orav-Kotta.** Habitat choice and feeding activity of benthic suspension feeders and mesograzers in the northern Baltic Sea. Tartu, 2004. 117 p.
90. **Maarja Öpik.** Diversity of arbuscular mycorrhizal fungi in the roots of perennial plants and their effect on plant performance. Tartu, 2004. 175 p.
91. **Kadri Tali.** Species structure of *Neotinea ustulata*. Tartu, 2004. 109 p.
92. **Kristiina Tambets.** Towards the understanding of post-glacial spread of human mitochondrial DNA haplogroups in Europe and beyond: a phylogeographic approach. Tartu, 2004. 163 p.
93. **Arvi Jõers.** Regulation of p53-dependent transcription. Tartu, 2004. 103 p.
94. **Lilian Kadaja.** Studies on modulation of the activity of tumor suppressor protein p53. Tartu, 2004. 103 p.
95. **Jaak Truu.** Oil shale industry wastewater: impact on river microbial community and possibilities for bioremediation. Tartu, 2004. 128 p.
96. **Maire Peters.** Natural horizontal transfer of the *pheBA* operon. Tartu, 2004. 105 p.
97. **Ülo Maiväli.** Studies on the structure-function relationship of the bacterial ribosome. Tartu, 2004. 130 p.
98. **Merit Otsus.** Plant community regeneration and species diversity in dry calcareous grasslands. Tartu, 2004. 103 p.
99. **Mikk Heidemaa.** Systematic studies on sawflies of the genera *Dolerus*, *Empria*, and *Caliroa* (Hymenoptera: Tenthredinidae). Tartu, 2004. 167 p.
100. **Ilmar Tõnno.** The impact of nitrogen and phosphorus concentration and N/P ratio on cyanobacterial dominance and N<sub>2</sub> fixation in some Estonian lakes. Tartu, 2004. 111 p.
101. **Lauri Saks.** Immune function, parasites, and carotenoid-based ornaments in greenfinches. Tartu, 2004. 144 p.

102. **Siiri Rootsi.** Human Y-chromosomal variation in European populations. Tartu, 2004. 142 p.
103. **Eve Vedler.** Structure of the 2,4-dichloro-phenoxyacetic acid-degradative plasmid pEST4011. Tartu, 2005. 106 p.
104. **Andres Tover.** Regulation of transcription of the phenol degradation *pheBA* operon in *Pseudomonas putida*. Tartu, 2005. 126 p.
105. **Helen Udras.** Hexose kinases and glucose transport in the yeast *Hansenula polymorpha*. Tartu, 2005. 100 p.
106. **Ave Suija.** Lichens and lichenicolous fungi in Estonia: diversity, distribution patterns, taxonomy. Tartu, 2005. 162 p.
107. **Piret Lõhmus.** Forest lichens and their substrata in Estonia. Tartu, 2005. 162 p.
108. **Inga Lips.** Abiotic factors controlling the cyanobacterial bloom occurrence in the Gulf of Finland. Tartu, 2005. 156 p.
109. **Kaasik, Krista.** Circadian clock genes in mammalian clockwork, metabolism and behaviour. Tartu, 2005. 121 p.
110. **Juhan Javoiš.** The effects of experience on host acceptance in ovipositing moths. Tartu, 2005. 112 p.
111. **Tiina Sedman.** Characterization of the yeast *Saccharomyces cerevisiae* mitochondrial DNA helicase Hmi1. Tartu, 2005. 103 p.
112. **Ruth Agurauja.** Hawaiian endemic fern lineage *Diellia* (Aspleniaceae): distribution, population structure and ecology. Tartu, 2005. 112 p.
113. **Riho Teras.** Regulation of transcription from the fusion promoters generated by transposition of Tn4652 into the upstream region of *pheBA* operon in *Pseudomonas putida*. Tartu, 2005. 106 p.
114. **Mait Metspalu.** Through the course of prehistory in india: tracing the mtDNA trail. Tartu, 2005. 138 p.
115. **Elin Lõhmussaar.** The comparative patterns of linkage disequilibrium in European populations and its implication for genetic association studies. Tartu, 2006. 124 p.
116. **Priit Kopper.** Hydraulic and environmental limitations to leaf water relations in trees with respect to canopy position. Tartu, 2006. 126 p.
117. **Heili Ilves.** Stress-induced transposition of Tn4652 in *Pseudomonas Putida*. Tartu, 2006. 120 p.
118. **Silja Kuusk.** Biochemical properties of Hmi1p, a DNA helicase from *Saccharomyces cerevisiae* mitochondria. Tartu, 2006. 126 p.
119. **Kersti Püssa.** Forest edges on medium resolution landsat thematic mapper satellite images. Tartu, 2006. 90 p.
120. **Lea Tummeleht.** Physiological condition and immune function in great tits (*Parus major* L.): Sources of variation and trade-offs in relation to growth. Tartu, 2006. 94 p.
121. **Toomas Esperk.** Larval instar as a key element of insect growth schedules. Tartu, 2006. 186 p.

122. **Harri Valdmann.** Lynx (*Lynx lynx*) and wolf (*Canis lupus*) in the Baltic region: Diets, helminth parasites and genetic variation. Tartu, 2006. 102 p.
123. **Priit Jõers.** Studies of the mitochondrial helicase Hmi1p in *Candida albicans* and *Saccharomyces cerevisia*. Tartu, 2006. 113 p.
124. **Kersti Lilleväli.** Gata3 and Gata2 in inner ear development. Tartu, 2007. 123 p.
125. **Kai Rünk.** Comparative ecology of three fern species: *Dryopteris carthusiana* (Vill.) H.P. Fuchs, *D. expansa* (C. Presl) Fraser-Jenkins & Jermy and *D. dilatata* (Hoffm.) A. Gray (Dryopteridaceae). Tartu, 2007. 143 p.
126. **Aveliina Helm.** Formation and persistence of dry grassland diversity: role of human history and landscape structure. Tartu, 2007. 89 p.
127. **Leho Tedersoo.** Ectomycorrhizal fungi: diversity and community structure in Estonia, Seychelles and Australia. Tartu, 2007. 233 p.
128. **Marko Mägi.** The habitat-related variation of reproductive performance of great tits in a deciduous-coniferous forest mosaic: looking for causes and consequences. Tartu, 2007. 135 p.
129. **Valeria Lulla.** Replication strategies and applications of Semliki Forest virus. Tartu, 2007. 109 p.
130. **Ülle Reier.** Estonian threatened vascular plant species: causes of rarity and conservation. Tartu, 2007. 79 p.
131. **Inga Jüriado.** Diversity of lichen species in Estonia: influence of regional and local factors. Tartu, 2007. 171 p.
132. **Tatjana Krama.** Mobbing behaviour in birds: costs and reciprocity based cooperation. Tartu, 2007.
133. **Signe Saumaa.** The role of DNA mismatch repair and oxidative DNA damage defense systems in avoidance of stationary phase mutations in *Pseudomonas putida*. Tartu, 2007. 172 p.
134. **Reedik Mägi.** The linkage disequilibrium and the selection of genetic markers for association studies in european populations. Tartu, 2007. 96 p.
135. **Priit Kilgas.** Blood parameters as indicators of physiological condition and skeletal development in great tits (*Parus major*): natural variation and application in the reproductive ecology of birds. Tartu, 2007. 129 p.
136. **Anu Albert.** The role of water salinity in structuring eastern Baltic coastal fish communities. Tartu, 2007. 95 p.
137. **Kärt Padari.** Protein transduction mechanisms of transportans. Tartu, 2008. 128 p.
138. **Siiri-Lii Sandre.** Selective forces on larval colouration in a moth. Tartu, 2008. 125 p.
139. **Ülle Jõgar.** Conservation and restoration of semi-natural floodplain meadows and their rare plant species. Tartu, 2008. 99 p.
140. **Lauri Laanisto.** Macroecological approach in vegetation science: generality of ecological relationships at the global scale. Tartu, 2008. 133 p.
141. **Reidar Andreson.** Methods and software for predicting PCR failure rate in large genomes. Tartu, 2008. 105 p.

142. **Birgot Paavel.** Bio-optical properties of turbid lakes. Tartu, 2008. 175 p.
143. **Kaire Torn.** Distribution and ecology of charophytes in the Baltic Sea. Tartu, 2008, 98 p.